The Science of Paintings

W. STANLEY TAFT, JR.
JAMES W. MAYER

Springer

The Science of Paintings

Springer
New York
Berlin
Heidelberg
Barcelona
Hong Kong
London
Milan
Paris
Singapore
Tokyo

The Science of Paintings

W. Stanley Taft, Jr.

James W. Mayer

With Contributions from:

Peter Ian Kuniholm

Richard Newman

Dusan C. Stulik

With 166 Illustrations, 28 in full color

Springer

W. Stanley Taft, Jr.
Department of Art
Cornell University
224 Tjaden Hall
Ithaca, NY 14853
USA
wst4@cornell.edu

James W. Mayer
Center for Solid State Science
Arizona State University
P.O. Box 871704
Tempe, AZ 85287
USA
james.mayer@asu.edu

Contributors

Peter Ian Kuniholm
Department of Art History
Cornell University

Richard Newman
Museum of Fine Arts,
Boston

Dusan C. Stulik
The Getty Conservation
Institute

Library of Congress Cataloging-in-Publication Data
Taft, W. Stanley.
The science of paintings / Stanley Taft, James W. Mayer ; with
contributions by Peter Kuniholm, Richard Newman, and Dusan Stulik.
p. cm.
Includes bibliographical references and index.
ISBN 0-387-98722-3 (hardcover : alk. paper)
1. Painting—Appreciation. I. Mayer, James W., 1930– .
II. Newman, Richard, 1951– . III. Stulik, Dusan, 1956– .
IV. Kuniholm, Peter. V. Title.
ND 1143.T34 2000
751—dc21 99-39642

Printed on acid-free paper.

Production managed by MaryAnn Brickner; manufacturing supervised by Joe Quatela.
Typeset by Matrix Publishing Services, Inc., York, PA.
Printed and bound by Maple-Vail Book Manufacturing Group, York, PA.
Printed in the United States of America.

9 8 7 6 5 4 3 2 1

ISBN 0-387-98722-3 Springer-Verlag New York Berlin Heidelberg SPIN 10707620

PREFACE

The beauty, mystery, joy, and inspired observation of the human spirit that paintings evoke result from a complex of intuitive and cognitive choices made by the artist. An understanding of the genesis of these choices can be as elusive as the resulting imagery, but great paintings seem to initiate in us a curiosity about the ideas, methods, and materials used by their creators. In the twentieth century connoisseurship has been enriched by the application of methods of scientific analysis. The results of these investigations into the physical properties of paintings have shed new light on their authenticity and individual histories as well as on the craft in general. Developments in the fields of physics and chemistry have allowed us to understand still more about how we perceive and interact with paintings.

This book is intended for those both inside and outside the field of art who wish to gain insight into the making of paintings. It is directed toward students, teachers, and scientists in engineering, physics, and chemistry as well as those in art, art history, and art conservation. This book grew out of the interdisciplinary undergraduate-level course Art, Isotopes, and Analysis taught at Cornell University by the two authors and supported in lectures and seminars by three of the contributing authors: Dr. Richard Newman, of the Museum of Fine Arts, Boston; Dr. Dusan Stulik, of the Getty Conservation Institute; and Prof. Peter Kuniholm, of Cornell University. Students enrolled in the course represented a broad range of majors and expertise in both art and science (they were not expected to have taken college-level math, physics, or chemistry). The course gave inspiration and structure to the book, which developed from a student text compiled by the authors and other contributors to the course. Much of the information in the Technical Appendices is derived from these lecture notes.

The book is divided into two sections: (1) nine chapters describing the structure of paintings, the differences in painting media, and the physical properties of painting materials. The nature of light and color and their interaction lead to a view beyond the eye, enhanced by x-radiation, infrared radiation, and nuclear radiation, enabling a deeper penetration into the painting. Analysis of pigments, binders, and support materials as well as the application of dating techniques is also described; (2) a list of references and technical appendices that provide, in detail, the physics and chemistry applicable to the topics covered in the main text. The problem sets and exams used at Cornell University for the Art, Isotopes, and Analysis course, as well as a solution set, are available through the publisher, Springer-Verlag.

The authors acknowledge the help and support of our Cornell University colleagues. Professor Donald D. Eddy, of the Department of English, has for many years taught The History of the Book, a course that was the inspiration for Art, Isotopes, and Analysis. Eddy also participated in the organization of Art, Isotopes, and Analysis and presented lectures on printing, binding, paper, and the history of books. Professor Peter I. Kuniholm, of the Department of the History of Art and Archeaology and director of the Aegean Dendrochronology Project, provided lectures and data on dendrochronology. Professor David D. Clark and Howard C. Aderhold, of the Department of Nuclear Science and Engineering, and Professor Albert Silverman, from the Department of Physics and Nuclear Science, gave support in the areas of physics and neutron-induced autoradiography. Peter Revesz provided proton-induced x-ray emission (PIXE) analysis of pigments. Debora Mayer, a private art conservator in Bedford, New Hampshire, and formerly at the Winterthur Museum, gave lectures on beta-radiography of works of art on paper and on paper fibers. We are indebted to the students at Cornell who attended our course and those who served as our undergraduate teaching assistants. These teaching assistants attended the course, carried out research projects, and participated as graders, advisors, and assistants.

This book is being used at Cornell University as a text in studio painting courses and at Arizona State University as a supplemental text in the course Patterns in Nature, which is intended for teachers of grades K–12.

Contents

APPENDICES 101

This page intentionally left blank

The Structure and Analysis of Paintings

1

1.0 Introduction

This book follows two lines (science and art) that run simultaneously. Each has been organized independently to explore a particular discipline or body of knowledge. The science component of the book takes ever closer views of matter and the interactions in nature that allow us to perceive paintings, from the phenomenon of light to the composition and dynamics of the atom. Techniques of analysis, which utilize these scientific principles, are used in an in-depth investigation of paintings. The book also explores the processes through which paintings are made, the materials to make them, and the information produced by scientific analysis.

The sequence of examples and topics is designed to give as clear an explanation as possible of the nature of paintings as objects. The sequence is also designed to explain the scientific laws that are at work in making it possible for the object to exist and for us to perceive it. Despite the differences in motivation on the part of artists, the social, political, and economic forces at work during the time in which the works were made, and the consequences of artistic invention, the objects we are analyzing live as objects and among objects as a part of our world. It is part of the intention of the book to give some feeling for the relevance of the works of the past to our lives today. The objects we will examine are as alive today as they were when they were made. This is not to say that the conditions under which the works were made have no consequence in our study of them. Quite the contrary. Many of the choices made by an artist were dictated by the current state of technology, economics, politics, and many other factors.

Paintings are also repositories of history. They have been subjected to the whims of man and the forces of nature. A study of the particular way time and the elements have affected these objects can reveal to us a great deal about the properties of the materials, and the way in which they were made.

1.1 What Is a Painting?

Paintings present us with images that either represent things, ideas, or events familiar to us or that have no connection to our own experience. In either case, we are often inspired, informed, and given pleasure by what we see. And what is it that we see? Paintings are essentially two-dimensional—an image painted on a flat surface. Most typically the surface is rectangular, and we view it hanging flat against a wall. The three-dimensional volumes of the figure and the deep space of the interior in *The Archangel Gabriel* by Gerard David (Color Plate 1) are illusions. The effectiveness of these illusions is dependent upon the skill of the painter, for despite the complexities of iconography, narrative, and the attachment of the viewer to the activity being depicted, these are simply images made with paint. In most cases, the paint is somewhat evenly distributed across the surface, reinforcing the two-dimensionality of the painting.

The fact that paintings have a material presence is often overlooked or is not fully appreciated. This is due in part to the profusion of art reproductions that, while providing us with the image, cannot adequately portray the surface or scale of the painting. When we view an actual painting, its material aspect can become very apparent to us. We see the image, and simultaneously we may also acknowledge that it is made with paint. The images in *Easter Monday* by Willem de Kooning (Color Plate 2) are clearly made of material we associate with paint. The texture of the paint is an integral part of the image. We may see that areas of color overlap one another in some way or that some areas of paint may be thicker than others. The paint may also have different surface characteristics or topography. Some areas may be very smooth and others heavily textured.

The whole surface may be extremely smooth—resembling enamel or glass. In David's *Archangel Gabriel* (Color Plate 1) we are more aware of the figure in the interior than the surface topography of the paint. We assume that the images are made with paint, but the character of the material is not as evident as the illusionistic texture of fabric, hair, and feathers. The topographical character of the paint—whether smooth, as in the David, or heavily textured in the de Kooning—is crucial to initiating a response from the viewer.

Paint may be manipulated to produce a wide range of reflective qual-

ities from shiny to matte. These effects are, for the most part, imperceivable in reproductions, but are an integral part of the painting and carefully considered by the painter.

Paint, of whatever surface texture or reflective quality, is composed of the same basic components. The component we perceive as color is known as *pigment*, which is most typically a fine powder of organic or inorganic material. The pigment is dispersed in a liquid, which allows it to be spread out and which binds the individual powder granules together and to the surface to which the paint is applied. This liquid, called the *binder*, can be one of a number of oils, egg, gum, or a synthetic polymer (acrylic, alkyd). The binder has the characteristic that when it dries it produces a stable paint film. A third component (sometimes absent) is the *vehicle,* or *diluent*. The vehicle is compatible with the binder: water with egg, gums, and acrylic polymers; turpentine or petroleum distillate with oils. When mixed with the pigment and binder, the vehicle allows the paint to be spread more easily and makes it a bit more transparent. It may also assist in the drying of the film. In all cases, the vehicle evaporates as the film dries.

The surface upon which the paint is applied is known as the *support*. It may be flexible material like cotton or linen canvas (stretched over a wooden frame, the *stretcher*, to give it stability as shown in Figure 1.1), or rigid panels of wood, metal, glass, or plastic. The walls and ceilings of buildings have also served as supports for paintings. Canvas has a distinct texture that in most cases can be easily recognized in the painting. The nature of the support material influences the way we see and interpret the painting. Some materials, such as coarse canvas, impart a softness to the surface, whereas a painting on a wooden or metal panel looks hard and smooth.

The support is first prepared with an application of *size*. Size is a diluted glue, most typically made from animal skins. The size prevents the binder in the subsequent layers of the painting from being absorbed into the support, thereby weakening the painting. In addition, the size prevents the penetration into the support of binders and vehicles that may have a deleterious effect on the support material. In the case of canvas, size also

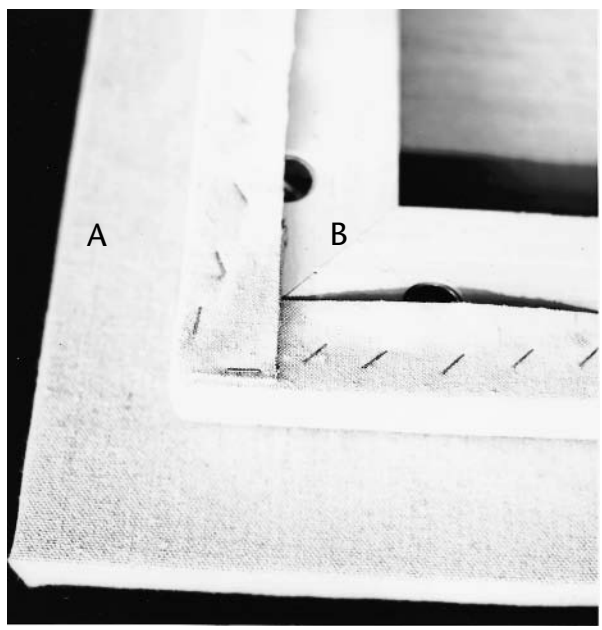

Fig. 1.1A,B. Canvas stretched over a wooden "stretcher" frame.
A: the surface that will receive the paint. B: the back of the canvas, showing how the fabric is attached to the stretcher.

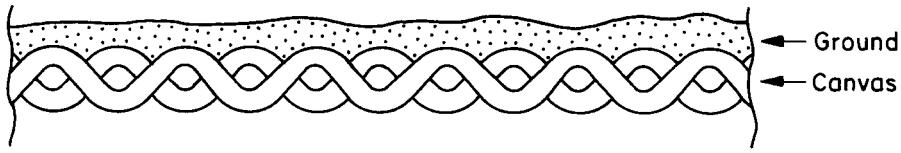

Fig. 1.2. The ground layer applied to the canvas.
This coating protects the fabric from the adverse effects of the paint. This view is called a cross section because it cuts across the layers of the painting, perpendicular to the surface view.

shrinks the fabric to a taut, smooth membrane (held, of course, by the stretcher).

A coating, or *ground*, shown in Figure 1.2, covers the sized support to further protect it from the adverse effects of binders and to block the absorption of the binder into the support. The ground is essentially a paint, made of materials compatible with the support material and the paint to be used over it. Gesso—a mixture of animal glue, chalk (calcium carbonate), and at times a white pigment—has been used for centuries as a ground for both wooden panels and canvas. The most common ground preparation used today is a gesso containing a binder of acrylic polymer, which replaces the animal skin glue used in traditional gesso. Traditional gesso grounds produce a white, opaque surface. In addition to its protective function, the ground also acts as a reflective surface beneath the paint film.

The illustration of a painting shown in Figure 1.3 is known as a *cross section,* which depicts the layers of a painting as seen from its edge, per-

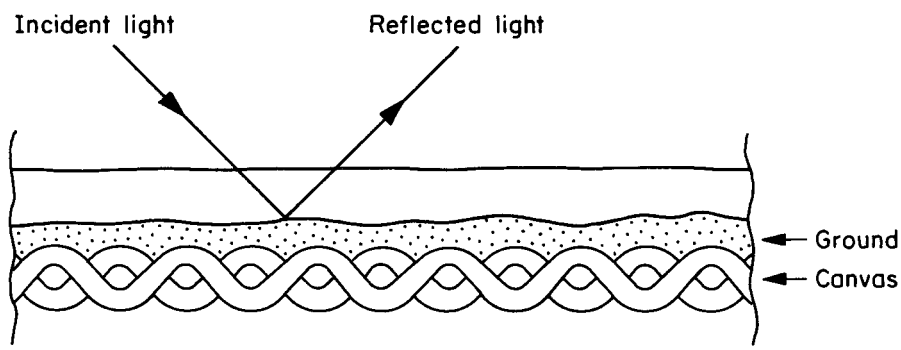

Fig. 1.3. Light passing through a layer of paint and reflected by the ground layer.
Not all paint films allow light to pass to the ground, and the amount of light reflected is dependent upon the characteristics of the pigment and binder components of the paint.

pendicular to the normal surface view. This view allows us to understand, in this case, how light interacts with the painting. As we will see in discussing the optical properties of paint films, light passes into the film and may penetrate as far as the ground. If the light is reflected back by the dense white surface, we will perceive luminosity in the painting, a quality cherished by many painters. Some grounds are not white, however. The painter may decide to add certain colors to the ground mixture to act as a base for overlaying colors. A cool tone (blue-gray or green) sometimes underlies the warm colors of flesh. A brilliant white ground may well impart desirable characteristics to the paint film, but to many painters it is a disturbing surface to face when starting a painting. A thin layer of color called an *imprimatura* may be applied over the ground to act in a way similar to a toned ground, and may also serve to seal a somewhat absorbent gesso. Painters sometimes find these colors useful as the painting develops. Areas of either toned ground or imprimatura may be visible in a finished painting.

The painting may be coated after completion with a thin layer of *varnish*. The varnish is a transparent liquid material that performs two primary functions: It protects the paint film from abrasions, pollutants in the atmosphere, moisture, and dirt, and it can alter the reflective characteristics of the paint. The painter may find that certain colors have dried matte while others have dried glossy. If the desired effect is a glossy surface, the application of a gloss varnish will make all colors uniformly glossy.

Figure 1.4 illustrates how these components of a painting fit together. Most paintings seen in cross section will resemble this drawing. The particular construction in Figure 1.4 has served the needs of many painters in the history of Western painting; however, there exist many variations on the theme. In an effort to satisfy the demands of the imagination, artists have experimented with many nontraditional painting materials and with methods that often stretch both traditional and nontraditional materials to the limit (and sometimes perhaps regrettably beyond the limit) of

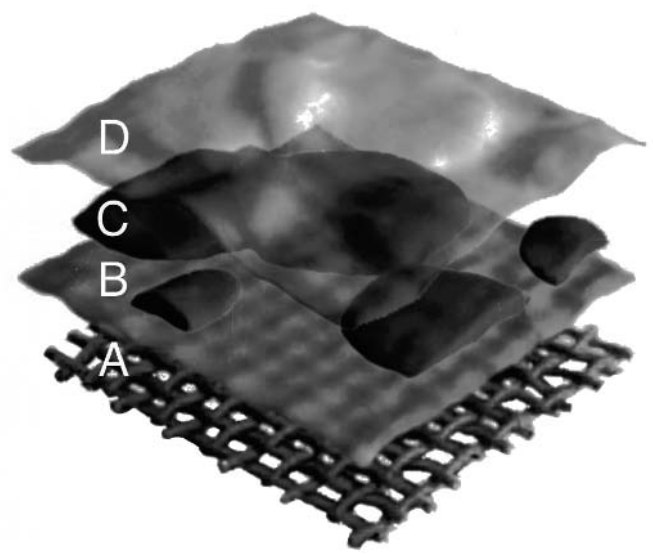

Fig. 1.4A,B,C,D. A typical painting in exploded view. Overlaying the canvas (A) is a layer of ground (B), followed by areas of paint (C). Covering the various applications of paint is a layer of translucent glaze or transparent varnish (D).

their abilities to produce a stable, perceivable object. *Woman with Hat* (1916) by Alexander Archipenko (Color Plate 3) is a very successful example of the use of traditional materials applied in nontraditional ways. It has a rather complex support made of wood, metal, papier-maché, and gauze. The image is made partly in relief and then painted. Experimentation is an innate part of the painting process and will manifest itself in more or less subtle ways.

1.2 CHOICES

What we see when we look at a painting—the image and our belief in it—is the result of choices in painting media, physical components, and the methods employed prior to and during the painting process. To a great extent, the number of choices, the way they are made, and the sequence in which they are used are influenced by the environment of the artist. Availability of materials, training, common practice, the demand of imagery, scale, and placement of the completed painting all influence these choices. We certainly cannot discount skill and invention as contributing factors in the making of the object, for they guide the use of materials, and, when the artist is truly inspired, allow us to be transported into the life of the painting.

The choices made to satisfy the particular requirements of one painting may well provide the viewer with a distinctly different sensory experience from a painting requiring different choices. In the late 1520s, the Florentine artist Jacopo Pontormo painted the *Deposition* altarpiece and *Annunciation* (Color Plates 4 and 5) for the Capponi Chapel in S. Felicita, Florence. The altarpiece is painted in oil on a panel and has a glossy, luminous, rich surface. The colors are very intense and range from very light to very dark. On an adjoining wall in the small chapel is the *Annunciation*, a fresco painting much different in character. Fresco is a method of painting on a wall while the plaster of the wall is still damp, or "fresh," as described in Section 2.2. Part of the difference between the paintings can be attributed to the effects of nature and time on the fresco, but there is also a significant visual difference resulting from the unique method used in fresco. The method is determined in large part by the nature of the materials. Fresco also has a much drier, less reflective, and somewhat matte surface. In addition, one cannot overlook the fact that the images are a part of the wall. The *Deposition* is painted on a panel and is separated from the architecture of the chapel by an ornate frame. The panel support does not assert itself, so we are led through the frame into the space of the painting as through a window. The space is crowded with figures, and there is very little to indicate the particular environment they occupy. We are transported from the world of the chapel into the world of the painting. By contrast, the angel and Virgin of the *An-*

nunciation are part of the architecture that surrounds the viewer. These figures are close to us; we see them as a part of our space. They are intimately integrated into the space of the chapel, flanking a window—a real window, across which the communication between them takes place, and which operates as a source of light for the chapel.

The life of the painting itself is as dependent upon these choices as the image. Albert Pinkham Ryder, a much admired American painter (1847–1917), produced paintings that are often mysterious, full of large swirling forms depicting strange landscapes or seascapes (Figure 1.5).

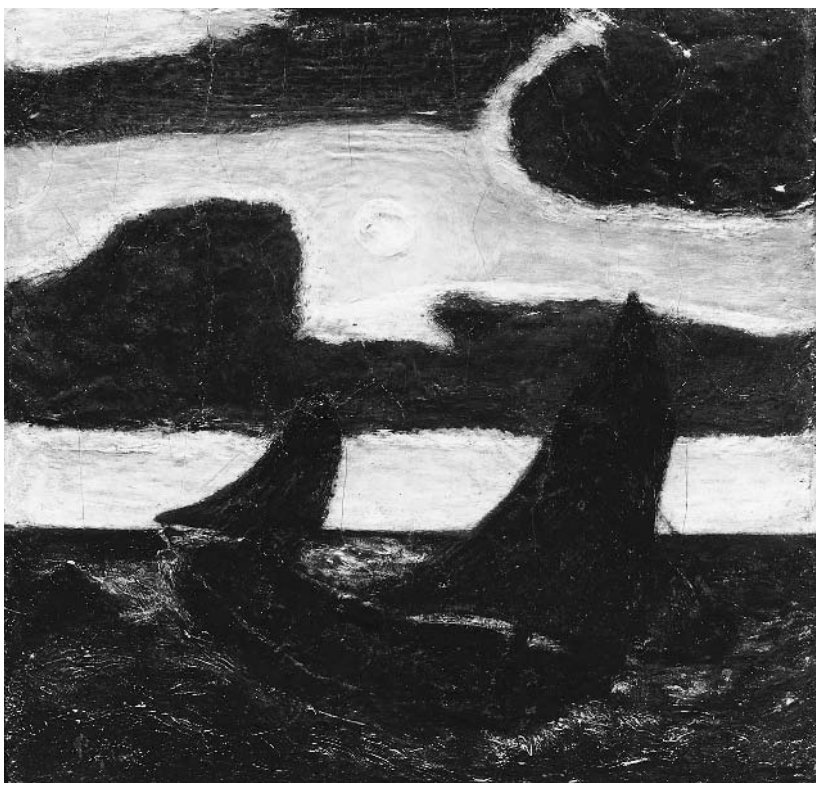

Fig. 1.5. *Moonlight Marine* by Albert Pinkham Ryder, late 1890s, Metropolitan Museum of Art. Oil on canvas, 11 1/2″ × 12″.
Cracks can be clearly seen throughout the surface of Ryder's painting. His unorthodox technique and choice of materials contributed to their presence. Although the cracks indicate a faulty and often delicate paint film, they somehow do not interfere with the appreciation of the painting. In fact, because of the prevalence of such cracking in his paintings, we have grown to expect them. A Ryder painting without cracks would be very surprising.

Many of the paintings are relatively small, and because of the scale, the texture and character of the surface are very evident when we view them either in a museum or in reproduction. Typically, passing across those painted large forms is a network of cracks. More than likely, the thickness of the paint, the materials used, and the process employed in building the layers of paint all contributed to the cracking. To the viewer the pattern of cracks seems to relate to the images; it is difficult to think of Ryder's paintings without them. But it is unfortunate at the same time that the unique qualities that make Ryder's paintings so compelling (the rich multilayer glazes, for example) also make them extremely fragile.

Painters over the centuries have been very attentive to the demands of particular materials. Methods of work have been developed to accommodate the characteristics of the materials used. If a pigment has proved to be unsatisfactory, it is either abandoned or used with a binding medium that allows it to remain stable. Often paintings incorporate more than one binding medium because the artist needs to use a range of pigments, some compatible with one binder, others compatible with a different binder. Likewise, the effects resulting from the use of one medium might be desired in one area of a painting, while the effects generated by the use of another medium are felt to be more appropriate for another part of the image.

The determination of what materials are suitable for a given situation, or indeed, what are suitable for the making of paintings in the first place, is often made through the study of the work of past masters. The methods of working and the application of a wide variety of materials to the process have been well documented. However, the innovations of painters of the past often fail to meet the demands of an artist's imagination.

Many artists have adopted materials designed for industrial applications. This has at times proved problematic, given the instability or impermanence of many synthetic materials, but it has also provided the artist with an ever-expanding source of permanent and easy-to-use materials. Well-established practices must frequently be modified, and unconventional materials or traditional materials used in unconventional ways may be called for. Experimentation of this sort is an integral part of the painting process and has advanced the craft steadily throughout its history. These investigations may also have the effect of liberating the artist's imagination. Some ideas lie dormant, waiting for the appropriate material to give them life.

1.3 Examination and Analysis

We have described a painting as an object made from a variety of materials carefully chosen by the painter. But how is it constructed, what are its materials, and how is our visual response generated by the result

of their combination? A series of analytical techniques has been developed to help answer these questions.

The techniques employed in the scientific analysis of paintings follow a sequence beginning with an external view with the unaided eye. Much information is available from this view, and the resulting perceptions both direct and assess further investigation by other techniques. Assisted by the optical microscope (Figure 1.6) and various other techniques that aid the eye, we can begin to look into and through the painting.

The interior view reveals a relationship between the elemental structures within a particle of pigment, for example, and the images on the surface of the painting. The external and internal views are aspects of the same phenomenon. They reinforce and amplify each other. The scientific analysis is a window through which we gain an appreciation of the structure of a painting just as paintings themselves are windows through which we may view ourselves and our world.

Fig. 1.6. Viewing a painting through a binocular microscope.
The microscopic view reveals aspects of the painting's construction such as the layering sequences of paint layers, pigment density, underpainting or underdrawings, as well as evidence of restoration, overpainting, losses, and alterations to the original work. Photo: J. Mayer.

A thorough scientific analysis is essential in deciding upon a course of treatment for an ailing work of art. The resulting information may allow one to avoid complications or damage resulting from the treatment itself. The success of any such treatment is, of course, dependent to a great extent on available technology. With the development of more sophisticated methods of assessing the condition of artworks, as well as determining the component materials and how they have been used, has come a more informed, restrained, and cautionary approach to treatment. Art historians have also benefited by the development of new applications of analytical technology. Attributions, deattributions, and reattributions are often more easily made after reviewing x-radiographs, infrared reflectograms, dendrochronological data, and pigment analyses. This material adds to the general knowledge about particular artists, their lives, working methods, chronologies of their work, and interrelationships with other artists.

Another benefactor of this information is the contemporary artist. Traditionally, artists learn about the craft of painting directly from masters, contemporary accounts of studio practices written by artists (Giorgio Vasari in his *Lives of the Artists* and *The Craftsman's Handbook* by Cennino d'Andrea Cennini, for example), and from artist's journals. The texts most used today were compiled by or with the assistance of scientists. Rutherford J. Gettens, George Stout, Ralph Mayer, and Max Doerner are a few of the modern writers on painting materials and techniques whose work is based on scientific investigation.

The techniques used in the analysis of works of art fall into the larger framework of analysis of the wide variety of materials that make up our

Fig. 1.7. Detail of painting *4 Squids* by Richard Birkett, 1986.
Paintings (in this case an object composed of oil paint on canvas) are typically viewed with the unaided eye and are appreciated with no other mediation. Additional information and an appreciation of different aspects of the object are achieved through the use of the same analytical techniques that are used to study, and therefore to appreciate, the integrated circuit shown in Figure 1.8.

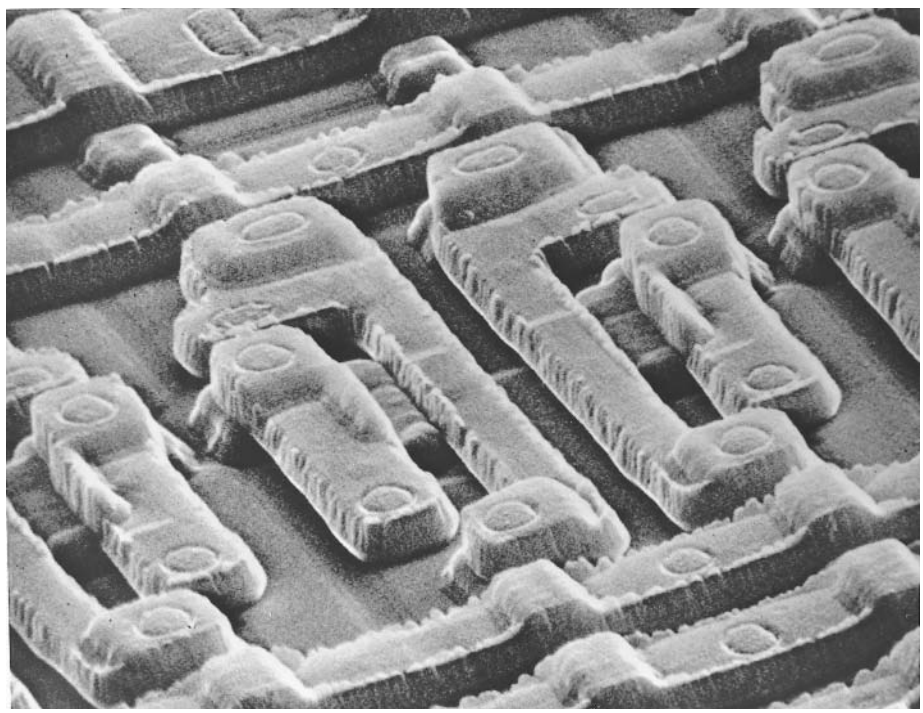

Fig. 1.8. A scanning electron micrograph of an electronic circuit.
This degree of detail of the surface typography and texture cannot be perceived with the unaided eye. Through the use of specialized techniques of analysis we are able to extend our view and knowledge of the object.

world today, from coatings on windows to the integrated circuits in our home computers. The analysis of the layers of paint that produce the image of a squid in the painting shown in Figure 1.7 can be performed using the same approach used in the analysis of the layers in the metal lines interconnecting electronic devices in the semiconductor surface shown in Figure 1.8. From a scientific viewpoint both the squid and the metal lines of the semiconductor are thin films with defined shapes and patterns. In terms of scale, they are vastly different, with the squid composed of patterns that are centimeters across and the metal lines thousands of times smaller. The details of the squid can be viewed with the unaided eye, while the metal lines cannot be seen without the aid of a high-powered scanning electron microscope. Yet, the analytical techniques developed for unraveling the structure of the components in semiconductor transistors have their counterparts in the laboratories of museum scientists and conservators to assist them in gaining a deeper understanding of the structures and physical properties of paintings.

PAINT 2

Contributed by DUSAN STULIK
The Getty Conservation Institute

2.0 PAINT

The paint used by artists to project their ideas and observations can be as simple as a mixture of pigment and binder, with pigment providing the color and the binder joining the particles of pigment together and to the support. A paint may also contain a vehicle that dilutes the pigment/binder mixture, allowing the paint to be spread more easily. Other materials may be added to the mixture to enhance the optical or textural characteristics, or to alter the working properties, by accelerating or slowing the drying of the film or by making it more or less fluid.

The choice of materials for these various functions is dependent upon the type of support the painter intends to use, the scale of the painting, its proposed environment, and the tactile and optical characteristics suitable to the artist's vision. Although many artists have experimented extensively in the hope of developing new techniques (Figure 2.1) or adapting new materials to suit their pictorial needs, most have followed common practice or historically established procedures. Innovations generally derive from these historical precedents, and the adoption of new materials such as acrylic polymers, vinyl, and alkyd resins, in their most common formulations, mimic to some extent conventional paints. These synthetic media do offer the painter an expanded range of textures, consistencies, and optical effects through the use of a number of additives.

In centuries prior to the Industrial Revolution and the development of manufactured paints, a painter was not only an artist, but also a "formulator of paints." Painters personally, or with the help of

assistants, made their own paints, mixing pigments with selected binding media (the material that holds the pigment together and bonds the paint to a support). Hands-on experience with paint preparation gave an artist a great understanding of artist's materials and their properties. Artists often followed a variety of traditional paint recipes. Differences in paint formulas proliferated as painters experimented with a multiplicity of binding media, seeking that special combination that would give their paints the desired optical and handling properties.

After the introduction of collapsible paint tubes in 1841 and the development of the paint industry in the eighteenth and nineteenth centuries, artists became separated from the paint manufacturing process, and most of them lost the motivation to learn the details of the paint-making trade. Artists became freer in the creative process, and the collapsible paint tubes allowed them to leave their studios and helped them to develop new styles of painting. We can say that without these technological advances in artist's materials there would not have been such art movements as Impressionism, which brought the painter out into the open air. The technological advances and diminishing knowledge of artist's materials by painters had, on the other hand, some serious negative effects. Using inadequate materials, working with poorly tested paints, and experimenting with paint formulas without an intimate knowledge of possible consequences sometimes had disastrous effects on the longevity of paintings.

Fig. 2.1. *Photo of Jackson Pollock,* Hans Namuth.
Many of Jackson Pollock's paintings consist of layers of paint marks produced by dripping very liquid paints onto canvas. In order to make this kind of image, Pollock adopted the unconventional application technique shown here.

Paint media, no matter how different they are from one another, share a common characteristic in that they are manufactured in essentially the same way. The pigment must be dispersed, or *ground,* as evenly as possible in the binding medium to take full advantage of the properties of both the pigment and the binder. The grinding process does not alter the morphology of the individual particles of pigment, but simply distributes them evenly within the binder (Figure 2.2a,b). Traditionally,

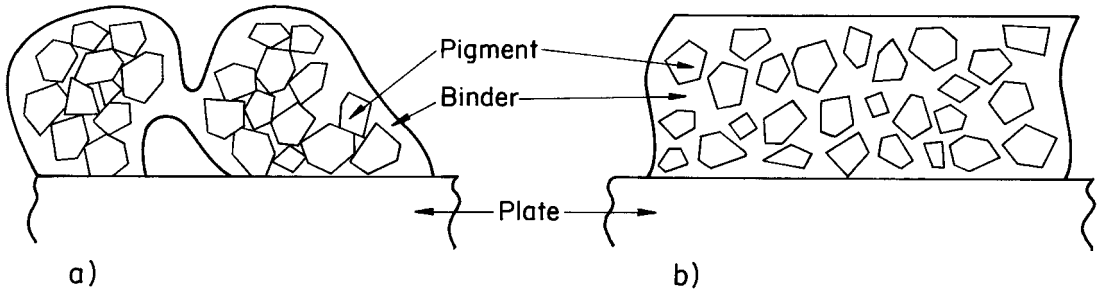

Fig. 2.2a,b. (a) Pigments (irregularly shaped particles) are combined with a binding medium into a stiff paste, which is then (b) ground on a flat plate to distribute the pigment particles uniformly within the binder.

Fig. 2.3. *A Dutch Studio in the Sixteenth Century*, engraving, Theodor Galle after Johannes Stradamus, Bibliothèque Nationale, Paris.
In the studio of a successful sixteenth-century painter, apprentices are busy assisting the master in a number of ways including the grinding, or preparation, of paint, shown on the far right.

the pigment and binder are first mixed into a stiff paste. This is then ground on a flat plate of glass or stone with a muller, a flat-bottomed glass or stone instrument held in the hands and pushed in a circular motion, demonstrated by the apprentices in the studio of a sixteenth-century painter in Figure 2.3. Although some painters today still grind their paint by hand, most purchase their paint preground by machines used by manufacturers to produce large quantities of paint (Figure 2.4) of uniform consistency and pigment distribution.

Fig. 2.4. A modern commercial three-roll mill producing, in this case, permanent green oil paint (Courtesy, Daniel Smith Artists' Materials.)

2.1 PIGMENT

A leading manufacturer of artist's paint currently lists at least 108 different colors of oil paint. The pigments selected for these colors are uniform in particle size, compatible with oil binders, are reasonably resistant to atmospheric gases and light, and are for the most part permanent. These modern pigments are also relatively uniform in consistency, workability, and drying time from color to color. Even though some of the 108 colors are mixes of two or more pigments (a *flesh* color might be a mix of reds, yellows, and titanium white), this represents an incredibly varied and comprehensive palette for the contemporary painter.

Modern high-quality artist's paints are manufactured to such exacting standards that the contemporary artist need not be terribly concerned about using impermanent or unstable colors. In fact, few painters take much notice of the pigments used in their paint and rarely have to consider the compatibility of the colors that they are mixing together on the palette. It is tempting to believe that whatever use is made of the paint, the results will be faultless.

By comparison, the options available to artists of the fourteenth through seventeenth centuries, for example, were very limited. The pigments commonly used during this period of Western painting numbered about fifteen. The most common were three blues, azurite (copper carbonate), ultramarine blue (lazurite), and smalt (cobalt glass); and possibly four reds, red lead (lead tetroxide), vermilion (mercury sulfide), iron oxide red, and carmine lake (made from the dried bodies of the cochineal, a South American insect). For many painters not all of these pigments were available at all times, and some (ultramarine blue, for example, made from the semiprecious stone lapis lazuli) were so prohibitively expensive that they could be used only on paintings for which the painter had received a substantial advanced sum for materials.

There were other colors available, notably simple earth pigments—yellows and browns. Dyes of various kinds and minerals were continually being developed for other industries. These materials were often tested for use by painters, and in some cases the palette was expanded significantly by this experimentation. The more common result was that these pigments turned out to be incompatible with other tried and true materials. They proved to be unstable in some way, either by changing color, fading, cracking, or by altering the materials placed in contact with them.

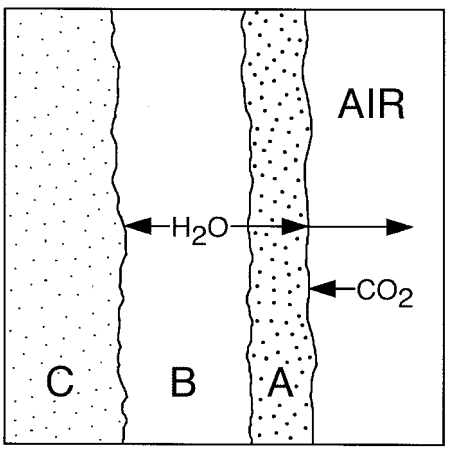

Fig. 2.5A,B,C. Diagram showing layers of plaster applied to a masonry substrate in the construction of a fresco painting.
Each layer is kept damp until after the succeeding layer is applied, and the colors are applied to the final layer before it dries, or within about eight hours. As the composite of layers dries, some water migrates from the surface back through the surface layer or *intonacco* (A), and *arriccio* (B) toward the masonry wall (C) while the rest evaporates into the air at the surface. Carbon dioxide is drawn into the plaster, transforming the calcium hydroxide into calcium carbonate. During this process, platelets of calcium carbonate lock the particles of pigment into the surface of the plaster. This process acts as the equivalent of an organic binder found in more conventional paints. See Appendix J for an analysis of a cross section of the *Detroit Industry* frescos by Diego Rivera.

Artists tend to be experimental by nature and are willing to try untested materials or procedures that suggest an improvement in the capacity of materials to project their ideas. Along with this air of curiosity there also exists a concern for permanence and general high quality. Although periodic experimentation has been the norm throughout history, most painters have had a rather conservative attitude about their choice of pigments. Powers of invention are focused on how to maximize through mixing the limitations of a small number of trusted colors.

What follows are descriptions of several types of paint and the methods of applying them. There are nearly as many variations of these methods and formulations of materials as there have been painters, but nearly all painters have based their approach on historical models that still define the art and craft of painting.

2.2 FRESCO

Fresco is an ancient technique of painting on masonry walls. The color in Diego Rivera's murals at the Detroit Institute of Arts (Color Plate 6) was applied to damp plaster (hence the term fresco, or "fresh" in Italian). The material used to paint frescos does not conform to our usual definition of a paint, which specifies the presence of a binder. The pigment is ground in water, which has no binding strength. Water is a vehicle, or diluent, which evaporates during the drying process. The water is used to dilute the pigment, allowing it to be spread easily over the plaster and to assist in the drying/binding process.

The binder is the result of a chemical process, resulting in a mechanical bonding of the particles of pigment. The color mixture of pigment and water is brushed onto a freshly plastered surface. The plaster is a mixture of slaked lime (calcium oxide in solution with water, forming calcium hydroxide) and an aggregate (sand, marble dust, or a volcanic ash called pozzolana). As the plaster dries, the particles of pigment are pulled into the surface of the plaster and locked in place by particles of calcium hydroxide, which convert to calcium carbonate as the plaster dries (Figure 2.5). The plaster acts as ground, support, and binding agent. Fresco is the one painting medium in which all of the component parts merge to form a single unit. A cross section from Rivera's mural (Figure 2.6) reveals a simple structure with pigment particles integrated within the surface of the lime mixture. (See Appendix J for an analysis of pigment–plaster integration.) Underlying the apparent simplicity of this medium, however, is a process complex in its chemical interactions and demanding in its execution.

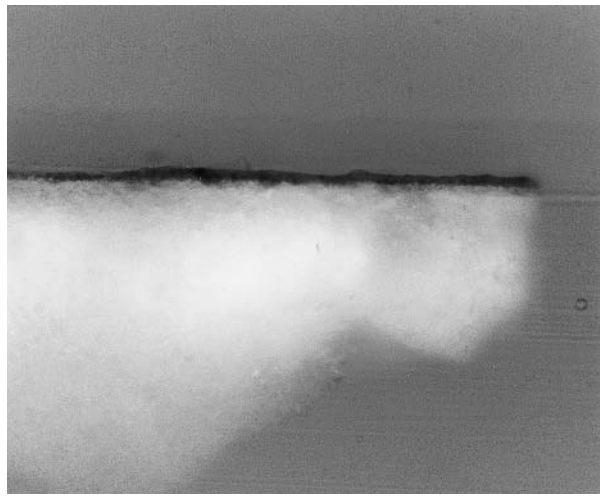

Fig. 2.6. A cross section from the fresco *Detroit Industry* by Diego Rivera showing the accumulation of pigment particles (thin dark band) at the surface of a layer of plaster. Although this band appears as a discrete layer, the pigment particles are actually interlaced with crystallites of calcium carbonate in the plaster. See analysis of this cross section in Appendix J.

Fresco is a marvelous medium for painting large-scale works that are meant to be assimilated into an architectural space. It is compatible with masonry and is durable and quickly executed. The difficulties for the painter are that extensive preparatory work must be done (in the form of sketches, full-size drawings called *cartoons* and small-scale color sketches), large areas must be painted quickly and without alteration, and the work of assistants and tradesmen must be orchestrated in the often cumbersome environment of scaffolding and restrictive architectural spaces.

The wall surface is built up of layers of different formulations of lime, water, and aggregate as shown in Figure 2.5. Each successive layer contains a greater percentage of lime, gradually increasing the binding power of the plaster. Layering ensures even, slow drying, which reduces the likelihood of cracking. Because most frescos are large in scale, the *intonacco*, or surface layer, is applied in sections that can be painted in one day before the plaster dries. These sections are called *giornate*, or a day's work. In addition to making the painting process more manageable for the

Fig. 2.7. The line drawing superimposed over a photo of *Vaccination* from *Detroit Industry* by Diego Rivera indicates the seams between giornate, or sections of the fresco completed in one day. The seams usually follow the contours of forms in the image.

painter, the seams between giornate act as expansion joints, alleviating some of the stresses on the surface that could lead to cracking. Figure 2.7 shows the arrangement of giornate for the section *Vaccination* from the mural cycle by Diego Rivera at the Detroit Institute of Arts. The seams are aligned with the edges of forms in the image. Complex color mixtures would need to be matched from day to day (nearly impossible to do given the inconstancy of pigment and plaster mixtures and the inevitable fluctuations of atmospheric conditions) should a seam pass through a form or area of the image. The schemes for the giornate are very carefully plotted when the cartoons are drawn. The image in the cartoon (Figure 2.8) is transferred directly to the damp plaster by means of pouncing (charcoal dust or pigment forced through a series of small punctures along the lines of the drawing), or by scribing along the lines in the cartoon with a pointed wooden or metal tool that incises the line into the soft plaster.

Painting of the image then proceeds in the prescribed sequence. Each giornate must be completed in 4 to 8 hours, after which time the plaster has dried too much to permit the adhesion of the pigment particles within its surface. The painting cannot be revived after the plaster dries to make alterations or corrections without having to chip away the *intonacco* and start over again. It is possible to paint over the fresco to make alterations, but this procedure requires the use of a binder in the paint (egg, casein, or animal glue have been used), which then produces a film on the plaster. In addition to making corrections, this technique, called *secco*, is sometimes used to apply pigments that are not compatible with lime (pigments containing copper, for example).

The finished state of a fresco has a somewhat dry, nonglossy ap-

pearance. The surface may become slightly more reflective with age or from having been burnished with a fine abrasive, a practice sometimes employed on Roman frescos. In most cases, there is no sense of the surface being coated with a layer of paint. The image is simply a part of the wall. Fresco has the potential to produce brilliant color as well as a feeling of monumentality through its affinities with architecture (Figure 2.9).

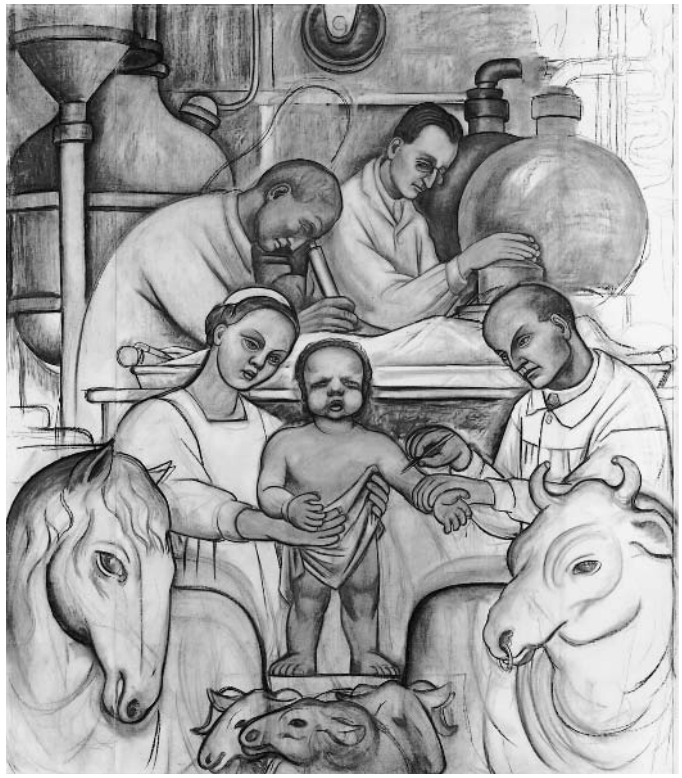

Fig. 2.8. *Vaccination*, Diego Rivera, 1932. Charcoal with red pigment, 2.55 × 2.20 m. Cartoon for south wall of *Detroit Industry*, Detroit Institute of Arts.
The cartoon is a full-scale drawing that is transferred to the prepared wall prior to painting.

2.3 TEMPERA

Tempera refers to paint containing a binder of egg. Its vehicle is water, which dilutes the paint but evaporates during drying. Tempera produces a very durable but somewhat brittle paint film. It is usually applied to a rigid wooden panel (Color Plate 7) that has been coated with gesso, a mixture of animal glue, water, chalk, and, at times, white pigment. The rigid support (typically made of wood) prevents the paint film from flexing enough to cause cracking or flaking. In order to maintain binding strength and avoid adhesion problems between layers, the paint must not be diluted excessively with water. As a result, tempera paint is not very fluid compared to other media. The paint dries rather quickly to an unusually luminous and brilliant film.

Tempera has sometimes been used in conjunction with other painting media. In fresco, it is the secco overlying the fresco when alterations are required, or it is used in the application of certain pigments (containing copper, such as azurite) that are incompatible with the alkalis in the plaster. It has also been commonly used as an underpainting, over which layers of opaque and/or transparent oil paint are applied. Because tempera dries quickly (within minutes), the painter can establish value and compositional arrangements without the delays required by the

Fig. 2.9. *Photo of Vaccination* in situ. North wall of *Detroit Industry*, Diego Rivera, 1932. Fresco.
It is only within the context of the architectural space in which they function that frescos can be fully appreciated. The painted image and the architecture of the space are fully integrated.

much more slowly drying oil medium, often requiring days of drying before subsequent layers can be applied. Alterations at this stage of the painting may be much easier to accomplish using the quicker-drying tempera. Some pigments, usually those containing high concentrations of copper (azurite or malachite), tend to discolor oil binders, so they have been ground in egg instead. Resulting paint films may have alternating layers of tempera and oil paint.

The *Annunciation*, by Dierick Bouts (Figure 2.10), was painted in a medium known as *distemper*. The binder is animal glue, usually made from the skin of rabbits. This is a very strong glue, used in gesso, and commonly used as an adhesive in the fabrication of furniture. As in the case with the egg binder used in tempera, animal glue is diluted with water. The paint is very brittle and often fragile. It must also be applied to a rigid support, or when applied to canvas, as in the case of the Bouts *Annunciation*, applied very thinly, almost as a kind of stain. When painted

Fig. 2.10. *Annunciation*, Dierick Bouts, c. 1450–55. Distemper on canvas, 90 × 74.5 cm, The J. Paul Getty Museum.
Distemper is a paint with a binder of animal hide glue. This example is unusual in that the paint was applied to a support of canvas. More typically, distemper is applied to a rigid support in order to compensate for the brittle character of the paint film. The paint in the *Annunciation* is extremely thin—almost a stain.

on canvas, the distemper has a very matte surface. It can produce a very luminous and highly reflective surface (similar to porcelain or enamel) if applied in layers on a panel.

Other media related to tempera are gouache and casein. Gouache has a binder of gum arabic, a natural gum produced by the acacia tree. Sometimes referred to as opaque watercolor, gouache is indeed extremely

opaque in normal usage. It dries very quickly to a matte surface. This, too, produces a rather brittle film. It is usually used on panels or paper.

Casein (an example is given in Chapter 3) shares some of the characteristics of tempera and gouache. It is diluted with water and dries to a matte film. The binder in this case is the solids of skim milk. Casein glue made from these solids is extremely strong and when dry is insoluble in water. Due to the insolubility of the dried film, casein lends itself to work requiring layers of color or to artists who rely on making revisions by overpainting. It produces a film with slightly more luster than gouache, and like gouache is normally used as an opaque color.

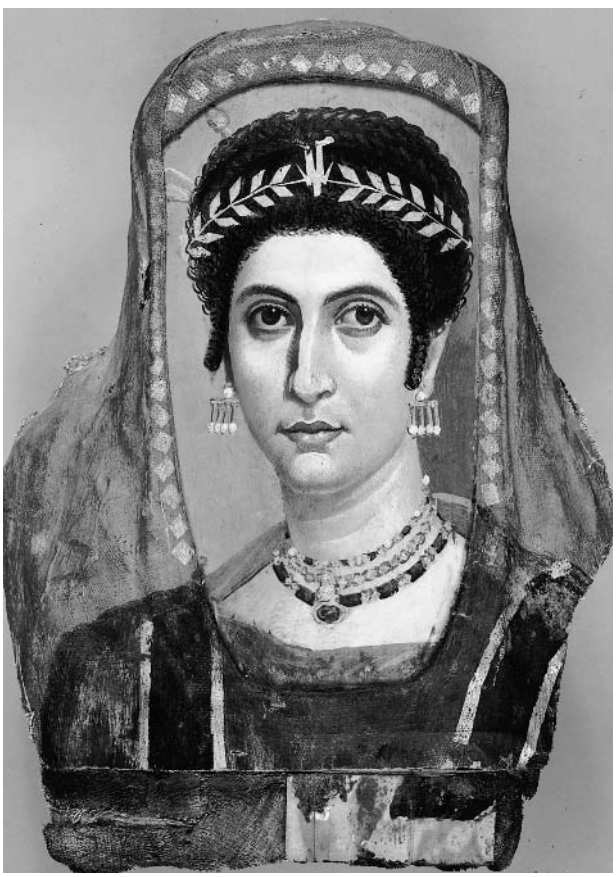

Fig. 2.11. *Portrait of a Woman*, Romano-Egyptian, c. A.D. 100–125. Encaustic and gilt on wood panel wrapped in linen, 55 × 35 cm. The J. Paul Getty Museum.
The presence of wax as a binder in the paint gives the painting a rich, luminous quality. Wax is also a relatively permanent substance, which accounts for the very good condition of many encaustic paintings from this period.

2.4 ENCAUSTIC

Wax has been used as a binding agent in paint since antiquity, and the most compelling examples of its use to date remain the famous portraits produced at Roman settlements in Egypt during the first and second centuries A.D. (Figure 2.11 *Portrait of a Woman*, J. Paul Getty Museum). The simplest method of wax painting is called encaustic, a term derived from Latin and referring to the use of heat, which is required to liquefy the colors. In modern usage, a bleached white beeswax is combined with pigment and resin (damar is commonly used). The heated, liquefied colors are applied to a rigid support by brush or palette knife. A wide range of textures is possible by varying the consistency of the paint through manipulation of working temperatures, both of the colors and the support material. For some effects, the painter heats the support panel in order to maintain liquidity in the paint for extended periods of time. Heat is also applied after application from above the surface to "burn in" the layers of color, ensuring adhe-

sion between layers. Encaustic paintings have a unique lustrous, rich, somewhat translucent surface.

Some of the attributes of wax have been incorporated into other media as well, through the admixture of wax as a binder or extender, or as a final coating. Beeswax is soluble in turpentine and compatible with the binders used in oil paint. To some extent, the admirable qualities of wax can be utilized when combined with oil paint without the complexities inherent in traditional encaustic technique. Heat is not required in the process, and the resulting paint film is much more flexible, making it suitable for application on flexible supports.

2.5 Oil

Oil paint, long considered the most versatile painting medium, contains a binder of oil. Typically linseed oil is used, although oils processed from other plants including poppy seed and walnut oil have also been used. The binder is diluted with spirits of gum turpentine, derived from several species of pine tree. As in the case with water-soluble paint media, the diluent evaporates as the paint dries. Many different materials, including marble dust, waxes, and thickened (polymerized) oils may be added to paint to produce a diverse range of textures and handling characteristics. Additives may also be used either to accelerate or retard drying (various oils and resins), to alter the transparency of the paint, as well as to affect its reflective properties (matte or gloss effects).

The oil is relatively slow drying (usually taking at least a day to dry to the touch, and sometimes years to dry completely), which can be seen as an advantage to the painter. Color mixing as well as the development of a range of textures across the painting surface can be produced by mixing one color into another before the paint dries (known as working "wet into wet"). One can detect in Color Plate 8a a very thickly applied paint surface. The cross section of paint from the same painting, as shown in Color Plate 8b, reinforces our impression that the colors were mixed wet into wet.

By applying layers of uniform or different consistencies over one another, effects can be created unattainable by any other medium. Painting in layers has been for centuries an effective way of mixing colors. An opaque color may be overlaid with a transparent color, producing a third distinct color. The transparency of the overlay colors is obtained by extending the paint with quantities of variously formulated oils and/or resins.

The film that results is very durable, water resistant, and much more flexible than many of the tempera-like paints. Oil paint can be applied both to rigid supports and to flexible supports like canvas or paper. Many painters of the fifteenth and sixteenth centuries who had adopted the oil

medium for its handling and optical qualities recognized as well the paint's ability to retain enough flexibility in a dry state to be relatively unaffected by the expansion and contraction of a stretched canvas. The development of the use of canvas as a painting support has allowed artists to create large-scale, easily movable paintings.

Traditionally, the procedures used in making an oil painting follow those common to fresco and tempera painting. Preparatory drawings and color studies are made, and once the image is resolved, it is transferred to the prepared support. A drawing of the image may be overlaid by an underpainting followed by opaque and transparent layers of paint. Although this remains the most meaningful and productive approach to many painters, other means are utilized by painters whose imagery must evolve as the painting is made. Preliminary drawings, underdrawings, and underpainting may not be necessary if a more direct approach is required. The careful building of the painting from one layer to another may also be reversed. The wet paint film is often wiped away, scraped, or sanded (when dry) and repainted—many times, in some cases—before the artist is satisfied with the result.

2.6 ACRYLIC

Rivaling oil paint in versatility is a modern paint formulated from a synthetic polymer generally referred to as acrylic polymer emulsion. It has been in use since the 1930s. Widespread use followed commercial manufacture of acrylic paints in the early 1950s. From the beginning of its use, artists have been attracted by its ability to dry quickly (often within minutes) and the tough, flexible film it produces. Because acrylic paint uses water as a diluent, the toxic fumes commonly associated with solvents used with oil paint are eliminated from the painter's studio. The use of water also simplifies thinning of the paint and cleanup of brushes and other equipment.

One of the most compelling qualities of acrylic paint is its uncanny resemblance (by means of manipulating the formulation of paint, diluent, and various additives) to the characteristics of a broad range of traditional paint media. It is sometimes difficult, at first glance, to distinguish oil paint from acrylic, or watercolor, tempera, and casein from acrylic. It can be thinned and used in washes on uncoated paper, or thickened and applied to gessoed canvas or panels. Additives can provide a matte or glossy surface as well as unlimited varieties of textures. The paint film is tough, flexible, and resistant to moisture. Acrylic also has unique qualities that artists have used to great advantage. It can be used as a stain on raw, unprepared canvas or when formulated to a particular viscosity, applied in very uniform layers producing surfaces that show

an absence of texture as shown by the painting *Superimposed Supremos* by David Diao (Color Plate 9).

For the mural painter, acrylic paints eliminate the complexities of building up the multilayered masonry support associated with fresco, being more compatible with modern building materials and methods. Revisions can be carried out directly and immediately without altering the surface of the wall. Images can also (on all supports) be developed by overpainting many layers. The painter need only wait until each layer is dry to the touch—a matter of minutes in most cases.

The acrylic polymer emulsion used as a binder is not quite as transparent as some other painting media and as a result produces a slightly less luminous film than that of oil paint, for example. Another disadvantage of acrylic paints (again the result of characteristics of the polymer emulsion) is that the binder cannot hold as high concentrations of pigment as other binders. The result is a slight reduction in tinting strength, or the power of a color to influence other colors mixed with it.

Binding media determine to a great extent a paint's handling, drying, textural, and optical characteristics. The analysis and identification of binding media is an essential part of the overall examination of paintings in the laboratory, and therefore we have devoted the following chapter to their description.

ORGANIC BINDERS 3

Contributed by R. NEWMAN, Museum of Fine Arts, Boston

3.0 INTRODUCTION

Paints almost always consist of pigments, which provide the color, and an adhesive material that binds the pigment particles together and joins them to the substrate to which they are applied. Rarely, one material could serve as both pigment and binder. For example, Paleolithic cave paintings (Figure 3.1) at least in some cases were probably done with clay-containing earth pigments; the clay component, when moistened, would have given the earth pigments enough stickiness to adhere to the cave walls. But in most instances, even in the earliest times, the adhesive or binder was a separate material that had to be mixed with the pigments. Animal fat has been identified as a binder in other Paleolithic cave paintings.

Traditional binding materials are all natural substances produced by living things (plants or animals). Some require no processing, while others have to be extracted from their source by some means. In modern times, naturally occurring materials have been supplemented by compounds synthesized in the laboratory, such as the resins used to bind modern acrylic paints and latex house paints. In this chapter only the natural organic binders will be discussed; Chapter 2 discusses modern acrylic paints.

One method of classification of natural binders is by the types of organic compounds of which they consist, as shown in Table 3.1. Another way is to group them by their solubility in water, as in Table 3.2. Paints that contain water-soluble binders can be diluted with water. Some paints that contain water-soluble binders remain soluble in wa-

Fig. 3.1. Black bison of the "Salon Noir" in the Niaux cave.
Upper Magdalenian period (10,500 B.C.) and have been found in a number of caves in France and Spain. The people who did this painting used a limited range of pigments, probably for the most part, locally available natural earths. At least in some cases, fatty material (perhaps animal fat) was mixed with the colors to serve as a binder.

ter after they dry (such as modern tube watercolor paints, which contain gums). Others are quite insoluble after they dry (for example, egg yolk). The non-water-soluble binders are substances that cannot be put into solution in water, although many can be dissolved in organic solvents such as turpentine or mineral spirits. It is possible to mix various binders together, something that has often been done. Even some water-soluble binders can be mixed with water-insoluble ones to produce emulsions that have attractive handling properties or optical qualities that appeal to artists.

The solubility, application, and handling properties of the different binders is ultimately related to their general chemical composition, and thus the scheme of Table 3.1 will be used to group the binders.

TABLE 3.1

Classification of Natural Binders by Composition

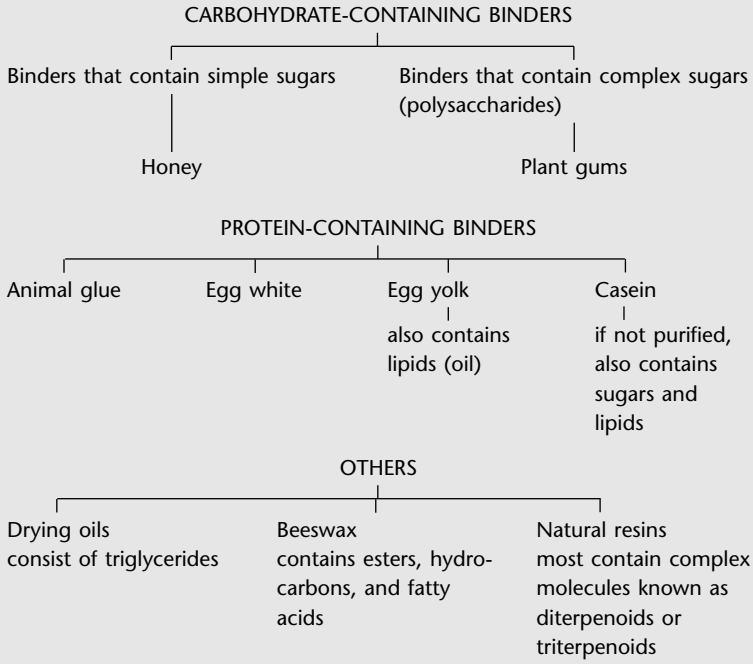

TABLE 3.2

Classification of Natural Binders by Solubility

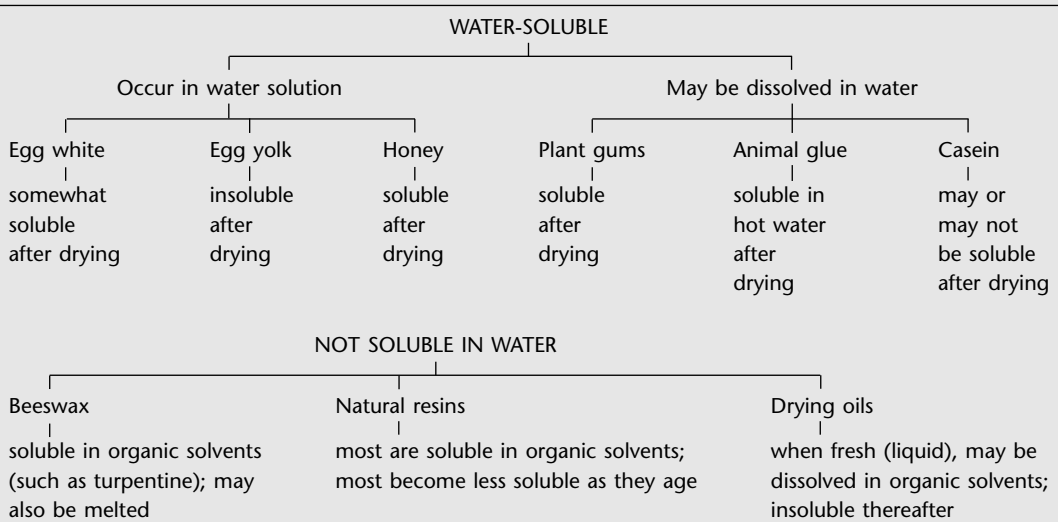

3.1 Carbohydrate-Containing Binders

Carbohydrates are compounds that contain carbon, hydrogen, and oxygen. The basic building blocks of carbohydrates are simple sugars, or (in the nomenclature of organic chemistry) monosaccharides. Some simple sugars contain five carbon atoms, others six. The six-carbon simple sugar known as glucose is probably the most abundant organic compound on the earth. Another common simple sugar is fructose, which is found in honey and many fruit juices. Simple sugars can be bonded together to form larger molecules. Disaccharides are carbohydrates that consist of two simple sugars bonded together (for the sake of convenience, we can call these individual simple sugar building blocks "units"). The most ubiquitous example in everyday life is table sugar (sucrose), a carbohydrate found in many plants. Each molecule of sucrose consists of one glucose unit and one fructose unit bonded together.

Many simple sugar units can be bonded together to form very large molecules, known as polysaccharides. Starch, found in grains such as wheat and corn, is a polysaccharide consisting of many glucose units bonded together. Like all natural polysaccharides, starch has no fixed chemical composition, but each "molecule" of starch appears to consist of from about one thousand to several thousand glucose units bonded together. Another common polysaccharide is cellulose, the principal structural material of plants. Like starch, cellulose consists of many glucose units bonded together, about 1,500 or more per molecule of cellulose.

3.1.1 Honey: Honey, while not a widely utilized binder, has probably found use in paintings at many times in the past. It may have been used in ancient Egypt; nearly 3,000 years later it was described as one of the binders in use by the painters of medieval European illuminated manuscripts. Also mentioned in association with manuscript illuminations were plant or fruit juices, which owed their stickiness to simple sugars or disaccharides. Like modern table sugar, honey and the sugars of fruit or plant juices can be easily dissolved in water. Once the sticky sugar solution dries, it can be readily redissolved in water. It seems likely that binders containing simple sugars would not have been used on artifacts that were intended to be subjected to the elements, as the paint layers they produce are very sensitive to moisture and are quite brittle.

3.1.2 Plant Gums: Plant gums are another example of natural polysaccharides. These are exudates from trees of many types. Although varying considerably in composition from one type of tree to another, they consist of very large molecules, each probably consisting on average of several thousand simple sugar units bonded together. In addition to simple sugars, gums usually contain sugar acids.

Some plant gums are soluble in cold water, some in hot water, while some are partly soluble in water and some are completely insoluble. Those that have been used as paint binders can be put into solution in water. The behaviors of starch, cellulose, and plant gums when placed in water are quite variable, and yet all of these materials are polysaccharides. The extreme variability, from the total insolubility of cellulose to the complete solubility of some gums, is related to the structure of the molecules. Simple sugars can be bonded together in several different ways, from long, chainlike molecules (as in cellulose) to highly branched, approximately spherical molecules such as the soluble plant gums. The polysaccharides with branched structures can be dissolved in water.

A great many types of plant gums were probably utilized in different times and places as binders for paints. Probably the most common is the material now known as gum arabic, which at this time can be found as an additive in many foods and is the binder of many modern commercial artist's watercolor paints (Figure 3.2). Gum arabic comes

Fig. 3.2. Winslow Homer. *The Adirondack Guide,* 1894.
Watercolor over graphite on paper. Paintings like this one were carried out with commercial watercolor paints, which were sold in pans or tubes. The paints were bound with natural plant gums, most commonly gum arabic. In this type of watercolor painting, the paints are usually thinned with water and applied in washes. Bequest of Mrs. Alma H. Wadleigh. (*Courtesy,* Museum of Fine Arts, Boston)

from a particular variety of the *acacia*, a shrublike tree of which there are hundreds of individual varieties that grow in many parts of the world. Acacia was one of the few trees that grew in ancient Egypt, and it is not a surprise that *acacia* gums were used as paint medium at that period. Gum arabic served as a major binder in European medieval manuscript illuminations and in traditional Indian manuscript paintings (Figure 3.3). Adding a little honey or sugar to a gum binder was recommended, probably for flexibility of the dried paint. Mixtures of more than one gum may have been used.

Among other gums that were used are the gums of fruit trees, such as peach, apricot, plum, cherry, and almond. All of these trees belong to the genus *Prunus*. Among examples of their applications are Central Asian cave paintings.

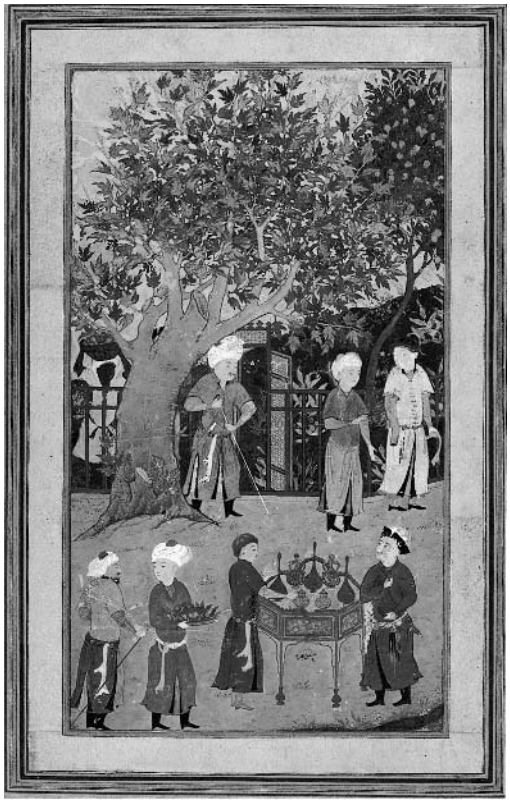

Fig. 3.3. Ascribed to Bihzad. *Garden Scene,* late 15th century; Persia; Timuria period.
Ink and colors on paper. Although the binder used in this painting is not known, it could well have been a natural plant gum, which documentary sources indicate was a common binder for such paintings. Most of the paint here was applied in fairly thick opaque layers, although thinner wash-like layers were used in places. Francis Bartlett Donation of 1912 and Picture Fund. (*Courtesy,* Museum of Fine Arts, Boston)

3.2 Protein-Containing Materials

Proteins are compounds that consist mainly of carbon, oxygen, hydrogen, and nitrogen; sulfur is also found in some. Just as simple sugars are the building blocks (or units) of carbohydrates, the basic building blocks of proteins are amino acids. About two dozen different naturally occurring amino acids are known. Various types, proportions, and numbers of amino acid units can be combined to form widely varying larger molecules. Individual amino acids are soluble in water, as are some of the very large proteins formed by the linking of hundreds or even thousands of amino acid units. As with polysaccharides, however, not all proteins are soluble; as with polysaccharides, the differences in solubility are largely due to the structure of the protein, or the manner in which the amino acids have been bonded together.

Individual amino acids are present in the blood of animals and in many other natural materials. Among examples of important natural proteins are keratin (found in skin, hair, wool, horn, and feathers), hemo-

globin, antibodies, and silk. Blood has probably occasionally been used as binder; however, the most important protein-containing binders are those discussed below.

3.2.1 Animal Glue: Today "glue" is a word loosely used to refer to many adhesive materials, natural and synthetic. In the context of traditional binding materials, glue refers specifically to a substance derived from boiling skins or connective tissues of certain mammals or parts of some fish. Whatever the source, the adhesive material is the protein collagen, which is a major structural material in mammals and fish. It is the major material found in the inner layers of the skin of mammals.

This protein has the unusual property of being soluble in hot water, but gelling as the solution cools to room temperature. The purified form of collagen is the familiar gelatin of "Jello" and other similar desserts and many food products. The gelled protein will go back into solution when reheated. Because of this property, as a paint medium the glue needs to be used hot. It was discovered long ago that this bothersome property can be circumvented by allowing the solution to sit for a few days and deteriorate. A medieval text on manuscript illumination notes this, and states, "It may smell bad, but will be very good."

Fig. 3.4. Tibet (Raktayamari). *Tanka,* 18th century.
This painting was carried out with thin opaque layers of paint bound with animal glue. Although the animal used to make the glue is not known, it could well have been the yak. Gift of John Goelet. (*Courtesy,* Museum of Fine Arts, Boston)

If water is allowed to evaporate out of the gelled solution, solid glue is left behind. This solid material can be put back into solution by soaking in water and heating.

Of all binding media, glue is almost certainly the one most widely utilized around the world. For example, it was a common

binder in paints in ancient Egypt. Glues have been important binders in many cultures. Buffalo-skin glue was used in manuscript paintings in ancient India, yak-skin glue in Tibet (Figure 3.4); and glue was probably the major binding medium of traditional Japanese and Chinese painting.

In medieval Europe, glue (also called size) was widely used in manuscript illuminations, and there is evidence that it was the binder in some medieval wall paintings, particularly in northern Europe. While painting on fabric was not as common as panel painting during the medieval period, there was a tradition of fabric painting in northern Europe. Such paintings seem to have usually been executed in an almost watercolor-like technique, using thin layers of glue-bound paint.

Fig. 3.5. Barnaba da Modena. *Virgin and Child,* Italian (Modenese), active 1361–83. Tempera on panel.
This painting was carried out with paints bound with diluted egg yolk, or egg tempera. Some Italian artists of around this time had also begun to experiment with oil paints, and some egg tempera paintings contain passages actually carried out with oils. Gift of Mrs. W. Scott Fitz. (*Courtesy,* Museum of Fine Arts, Boston)

3.2.2 Egg White and Egg Yolk: Both the white and yolk of eggs can be used as binders; probably they were most often used separately, but they can be mixed together.

Dried egg white is about 90% protein by weight. Over half of the protein is a type known as ovalbumin. A small amount of another protein is what gives egg white its stringy property as it comes from the egg. Whipping breaks apart the stringy protein, and the solution below the froth produced by the whipping contains enough of the protein to be useful as a binder. Egg white has probably not been widely utilized as a binder. The best known examples, described by surviving documents, are medieval European manuscript illuminations. The term *glair* is often used to describe egg white in this context. After egg white dries, it continues to be soluble for the most part in cold water.

Egg yolk is very different in composition and properties from egg white. As it comes from the egg, yolk consists of minute spherical droplets

Fig. 3.6. *Bent-corner chief's chest,* ca. 1850. Coastal British Columbia, Canada. Yellow cedar, red cedar, red and black pigments (Chine vermilion and red ochre). H: 25 in., L: 40 in., and D: 25 in.
The low-relief carved designs on this box were painted with pigments bound with salmon eggs, which were usually chewed before being mixed with the colors. Gift of a Friend of American Decorative Arts and Sculpture. (*Courtesy,* Museum of Fine Arts, Boston)

of oil suspended in a water medium. Dried yolk consists of about one-third protein and two-thirds other types of compounds. These other compounds are predominantly oil, which is similar chemically to the oils used for painting that are discussed below.

Salad dressings that consist of oil and vinegar need to be continually shaken to disperse droplets of the oil in the water phase (vinegar) to form an emulsion. If let sit, the water phase and oil separate. Egg yolk is also a mixture of an oily phase and a water phase. Egg yolk is a stable emulsion of these two insoluble classes of material, naturally stabilized by a compound called lecithin, which also stabilizes such foods as mayonnaise.

As a medium, egg yolk is usually diluted with some water and mixed with pigments. After it dries, it can no longer be dissolved in water, a property that distinguishes it from all of the other, water-soluble, media. Many proteins that are found in solution in water in nature, such as those in egg yolk, undergo transformations as they are heated or dried.

These transformations (called denaturation) mean that once heated or dried, these proteins can no longer be put back into solution in water.

While egg yolk could have been utilized by many cultures, the best-known examples of its use are in medieval and Renaissance Europe. Cennino Cennini, in his well-known book on painting, described the practice of painting with egg yolk paints, which were widely used in Italy (Figure 3.5). This type of painting is usually referred to as egg tempera, or simply tempera. Paints based on a salmon-egg medium were used by various groups of Native Americans: An example is shown in Figure 3.6.

3.2.3 Casein: Casein is the name for a mixture of proteins that can be separated from milk. Milk solids consist of about one-fourth protein. The other materials in milk solids are milk sugar and oil. Preparation of curds

Fig. 3.7. William Morris Hunt. *Gloucester Harbor,* about 1877. U.S., 1824–1879. Oil on canvas.
Analysis shows that this painting was carried out with casein-bound paint mixed with oil. Depending on how it is prepared, a casein binder may be nearly pure protein, or may contain some sugars or oils from the original milk source in addition to the milk proteins (casein). Milk sugar was found in this painting. Gift of H. Nelson Slater, Mrs. Esther Slater Kerrigan, and Mrs. Ray Slater Murphy, in memory of their mother, Mabel Hunt Slater. (*Courtesy,* Museum of Fine Arts, Boston)

and thorough washing of them can largely separate the protein from the other components. Mixing curds, or cheese, with lime yields a very strong adhesive that is virtually insoluble once it sets. Casein glues or adhesives have been used since ancient times.

Casein has also been used as a paint medium, probably since ancient times, possibly in many parts of the world, although the early history of its use for this purpose is not very well known. Paints made from milk were popular house and decorative paints in early America, and commercially manufactured casein paints became available about the beginning of the twentieth century.

Two large canvas paintings by William Morris Hunt in the Museum of Fine Arts, Boston, were painted with casein-bound paints (Figure 3.7).

3.3 OILS

There is a large class of diverse natural compounds known as lipids. One major subgroup of lipids are fats and oils. These are the main constituents of the storage fat cells in plants and animals. Fats are materials that are solid at room temperature, while oils are liquid, but both are quite similar in chemical composition. Examples are coconut butter, bacon grease, and cooking oils such as corn, safflower, and olive. The oil found in egg yolk and unwashed milk solids is of the same general type. Most of these oils are "nondrying" or "semidrying" in nature: If spread in a thin film and exposed to air, they remain liquid or become somewhat solid. A few other types of oils are "drying" in nature; they can form solid films when exposed to air. The major drying oils are linseed, walnut, and poppy-seed.

That some oils are capable of drying was known as early as classical antiquity, but their application for decorative and artistic purposes seems not to have occurred until much later. The earliest documentary references to such uses for oils are in recipes for varnishes or protective coatings for wood, stone, etc. These early recipes involve mixtures of oil and natural resins. It would appear that drying oils were first utilized in this fashion. Later, in medieval times, they were mixed with colors for decorative painting, and eventually came to be used by panel painters.

The earliest known European oil paintings are a series of late thirteenth-century Norwegian altar frontals. There are some indications that these actually may have been painted with a mixture of drying oil and egg yolk. Analytical work suggests that linseed oil was the common oil in these early oil paintings, as well as in the paintings of the fifteenth-century Netherlandish painters, which are the earliest accomplished European paintings essentially done with drying oils. An example is *St. Luke Drawing the Virgin,* by Rogier van der Weyden, a painting done mainly with a linseed oil medium (Figure 3.8).

Fig. 3.8. Rogier van der Weyden. *Saint Luke Drawing the Virgin and Child,* about 1435. Flemish, 1400–1464. Oil on panel.
Like most other early Netherlandish panel paintings, this painting was carried out mainly with oil paints. As here, linseed oil was apparently the most commonly-used oil. Some early Netherlandish paintings contain passages carried out with protein-containing paint, or protein-oil mixtures. This seems to be the case with some of the underpainting on this panel. Glazes used by early Netherlandish painters sometimes were made from drying oils mixed with a little natural resin. Gift of Mr. and Mrs. Henry Lee Higginson. (*Courtesy,* Museum of Fine Arts, Boston)

Linseed and walnut oils seem to have been the most common oils; the former was pressed from the seeds of the flax plant, a plant that also was the source of linen, while the latter was pressed from the seeds of walnut trees. Later, mainly during the later nineteenth century, poppy seed oil was popular.

All of the drying oils and nondrying oils consist principally of compounds called triglycerides, formed from glycerol (a type of alcohol) and fatty acids. There are many types of fatty acids, and the types and relative proportions found in different oils vary, as even do the amounts between different samples of a particular type of oil that come from different geographic sources.

The drying of paints with glue, gum, egg white, or egg yolk binders mainly involves evaporation of the water in which they are dissolved or dispersed. Drying oils contain no solvent; they dry by a complex series of chemical reactions involving atmospheric oxygen.

Drying oils do not all dry at the same rate. Painters would naturally seek faster drying oils. But the same reactions that lead to drying also result in yellowing as the oil film ages. And unfortunately, faster drying oils also yellow more than do slower drying oils. The yellowing of the oil medium would have a quite noticeable effect on white passages (turning them a dirty white) and blue passages (turning them greenish); effects of yellowing would be much less obvious in passages of other colors, such as green, yellow, or red. Apparently, quite early in the history of oil painting artists were aware of this, and more than one type of oil may be found in a given painting. The slower drying walnut typically is found in blue or white paints. The faster drying linseed is more likely to be found in other passages, where its greater tendency to yellow would not present much of a problem.

It seems certain that "pure" oil painting was stimulated in Italy by the example of Flemish oil paintings. One of the Italian artists who first experimented with oils was Cosimo Tura. His *Allegorical Figure,* in the National Gallery, in London, dated to about 1460, is a unique document. It appears to have been begun in egg tempera, following the traditional Italian practice. Perhaps a year or two later Tura seems to have entirely repainted it in oil. The layer structures of the oil painting are quite similar to those found in early Flemish oil paintings. The painting may have been done in Ferrara, where some works by Roger van der Weyden are known to have been located. Tura used walnut oil in white passages, linseed in passages of other colors.

3.4 WAXES

Waxes are a class of materials that can be of animal, vegetable, or mineral origin. For artistic purposes, the most important one historically has been beeswax. Chemically, beeswax contains some free fatty acids, hydro-

carbons (compounds consisting only of carbon and hydrogen), and esters formed from alcohols and fatty acids. Beeswax can be dissolved in organic solvents such as turpentine, and it can also be easily melted. While wax was known in ancient Egypt, and may have been used as a binding medium, the major use of this medium in antiquity occurred in Greek and Roman times. While no examples remain, there are descriptions pointing to the importance of the wax medium, which is usually known as "encaustic," derived from the Latin for "burned in." Since it is doubtful that suitable solvents for wax were known in ancient times, wax paintings were probably done by melting the wax/pigment mixtures and applying them with a heated metal tool or brushes to panels, which were also probably heated.

The earliest surviving wax paintings are a large group of portraits done in the Fayum region of Egypt, around the second century B.C. to the second century A.D. These paintings probably reflect Greek and Roman practice, not a native Egyptian tradition (Figure 3.9).

Other waxes, some quite different in composition from beeswax, have been used in sculptures and for other purposes, but beeswax has been the only wax of importance in the history of painting.

In the nineteenth century there was renewed interest in painting techniques of antiquity. That wax had been a common binder in paintings of classical times was known, and a number of artists began to experiment with the material. Some artists

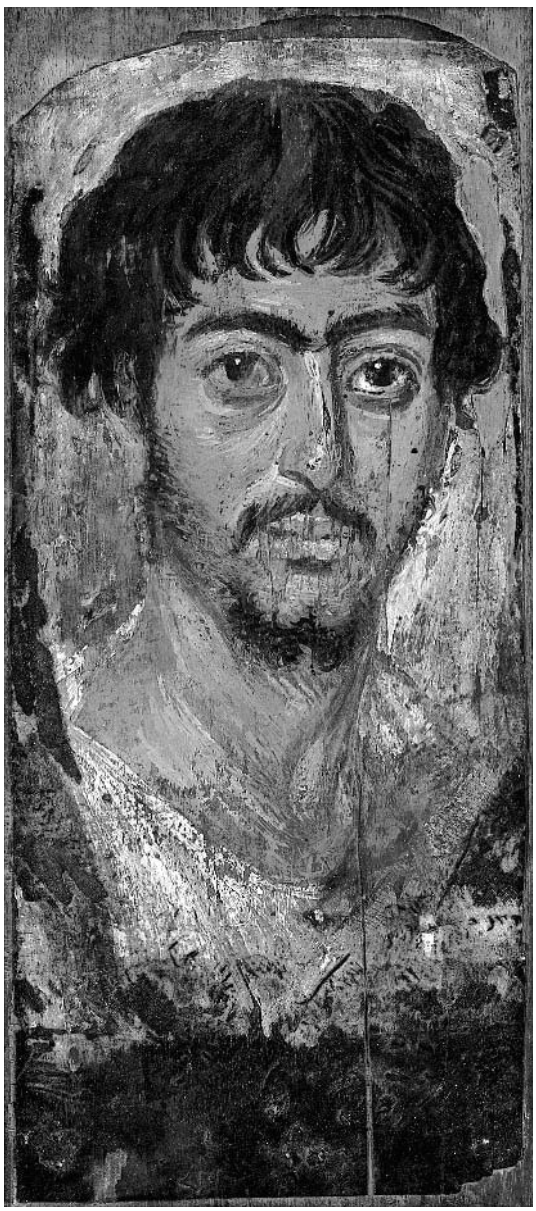

Fig. 3.9. *Portrait of a Man,* Graeco-Roman (the Fayum). Painted wood.
Many paintings carried out during the Roman period in Egypt were done with the "encaustic" or wax medium. The wax used was beeswax, which may have been heated in an alkaline solution, which would have chemically broken down some of the compounds found in the pure natural material. In order to be used, the wax colors had to be melted. They could then be quickly applied with a brush, and reworked locally on the panel with heated metal tools. Gift of Egypt Exploration Fund. (*Courtesy,* Museum of Fine Arts, Boston)

Fig. 3.10. Arthur Garfield Dove. *Square on the Pond,* 1942. U.S., 1880–1946. Wax-based paint on canvas.
Many paintings from the later part of this American artist's career, such as this one, were done with a mixed medium that contained wax as well as drying oil, and possibly smaller amounts of other binders (such as resins and proteins). To make his medium, Dove heated beeswax in an alkaline solution until it formed a creamy emulsion, which was then mixed with some oil. Gift of the William H. and Saundra B. Lane and Henry H. and Zoe Oliver Sherman Fund, M. Theresa B. Hopkins Fund, Seth K. Sweetser Fund, Robert Jordan Fund and Museum Purchase. (*Courtesy,* Museum of Fine Arts, Boston)

used unusual combinations of materials, such as oils, waxes, and resins. One example was Arthur Dove, an early twentieth-century American abstract painter, who experimented extensively with wax (Figure 3.10).

3.5 Natural Resins

Natural resins are sticky, water-insoluble substances that exude from a wide variety of trees. Most consist of compounds known as terpenoids. The resin that exudes from some types of trees contains copious amounts

of natural solvents. One example is pine resin, from which turpentine, a natural solvent is distilled. Resins were known in ancient Egypt, and quite probably earlier. In Egyptian times, they were used in varnishes and figured in mummification procedures, among other uses.

A bewildering variety of resins are known. In Egyptian times, perhaps pine resin and Chios turpentine, a type of resin that came from trees growing in northern Africa and on the island of Chios, were the best known. During the early Middle Ages, treatises mention many other varieties, including sandarac, Venice turpentine (larch resin), and amber. Resins that became popular in furniture varnishes and other applications during the nineteenth century included copals (of which there are many varieties), mastic, and damar.

Many of these resins can be dissolved, usually with heating, in oil. They can also be put into solution in organic solvents such as turpentine, although such simple resin solutions were probably not used until the eighteenth or nineteenth century. Some resins are only partially soluble in oil or solvents, but can be made more soluble by first heating them, which partially breaks down their structures. Amber and some copals need to be treated in this fashion in order to be made into varnishes.

Aside from picture varnishes, the major use of resins in oil paintings was in glazes. An oil–resin medium produces a rich, shiny paint layer, well suited to glazes. One popular color in European medieval and later periods is known as copper resinate. It was often made by dissolving a green pigment (verdigris) in a mixture of oil and resin. Pine may have been the major resin used for this purpose.

The Painter's Color and Light

4

4.0 Color, Light, and Space

In the world around us, color appears to be attached to everything we see. It changes as the light changes, but usually within predictable limits, or at least we recognize that a color linked to an object appears a certain way in a certain kind of light. We are conditioned enough by this that we often identify an object by its color. And we are conditioned enough by the change of light to recognize the same object by color even though the condition of light has changed the color of the object.

By sensing space, and locating objects within it, we can move about within that space in a fairly comfortable way and understand the relationships between the things that occupy the space. The visual perception of space is dependent on light, or on how a space or object is illuminated. The direction from which the light travels toward the object, and at what intensity, can make a dramatic difference in how we place that object in our field of vision. The effect of light on objects and spaces also tells us a great deal about the source of light. The relative density of shadows and the intensity of illuminated surfaces can indicate a sunlit morning or a night under artificial light (Figure 4.1a,b).

In the world of paintings we are faced with circumstances much different from our view of the world around us. Images in paintings are revealed to us on two dimensional surfaces that in many cases echo the images that appear before us as we move about in our familiar environments. We see images of people and objects occupying

(a) (b)

Fig. 4.1a,b. Photographs of a tree under different lighting conditions: (a) on a sunlit morning and (b) at night under artificial illumination. The arrangement of light and dark areas is, for the most part, reversed in these two photographs and indicates to us lighting conditions typical of different times of the day.

spaces as *we* occupy spaces. However, we must keep in mind that the painter has made this experience for us without many of the conditions that perceptually reveal our environment to us. There is no *real* spatial depth in the painting. There is no source of light within a painting. There is no movement or change of light in a painting. All of these conditions are implied, and if we are to be led to believe that they exist within the painting, they must be supplied by the painter.

We have little difficulty believing much of what we see in the world aided by our perception of space, movement, light, and color. Even at times when we question what we see, we test the disbelief against other experiences. Painters have learned to utilize events in nature to help extend this atmosphere of belief into their paintings. The dove above the Virgin's head in Gerard David's *Annunciation* (Color Plate 9), presented in such an extraordinary way, and the halo behind the Virgin's head exist within the context of the pictorial space of the painting and are acceptable to us within that context. The dove occupies space just as the book, *in the painting,* occupies space, and both appear to be illuminated by the same light source. Light is common to paintings and nature, and is our conduit into the world of the painting. It is not surprising, then, to see that a study of the dynamics of light and color in nature is the key to understanding events in a painting.

4.1 COLOR CHARACTERISTICS

Homage to the Square—Saturated, a painting by Josef Albers (Color Plate 10), is composed of overlapping red squares. The squares differ from each other, and these differences can be accurately described by noting three characteristics: *hue, value,* and *saturation*. Hue identifies the color (red, in this case) as distinct from other hues (yellow, green, or violet, for example). Value is the lightness or darkness of the hue as it relates to a scale of white to black (Figure 4.2). We can distinguish one square from another, in part, by their differences in value; one red appears lighter or darker than the others (Color Plate 11). Saturation (sometimes referred to as intensity or chroma) is the purity of the hue. A fully saturated hue is one that is not diluted by the admixture of white. A color of reduced saturation is said to be *neutralized* to some degree, with a fully neutralized color resembling the color gray. These three characteristics are utilized by scientists interested in a precise identification of colors as well as by painters assessing color relationships or identifying an observed color.

Painters are also interested in the designation *color temperature,* a property not easily defined. The temperature of a color is purely perceptual; it cannot be quantified in the same ways as hue, value, and saturation. A color may be seen to be warm or warmer (relative to other colors), or cool/cooler. Most people would acknowledge that yellow is warm and blue is cool. Orange and red are also considered warm, and green, purple, and gray are cool. In addition to distinctions between hues, painters make the distinction between warm and cool varieties of the same hue. And for the most part, one can identify warm and cool reds, greens, yellows, etc. Some colors seem to present problems. For example, it is sometimes difficult to get wide agreement on what is a warm blue and what is a cool blue. This determination is largely the result of informed intuition on the part of the painter. There is, however, a rather straightforward way of making this judgment. In many cases, when a cool color is mixed with another cool color, or a warm color with another warm color, the resulting color will be similar in saturation to each of the components. If a cool color and warm color are mixed, the saturation of the resulting color will be reduced to some extent, tending to neutralize it. This is, in fact, one of the many ways painters manipulate

Fig. 4.2. The increments of a gray scale illustrate the concept of relative values arranged in order from white to black.

or modulate a color. One can produce a purple by mixing a red and a blue. By mixing a cool blue and a cool red (ultramarine blue and alizarin crimson, for example) a bright, fully saturated purple will result. By mixing a warm blue (cerulean) and a cool red (alizarin crimson), a grayed purple results.

To describe a single color is fairly straightforward and can be done very accurately, but it is a description of a color isolated from all other colors. Once a color is placed adjacent to another, many variables come into play, and one begins to see why Josef Albers (in his book *The Interaction of Color*) noted that color is "the most relative medium in art." These variables are the "interactions" of colors. The word *interaction* is appropriate in that colors do actively influence one another. Colors assume spatial relationships. A color's apparent position in space relative to another color is dependent upon the interrelationships of saturation, value, and temperature. In most cases, fully saturated, light, and warm colors tend to advance toward the viewer, while neutralized, darker, and cooler colors tend to recede. Depending upon the proximity of a color to areas of different hue, value, intensity, shape, and size, these spatial relationships can be reversed. In some carefully orchestrated situations, areas of color of different hue, value, and saturation may be made to reside in the same position in space. This positioning of colors in space can occur without the colors being attached to recognizable images, as we can see in purely abstract, nonobjective works of art. The visual activity in Piet Mondrian's painting *Composition 1916* (Color Plate 12) is as dependent upon the spatial relationships among the colors as on changes in value, intensity, and size of the shapes. The gray field acts primarily as space, with the more intense yellows, pinks, and blues displaced forward and backward against the black linear elements as the eye moves across the surface.

4.2 AFTERIMAGES

If one's attention is focused on an area of a single color for thirty to sixty seconds and then shifted to a field of white (Figure 4.3), the eye will sense a color other than the first one covering the white field. The second color is *complementary* to the first color. For example, red will produce an afterimage of green, and blue will produce an orange afterimage. The complementary afterimage appears as a luminous transparency. The effect is similar to that obtained by viewing the white surface through a colored filter. Because the color does not reside

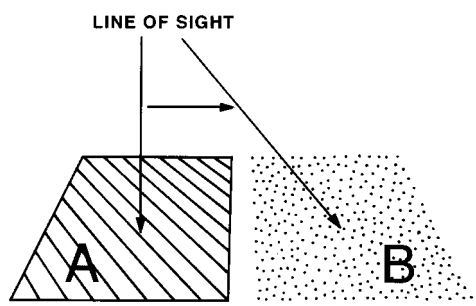

Fig. 4.3A,B. Color **A** is viewed for 30 to 60 seconds. The eye then focuses on a spot some distance away. A different color will be perceived in the same shape as **A.** Color **B** is the complement of **A**.

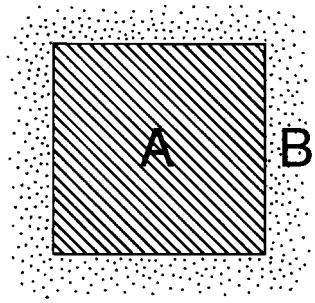

Fig. 4.4A,B. Color **A** is located on a white field. Retinal fatigue produces the color **B** halo surrounding **A**. Color **B** is the complement of **A**.

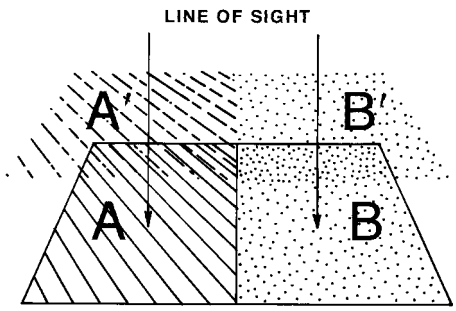

Fig. 4.5A,B. Two areas of color **A** and **B**, a complementary pair, are viewed adjacent to each other. Complementary afterimages **A′** and **B′** are also present due to the effect illustrated in Figure 4.4.

on the white surface, we can assume that it is a sensation generated in the eye (See Section 5.6 *The Eye and Color Sensation*).

The afterimage phenomenon affects many of the choices made by a painter. An optically generated complementary color will not only fill a prescribed white field; it will spill out in all directions from the primary color source (Figure 4.4). If two areas of color, one the complement of the other, are placed adjacent to each other, an optically generated complement of some degree of intensity will overlie each of the areas (Figure 4.5). Think again of the afterimage as a color filter suspended before the eye. Since the overlay will be of the same color as that lying beneath it, and because the afterimage appears as a colored light, we will sense that the field of color has become more luminous and intense. Complementary colors are always more intense when they are in close proximity to one another than when they are isolated or surrounded by other colors. Note how the complementary colors red and green in van Gogh's *La Berceuse* (Color Plate 13) amplify each other to create a brilliant, intense, and massive foreground.

Value relationships are affected in the same complementary way as hue relationships. White will look lighter and black darker if they are placed next to each other. When colors that are not complementary are placed adjacent to one another, the same optical behavior will bring about a different effect. An area of yellow in a field of red will appear more greenish than the same yellow residing in a field of blue-violet. The yellow is being altered by the complement of red, which is green. The blue-violet intensifies the yellow with the overlay of its complement, which is yellow. The manipulation of one color by another through complementary overlay is known as *simultaneous contrast.*

4.3 SIMULTANEOUS CONTRAST

Included in Aristotle's book *On Sense and the Sensible* is a description of the three primary ways of mixing colors. One approach is to mix a quantity of one color of paint with a quantity of another color, producing a

third, distinctive color of paint, ready to be applied to the painting surface. A second is to place a transparency of one color over an area of another color. In most cases, the transparency is accomplished by adding binder or diluent to the paint to disperse the particles of pigment. Light is then allowed to pass through the transparent layer to interact with the area of color beneath. Color signals from both the transparency and the underlying color mix as they are reflected to the eye, producing a third color sensation (see Section 5.5). The third way to mix colors is to intersperse many small areas (dots or small brushstrokes) of two different hues. Viewed from a distance, the small areas of color appear to blend together to form a third color. The mixing in this case is known as *optical mixing*. Signals from each color are transmitted simultaneously to the eye. The amount of optical mixing is dependent on the size of the individual areas of color (the small dots used in commercial color printing cannot be sensed as individual dots without magnification, for example).

Throughout the centuries, artists have benefited from their close association with the scientific community, incorporating for their own purposes developments in optics, chemistry, and physics. In the mid-nineteenth century scientific investigations into the fundamental properties of light and matter had a direct influence on the work of some of the most innovative artists of the period.

In 1839, the French chemist Michel-Eugène Chevreul published a book titled *The Principles of Harmony and Contrast of Colors*. Chevreul worked at the tapestry workshop Les Gobelins in the dyeing department. Here he carried out experiments with various dyes in an attempt to increase or alter the intensity of colors. Tapestries are made by weaving colored yarns together to form images. Masses of color, areas of modulation of color, gradations of value, are all made up of thousands of tiny loops of colored wool (Color Plate 14). They are essentially small single-color dots that, when carefully organized, mix at a distance to create the desired modulation. Because of the relatively small scale of the color dots, our eyes cannot perceive individual color sensations. The separate color signals merge, or *optically mix,* into larger areas of color, shape, and image.

Chevreul realized that optical mixing was not the only dynamic at work when colors were placed adjacent to one other. He found that by utilizing the phenomenon of simultaneous contrast, he could alter the perception of a color by the choice of adjacent colors. He could even increase the perceived saturation of a color. More could be done, in fact, through juxtaposition than through the development of new dye colors. One of the remarkable things about his discoveries was that the effects were predictable.

The Principles of Harmony and Contrast of Colors was directed as much to painters as it was to scientists and dyers of wool. Chevreul gave the advice to painters that they be observant of the effects of various

kinds of light or shade on local color (the inherent color of an object) in the world around them. Although he seems to have been oriented toward a realist view of painting, that is, that the painter should faithfully replicate what is perceived in nature, he does suggest that some liberties be taken at times to accommodate an aesthetic ideal. It was the particular combination of his views on painting and observations on the perception of color that struck a chord with painters of his time.

Chevreul's work suggested to painters that color could be thought of as independent of the objects and elements of nature. One could see that by understanding the dynamics of simultaneous contrast, many of the perceptual functions within a painting that were performed by pictorial description (drawing), could be performed by color, or at least the use of color could reinforce other means of description. The illusion of space, for example, could be created simply by placing one color against another. One color could make an adjacent color appear more intense and therefore advance spatially toward the viewer. Because the principle of simultaneous contrast effects differences in value as well as hue, darks could be made to seem darker, and lights, lighter. These perceptual characteristics have offered the painter a much expanded visual vocabulary with which to construct paintings.

Fig. 4.6. *Judith with the Head of Holophernes,* Artemisia Gentileschi, c. 1625. Oil on canvas, Detroit Institute of Arts.
One of the more conventional ways to suggest luminosity in a painting is to offer clues to the viewer through images of light and their effects on the spaces and objects around them.

Perhaps the most dramatic manifestation of the laws of simultaneous contrast as described by Chevreul can be found in the work of the French painter Georges Seurat (Color Plate 15). Seurat applied dots of color in a nearly uniform distribution over the entire surface of the painting (sometimes even including the frame). Small brushstrokes of color (often fully saturated primary and secondary hues) were applied to the painting in combinations that served a number of functions. The combinations of

separate dots of color mix optically to produce in the eye the sensation of masses or gradations of more complex color. He *mixed* purple, for example, by distributing dots of red and blue evenly over the surface, sometimes layering the colors as well (Color Plate 16). Fully saturated as well as more complex and modulated colors were combined to produce in the eye a very full range of sensory response, from intense fields of dense, uniform color, to grayed, neutralized fields of color. The resulting color fields can be as simple as a fully saturated purple made of red and blue components, or as complex as a purplish-gray containing blue, pink, sienna, green, and yellow (Color Plate 17). Warm and cool colors could be combined in this way along with complementary colors to produce neutral or grayed tones. In the case of grayed optically mixed color, there is an undertone of intensity due to the presence of relatively saturated color. We see and understand the area as neutral, but we sense the intensity within it.

Another function of Seurat's technique was to produce the sensation of luminosity. Afterimages generated by the small dots of color produce the sensation of many small colored light sources distributed across the painting surface. The more traditional (and often as effective) approach is to suggest luminosity through depiction: The viewer senses the light conceptually as the mind accepts the image as a real experience as in Artemisia Gentileschi's *Judith with the Head of Holophernes* (Figure 4.6). A light source is given within the pictorial space of the painting, and its effect is clearly shown on the surfaces adjacent to it.

Not all painters place so much importance on the implication or representation of light in their work. However, the light that surrounds the work is of critical concern to all painters. It is the medium by which the color, image, message (in fact, nearly all that the painting has to offer) is transmitted to the eye of the viewer.

Color and Light 5

5.0 Introduction

Painters rejoice in colors, and their palettes reflect their exuberance. Robert Delaunay's use of color in his painting *Homage à Blériot* (Color Plate 18) echoes the spectral colors found in nature, i.e., the rainbow. It shows light interacting with objects that appear outlined in a spectral halo. In order to fully understand the work of the painter, the viewer must sense the color within it. Here we ask how color is sensed by the viewer. To answer the question we need to specify how color is described and how color information is received by the eye. The starting point for an understanding of color is a description of light.

We see a red object as red when light strikes and reflects from that object and then triggers a response in the photoreceptors in the eye. The response from the eye is sent to the brain, where the signal is processed and identified as "red."

What we sense as the normal ambient or "white" light that surrounds us carries the signals that contain color information. When we view a red object, the light reflected from the object carries the signal that triggers the "red" response in the eye. All color sensation is initiated by strengths of the signals contained in the light incident on the eye.

In conditions of low light intensity (at night or in interior unlighted spaces) very little color response is noted. Objects appear in various shades of gray. That is, an object that appears red in daylight now appears gray. This effect can be experienced in an enclosed room with a variable intensity light source illuminating a red object. As the light

intensity is decreased, a vividly colored red object is perceived as losing its "redness." The object has not changed, only the light intensity. The "red" object is now "gray" because the light intensity is not high enough to trigger a "red" response in the eye.

5.1 Light: Photons and Waves

The starting point for a description of color is a description of light. For that, we start with a beam of white light (Color Plate 19). When the beam of white light passes through a prism, the white light is split into many colors. As will be decribed later in detail, the beam of white light contains spectral color signals from red through violet. The prism separates the signals into the individual components.

Isaac Newton demonstrated in 1672 that light could be split into many colors by a prism, and he used this experimental concept to analyze light. The colors produced by light passing through a prism are arranged in a precise array, or spectrum, from red through orange, yellow, green, blue, indigo, and into violet. The order of colors is constant, and each color has a unique signature identifying its location in the spectrum. The signature of color is the wavelength of light.

Somewhat less than one hundred years after Newton's discoveries, James Clerk Maxwell showed that light is a form of electromagnetic radiation. This radiation includes radio waves, visible light, and x-rays. Figure 5.1 shows electromagnetic radiation as a spectrum of radiation extending beyond the visible spectrum to include at one end radio waves and at the other end gamma rays. The visible light region occupies a very small portion of the electromagnetic spectrum. The light emitted by the

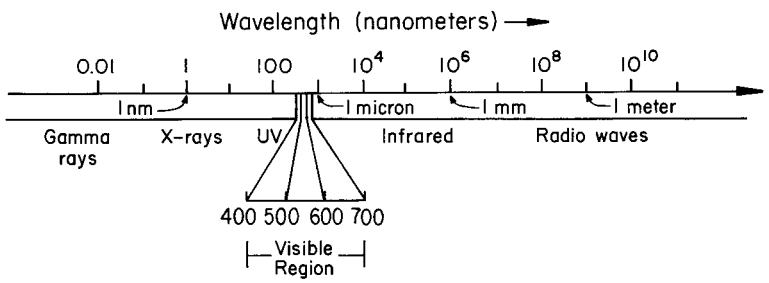

Fig. 5.1. The electromagnetic spectrum, which encompasses the visible region of light, extends from gamma rays with wavelengths of one hundredth of a nanometer to radio waves with wavelengths of one meter or greater.

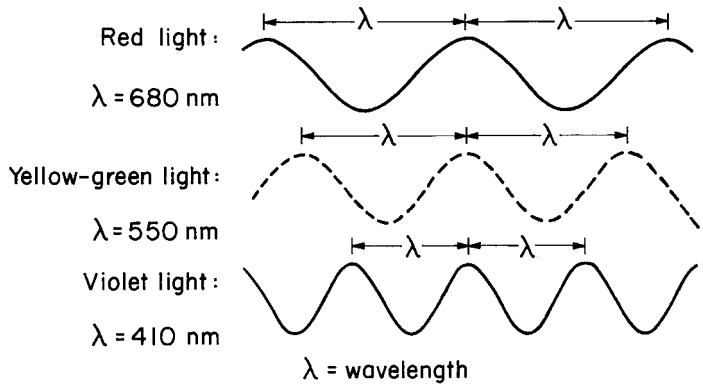

Fig. 5.2. A wave representation of three different light hues: red, yellow-green, and violet, each with a different wavelength λ, which represents the distance between wave crests.

sun encompasses the visible region of the electromagnetic spectrum and extends beyond the red (into the infrared) on one side and beyond violet (into the ultraviolet) on the other with a maximum intensity in the yellow range of visible light.

When we consider light as an electromagnetic wave, a color's spectral signature may be identified by noting its wavelength. We sense the waves as color, violet being the shortest visible wavelength and red the longest. Visible light is the range of wavelengths within the electromagnetic spectrum that the eye responds to. Although radiation of longer or shorter wavelengths is present, the human eye is not capable of responding to it.

Three typical waves of visible light are shown in Figure 5.2. The wavelength is the distance from one wave crest to the next, and is represented by the Greek letter lambda, λ. The violet light depicted in the figure is electromagnetic radiation with wavelength of 410 nanometers, and the red light has a wavelength of 680 nanometers.

The nanometer is a unit of distance in the metric scale and is abbreviated as nm. One nanometer (nm) equals one thousand millionths of a meter (m), or 1 nm = 10^{-9} m. One nanometer is a distance too small to be resolved in an optical microscope, but one micron (μm), which is one thousand nanometers, can be resolved (1 micron = 1000 nm). The view of three red blood cells shown in Figure 5.3 includes a one-micron marker superimposed on the bottom cell to the right. The wavelength of blue-green light is about one-twelfth the width of a blood cell. The wavelengths of visible light are smaller than common objects such as the thickness of a sheet of paper or the diameter of a human hair. Both of these are about one hundred microns thick, which translates to distances greater than one hundred wavelengths of visible light.

As we move through the visible spectrum of violet, blue, green, yellow, orange, and red, the wavelengths become longer. The range of wavelengths (400–700 nm) of visible light is centrally located in the electromagnetic spectrum (Figure 5.1). Infrared and radio waves are at the long wavelength side, while ultraviolet (UV), x-rays, and gamma rays lie at the short wavelength side of the electromagnetic spectrum. Radiation with wavelengths shorter than 400 nm cannot be sensed by the eye. Light with wavelengths longer than 700 nanometers is also invisible. In

the analysis of works of art, the regions of the spectrum encompassing x-rays and infrared radiation are of great interest. Radiation in these regions is used to examine the structure of paintings much the same way that x-rays are used in medical diagnostics, ultraviolet (UV) rays in forensic analysis, and infrared in nighttime reconnaissance. We can use this broad region of the electromagnetic spectrum to look beyond the visible appearance of a painting.

For example, by use of equipment sensitive to infrared radiation we can look beneath the layers of paint. The infrared reflectogram of the *Portrait of a Man* shown in Figure 5.4a reveals an extensive underdrawing (Figures 5.4b and 5.4c) otherwise not visible to the unaided eye. The use of infrared techniques is described in more detail in Chapter 7, "Beyond the Eye."

We can describe light as electromagnetic waves with color identified by its wavelength. We can also consider light as a stream of minute packets of energy called *photons,* which create a pulsating electromagnetic disturbance. A single photon of one color differs from a photon of another color only by its energy.

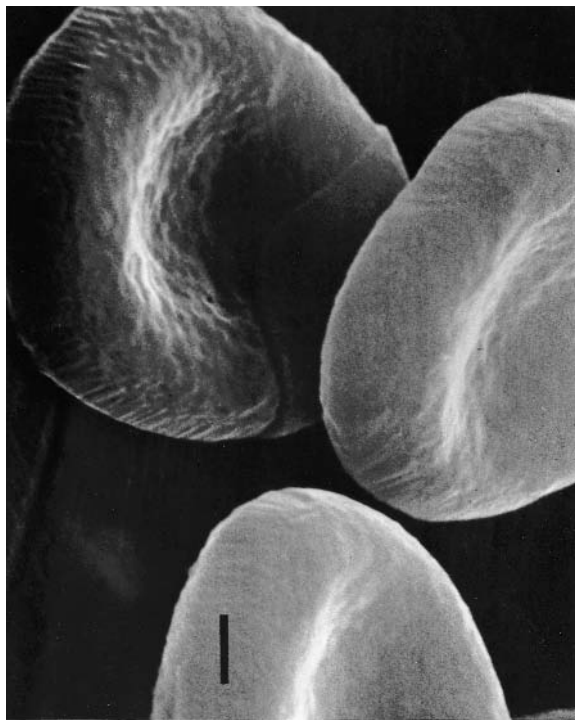

Fig. 5.3. A scanning electron microscope image of three red blood cells. The black bar overlying the blood cell on the bottom represents a distance of 1000 nanometers (or 1 micron), which is approximately 2 wavelengths of the yellow-green light shown in Figure 5.2.

In the analysis of art and in the description of light, the most convenient unit of energy to use is the *electron volt*, abbreviated eV. The electron volt is the energy gained by an electron that moves across a positive voltage of one volt (V). For example 1.5 electron volts is the energy gained by an electron moving from a negative metal plate to a positive plate, both of which are connected to the terminals of a common 1.5 volt "C" battery.

Visible light is composed of photons in the energy range of around 2 to 3 eV (Figure 5.5). As the energy of the light increases, the wavelength decreases. Orange light with a wavelength of 620 nanometers is composed of photons with energy of 2 eV. It is light with energies in the range of 1.8 to 3.1 eV that triggers the photo receptors in the eye. Lower energies (longer wavelengths) are not detected by the human eye but can be detected by special infrared sensors. Higher energies (shorter wavelengths) such as x-rays are detected by x-ray sensitive photographic film or again by special devices.

(a)

(b)

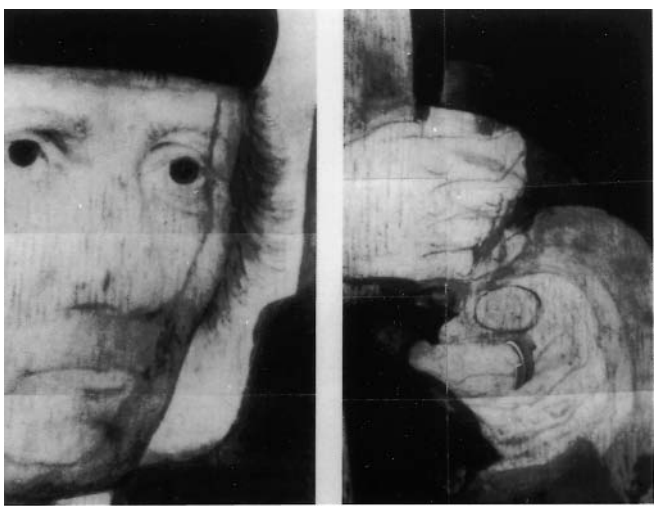

(c)

Fig. 5.4a,b,c. *Portrait of a Man*, attrib. Jan Mostaert, c. 1473–1555/6, 41.9 × 33.1cm, The Saint Louis Art Museum.
Infrared reflectography reveals (b and c) underdrawings that do not conform to the image of the man in the painting as we would view it with the unaided eye (a). The painter chose to alter the location of various contours as the painting progressed on top of the underdrawing.

Light rays are composed of photons whose energy corresponds to a color from red to violet. The intensity or brightness of the light is defined by the flux, which is the number of photons passing through a unit area in a unit time, for example, the number of photons per square centimeter per second. A more detailed description of light energy and wavelength is given in Appendix A.

A spectroscopically pure color has light of only one wavelength. Graphically, this would be displayed as a solid line located at a point along the wavelength scale (Figure 5.6). The height of the line indicates its flux, or intensity. For comparison, the dashed line indicates a "pure" green light whose intensity is less than that of the red light. Colors are seldom spectroscopically pure, that is, composed of a single wavelength of light. A sensed color such as green or red will be composed of a number of photons whose wavelengths are closely spaced around that of the pure color. Figure 5.7 shows an intensity versus wavelength diagram for two groups of photons, one group for a particular green light and the other for a particular red light. For example, the green light is composed of photons with maximum intensities around wavelengths of 520 to 530 nanometers. Other green lights would have different intensity versus wavelength distributions. In Figure 5.8, a smooth curve is drawn through the points of maximum intensity at each wavelength. The curve for the red light is higher than that for the green light, indicating that the red light is more intense (possesses greater photon flux) than the green one.

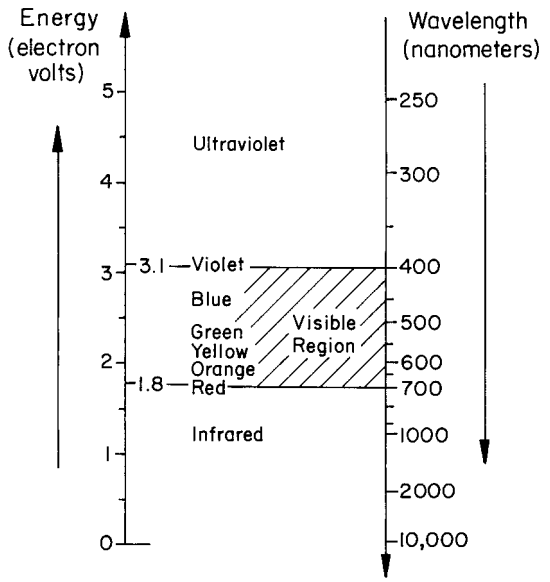

Fig. 5.5. Diagram showing the visible region of the electromagnetic spectrum in terms of wavelength and corresponding energies. The visible region extends from 400 nm to 700 nm (wavelength) with corresponding energies of 3.1 to 1.8 electron volts (eV).

The spectral range of the red color in Figure 5.8 indicates that this specific red color cannot be represented by a single wavelength. However, if we specify a wavelength in the visible range on the electromagnetic scale, we can attribute a color to it. That is, laser light with a single wavelength of 650 nanometers looks red. Optical instruments can be used to measure the intensities and wavelengths of the components of light. In carrying out these measurements one finds that a given color can be produced by light of two or three wavelengths; for example, yellow can be produced by a combination of red light and green light. Most, but not all colors can be produced by mixing lights of three "primary" colors—red, green, and blue.

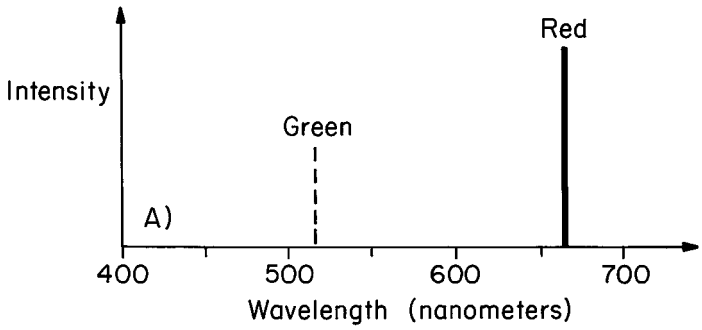

Fig. 5.6. The intensity vs. wavelength of a pure red light (solid line) at 670 nm. The height of the line indicates the intensity, or number of photons per second. A pure green light at 520 nm is shown with less intensity (lower height of dashed line) than that of the red light.

We show the major spectral colors in Figure 5.9a as a linear sequence from red at 700 nm to violet at 400 nm. A circular sequence of these same spectral colors, the color wheel first attributed to Isaac Newton, is shown in Figure 5.9b. The progression of colors from red through violet is identical to that on the linear scale. The circular wavelength scale outside the color wheel shows the wavelength connection between the linear and circular sequences. The purple region in the color wheel represents a notable difference between the two sequences. Colors in this purple portion of the color wheel are composed of mixtures of wavelengths and cannot be represented by a single wavelength.

No single wavelength exists for the color purple. Purple can be created with a mixture of wavelengths in both the red and the violet. In the text, purple is also referred to as magenta (Figures 5.15 and 5.17).

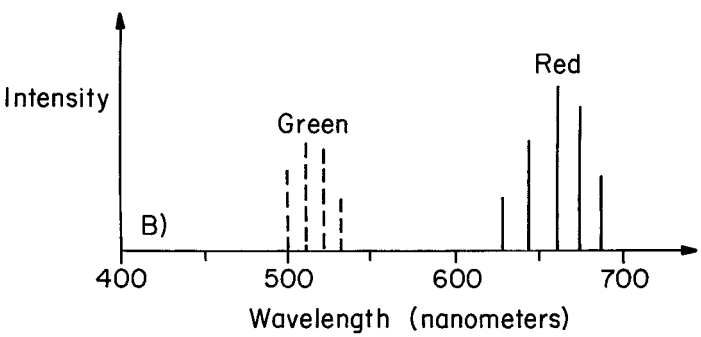

Fig. 5.7. Red light as perceived by the eye is composed of a number of pure red lights of different intensities and wavelengths as represented by the five solid lines. Green is represented in the same way. Any color of light perceived by the eye is composed in a similar way.

5.2 THE COLOR OF OBJECTS

As we look at a painting, the color we see exists due to light illuminating the painting, interacting with the layers of pigment and varnish and reflecting back to the eye. In the previous section we described color as light of specific wavelengths and intensities. Here we consider the color of an object illuminated by white light. Color is produced by the absorption of selected wavelengths of

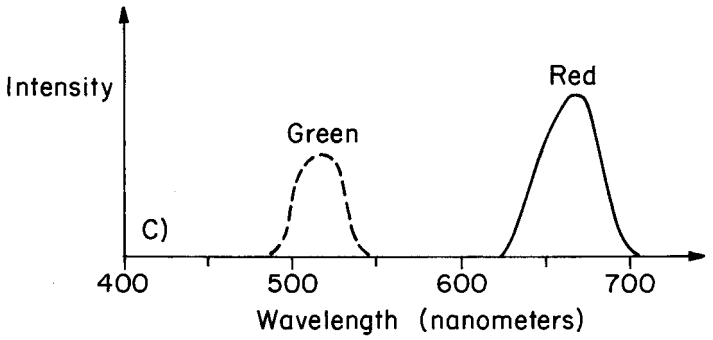

Fig. 5.8. By connecting the heights of the lines in Figure 5.7, an envelope (curved line) is generated that represents, in this illustration, the colors green (dashed line) and red (solid line) as they are perceived by the eye.

light by an object. Objects can be thought of as absorbing all colors except the colors of their appearance, which are reflected as illustrated in Figure 5.10. A blue object illuminated by white light absorbs most of the wavelengths except those corresponding to blue light. These blue wavelengths are reflected by the object.

White light is considered to be a mixture of all wavelengths at uniform intensity. A white object illuminated by white light reflects 100%

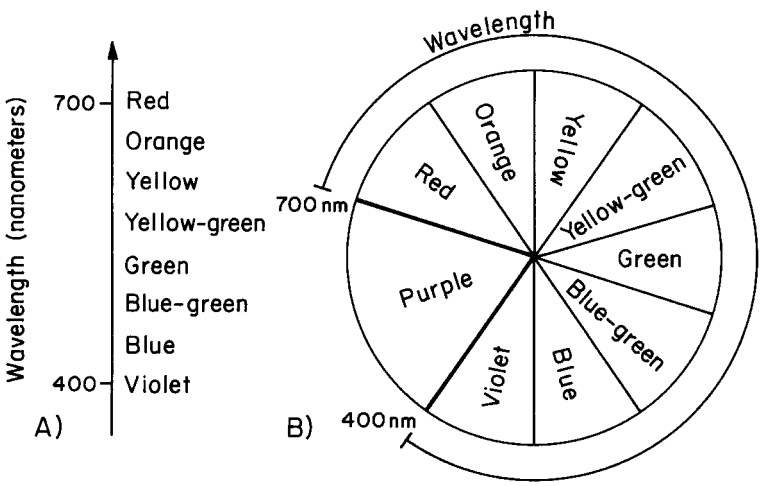

Fig. 5.9A,B. The region of visible light in wavelengths shown as a linear arrangement (A) and as a circle (B) as conceived by Sir Isaac Newton. The color purple shown in the color wheel (B) is composed of a mixture of light in the red and violet regions of the spectrum. Purple cannot be represented by a single wavelength of light.

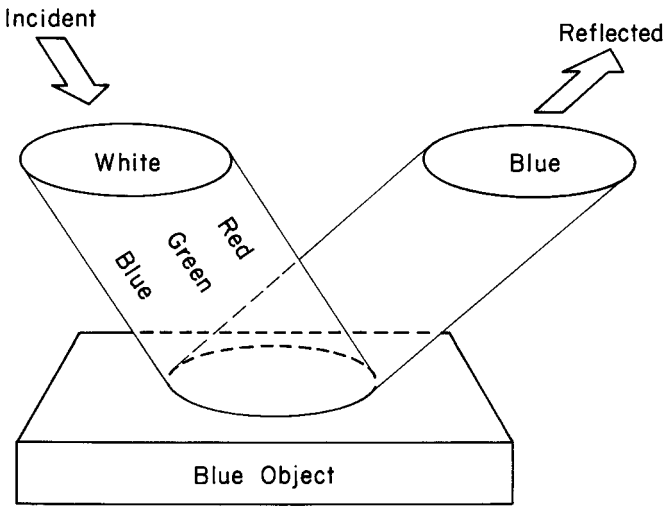

Fig. 5.10. White light composed of all wavelengths of visible light incident on a pure blue object. Only blue light is reflected from the surface.

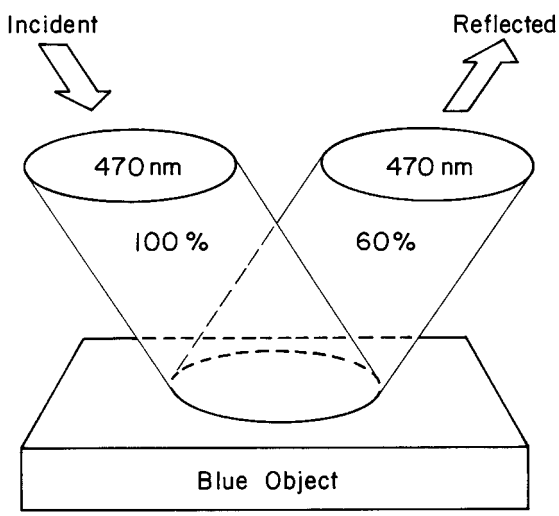

Fig. 5.11. This blue object reflects 60% of the incident blue light of 470 nm and absorbs 40%. Different blue objects will reflect and absorb light in different ratios.

of the illuminating, or incident, light at all wavelengths. Colored objects never reflect 100% of incident white light. Varying amounts of light of wavelengths within the visible spectrum are absorbed by the object. The amount of reflected light can be measured one wavelength at a time through the sequence of wavelengths within the visible spectrum. Figure 5.11 shows the measurement concept of incident blue light of 470 nm. For the measured blue object, 60% of the incident blue light is reflected, and therefore 40% is absorbed. The relationship between reflectance and wavelength is given in Figure 5.12. The single line shows that the light is monochromatic with one wavelength at 470 nm. The height of the line shows the intensity of the reflected light (60%). The remainder of the light (40%) is absorbed.

A blue object illuminated by white light will reflect a mixture of wavelengths. The dominant color is blue, but other wavelengths in the green and red can also be reflected. This is illustrated by the curve in Figure 5.13, which shows the reflectance versus wavelength for a blue object. This curve is called a spectral reflectance curve. At a wavelength of 470 nm (in the blue portion of the visible light spectrum), 60% of the light would be reflected back from the blue object. There is a significant amount of light reflected at wavelengths corresponding to the green, yellow, and red portions of the visible spectrum. For

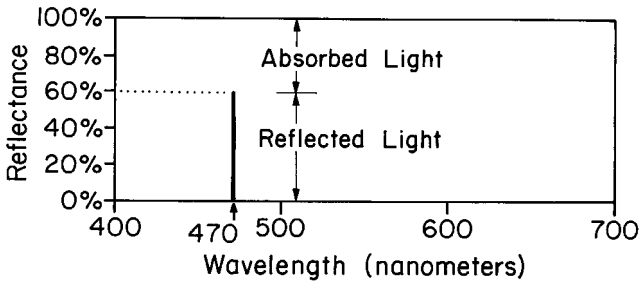

Fig. 5.12. The reflected light from the blue object in Figure 5.11 is shown graphically as reflectance vs. wavelength. The vertical height of the solid line indicates a reflectance of 60% for blue light at a wavelength of 470 nm.

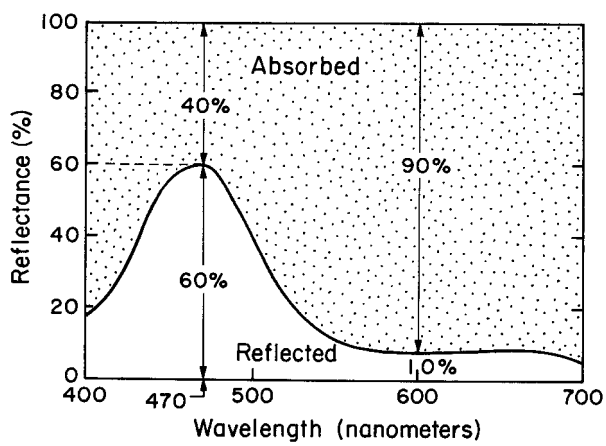

Fig. 5.13. The reflectance of the particular blue object in Figure 5.11 when illuminated by white light can be described by a reflectance vs. wavelength curve. Although the dominant reflectance (60%) is at 470 nm, reflectance at smaller intensities occurs at all wavelengths. Even though the object is perceived as blue, there is a 10% reflectance in the red region at 600nm.

example, 10% of 600 nm wavelength light (yellow) would be reflected, and the remaining 90% would be absorbed.

5.3 COLOR: ILLUMINATION AND METAMERISM

Colors that match in one set of viewing conditions but not in others are said to be metameric. Such colors are called metamers, and the phenomenon is called metamerism. The spectral reflectance curves of metamers are different, but they intersect, usually at three or more wavelengths, between 400 and 700 nm. The greater the differences between the reflectance curves, the more readily the metamerism will become apparent when viewing conditions are changed.

Different colors have different reflectance curves; blue objects have a higher reflectance in the blue region of the spectrum, red objects in the red. White objects have a high reflectance over all wavelengths. These spectral reflectance curves are determined by directing a beam of light of a given wavelength and known intensity on a layer of pigment and measuring the intensity of light that is reflected back. The measurements are repeated at different wavelengths from 400 to 700 nm.

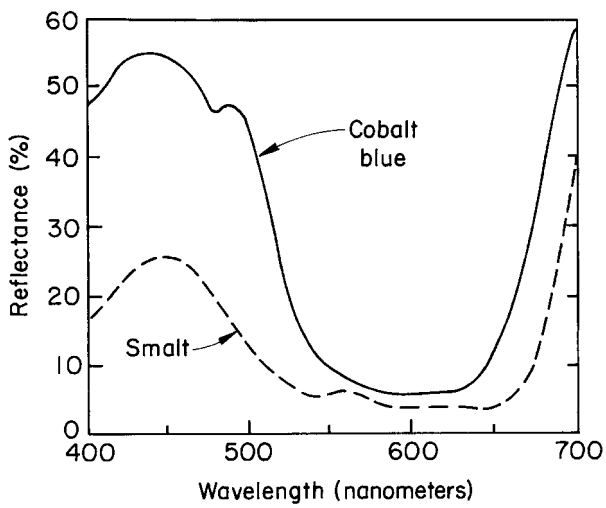

Fig. 5.14. A graph of the reflectance versus wavelength of two blue pigments considered to be the same hue: the traditional blue pigment, smalt (dashed line), and a modern blue pigment (cobalt blue), which has a higher reflectance in the red than smalt. These results indicate that these two blue pigments have different reflectivities at different wavelengths. Consequently, the pigments will appear different under different illumination conditions (daylight, artificial illumination).

Even colors that appear the same may not have the same spectral reflectance curve. For instance, there is a difference in the spectral response of traditional and modern pigments of the same hue. In Figure 5.14 we compare the reflectance of a traditional blue pigment, smalt (dashed line), with its modern counterpart, cobalt blue (solid line). Smalt is made of powdered glass colored with cobalt oxide. Cobalt blue, discovered in 1802, is made with a mixture of cobalt oxide and aluminum oxide. Cobalt blue has a higher reflectance in the red than smalt. These differences in reflectance mean that the blue pigments will have a different appearance to the eye when viewed under different illumination conditions. Metamerism becomes an important consideration in the restoration of older paintings that require

in-painting with modern pigments to replace areas of loss of original paint.

Metamerism is also of consequence to the painter. A painting produced under one lighting condition but viewed under a very different one will reveal color relationships unintended by the painter. The maintenance of very subtle tonal shifts and color resonances, effected (often catastrophically) by this change of illumination, is of great interest. The contemporary painter Avigdor Arikha (see "Duncan Thomson talks to Avigdor Arikha" in the journal *Modern Painters,* Spring, 1990), dedicated to working from observation, is particularly discriminating about the condition of light that reveals his subject and therefore his painting. "Tonal painting, or any painting painted in daylight, must be viewed in daylight, for which there is no replacement yet. Imagine a concert hall whose acoustics falsified pitch: Schubert off by a fraction. What an offense to the ear!" A meaningful interpretation of a painting is often dependent upon such subtle distinctions. Certainly, the painter takes great pains to leave a painting in a particular state. For a certain color to disappear, or appear as another hue or value, is to ensure that the painting will be read in a much different way than was intended.

5.4 Additive Color

White light is a mixture of all wavelengths of the visible spectrum. We can select three individual color lights from the visible spectrum that in combination or by themselves will produce the complete range of colors including white. These three specific colors of light are red, blue, and green.

Any two colored lights may be mixed on a white substrate to produce a third distinct color. Incident primary red and blue lights produce the color magenta (Figure 5.15). Similarly, superimposed beams of primary blue and green produce cyan (blue-green). Superimposed beams of primary blue, green, and red will produce white light. This production of white light is just the reverse of the production of a spectral array resulting from white light incident on a prism. In Figure 5.16 the region occupied by all three beams is white (W). The region oc-

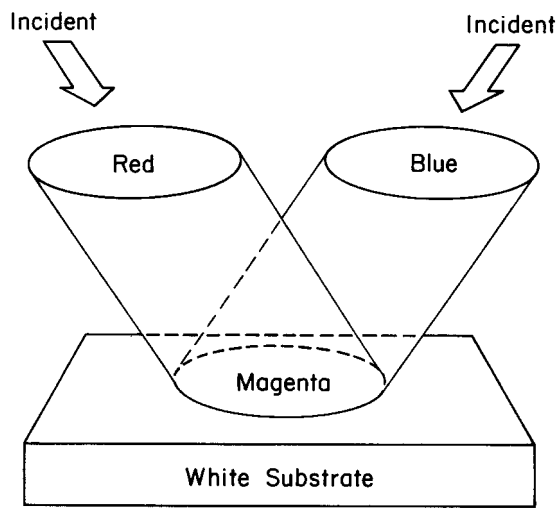

Fig. 5.15. The color magenta (purple) is produced by the addition of red and blue light incident on a white substrate.

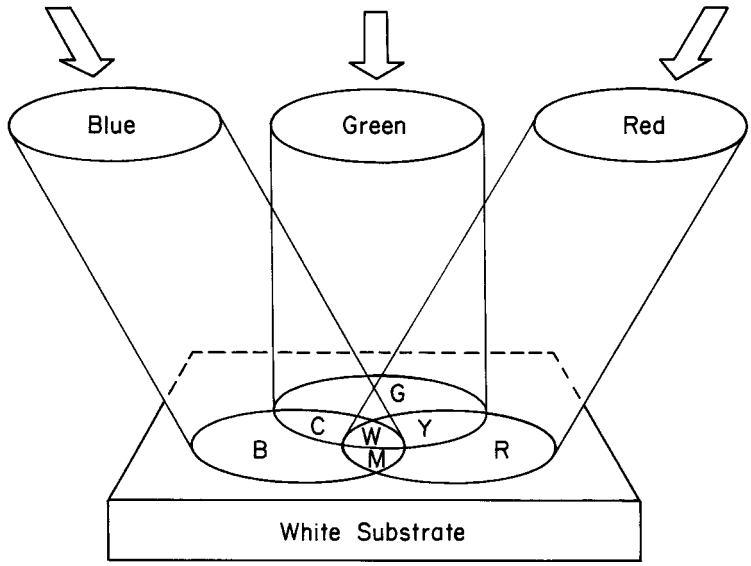

Fig. 5.16. The colors blue (B), cyan (C), green (G), yellow (Y), red (R), magenta (M), and white (W) are produced by the addition of beams of blue, green, and red light incident on a white substrate. This shows that white can be produced by the additive mixtures of these three pure colors, referred to as additive primaries.

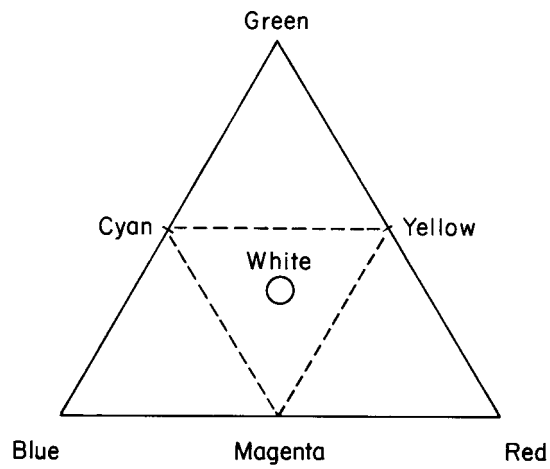

Fig. 5.17. The color triangle with the primary additive colors (blue, green, and red) at the corners and the secondary additive colors (cyan, yellow, and magenta (purple)) at the edges.

cupied by overlapping beams of red and green is yellow (Y); of green and blue is cyan (C); and of red and blue is magenta (M). Another representation of these relations is given as a color triangle in Figure 5.17. Red, blue, and green are primary additive colors. The addition of these three colors produces white, represented by the open circle in the center of the triangle. Cyan, yellow, and magenta, also in a triangular relationship and represented by the dashed line, are secondary additive colors.

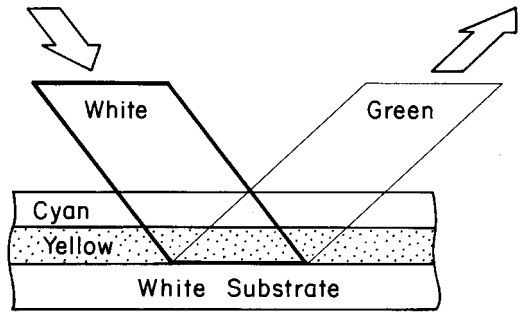

Fig. 5.18. Subtractive color is illustrated by white light incident on a translucent cyan layer (red absorbed), on a translucent yellow layer (blue absorbed); and then the remaining (nonabsorbed) green light is reflected from the white substrate.

5.5 Subtractive Color

Just as additive color mixing refers to the process of adding colored lights, the subtractive process refers to the removal of certain wavelengths of light as a result of absorption. This is the condition when we observe light reflected from objects. It is the mixing of subtractive primary colors that determines the observed colors in painting media.

Subtractive color mixing can be illustrated by illuminating with white light superimposed layers of translucent color on an opaque white substrate. In Figure 5.18 a layer of translucent cyan is superimposed over a layer of translucent yellow. As the incident white light passes through the cyan layer, red wavelengths are absorbed. Blue wavelengths are absorbed in the passage through the yellow layer. The light reflected from the white substrate is green. This is an example of how painters are able to mix colors through the use of translucent glazes.

5.6 The Eye and Color Sensation

So far in this chapter we have discussed light and colors measured by optical instrumentation. Color identification as used by the painter depends on the response of the eye. Our perception of color arises from the composition of light—the energy spectrum of photons that enter the eye. The retina, located on the inner surface of the back of the eye (Figure 5.19), contains photosensitive cells. These cells contain pigments that absorb visible light. Of the two classes of photosensitive cells, rods and cones, it is the cones that allow us to distinguish between different colors. The rods are effective in dim light and sense differences in light intensity—the flux of incident photons—not photon energy. So in dim light we perceive colored objects as shades of gray, not shades of color.

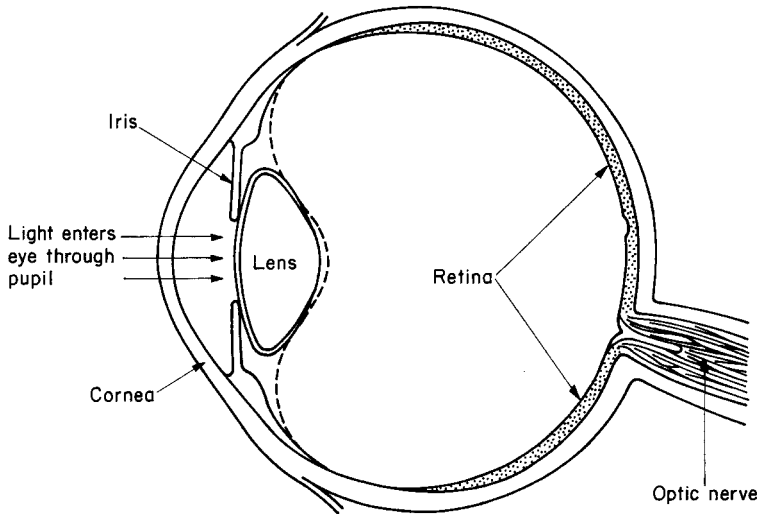

Fig. 5.19. A cross-sectional representation of the eye showing light entering through the pupil. The photosensitive cells, cones and rods, are located in the retina: Cones respond to color, and rods respond to light intensity.

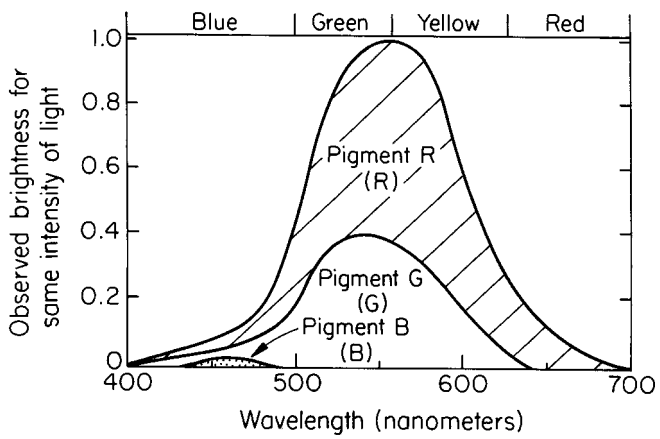

Fig. 5.20. The response of the three cones to incident light: Cone R (pigment R) has a maximum sensitivity in the orange-red, cone G (pigment G) in the green-yellow, and cone B (pigment B) in the blue portions of the visible spectrum. The sensitivities of the three cones overlap, and the perceived color is due to the relative response of the three cones.

Color is perceived in the retina by three sets of cones, photoreceptors with sensitivity to photons whose energy broadly overlaps the blue, green, and red portions of the spectrum. Color vision is possible because the sets of cones differ from each other in their sensitivity to photon energy. The sensitivity of the cones to light of the same intensity (the same photon flux) but different wavelengths (energy) is shown in Figure 5.20. The maximum sensitivity is to yellow light, but cone *R* has a maximum in the red-orange, *G* in the green-yellow, and *B* in the blue. The sensitivities of the three cones overlap. For every color signal, or flux of photons, reaching the eye, some ratio of response within the three types of cones is triggered. It is this ratio that permits the perception of a particular color.

The afterimage phenomenon discussed in Chapter 2 is due to fatigue in the cones. If we stare at a blue object on a white background, the cones in the retina are activated by the photon flux from the blue color. The red, blue, and green pigmented cones respond to the mix of photons of various wavelengths in a proportion representing that color. After a period of time, these cones become fatigued. If the blue object is removed, an image appears on the white background. The cones that are not fatigued signal the image color response, and consequently the afterimage is in the complementary color of the real object.

Optics of Paint Films 6

6.0 Introduction

Our perception of a painting depends on the interactions between light and the layers of paint. The interaction of light with the surface of a painting allows us to sense the texture (smooth or rough), the paint thickness, and the transparency or opacity of the paint. Light does more than interact with the surface. Light penetrates into the paint film, and the colors become visible due to the interaction of light with pigments, binders, varnishes, and other components of a painting. Whether a painting is made of a single layer or multiple layers of paint, there is a common basis that describes the interaction of light. Light is reflected, absorbed, and transmitted by the paint film. In *Holy Women at the Sepulcher* by Peter Paul Rubens, (Color Plate 20), the light illuminating the women acts as a significant component of the narrative. The effect of the image of light in the painting is reinforced by the use of transparent layers of color allowing light to penetrate deeply into the paint film.

In the next sections we discuss the behavior of light in terms of reflection, refraction, and absorption. These optical interactions determine to a great degree how we interpret a painting.

6.1 Reflection

Polished metal surfaces reflect light much like the silver layer on the back side of a glass mirror. A beam of light incident on the metal sur-

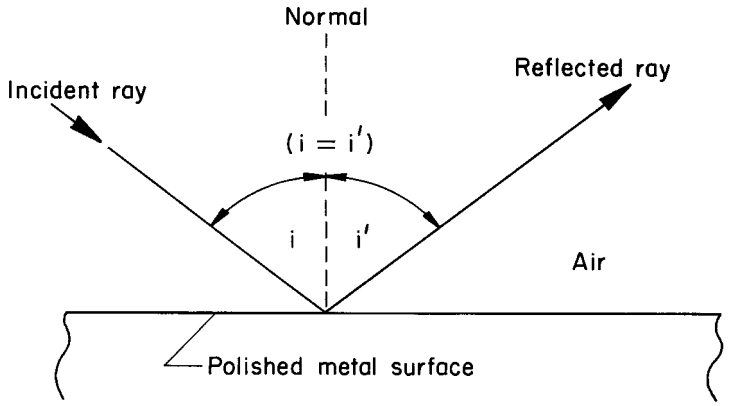

Fig. 6.1. Light ray reflected from a metal surface with angle of incidence i equal to the angle of reflectance i'. The dashed line (normal) is perpendicular to the sample surface.

face is reflected. Reflection involves two rays—an incoming, or *incident*, ray and an outgoing, or *reflected,* ray. In Figure 6.1 we use a single line to illustrate a light ray reflected from a surface. The law of reflection requires that the two rays be at identical angles but on opposite sides of the *normal,* which is an imaginary line (dashed in Figure 6.1) at right angles to the mirror surface at the point where the rays meet. We show in Figure 6.1 that the angles of incidence i and reflection i' are equal by joining the two angles with an equal sign. All reflected light obeys the

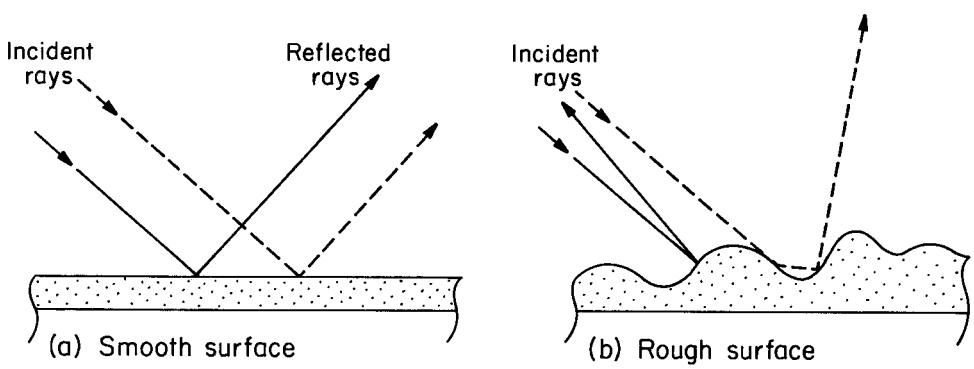

Fig. 6.2a,b. Light reflection from (a) smooth surface (specular reflection) and (b) rough surface (diffuse reflection). In both cases the angle of incidence equals the angle of reflection at the point that the light ray strikes the surface.

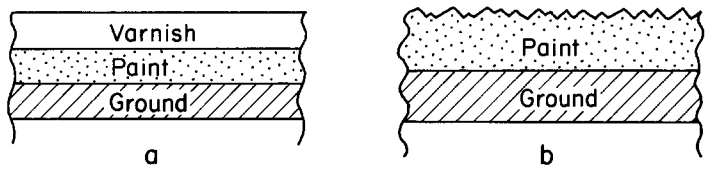

Fig. 6.3a,b. Cross sections of paintings with (a) varnish-covered surface and (b) rough paint surface without a varnish overlayer. The rough surface (diffuse reflection) will appear matte.

relationship that the angle of incidence equals the angle of reflection. Just as images are reflected from the surface of a mirror, light reflected from a smooth water surface also produces a clear image. We call the reflection from a smooth, mirrorlike surface *specular* (as shown in Figure 6.2a). When the surface of water is wind-blown and irregular, the rays of light are reflected in many directions. The law of reflection is obeyed, but the incident rays strike different regions that are inclined at different angles to each other (Figure 6.2b). Consequently, the outgoing rays are reflected at many different angles, and the image is disrupted. Reflection from such a rough surface is called *diffuse* reflection.

The surface of paint layers reflects light in much the same way as water. The smooth varnished surface of the painting shown in cross section in Figure 6.3a causes specular reflection and appears shiny, while the rough surface of the painting in Figure 6.3b has diffuse reflective properties and appears *matte,* or dull.

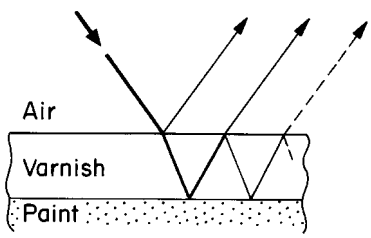

Fig. 6.4. A ray of light incident on a transparent varnish layer is both reflected from the air/varnish surface and transmitted through the layer, where it is reflected at the varnish/paint interface. The outgoing ray at the varnish/air surface is both reflected and transmitted.

Light is reflected when it is incident on a surface or interface between two different materials such as the surface between air and water, or air and paint, or varnish and paint. The reflection of light from varnish and paint layer interfaces is sketched in Figure 6.4. The ray of light incident on the layer of varnish is partially reflected and partially transmitted through the transparent material. At the interface with the paint layer, the transmitted incident ray is reflected and transmitted through the varnish to the varnish/air interface. This ray is then partially reflected internally and partially transmitted into the air. Each time a ray of light strikes a boundary between two materials, such as air/varnish or varnish/paint, some of the light is reflected. The laws of reflection are obeyed at all interfaces. The amount of reflected light at the interface depends on the differences in *refraction* between the two adjoining materials.

6.2 REFRACTION

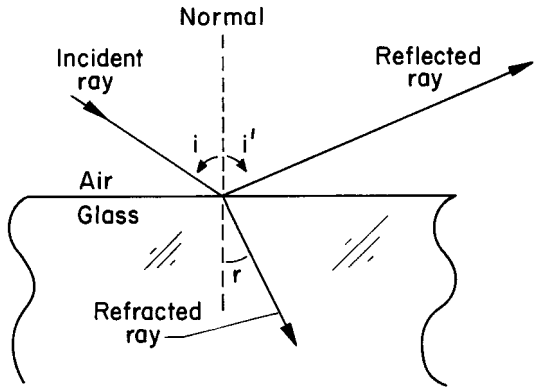

Fig. 6.5. Light in air incident on a glass surface where it is partly reflected at the interface and partly transmitted into the glass. The direction of the transmitted ray is changed at the air/glass surface. The angle of refraction r is less than the angle of incidence i.

Optical properties of materials are characterized in part by their refraction of light. Light incident at the interface between two materials has a transmitted component whose direction changes as it passes the interface. For example, rays of light change direction, or are "refracted," when passing from air into glass. As shown in Figure 6.5, one component of light is reflected, while the other component is refracted. The refracted beam changes direction at the interface and deviates from a straight continuation of the incident light ray. A similar effect can be seen in the apparent bend in a straight stirring rod immersed in a liquid. In Figure 6.6a the beaker is filled with air, and hence the entire length of the rod is in the same medium, air, and appears straight. The beaker in Figure 6.6b is partially filled with water. The stirring rod therefore passes through two media, air and water. At the air/water interface the rod appears to bend.

The change in direction of light as it passes from one medium to another is associated with a change in velocity. When visible light in air en-

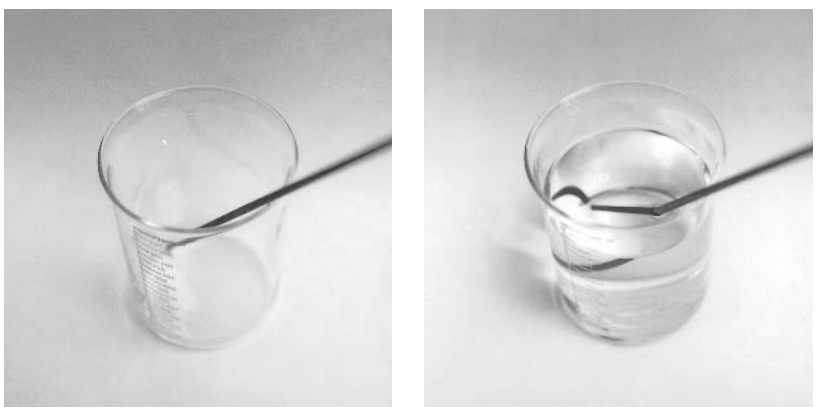

(a) (b)

Fig. 6.6a,b. Photographs of a stirring rod in a beaker. Photograph (a) is of an empty beaker, and the glass rod appears straight. Photograph (b) is of a beaker partially filled with water. The rod appears to be bent at the water surface.

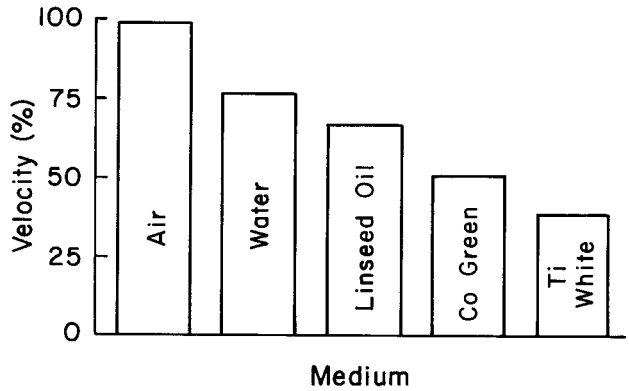

Fig. 6.7. Bar chart of the velocity of visible light in different media. The value of 100% refers to the velocity of light in a vacuum.

ters a medium such as glass, the velocity of light decreases to 75% of its velocity in air, and in other materials the decrease can be even more substantial. For example, in binders such as linseed oil, the velocity decreases to 66% of its velocity in air. Figure 6.7 displays in bar chart format the velocity of light in different media. The 100% value is the velocity of light in a vacuum. For air, the velocity is 99.7% of the speed in a vacuum. For some pigments such as titanium (Ti) white, the velocity decreases to 40%.

Refraction is an effect that occurs when a light wave passes a boundary from one medium into another in which there is a change in veloc-

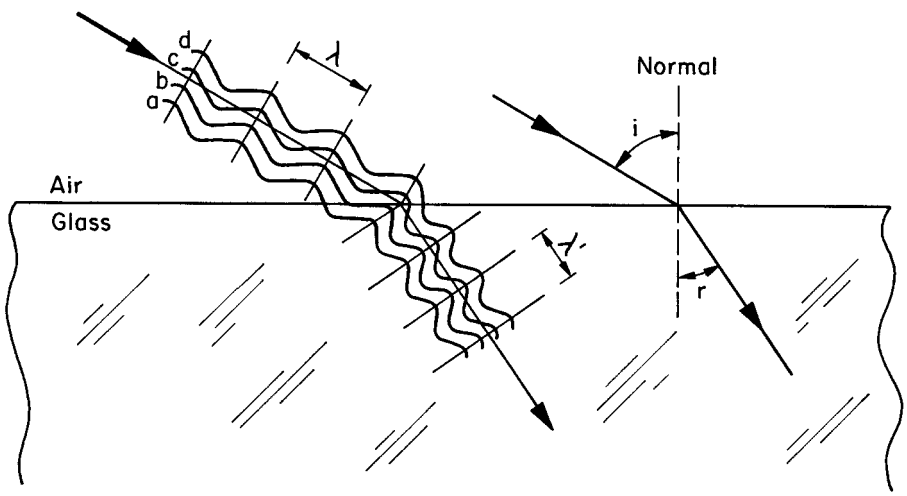

Fig. 6.8. Light waves of wavelength *l* incident on glass change direction and wavelength when transmitted into the glass.

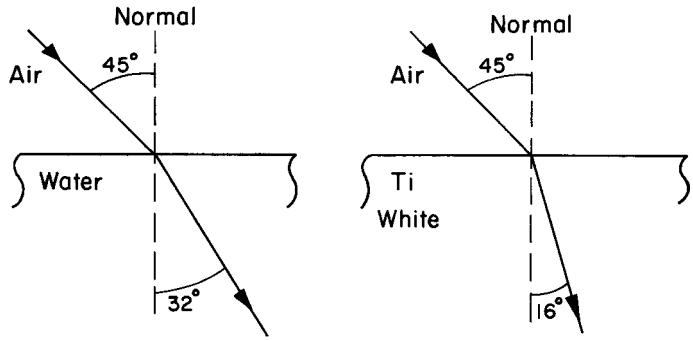

Fig. 6.9. Light incident at 45° on water and Ti white. The angles of refraction (32° for water, 16° for Ti white) are determined by the refractive indices, which are 1.33 for water and 2.5 for Ti white. The reflected components are not shown.

ity of the light. Light is therefore refracted when it crosses the interface from air into glass, in which it moves more slowly. We illustrate refraction in Figure 6.8 by representing incident light as parallel waves with a uniform wavelength, lambda, λ. As the light enters the glass the wavelength changes to a smaller value, lambda prime, λ'. Wave *a* passes the air/glass interface and slows down before wave *b*, *c*, or *d* arrives at the interface. The break in the wave front intersecting the interface occurs when waves *a* and *b* have entered the glass, slowed down, and changed direction. At the next wave front in the glass, all four waves are now traveling with the same velocity and wavelength λ'.

The waves are continuous and remain connected as they pass from one medium to another. The wave inside the new medium is moving more slowly. For waves traveling at an angle to the surface, this slower velocity causes the waves to change direction. The greater the change in velocity, the greater the change in direction. Figure 6.9 shows the change in direction for light in air incident at 45° both on water with refracted angle of 32° and on Ti white with a refracted angle of 16°. These angles correspond to the differences in velocity shown in Figure 6.7.

The ratio of the velocity of light in a vacuum to the velocity of light in a medium is referred to as the medium's *refractive index*. Refractive indices are most easily determined from the measured values of the incident angle and the angle of refraction and their geometric relationship described in Appendix B. Values of the refractive indices for the media shown in Figure 6.7 are given in Table 6.1. A more comprehensive list of values

TABLE 6.1

Values of Refractive index

Medium	*Refractive Index*
Air	1.003
Water	1.33
Linseed Oil	1.48
Cobalt Green	2.0
Titanium White	2.5

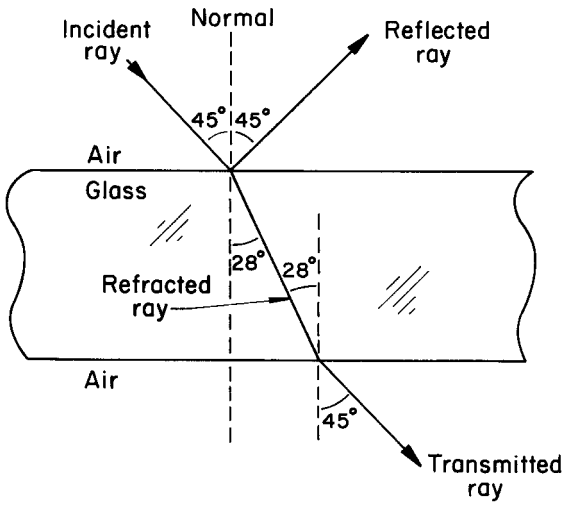

Fig. 6.10. Light incident on a glass plate. The reflected part of the ray is shown along with the light path for the refracted component.

of the refractive index is given in *Appendix B, Table B.1.*

Refractive indices correlate to the perceived relative transparency or opacity of a medium. The media above, commonly found in paintings, range from water (a diluent in many paints) with a refractive index of 1.33 and very transparent to titanium white with a refractive index of 2.5 (a very opaque white pigment).

The path of light in air incident on and transmitted through a glass plate is shown in Figure 6.10. The angle of the incident ray to the normal is 45° and equals that of the reflected ray. The transmitted ray is refracted at an angle of 28° to the normal and exits the glass at an angle of 45° to the normal, an angle equal to that of the incident ray. This explains why, for example, the image we see through a flat-glass window pane is virtually unchanged from that seen through an open window.

6.3 SCATTERING OF LIGHT

The transparency or opacity of a paint layer depends on the amount of scattering and absorption of the light. Scattering in paint films is the deflection of light rays by pigment particles suspended in a binding medium. Scattering depends on the difference in index of refraction between the paint pigment particle and the surrounding binding medium. If the difference in the refractive indices of the pigment particle and the binding medium is large, then the pigment deflects light effectively. For example, a particle of titanium oxide white pigment with a refractive index of 2.5 suspended in a medium of linseed oil with a refractive index of 1.5 will scatter light very effectively. A particle of ultramarine blue pigment with refractive index of 1.5 suspended in the same linseed oil medium will appear transparent because the refractive indices are closer on both sides of the interface, and little scattering will take place. Painters utilize the differences in opacity and transparency resulting from these relationships in organizing many aspects of their paintings, including the mixing of colors and the sensation of luminosity in the paint films.

The size of the pigment particle also influences the amount of scattering. Particles of about the same size as the wavelengths of visible light are more effective in scattering visible light than particles much larger or smaller. For example, centimeter size titanium oxide crystals are transparent, but when ground down to about 500 nanometers they scatter visible light very strongly. The amount of scattering also depends on the density of particles (number per unit volume) in the medium. The higher the density, the greater the amount of scattering. White correction fluid is a dense aggregation of titanium oxide particles suspended in a liquid medium. The opacity of the correction fluid is determined by the density as well as the difference in refractive index and the particle size.

6.4 Absorption of Light

As we pointed out in Chapter 5, the mechanism for the production of color by materials is the selective removal of certain wavelengths (or energies) of light from the electromagnetic spectrum. The light penetrates into the material and encounters light-absorbing pigment particles for this selective removal to occur. A photon transfers all of its energy to the absorbing pigment and is "lost," absorbed, that is, from the light beam. The nonabsorbed photons are scattered (or reflected) back from the pigment particle, producing the sensation of color specific to the pigment.

The absorption of light is illustrated by a beam of light of given intensity (or flux of photons) that penetrates into a material containing a given density of pigment particles that absorb or transmit the photons. The photons penetrate into the material and are absorbed at different depths (Figure 6.11). We also show in Figure 6.11 that some pigments (shaded) will not absorb certain photons. For example, red pigment particles will not absorb photons of light with wavelengths of around 700 nm, but will absorb photons of light with wavelengths of 400–500 nm (blue).

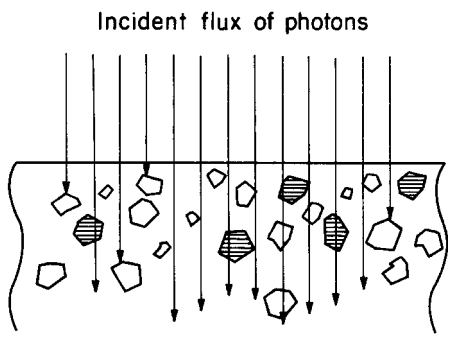

Fig. 6.11. Flux of photons incident on a transparent medium containing pigment particles, which either absorb the photons (unshaded particles) or transmit the photons (shaded particles).

The amount of light that is absorbed is not dependent on the intensity of the incident light, but is determined by the density of pigment particles. If the concentration of pigment particles is increased, the amount of absorption is increased and the amount of transmitted light is decreased. The intensity of light passing through a layer of paint will decrease with depth.

Paints with high concentrations of pigment and relatively small amounts of binder (casein, for

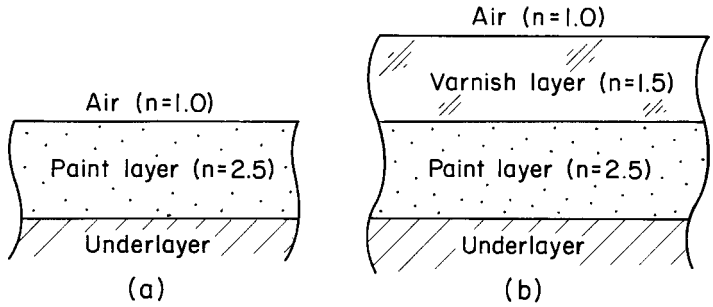

Fig. 6.12a,b. Cross section of paint film (a) without and (b) with varnish layers. The values of the refractive indices are given in parentheses.

example) rely mostly on surface absorption of light to produce color. The color of these paints changes dramatically when they are covered with varnish (Color Plate 21). The simplest change in appearance is the change from a rough matte surface (diffuse reflection when light is scattered in all directions from an irregular surface) to a smooth, glossy surface (specular reflection, where light is reflected in one direction). The varnished paint surface is glossy, and more light is reflected from the varnish surface than from the uncovered paint, leaving less light to be transmitted to and absorbed by the paint layer. This is the source of the darkening effect of a varnished surface. Darkening results from the lower light intensity incident on the paint layer under the varnish.

When the varnish layer is applied, we change the index of refraction relations as shown in Figure 6.12. The reflection of light at the paint layer under a coat of varnish is less than that for the unvarnished paint layer because the difference in refractive indices is smaller at the paint–varnish interface than at the paint–air interface. Once inside the varnish layer, a greater percentage of the light is transmitted into the paint. As a result, more light can be absorbed by the pigment particles, and this will lead to a deeper and richer color.

This concept is applied by painters through the use of a *glaze,* which is a colored, translucent layer of paint applied over another layer of color. The underlying color is typically opaque, although multiple layers of glaze are sometimes used. The light reflected from the opaque underlayer is filtered by the translucent glaze, resulting in a desired change in color. The colors produced by glazing techniques follow the subtractive color relationships (described in Chapter 5) arising from the absorption and scattering of light by pigment particles in the glaze. Glazes, like varnishes, darken the underlying color slightly and increase the reflective properties of the paint film.

6.5 FLUORESCENCE

Photons of visible light are not absorbed in layers of varnish and binding media but are transmitted through them. In contrast, the higher-energy photons in the ultraviolet (UV) region of the spectrum are strongly absorbed in varnishes and binding media.

The absorption of ultraviolet photons results, in some cases, in the emission of photons in the visible region of the spectrum. The absorption of light photons of high energy and reemission of photons of lower energy, in the visible region, is commonly called fluorescence.

The fluorescence of varnishes under an ultraviolet lamp allows us to distinguish the normally transparent (in the visible) varnish film from the underlying paint film. When varnish is removed during restoration of a painting the conservator can be guided in the process by periodic examination under ultraviolet illumination, as shown in Figure 6.13. Aged varnishes have different fluorescent properties than new varnishes, and some modern pigments fluoresce differently than traditional pigments. Thus examination of a painting under ultraviolet light can often reveal retouched or restored areas.

Fig. 6.13. *Portrait of Francis I* by Joos van Cleve in restoration. Fluorescence under ultraviolet illumination with varnish partly removed. Cloudy regions are those still covered with old varnish layers. (*From* B. Marconi, *Application of Science in Examination of Works of Art*, pp. 246–254 (Museum of Fine Arts, Boston, 1965).

Ultraviolet radiation is strongly absorbed in pigments and paint layers. It is so strongly absorbed that through prolonged exposure, the energy transmitted to the paint can cause fading and color changes. The potential of this sort of damage has led museums to forbid the use of flashbulbs (which produce an ultraviolet component in their light) in taking photographs.

BEYOND THE EYE 7

7.0 INTRODUCTION

Paintings are constructed by the artist to be viewed in the visible region of the electromagnetic spectrum, wavelengths from 400 to 700 nm. They are normally viewed in reflected light, where the transmission, absorption, and reflection of photons by pigments in the paint layers define the work of art through color.

Some characteristics of pigments permit us to gain access to aspects of the painting unavailable to us under normal viewing conditions. The underlayers of the finished painting, for example, are not always visible to the unaided eye. Underdrawings, executed with charcoal, dark pigmented inks, or paints often are used to assist the painter in composing the image. Painters may make numerous revisions of the image, called *pentimenti*, as the painting develops. These underlayers are most often covered by successive layers of paint. We can detect these underlayers by using photons that penetrate through the outer layers. The human eye is now assisted by equipment that detects radiation outside the visible spectrum, in the x-ray and infrared regions.

7.1 PIGMENT RESPONSE IN THE INFRARED

In the infrared portion of the spectrum the wavelengths are greater than 700 nanometers with photon energies less than 1.8 electron volts (eV). These infrared photon energies, typically around 1 eV, are so low

that the photons are not absorbed by most pigments. The paint layers are therefore relatively transparent to infrared radiation. Infrared radiation penetrates the upper paint layers but is absorbed by dark preliminary drawings that reside beneath them. The remaining radiation is reflected by white or light-colored grounds. With the aid of infrared-sensitive photographic equipment, the underdrawing can be seen be-

(a)

(b)

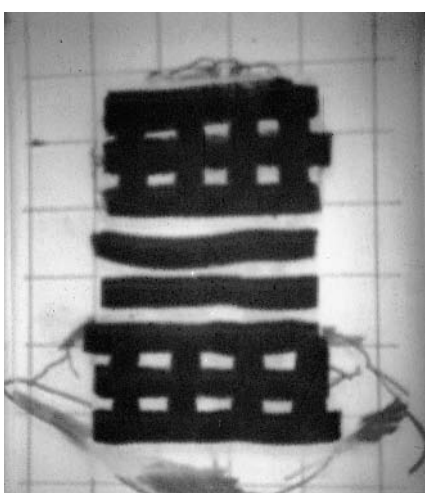

(c)

Fig. 7.1a,b,c. Demonstration of infrared reflectography. (a) Photograph of charcoal drawing in visible light, (b) photograph of layers of overpainted colors that hide the charcoal drawing, (c) infrared reflectogram revealing the charcoal drawing beneath the paint layer.

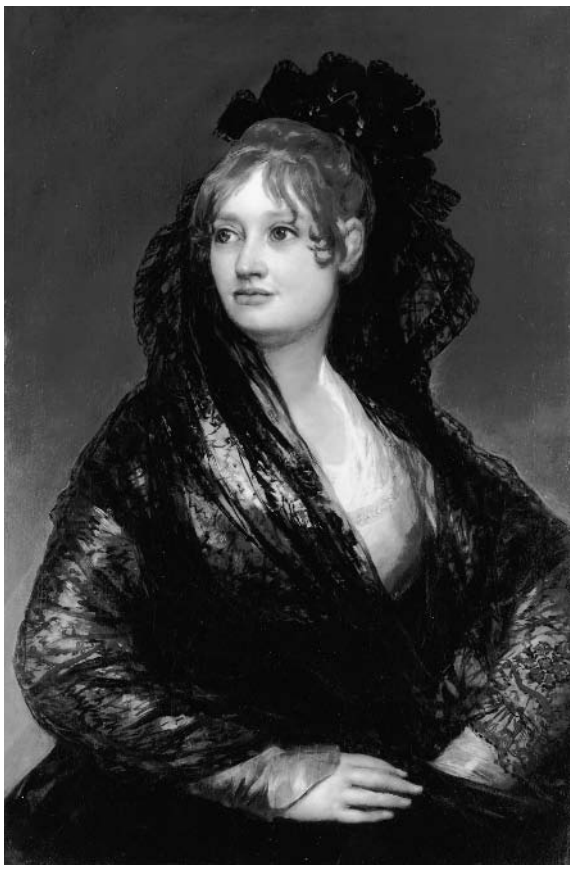

(a)

cause of the difference between absorbed and reflected radiation.

A particularly convincing demonstration of the transparency of pigments to the infrared is provided in Figure 7.1. First, an underdrawing is made using charcoal on a white ground. A layer of paint consisting of different colors is then applied to the drawing. Finally, the composite drawing/painting is viewed with an infrared-sensitive video camera, clearly revealing the image of the underdrawing in the infrared display.

Different pigments have different reflection and absorption properties at different wavelengths. When viewed in the visible range of the spectrum each pigment has a certain thickness that is required to cover up or hide an underlying pigment. To make the underdrawings observable, the hiding ability of the paint has to be minimized. The paint layer thickness cannot be modified, and therefore infrared radiation is

(b)

(c)

Fig. 7.2a,b,c. (a) Francisco Goya, *Doña Isabel de Porcel*. Oil on canvas, 32 1/4 × 21 1/2 inches, National Gallery, London. (b) Infrared reflectogram detail showing the presence of an eye beneath the portrait of Doña Isabel. (c) X-radiograph showing a more complete image of the overpainted portrait.

used because absorption and scattering are reduced in that region of the spectrum.

As the wavelength increases into the infrared region, the amount of scattering decreases for pigment particles embedded in a binding medium. The decrease in scattering leads to less reflection by the pigments. Because the photons are not absorbed they continue to penetrate through the paint layers. At the ground layer of a painting the photons are strongly absorbed by the underdrawing (charcoal or dark-colored ink) and universally reflected by the white pigments in a typical ground. Differences between areas of reflection and absorption are therefore detected.

Doña Isabel de Porcel, by Francisco Goya, provides an example of the penetration of infrared radiation through a paint film. The image seen in visible light (Figure 7.2a) gives no indication of the existence beneath it of an unrelated portrait. The infrared image (Figure 7.2b) shows the eye and eyebrow of the hidden portrait. We are able to detect this image because pigments used to paint the eye absorb photons in the infrared region, while surrounding light-pigmented areas reflect the photons. A more complete image of the overpainted portrait is provided by the x-radiograph shown in Figure 7.2c.

7.2 Pigment Response to X-rays: Absorption

In the x-ray portion of the electromagnetic spectrum the wavelengths are around 1 nanometer, a distance nearly one thousand times smaller than wavelengths in the visible spectrum. Consequently, the photon energies are a thousand times greater than the energies of photons in the visible region. In the x-ray region, photon energies are typically in the range of 1,000 to 20,000 electron volts (1 to 20 kiloelectron volts, or keV) with an upper level in the range of 100 keV. Above that level, photons in the range of 1 million electron volts (MeV) are called gamma rays. These photon energies are so high that the photons are not absorbed by most pigments. The paint layers are therefore relatively transparent to x-rays. The mechanism for the absorption of x-ray photons is the same as that in the infrared and visible regions of the electromagnetic spectrum. The energy of the x-ray photon is given up to a particle of pigment, and the photon is lost from the incident beam of x-rays. Those photons not absorbed from the beam continue to pass through the painting.

The amount of absorption of x-rays depends on the density of electrons in a given area of a painting. The energy of x-ray photons is absorbed by electrons, but only in regions of high electron density. Elements such as lead and mercury strongly absorb x-rays, because atoms of these elements contain high numbers of electrons (lead with 82 electrons and

mercury with 80). Lead is common in white pigments (flake white), and high concentrations of mercury are present in the red pigment vermilion. The distribution of pigments containing x-ray absorbing elements is easily distinguished against a background of nonabsorbing pigments. An x-radiograph of Jean Honoré Fragonard's *A Young Girl Reading* (Figure 7.3a) is shown in Figure 7.3b. A portrait residing beneath the figure of the young girl is revealed because the presence of white lead in that region of the painting absorbs most of the x-rays incident on the painting. Those x-rays not absorbed pass through the paint film and canvas to film mounted behind the painting. The film is exposed by these x-rays, producing the dark areas in the x-radiograph. This process is similar to medical x-radiography.

In addition to the image revealed by the presence of lead white, we also see evidence of the wooden stretcher frame as well as the nails used to secure the canvas to the frame. These images also result from the absorption of x-rays, but in this case, the x-rays are absorbed by high concentrations of elements containing atoms with low numbers of electrons.

(a)

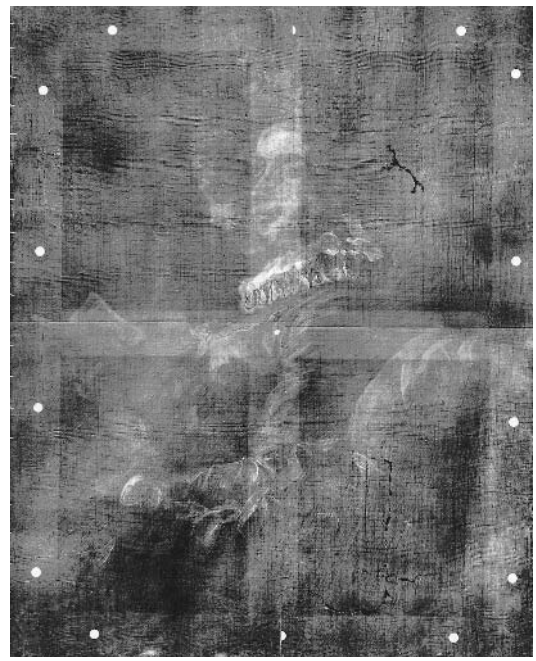

(b)

Fig. 7.3a,b. (a) Jean Honoré Fragonard, *A Young Girl Reading*, c. 1776. Oil on canvas, 32 × 25 1/2 inches (National Gallery of Art, Washington). (b) X-radiograph showing tears in the canvas and the portrait head underneath the image of the girl. (X-radiograph from Barbara Berrie, National Gallery of Art, Washington.)

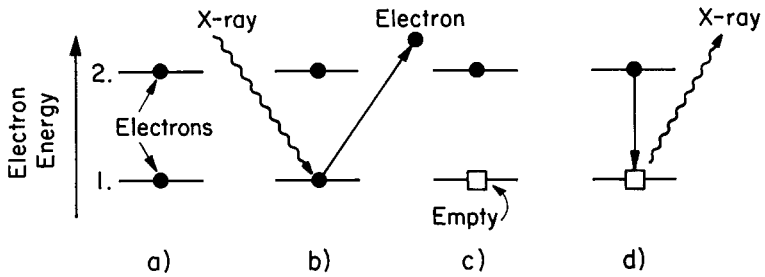

Fig. 7.4a,b,c,d. Schematic of x-ray emission from electrons that occupy two energy levels: (a) energy levels occupied by electrons; (b) incident high-energy x-ray ejects electron from level 1; (c) empty state in level 1; (d) electron makes transition to empty state in level 1 and emits an x-ray to conserve energy in the transition process.

7.3 Pigment Response to X-rays: Emission

Pigments have been characterized by their color and their relative transparency to infrared and x-radiation. The induced emission of x-rays also provides a means for pigment identification. An incident x-ray photon is absorbed and an electron is ejected from the atom, leaving an unfilled state. There is a specific set of energy states occupied by the electrons. No two electrons can occupy the same state. An electron in the atom makes a transition to fill the empty state, and an x-ray is emitted. The energy of the emitted x-ray is given by the energy lost by the electron that has made the transition between the two states, as shown in Figure 7.4. The emitted x-rays are detected and their energies measured. The measured energy values identify the specific elements contained in the pigment, and the number of x-rays emitted indicates the amount of the element. Pigments are composed of specific elements, each of which has a specific number of electrons and electron energy levels. For example, vermilion is composed of atoms of mercury with 80 electrons and sulphur with 16 electrons. Electron binding energy levels are those required by an incident photon to remove an electron from an atom.

An electron in mercury requires

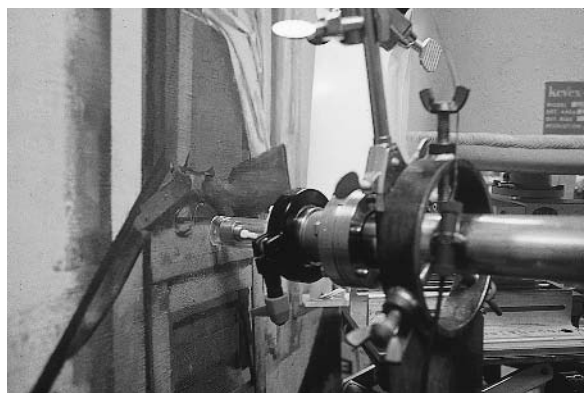

Fig. 7.5. Examination by proton-induced x-ray emission (PIXE) of the elemental composition in an oil paint film. The round stainless-steel tube directed toward the shotgun image in the painting is the end of a proton beamline that allows energetic protons to induce x-ray emission. The detector for measurement of x-ray energies is not shown. Courtesy of W.S. Taft and P. Revesz, Cornell University.

83,000 eV to be removed from the atom, whereas sulphur electrons require a much lower energy of 2,500 eV (see Appendix F, Table F.3, Electron Binding Energies). Each atom has a unique set of electron energy levels. The laws of quantum mechanics, established in the first half of the twentieth century, have led to a rigorous and exact description of the energy levels within the atom. The procedure shown in Figure 7.5, proton induced x-ray emission (PIXE), identifies the elements present (and therefore pigments) in localized areas of the painting of about 1 mm in diameter. Other methods of identifying pigments such as x-ray diffraction are discussed in Appendix E.

7.4 Pigment Response to Neutrons

A beam of neutrons incident on a painting will induce reactions within the elements present in the pigments. These reactions lead to the emission of beta rays and gamma rays. As is the case in x-ray emission, the energies of the emitted gamma rays identify the elements. Beta-ray emission allows one to examine the distribution of elements across a painting in a manner similar to x-radiography. An autoradiograph of Anthony Van Dyck's *Saint Rosalie Interceding for the Plague-Stricken of Palermo* (Figure 7.6a) reveals a self-portrait sketch painted in bone black oil paint residing beneath the image of Saint Rosalie (Figure 7.6b). Bone black pigment contains high concentrations of phosphorous, which when activated by neutrons generates through the emission of beta rays an image on film. Such exposures are timed to produce images of selected elements.

Neutrons are one of the constituents of nuclear matter and may be generated in a nuclear reactor. A flux of neutrons incident on the surface of a painting will penetrate the materials and be selectively absorbed by the elements in the pigments. The absorbed neutron causes a rearrangement of the nuclear structure of the element, leading to instability. The unstable nucleus moves toward a stable configuration by emitting a variety of nuclear particles such as beta rays and gamma rays. This process is referred to as radioactive decay. The rate of radioactive decay varies widely for different elements. The rate of decay is characterized by the "half-life," which is the time required for one half of the radioactive nuclei to decay.

The products of radioactive decay and their energies vary from element to element. In neutron-induced radioactive decay, the pigments are identified by the energies of the emitted gamma rays. Through the use of a gamma ray detector, one is able to document the elemental composition of a given pigment. The pigments also provide a picture of their location in a painting by the emission of beta rays, which expose film placed in contact with the surface of the painting. This process is called

(a)

(b)

Fig. 7.6a,b. (a) Anthony Van Dyck, *Saint Rosalie Interceding for the Plague-Stricken of Palermo*, c. 1624. Oil on canvas, 39 1/4 × 29 inches, The Metropolitan Museum of Art, New York. (b) A neutron-induced autoradiograph of Van Dyck's painting showing the self-portrait painted in bone black residing underneath the image of Saint Rosalie.

autoradiography because emission from the pigments themselves provides the image rather than an external beam.

The oil painting shown in Figure 7.7a was made to take advantage of the unique image-producing qualities of neutron-induced autoradiography. It is composed of layers of images superimposed upon one another beginning with the head painted in raw umber. Over the image of the head lies a grid of blue lines followed by squares of the same cobalt blue color. Once the painting was completed, it was exposed to a flux of neutrons produced in a nuclear reactor designed for research purposes. The intervention of the neutron flux initiated the radioactive decay of a variety of elements present in the pigments. The emission of beta rays incident on photographic film in contact with the painting surface produced a series of images, three of which are shown in Figures 7.7b,c, and d. Film exposures are timed to correspond to the decay rate of specific elements. In the first exposure, (Figure 7.7b) made 15 minutes after activation and of 10 minutes duration, atoms of cobalt altered by the flux of neutrons (or isotopes, in this case cobalt 60m) provide a strong image of the blue lines and checkerboard pattern. The large shape of cadmium red, which in the painting overlie the blue color, blocks some of the beta radiation being emitted by the cobalt. A very light image of the head can also be seen, which in the next exposure is much stronger. In the second exposure (Figure 7.7c) a picture of the distribution of man-

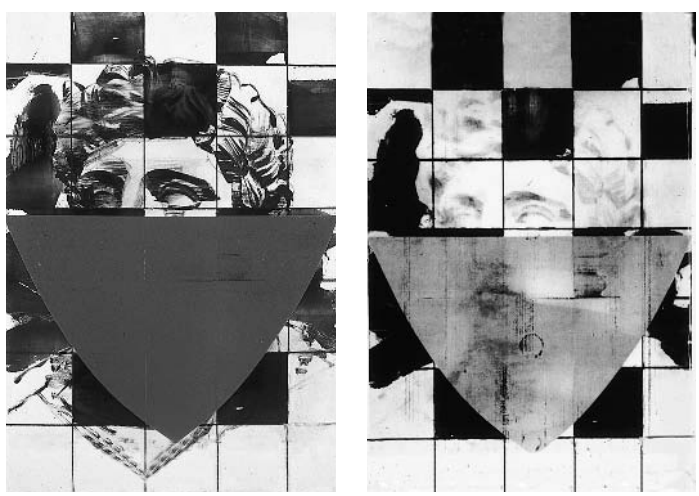

Fig. 7.7a,b. (a) Painting of a head partially obscured by a grid and checkerboard in blue and a red shape. The head is painted in raw umber containing manganese, overlain by grid lines and squares painted in cobalt blue. The red shape is painted in cadmium red. (b) First autoradiograph of the painting produced by beta radiation emitted by the isotope cobalt 60m. Exposure is for 10 minutes, beginning 15 minutes after activation. (*Continued on pg. 85.*)

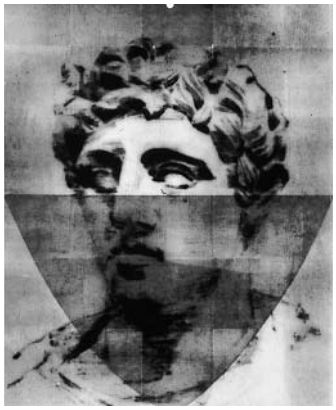

(c)

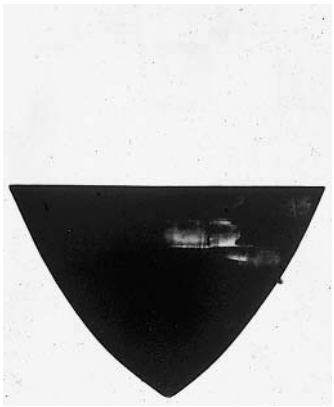

(d)

Fig. 7.7c,d. (c) A 2-hour exposure beginning 2 hours after activation produced this autoradiograph generated by the isotope manganese 56. (d) Third autoradiograph with dominant image of Cadmium. The exposure was begun 4 days after activation, for a period of 2 days.

ganese (present in the pigment raw umber used to paint the head) appears in an exposure taken during a period of 2 hours beginning 2 hours after activation. The cobalt isotope has by now degraded to such an extent that its beta radiation emission cannot be detected. For cadmium (the large shieldlike shape), the exposure was taken over a two-day period beginning four days after activation. It is shown in Figure 7.7d. The variations in value in the shape indicate differences in density of cadmium isotopes and therefore differences in thickness of the paint, even though in Figure 7.7a the red color appears as a uniform coating. Just beginning to be detected is a second isotope of cobalt (cobalt 60) with a much longer half-life than cobalt 60m.

7.6 Overview

The finished state of a painting often consists of more than a single layer of paint. The image may evolve through a process of revisions to the initial subject or may be painted over an unrelated image. Some of the unique characteristics of pigments allow us to appreciate the image in visible light, while other characteristics allow us to see the underlayers and therefore to gain an understanding of the process employed in making the painting. Some of the processes described in this chapter (infrared reflectography and x-radiography) are commonly used by conservators, curators, and art historians to study the material composition of paintings and the working methods employed by artists.

Detection of Fakes 8

8.0 Introduction

The word "fake" has many connotations, including fraud, deception, and forgery. Here, we explore the procedures and methods that can be used to determine whether a painting has been wrongly attributed to a given painter.

Forgeries are endemic in the art world. When millions, even tens of millions of dollars, are involved in the purchase of works of art, it is expected that spurious paintings will be represented as authentic works by master painters. The provenance or history of a painting can be murky. In the upheavals after World Wars I and II, there were a number of paintings acquired by art dealers, private collectors, and museums. Some provenances were sketchy. The art collections of estates have been sold with uncertain histories of the acquisitions. It is difficult to trace the history of a painting as it passes from one collection to another over the centuries. It may be difficult to obtain the ironclad provenance required to authenticate a work of art.

Anyone who carries out analysis of works of art is most likely to be asked to evaluate a recently found work of art by a well-known painter. Picasso was a prolific painter, and it is not uncommon to hear of claims that long-forgotten early works of his have been discovered in an attic. Walter McCrone (*Microscope,* vol. 38, pp. 289–98 (1990)) relates how 1500 pastels and drawings by Mikhail Larionov were discovered in a trunk in Moscow in 1985. Presumably the collection was left in Moscow when he moved to Paris in 1915. After his analysis of the pigments, McCrone concluded that the pastels date from after 1940

and must have been executed after 1957 because of the presence of pure TiO_2 (rutile) in the pigments.

Another example is that of Han Van Meegeren who was called the "most audacious and successful forger of modern times" (Hope B. Werness in *The Forger's Art*, edited by D. Dutton, University of California Press, Berkeley, California, 1983). His most famous forgery is the *The Supper at Emmaus,* which he convinced the art world in 1937 was a genuine Jan Vermeer. In an effort to avoid conviction for collaboration with the enemy (his *The Adulteress* had ended up in Hermann Göring's collection), Van Meegeran confessed to the lesser crime of forgery in 1945.

An exhibition of Rembrandt's work, *Rembrandt/Not Rembrandt*, at the Metropolitan Museum of Art, in New York, explored the issue of authenticity. In volume 1 of the two-volume catalog of *Rembrandt/Not Rembrandt* (The Metropolitan Museum of Art, New York, 1995), Hubert von Sonnenburg points out that "No other seventeenth century painter has been imitated to the degree Rembrandt was from the very beginning of his career." Even a Rembrandt signature is not necessarily a proof of authenticity. Signatures of artists like Rembrandt are often added to works of lesser artists. Von Sonnenburg discusses the scientific methods used in studies of the authenticity techniques that we will cover in the remainder of this chapter. For example, von Sonnenburg makes extensive use of x-radiography and autoradiography to analyze the structure beneath the surface of Rembrandt's paintings.

8.1 A Successful Forger

It is difficult to be a successful forger. Not only must the forger possess impressive artistic skills, he must have a general knowledge of a particular historical period as well as an understanding of the materials and methods employed by artists of the period.

One starts with the support—for European paintings the choices are wooden panels or canvas, depending on artist, time period, and geographic location. Both types of support can be easily dated, so the supports must be obtained from a painting of the period. Oak wood, used in imitating the Flemish period, can be dated by dendrochronology (Appendix L), the examination of growth ring patterns. Painters working in Italy commonly used poplar wood for panels. There are no tree-ring chronologies for poplar, so Italian panels cannot be dated in the same manner as Northern European panels. Sometimes panels can be identified as cut from the same tree. In the 1600s and later, oak panels were bought ready-made, in standard sizes from guild members with a monopoly in panel-making. Painters could purchase the panels in batches

from particular panel-makers. The use of panels as a support may not be the optimum choice for the forger because they are so easily dated.

The choice of canvas as a support for fakes has its own set of problems when a fake is advanced as authentic. Canvas can be dated by carbon-14 techniques. This dating technique was used to determine the harvest year for the flax from which the Shroud of Turin was woven. The Shroud of Turin is widely believed to be the burial shroud of the crucified Jesus Christ. The carbon date, however, is the middle of the fourteenth century (H. Gove, *Relic Icon or Hoax? Carbon Dating the Turin Shroud*, Institute of Physics Publishing, Bristol UK (1996)).

In order to mimic an authentic support, one must obtain an old painting of the correct age and location (trusting that it is not a contemporary forgery) and scrape away the paint film, leaving the original ground intact. As discussed in the earlier chapters, the ground is a layer or series of layers that prepares the support for the paint. The ground fills the weave of the canvas and acts as a barrier to the absorption of the paint by the fabric. The ground may be a single or double layer, white or colored.

The choice of pigments is what causes the forger the most trouble. Pigment usage changes over time. Velasquez used for a yellow pigment the synthetic lead–tin oxide made by fusing together lead oxide and

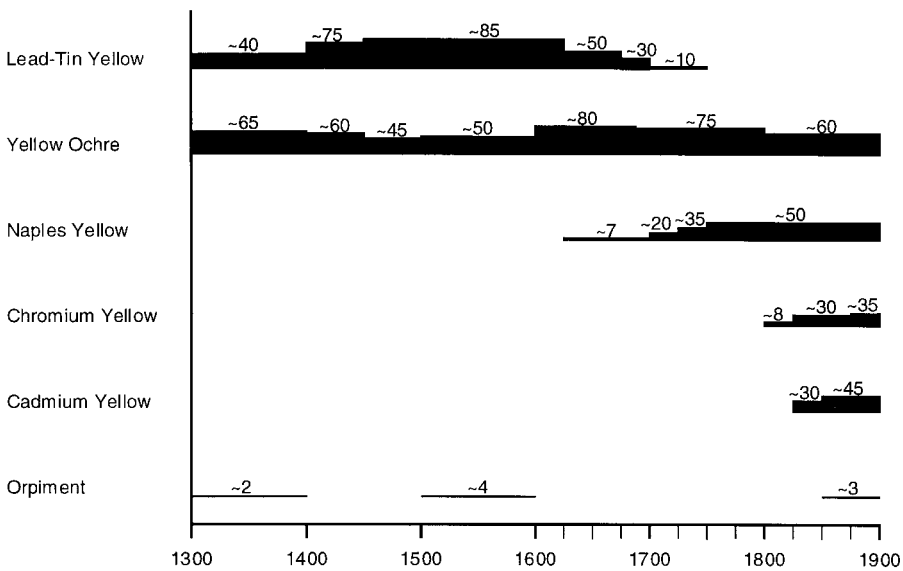

Fig. 8.1. Frequency pattern of yellow pigments in European easel painting 1300–1900 (*From* Hermann Kuhn, 1973).

molten tin. This lead–tin yellow pigment was used by artists from about 1300 to the mid-1700s. Figure 8.1 shows the number of times (normalized to 100 paintings) different yellow pigments have appeared in European easel paintings (H. Kuhn in "Terminal Dates for Paintings from Pigment Analysis" in *Application of Science in Examination of Works of Art*, edited by W.J. Young, published by Museum of Fine Arts, Boston (1973)). This information is based on examinations at the Doerner Institute, Munich, of authenticated paintings from 1300 to 1900. The information in the figure indicates that a painting containing Naples yellow (also called antimony yellow, lead antimonate) is with the high probability not earlier than the seventeenth century. Lead–tin yellow was the most common yellow pigment in the fifteenth, sixteenth and seventeenth centuries. The presence of lead–tin yellow in a painting indicates that the painting was executed before the middle of the eighteenth century. Chrome yellow (lead chromate) and cadmium yellow (cadmium sulfide) were introduced after 1800.

Among fakes detected by yellow anachronisms, a still life by Zurbarán deserves mention. It was purchased by the St. Louis Art Museum in 1942 as a work by the Spanish master, Francisco de Zurbarán (1598–1664), but came under suspicion when the museum curators learned that there was an almost identical painting in the Norton Simon Foundation collection. When the paintings were put side by side, art experts visually adjudged the St. Louis version to be somewhat inferior and downgraded its attributon to Zurbarán's son, Juan. However, even this later, seventeenth-century, dating could not be maintained once cadmium yellow had been detected in the lemons clustered on a platter. Cadmium yellow came into common use after 1800.

Another tip that a painting is not old, but made in modern times, is the forger's use of titanium dioxide, TiO_2. Titanium dioxide, or titanium white, has the greatest hiding power of any of the white pigments. It is the pigment used in correction fluid, or "whiteout." Titanium dioxide, TiO_2, occurs in two crystalline phases, anatase and rutile, both of which occur in nature. For paints it has a composition of 30% titanium diox-

TABLE 8.1

History of the Use of Titanium White Pigment*

Year	*History*
1791	The element titanium discovered
1821	Titanium dioxide (TiO_2) studies
1900	TiO_2 as yellow enamel opacifier
1913	Norwegian TiO_2 pigment patent
1919	Production of anatase/$BaSO_4$ pigment
1919	House paint (cream color)
1923	Anatase artist's paint (TiO_2/$BaSO_4$)
1925	Anatase artist's paint (TiO_2/$CaSO_4$)
1926	First white anatase pigment
1930	Gradual acceptance by artists
1934	Suggested for watercolors and tempera
1939	Production of rutile TiO_2/$BaSO_4$ pigments
1941	Production of rutile TiO_2/$CaSO_4$ pigments
1942	Suggested for oil-base paints
1957	Production of high quality (pure rutile pigment)

*SOURCE: W. McCrone, "1500 Forgeries" *The Microscope*, Volume 38, pp. 289–98 (1990)

ide and 70% barium sulfate. Titanium white is a pigment product of the 1900s (see Table 8.1). It is such a good white that a forger might be tempted to use it. To do so, however, could be the forger's undoing.

If the forger has taken scrupulous care to choose the right support, ground, pigment, binder (the choice is often between linseed and walnut oils), varnish, and signature, he must find a method to convincingly age the painting. The painting must look old, with age crackle (craquelure, the network of cracks in a painting, especially the varnish) appropriate to the purported period of the painting. Van Meegeren gave a painting the appearance of age by applying a light coat of varnish and rolling the painting around a cylinder to induce the age crackle (Hope B. Werness, *The Forger's Art*). For *The Supper at Emmaus*, Van Meegeren covered the entire surface with india ink, allowing the ink to penetrate the cracks in order to replicate the centuries of fine dust that accumulates in the cracks. The use of india ink as "old dust" is an indicator of fraud, and the ink can be detected by microscopic examination of the crackle.

The successful forger, in the end, is a kind of unscrupulous genius—part artist, art historian, materials scientist, and salesperson.

8.2 VISUAL EXAMINATION

We begin our objective study of authenticity by establishing the same line of inquiry that a museum does when receiving a new acquisition. Examination into the authenticity of a painting generally follows the sequence employed in determining treatment of a damaged or deteriorated painting.

The first step is to look at the painting. The use of the human eye is the most effective examination method (Color Plate 22). Visual examination by an art historian, curator, or conservator who is familiar with the production of the artist to whom a work is attributed is the first in a series of technical steps in laboratory analysis. It is in the first glance at a painting that one's visual encounter may stir doubts about authenticity.

Photography in normal, infrared (IR), and ultraviolet light is the next stage in the process. Photographs of the front of the painting under normal illuminations are accompanied by photographs using raking or tangental illumination to bring surface irregularities into bold relief.

Infrared reflectography (Chapter 7) allows a view beneath the surface. Underdrawings contrasting with a white ground show up in the IR and through their correlation with subsequent layers of painted images may indicate how images evolve as the painter considers issues of iconography, description, and composition. These layers are in varying degrees transparent to IR. In the same vein, x-radiography allows a view beneath the surface. With this proceedure one does not rely on the transparency

of paint to infrared radiation, but instead utilizes the increased absorption of x-rays by pigments containing high-atomic-number elements such as lead white or mercury, which is present in the color vermilion. The x-radiograph of Color Plate 23 given in Figure 8.2 shows the white areas in the face and in the book due to the presence of white lead. X-radiographs are used to reveal revisions (pentimenti) in the painting and the structure of the support on which the ground and subsequent layers have been applied.

In the search for fakes, infrared reflectography and x-radiography play an important role. Because underdrawings and revisions are quite common in authentic paintings, their absence might suggest chicanery. The lack of underdrawings or pentmenti alone, however, is not proof of fakery.

Fig. 8.2. X-radiograph of *Madonna* by Bartola.
(Courtesy of Laboratoire de Recherche des Musées de France (LRMF)).

8.3 Dating and Pigment Identification

At this point we go beyond routine visual examination procedures and attempt to date the painting. The suspect work of art can be dated by dendochronology (Appendix L) if a wooden panel support is used or by carbon-14 techniques (Appendix K) if a canvas is used as support.

One can also reach conclusions about a painting's date by determining the elemental composition of inorganic pigments. Element identification can be made by x-ray fluorescence, XRF (Appendix F), or by particle-induced x-ray emission (PIXE) (Appendix F). In both cases, a fingerprint of the elements is provided by the energies and intensities of the emitted x-rays that are characteristic of the element. Once the elemental composition is known, the pigment can be identified. The earliest date of pigment use can then be compared to the purported date of the painting. For example, Table 8.2 gives a list of blue pigments in use since 1700. A painting from 1780 containing cobalt stannate would be suspect.

Color Plate 24 is the portrait of a Madonna and child, in the same style as Color Plate 23 and attributed to the same artist. However, the position of the hands of the Madonna seemed "wrong" to the curator at the Louvre Museum in Paris. She asked for a further examination. Color Plate 25 shows Michel Menu at the particle accelerator with the painting of Color Plate 24 in the background preparing for pigment analysis by particle-induced x-ray emission (PIXE).

TABLE 8.2

Dates of Some Blue Pigment Use*

1700	Prussian blue, ferric ferrocyanide
1802	Cobalt blue, cobalt aluminate
1824	Ultramarine (artificial), sodium aluminum silicate
1850	Cerulean blue, cobalt stannate
1935	Manganese blue, barium mangenate

*SOURCE: San Francisco Museum of Art Conservation Laboratory

PIXE analysis indicated that the red blouse in Color Plate 24 contained the element cadmium. This is a direct tip-off that the painting is a modern fake. Table 8.3 shows that cadmium red pigments are post-1900. The painting was thought to be dated at around 1600.

To produce analytical images outside the range of human vision, a few museums have used, in addition to low-energy photons (infrared reflectography) and high-energy photons (x-radiography), nuclear reactors to produce neutron activation known as autoradiography (Chapter 7 and Appendix G). The painting takes its own picture with the emission of energetic electrons (beta rays) during radioactive decay of neutron-activated pigments. The technique has been used in extensive studies of Rembrandt (Maryan Ainsworth, et al. *Art and Autoradiography*, The Metropolitan Museum of Art, New York (1987)) and de La Tour (Claire Barry in Philip Conisbee, *Georges de La Tour*, National Gallery of Art, Washington (1996)), and presently the State Museum of Berlin is involved in autoradiographic examinations of works by various artists.

Autoradiography documents the location of many of the inorganic elements in a painting. Not all elements are shown because not all elements form radioactive products or have decay rates detectable within the time constraints of the procedure. The images resulting from detectable pigments reveal an orchestration of visual components which

TABLE 8.3

Dates of Cadmium-Containing Pigments*

1910	Cadmium red, cadmium sulfo-selenide
1926	Cadmium red lithopone, cadmium sulfo-selenide with barium sulfate
1846	Cadmium yellow, cadmium sulfide, CdS
1927	Cadmium yellow lithopone, cadmium sulfide with barium sulfate

*SOURCE: San Francisco Museum of Art Conservation Laboratory

generally follows a characteristic pattern associated with a particular artist or period. Autoradiographs, therefore, are helpful in authenticating and dating paintings. Analysis of autoradiographs of a painting attributed to de La Tour showed it to be a workshop copy of a famous lost original.

8.4 SAMPLING

Methods of analysis are called destructive or invasive when they require the removal of a sample of material from a painting (even extremely small, microscopic ones). The samples are taken from the edges of paintings or from areas of loss (lacunae). The samples are generally less than a millimeter in size, but even so, painting curators are offended by any loss.

Once obtained, the samples are subjected to a number of analytical methods. Optical microscopy reveals the structure of the paint layers from the ground to top varnish layers. Photomicrographs give a clear image of the layer stratigraphy. Refractive indices can be determined, and polarized-light microscopy is used to study the structure of pigment particles. Ultraviolet-light microscopy gives the fluorescent properties of the pigment; scanning electron microscopy provides particle size and morphology; and combined with x-ray emission, energy-dispersive spectroscopy gives elemental composition. X-ray diffraction analysis gives the crystal structure and thus completes the identification of the compound: composition, crystal structure, color, and refractive index. Various methods of chemical analysis identify organic binders and pigments.

The modern forger realizes that the chemical analysis of samples of pigments, grounds, and supports must face rigorous analysis. The forger cannot hope for forgiveness once scientific analysis is undertaken. Too much is known about pigment types and history to pass off a modern-day pigment as representative of that used in prior centuries.

8.5 FAKE/NO FAKE

Unfortunately, forgery continues. In spite of the vast array of analytical techniques that can be applied to the authentication of paintings, many fakes continue to enter the art market. We want to believe that there has been hidden somewhere for decades a lost Matisse or van Gogh just waiting to be discovered. The financial rewards for discovering such a painting are staggering, so forgers continue to take their chances and cover their tracks. In most cases, it is only when a painting is considered for

acquisition by a museum that proper and thorough analysis might reveal it to be a fake. Most major museums now have analytical laboratories in addition to the considerable resources of curators, conservators, and research staff that all together provide the connoisseurship to determine authenticity.

Object of Interaction 9

9.0 Beyond Analysis

The analysis of paintings provides extremely valuable information to those concerned with the conservation, authenticity, and art-historical aspects of these very complex art objects. Analysis also establishes for the practicing artist a body of practical knowledge concerning historical methods and materials. We have made the general argument that the information obtained through scientific methods of analysis in conjunction with an understanding of how paintings interact with the forces of nature expands our appreciation of paintings.

That said, it is important to recognize that paintings most often reveal their potential in the most elemental and direct way—simply by being viewed. The medium of light becomes a means of activating what might at first seem a passive relationship between painting and viewer. The phenomenon of a painted blue shape perceived as a blue shape by the viewer is dependent on true interaction between painting and viewer. The painting as an object is constructed in such a way as to utilize the physical characteristics of matter and light as well as the physiological mechanics of vision. Understanding the process of interaction adds a level of appreciation for the potential that paintings have for generating profound experiences for their viewers, but paintings project their most profound truths by means outside of the realm of analysis and historical relativity—sensory reception initiating psychological, physical, and emotional responses.

The use of analytical technology raises some very difficult questions. Artists have, through a series of decisions and actions, left us paintings that have a very particular construction and image. Setting

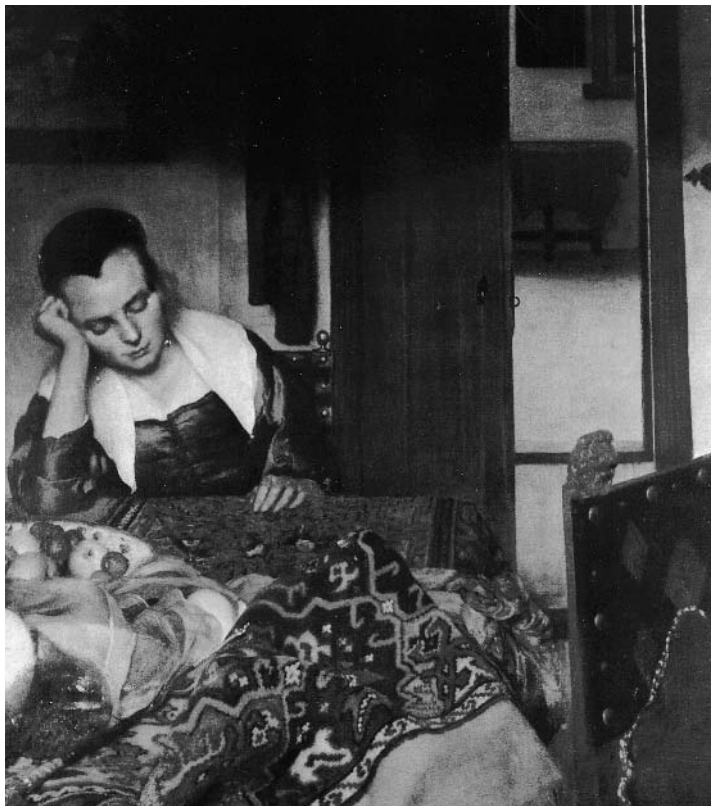

Fig. 9.1. *A Girl Asleep,* Jan Vermeer, c. 1657. Oil on canvas, 87.6 × 76.5 cm. The Metropolitan Museum of Art.

aside the effects on construction and image imposed by the forces of history and nature, we assume that what the artist has intended to express (or has discovered through the act of painting) is present in the painting *as we see it*. The artist has decided that it is finished or for some reason has abandoned it in its present state. All layers below the surface, including grounds, underdrawings, underpaintings, pentimenti, even areas of paint scraped away, have an effect on what is projected from the surface of the painting, but the artist has chosen not to make them visible. We are given only *what we see*. Until recent times, *what we see* has meant *what we see using only our eyes*. Since *what we see* can now mean *what we see with our eyes unaided or aided by various technologies,* are we compelled to reinterpret what is recognized as the information or experience generated by a painting? And is this reinterpretation then a violation of the intentions of the artist?

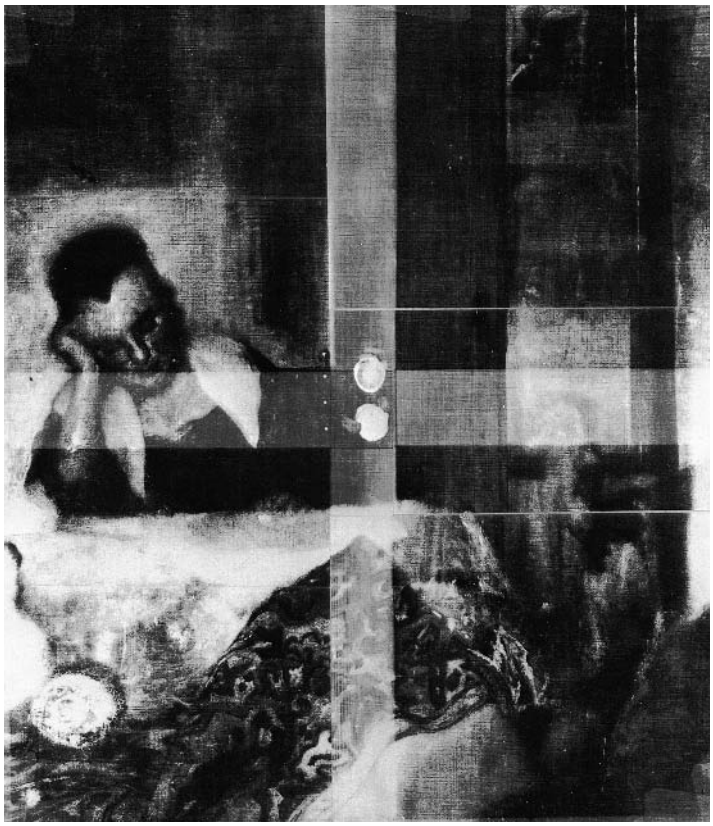

Fig. 9.2. X-radiograph of *A Girl Asleep* by Jan Vermeer.
One can detect in the area of the doorway on the right side of the painting vestiges of an image of a man with a broad-brimmed hat and just below center, a dog turned away from the viewer.

For some, the reinterpretation of a painting based on the reading of analytical data might seem a violation of what has been left to us by the painter. This is most likely the case when the iconography in the painting has changed dramatically from layer to layer. A case in point is the painting *A Girl Asleep* by Jan Vermeer in the collection of the Metropolitan Museum of Art (Figure 9.1). It was revealed through x-radiography and neutron-induced autoradiography that a number of images had been edited by the painter from the state we perceive visually. One can speculate that the retrieval of these images (a man in an adjoining room and a dog passing through a connecting doorway, for example, shown in Figure 9.2), helps to form a narrative for this very enigmatic painting. The overpainting of these images could have resulted from the painter hav-

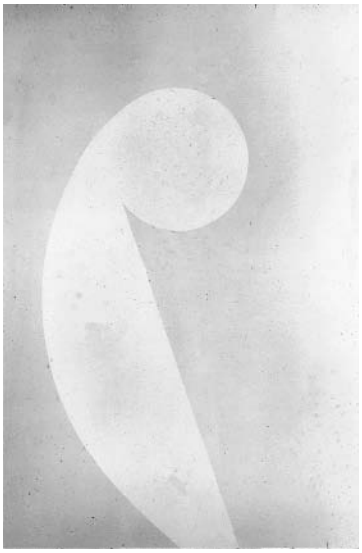

Fig. 9.3. X-radiograph of *Viol*. The image has been selectively retrieved from a layer beneath the surface. X-rays are absorbed by the pigment vermilion in the central shape due to the high concentration of mercury

ing changed the narrative, or an attempt at synthesis or clarity—to eliminate overly symbolic or descriptive elements. We do not know the motivation, but we are compelled in some way to reconcile the recovered information with what we understand the painting to mean based on what we see on its surface.

In contrast with this perceived sense of intrusion, the painting *Viol* shown in Color Plate 26 was intended to take advantage of a number of the analytical procedures described in this book. Throughout the process of making the painting, the choices of imagery, color, and other aesthetic concerns were orchestrated to be interpreted through the intervention of x-radiography, neutron-induced autoradiography, and infrared reflectography. The resulting images (Figures 9.3, 9.4, 9.5) are considered to be works of art on their own terms as well as aspects of the original painting. These supplementary images have very little analytical value, but operate as a way to make visible the compositions and recompositions of the visual material held within the layers of the painting. Whatever is covered by the surface layer of paint is meant to be retrieved.

It may seem curious that paintings retain the qualities that have been appreciated by viewers for hundreds

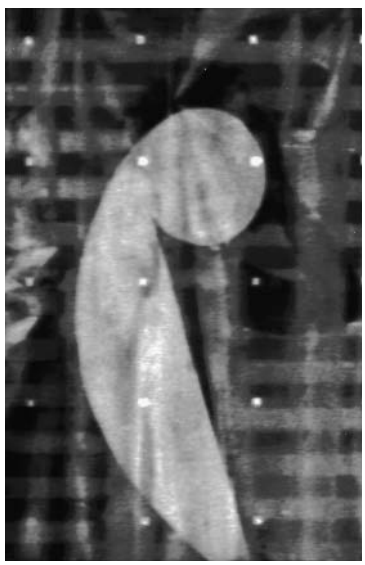

Fig. 9.4. Infrared reflectogram of *Viol*. A composite image of the same shape shown in Figure 9.3 partially obscuring a dark figure against a field of horizontal stripes. Some pigments, such as the vermilion shape, are highly reflective to IR radiation, while the dark colors used for the figure (raw umber) and the stripes (cobalt blue) absorb the radiation.

Fig. 9.5. Neutron-induced autoradiograph of *Viol.*
In this exposure, beta radiation is being emitted by several radioisotopes, allowing the figure to become more visible. The vermilion shape shown in Figures 9.4 and 9.5 is now invisible. The large areas of gray surrounding the figure result from the presence of gold leaf in the painting.

of years in spite of our *new* view. Paintings survive the intrusions of analysis in much the same way that humans do in spite of x-radiographs, blood tests, CAT scans, and the Human Genome Project. One appreciates the painting-as-image through the characteristics of the painting-as-object, but there remain aspects of identity (the essence of identity perhaps) that confound analysis, that are the inexplicable qualities that compel us to interact with a work of art in the first place.

This page intentionally left blank

A P P E N D I C E S

This page intentionally left blank

Photons, Electrons, and the Photoelectric Effect

A

The focus in this book is on the interaction of electromagnetic waves with electrons contained in the pigments, binders, and support that comprise a work of art.[1] These waves have wavelengths that range from 1 nanometer (10^{-9} meter) for x-rays to 1 kilometer (10^{3} meters) for radio waves. Wavelengths of visible light are in the range of 400 to 700 nanometers (nm). In this appendix we consider the formulation of photon wavelength and energy as well as the absorption of a photon by an electron.

Moving waves can be described by their frequency, or number of waves per second, as well as by their wavelength. If a train of waves is moving past a stationary observer at a frequency of f complete cycles, or waves, per second, and if each of these has a wavelength of λ centimeters per cycle, then the wave must be moving at a speed of v cm per second. The velocity (v), wavelength (λ), and frequency (f) are related by

$$\text{velocity} = \text{frequency}\left(\frac{1}{\text{time}}\right) \times \text{wavelength(distance)} = \frac{\text{distance}}{\text{time}},$$

$$v = f\lambda. \tag{A.1}$$

All electromagnetic radiation moves in a vacuum at a universal speed. This is the speed of light, c = 30,000,000,000 centimeters per second (usually written in powers of ten, $c = 3 \times 10^{10}$ cm/sec). The

[1]Information is also available on the Internet in Readings and Activities in Patterns in Nature. http://acept.la.asu.edu./PiN

universal speed of light in a vacuum goes against our intuition: We would expect that high-energy (short wavelength) radiation would move faster than low-energy (long wavelength) radiation. We can consider light as a stream of minute packets of energy, photons, which create a pulsating electromagnetic disturbance. A single photon differs from another photon only by its energy. In empty space (vacuum) all photons travel with the same velocity. Photons are slowed down when they pass through different media such as water, glass, or even air. This slowing down accounts for the refraction, or bending, of light by optical lenses. The energy of the photon is not changed, but the wavelength is. Photons of different energies are slowed by different amounts, which leads to the dispersion of light and the appearance of rainbows.

Because the speed of light in a vacuum is constant, if we know either the frequency or the wavelength of electromagnetic radiation we can calculate the other quantity from equation A.1. The frequency of the electromagnetic vibration we call light is given in units of "hertz" (abbreviated Hz and named after Heinrich Hertz (1857–1894) a famous German investigator of electromagnetism). One hertz is one vibration per second; the range of the pure spectrum perceived by the eye extends from about 4.3×10^{12} Hz in the red range to about 7.5×10^{12} Hz in the violet.

This aspect of the discussion suggests that light, and other electromagnetic radiation, is composed of waves. It was very disturbing, therefore, when phenomena were discovered (around 1900) that clearly indicated that light is made up of particles, called photons. One such phenomenon involved the *photoelectric effect*. It was known that if one shines a beam of light on a clean surface of a metal, electrons will be ejected from the metal. The process is shown in Figure A.1. The light has to exceed a certain energy to remove electrons from the metal surface. If the light has more than the minimum energy required, then the extra energy will be given to the ejected electrons as kinetic energy of motion.

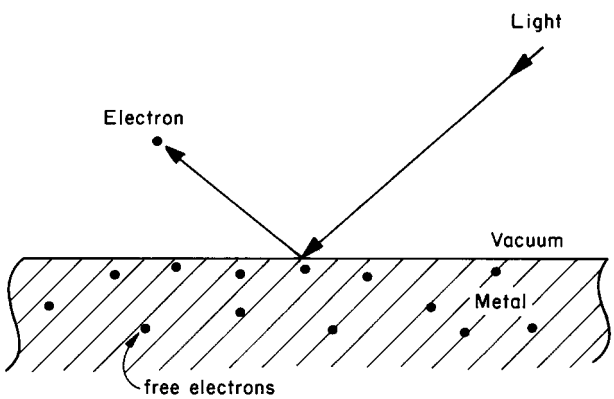

Fig. A.1. In the photoelectric effect a photon incident on a surface (here a metal surface in a vacuum) transfers its energy to an electron, which leaves the surface and is detected. The photoelectric effect demonstrates the particle nature of light.

In this discovery light of a single wavelength behaved as if it consisted of separate particles, photons, all with the same energy, with each ejected electron being the result of a collision between one photon and one electron in the metal. Greater intensity of light meant only that more photons were hitting the metal

per second and more electrons were ejected, not that there was more energy per photon. The energy of the outgoing electrons depended on the frequency of light used.

The energy (E) of the incoming photons was found to be directly proportional to the light frequency (f), which can be written as

$$E = hf \tag{A.2}$$

in which h is a constant.

Max Planck first proposed this relationship between energy and frequency in 1900 as part of his study of the way in which heated solids emit radiation. The constant h is called Planck's constant in his honor and has a value $h = 4.136 \times 10^{-15}$ eV sec.

For photons, the property most readily measured is their energy. The different colors of light, for example, are thought of as representing photons of different energies. The link between the particle theory and the wave theory lies in Planck's fundamental postulate of quantum theory given by equation (A.2).

There is an inverse relation between the energy E of the photon and the wavelength:

$$\text{Energy } (E) = \frac{\text{constant}}{\text{wavelength } (\lambda)} \tag{A.3}$$

The energy E in equation A.3 can be expressed in many units. In the analysis of art and in the description of light, the most convenient unit of energy to use is the electron volt, abbreviated eV. In terms of wavelength λ in nanometers (nm) and energy E in electron volts (eV), equation (A.3) can be expressed for light traveling in a vacuum as

$$E \text{ (eV)} = \frac{1240}{\lambda \text{ (nm)}} \tag{A.4}$$

and shown in Figure A.2.

The constants and numerical relations in equations (A.3) and (A.4) are found from Planck's equation (A.2) by writing the relationship for frequency (f) in (A.1) as

$$f = \frac{c}{\lambda}, \tag{A.5}$$

where c is the velocity of light in vacuum so that Planck's equation becomes

$$E = \frac{hc}{\lambda}. \tag{A.6}$$

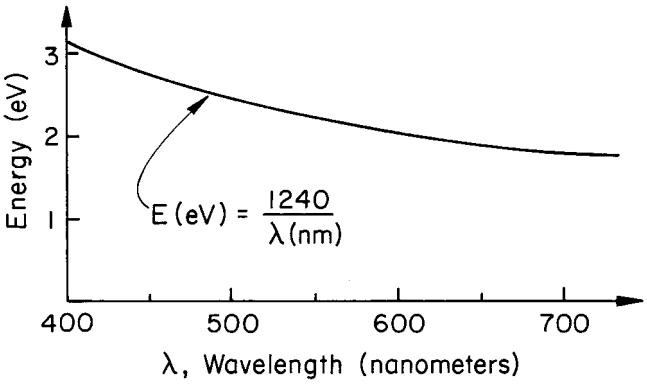

Fig. A.2. A curve that shows the relationship E (eV) = 1240/λ (nm) given in (A.4) for the energy in eV versus photon wavelength in nanometers for the visible region of the electromagnetic spectrum.

The value of Planck's constant h is 4.136×10^{-15} eV sec and the velocity of light c is 3×10^8m/sec, or 3×10^{17} nm/sec, so that $hc = 12.4 \times 10^2$, or 1240 eV nm.

We use nanometers (nm) and electron volts (eV) in this text. Other units for the wavelength λ, the distance between two crests of the light wave, are centimeters (cm), micrometers or microns (μm), where 1 micron = 10^{-4}cm, and angstrom units (Å), where 1 Å = 10^{-8} cm.

Visible light is composed of photons in the energy range of around 2 to 3 eV (Chapter 3). Orange light with a wavelength of 620 nanometers is composed of photons with energy of 2 eV. It is the energy range of 2 to 3 eV that triggers the photoreceptors in the eye. Lower energies (longer wavelengths) are not detected by the human eye but can be detected by special semiconductor infrared sensors. Higher energies (shorter wavelengths) such as x-rays damage human tissue and are detected by x-ray sensitive photographic film or again by special semiconductor devices.

Light rays are composed of photons whose energy or wavelength specifies a color from red to violet. An increase in the intensity or brightness of a light source increases the number of photons per unit area, or flux. *Brightness* of light refers to the *flux* of photons *not* their *energy*.

REFRACTION, REFLECTION, AND DISPERSION

B

The velocity of light *in vacuum* is constant for all wavelengths of light. When light enters a *medium* such as glass, the velocity of light decreases. In glass there is a decrease in velocity of 33% (velocity changes from 3 to 2×10^{10}cm/sec), and in other materials the decrease can be even more substantial, 50 to 60%.

A beam of light in air will change direction, be refracted, when entering glass at an angle to the surface normal; this bending of the beam is called refraction.[1] Refraction is an effect that occurs when a light wave passes at an angle to a boundary from one medium to another in which there is a change in velocity. Consider the case where light enters a medium where the wave velocity decreases. The wave inside the new medium is moving slower; therefore, since it remains connected to the faster-moving wave in the old medium, the wave turns, becoming more nearly parallel with the boundary, as shown in Figure B.1. The greater the change in velocity, the greater the change in direction.

B.1 INDEX OF REFRACTION

Refraction refers to the change in direction of light resulting from the change in the velocity as light passes from one medium into another.

[1]Information is also available on the Internet in Patterns in Nature under Readings on Reflection and Refraction. http://acept.la.asu.edu/PiN

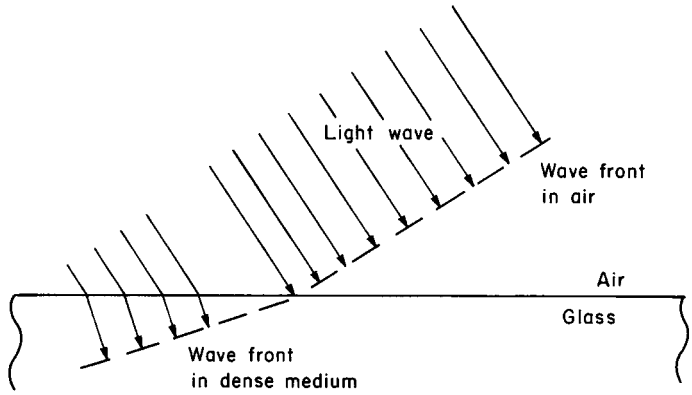

Fig. B.1. Schematic illustration of a wave front of a light wave in air incident on a transparent medium (here, glass) that has a greater density (higher refractive index) than that of air. The wave moves more slowly in glass than in air, and consequently the wave is bent at the air/glass interface to accommodate the transition between the faster motion in air and the slower motion in glass.

Figure B.2 shows the angle of incidence i and the angle r of the refracted beam measured to the normal (an imaginary line perpendicular to the interface between the two media). The photon energy does not change, and therefore the wavelength must decrease (Equation (A.3) in Appendix A). Only when the light beam is traveling perpendicular to the surface of the material will a change in velocity occur without a change in

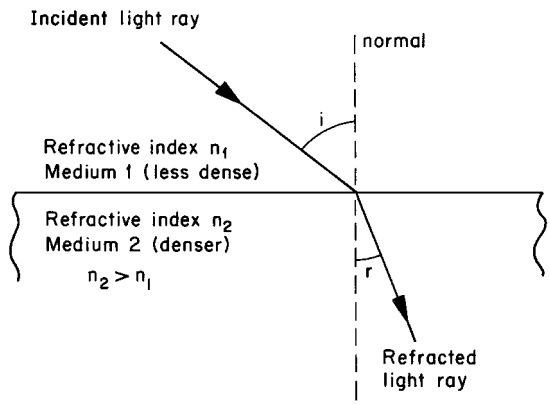

Fig. B-2. The refraction of light rays for a light ray in a less dense medium (index of refraction n_1) incident at an angle i from the normal to a more dense medium (index of refraction n_2). The refracted light ray is at an angle r to the normal, where the magnitude of r is less than i.

the direction of the light beam. Every medium produces a characteristic velocity for a specified wavelength of light.

The *refractive index* n *of a medium* refers to the ratio of the velocity (c) of light in a vacuum to its velocity (v) in the medium of interest.

$$n = \frac{c \text{ (vacuum)}}{v \text{ (medium)}}, \tag{B.1a}$$

which can be rewritten in terms of velocity as

$$v = \frac{c}{n}. \tag{B.1b}$$

Varnish has a refractive index of 1.5, so that visible light will travel 1.5 times slower in varnish than in a vacuum. The refractive index for a perfect vacuum is 1. The refractive index for air is 1.003. For convenience, air instead of vacuum will be used as the reference medium; the values of n for air differ insignificantly ($\approx$0.3%) from that in a vacuum.

There is a direct method of obtaining n in transparent materials by measuring the angular relation between incident and refracted beams of light. The index of refraction can be obtained from the ratio of the sine of the angle i to the sine of the angle r. Snell's law, formulated in 1621 by Willebrod Snell, gives the relationship

$$\frac{n_2}{n_1} = \frac{\sin i}{\sin r}, \tag{B.2}$$

where n_1 is the index of refraction of the less dense medium and n_2 is the refractive index of the denser medium. If air is the less dense medium we set $n_1 = 1.00$; then Snell's law is reduced to

$$n_2 = \frac{\sin i}{\sin r}. \tag{B.3}$$

The sine relation is shown in Figure B.3. The ratio sin i/sin r is a constant for a given material and a given wavelength.

The refractive index of the material is a useful parameter for discussing how a material affects light. Table B.1 contains values of the refractive index for selected natural materials used in pigments and binders.

The values of the refractive index n for clear materials vary from 1.33

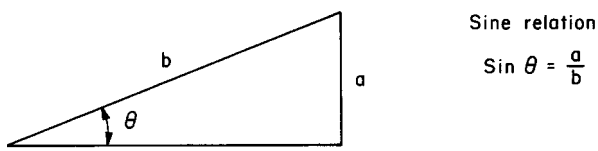

Fig. B.3. A right triangle is used to illustrate the geometric relation sin $\theta = a/b$.

TABLE B.1

Index of Refraction *n* for Pigments, Binders, and Others

Material	*n*	*Material*	*n*
White		*Red*	
Titanium dioxide (rutile)	2.71	Vermilion	2.97
White lead (lead carbonite)	2.04	Red lead	2.41
Zinc white (zinc oxide)	2.01	Cadmium red	2.64–2.77
Blue		*Binders and Diluents*	
Cerulean blue	1.84	Water	1.33
Azurite	1.78	Gum arabic solution 10%	1.334
Cobalt blue	1.74	Gum arabic solid	1.476
Prussian blue	1.56	Egg tempera	1.346
Ultramarine, natural (lazurite)	1.50	Glue solution, 10%	1.348
		Spirits of turpentine	1.47
Green		Poppy-seed oil	1.469
Green earth	2.5–2.7	Walnut oil	1.477
Chromium oxide green	2.5	Linseed oil	1.478
Cobalt green	1.94–2.0	Tung oil	1.517
Malachite	1.81	Venice turpentine	1.53
		Mastic	1.536
Yellow		Shellac	1.516
Orpiment	2.74	Beeswax (molten 74°C)	1.442
Cadmium yellow	2.35–2.48		
Massicot (litharge)	2.63		
Naples yellow	2.01–2.28	Diamond	2.418

Mean index of refraction *n* for pigments, binders, and other materials of interest in art. Mean index calculated for uniaxial and biaxial crystals from the procedure by Brill. (Brill, *Light* (Plenum Press, New York, 1980)), page 83.

for water to a value of 2.71 for rutile, a form of titanium dioxide, TiO_2. The values of the refractive index vary for different orientations of the light to the crystallographic axes of crystal materials. In Table B.1 we use an average value of the refractive index because the pigment crystallites in paint are randomly oriented with respect to one another. An average value is also used for liquid-based media, such as binders (linseed oil).

B.2 Reflection and Scattering

When light is incident on a transparent material such as glass, the light is reflected from the surface as well as refracted as it passes into the material. As shown in Figure B.4, the angle of incidence i is equal to the angle of reflection i':

$$\text{angle of incidence } (i) = \text{angle of reflection } (i') \tag{B.4}$$

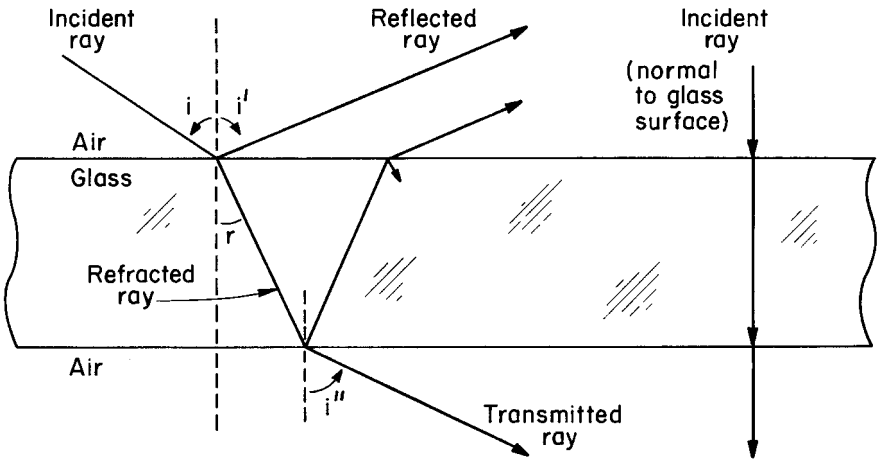

Fig. B.4. The paths of rays of light incident on a glass plate at angle of incidence i and then about 4% reflected at the air/glass interface and the remainder refracted at an angle r. As the light ray exits at the glass/air interface a portion is reflected and the remainder is refracted, so that the path of the transmitted ray is parallel to that of the incident ray (angle i = angle i'').

The amount or intensity I of the reflected light depends on the difference in the refractive indices n_1 and n_2, where n_1 is the refractive index of the incident medium and n_2 is that of the reflecting medium. The ratio of intensities is

$$\frac{I_{reflected}}{I_{incident}} = \left(\frac{n_2 - n_1}{n_2 + n_1}\right)^2. \tag{B.5}$$

If the incident medium is air, $n_1 = 1$, then

$$\frac{I_{reflected}}{I_{incident}} = \left(\frac{n_2 - 1}{n_2 + 1}\right)^2. \tag{B.6}$$

If the light is incident in air on glass with refractive index of $n = 1.5$, then

$$\frac{I_{reflected}}{I_{incident}} = \left(\frac{1.5 - 1}{1.5 + 1}\right)^2 = 0.04,$$

or 4% of the incident light is reflected from the glass surface.

When exiting the glass, the light rays are again refracted as the rays pass the interface between a denser medium, glass, to a less dense medium, air. Snell's law is obeyed, and the rays are bent away from the normal and now become parallel to their original direction when inci-

dent on the glass. This confirms common observation that one does not see dispersion of white light when viewing a light source through a plate of glass whose faces are parallel to each other. These paths are shown in Figure B.4.

In tracing the paths of light rays through the interfaces between various media, two facts stand out:

(a) Light paths are reversible and obey the same angular relations from either direction.

(b) Light is reflected and refracted at every interface where there is a change in the index of refraction across the interface. Even an uncoated sheet of glass acts as a mirror so that you can observe, albeit faintly, your own image reflected from the glass.

If light is inside a material such as glass with a larger refractive index n_2 than that of the material outside such as air, n_1, there is an angle, the critical angle of incidence, beyond which the light is reflected *back* into the material and does not escape. This is *total internal reflection*. The critical angle i_c is given by

$$\sin i_c = \frac{n_1}{n_2}. \tag{B.7}$$

For light exiting glass, $n_2 = 1.5$, the relation becomes

$$\sin i_c = \frac{1.0}{1.5},$$

and the value of the critical angle of incidence is 41°. Light in glass at any angle of incidence to the normal that is 41° or greater will be reflected from the glass–air interface back into the glass. The shaded area in Figure B.5 is the angular region where light is reflected back into the glass. The greater the difference in the two indices of refraction, the smaller the amount of light that can escape. For example, titanium dioxide with $n = 2.71$ has a smaller critical angle at the air–titanium dioxide interface than that of the air–glass interface. A coating of particles of titanium dioxide, for example the white correction fluid called whiteout, appears opaque because less light leaves the particles once it penetrates into the material.

The amount of light reflected or scattered from particles such as paint pigments depends on the size of the particles relative to the wavelength of light. There is a general observation that for dimensions greater than the wavelength of light, the smaller the particle, the more light is reflected. For example, if one takes colored glass and breaks it into small pieces, there is an increase in the amount of reflected, as opposed to transmitted, light. There is an increase in surface area with angled sides provided by the pieces of glass, so that the light is scattered. The smaller the pieces of glass, the higher the ratio of scattered light to transmitted

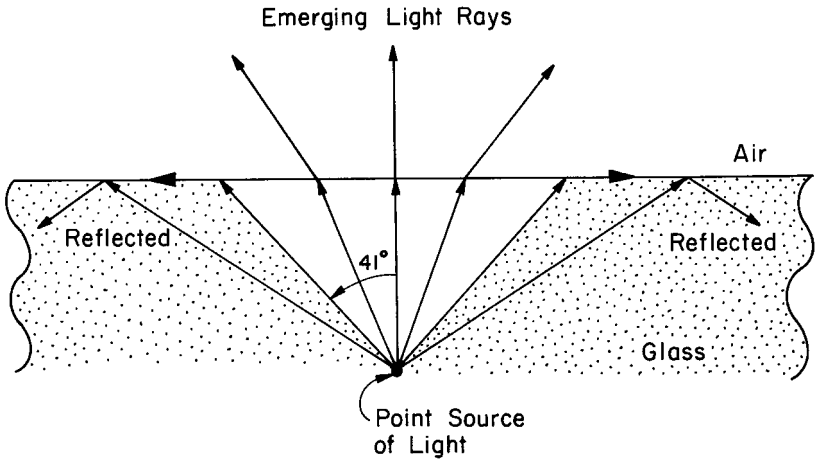

Fig. B.5. The internal reflectance at an glass/air interface for light rays from a point source in glass. Light rays incident at angles to normal greater than the critical angle (here, 41° for glass to air) do not leave the material and are reflected at the glass/air interface.

light. If the pieces are pulverized, the colored glass appears almost white, although the color component in the glass is still present. Particles that are large compared to the wavelength of visible light do not scatter colors selectively. If particles are much smaller than the wavelength of light (for example a tenth the wavelength), the shorter wavelengths, the blues, are scattered more strongly than the longer wavelengths, the reds. The sky appears blue because of light scattered from small particles and gas molecules in the air.

B.3 DISPERSION

The index of refraction or decrease in velocity depends on wavelength, with the velocity decrease more pronounced for blue light than for red. Thus, when parallel beams of red and blue light enter glass, the blue light is bent more at the air/glass interface than the red light (Figure B.6). This spreading of the beam is called dispersion. The dispersion curve in the visible region of crown glass is shown in Figure B.7. Although the difference in refractive index between that for blue, $n = 1.51$, and red, $n = 1.495$, is small, the difference is sufficient to cause a noticeable spread, or dispersion, in the two paths of red and blue light.

In 1672, Newton showed experimentally that a beam of white light, when passed through a glass prism, is decomposed into a spectrum con-

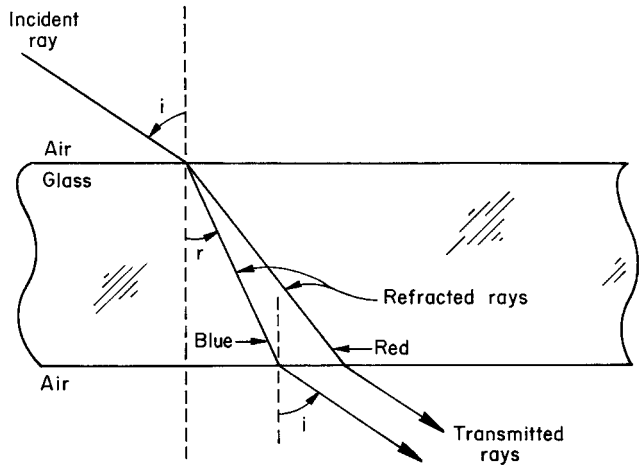

Fig. B.6. Incident rays of red and blue light are refracted through different angles at the air/glass interface and emerge at the glass/air interface so that the transmitted rays are parallel to the incident rays.

sisting of a large number of colors, from the red to the violet, which gradually merge into each other, and that these colors are components, not modifications, of white light. Figure B.8 shows this well-known property of transparent materials and light. The explanation lies in the fact that light of all wavelengths travels at the same velocity in empty space, but light in any other medium does not travel with the same velocity for

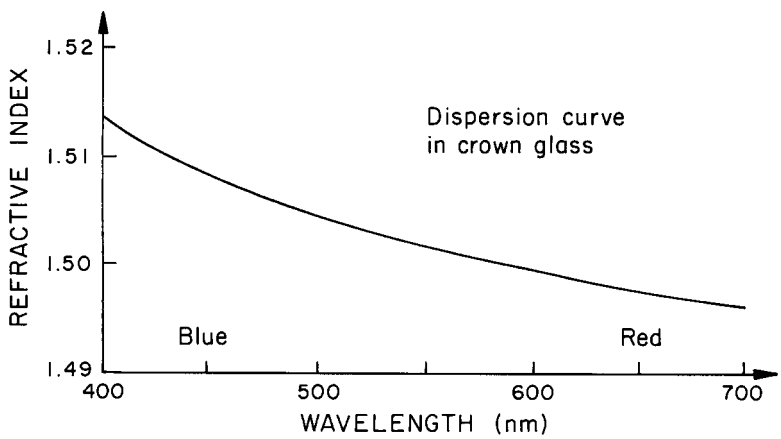

Fig. B.7. The dispersion curve of the refractive index n versus the wavelength in the visible region of the spectrum for a colorless crown glass. (*Adapted from* K. Nassau, *The Physics and Chemistry of Color* (Wiley-Interscience, New York, 1983)).

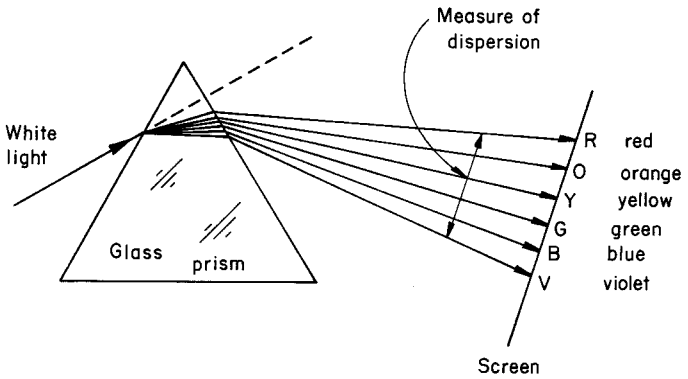

Fig. B.8. The production of the spectrum of visible light by white light incident on a triangular glass prism.

all wavelengths. The dispersion produces colors in intervals ranging from the longest to the shortest wavelength, red, orange, yellow, green, blue, and violet, as shown in Figure B.8.

The case of normal dispersion is observed for colorless transparent media. It is "normal" because red light (longest wavelength) has the greatest velocity in such media and the least dispersion, while the violet light (shortest wavelength) has the least velocity and the greatest dispersion. The other colors are divided sequentially between red and violet.

B.4 Varnishes and Refraction

The color of tempera paint changes dramatically when covered with varnish or mixed with a binder. The simplest change in appearance is the change from a rough matte surface (diffuse reflection, where light is scattered in all directions from an irregular surface) to a smooth, glossy surface (specular reflection, where light is reflected in one direction).

Tempera and pastels are paints with highly concentrated pigments, i.e., there is very little binder medium in the paint. The light interacts directly with the paint pigments without passing through an intermediate layer. The paints mostly rely on absorption and surface reflection of light to produce color. When a varnish layer is applied to the tempera, we change the index of refraction relations as shown in Figure B.9. Here we assume average values of refractive index for the varnish ($n = 1.5$) and for the concentrated pigment ($n = 2.6$).

The difference in refractive index Δn between the air and the pigment is 1.6, but when the varnish layer is applied, two interfaces exist.

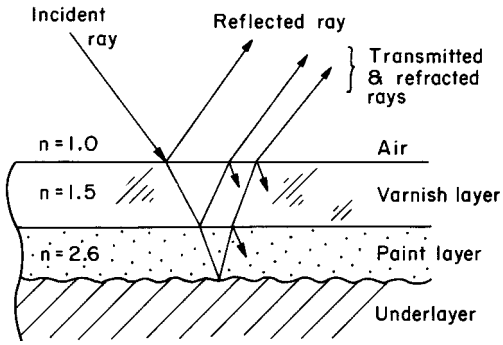

Fig. B.9. Paths of light incident in air on and reflected from a painting with a layer of varnish (refractive index $n = 1.5$) on a paint layer with a refractive index $n = 2.6$).

One is between the air and varnish, with $\Delta n = 0.5$, and the other is between the varnish and paint, with $\Delta n = 1.1$. The varnished paint surface is glossy, and more light is reflected from the varnished surface than from the unvarnished surface, leaving less light to be transmitted to and absorbed by the paint layer.

The reflection of light at the paint layer under a coat of varnish is less than that for the unvarnished paint layer because Δn is smaller at the paint–varnish interface than at the paint–air interface. Once inside the varnish layer, a greater percentage of the light is transmitted into the paint. As a result, more light can be absorbed by the pigment particles, and this will lead to a deeper and richer color.

B.5 Hiding Power

Hiding power is the measure of a paint's ability to cover a surface opaquely so that an underlying paint cannot be seen in visible light. Absorption is one factor in the hiding power of a paint. Darker colors absorb more intensely than lighter colors and hence have a greater hiding power.

The refractive index can play a major role in determining hiding power. The amount of light scattered or reflected from the interface of a composite of two materials depends strongly upon the difference between the indices of refraction of the two media. If the difference in the index of refraction is large at an air–surface interface, then the surface will be a good scatterer of light, and its transparency will be reduced. If there is no difference, then no light will be scattered at the interface, and all the light will pass into the material. For example, a glass object will "disappear" when it is immersed in a clear, colorless liquid if the index of refraction of the liquid is matched to that of the glass so that no light is deflected at the glass–solution interface. Hence the glass cannot be seen.

Consider the pigment–vehicle interface in a paint. If the difference in the refractive indices of the pigment and vehicle is large, then the pigment will be a good scatterer of light, and its opacity, or hiding power, will be large. The value of Δn is defined by

$$\Delta n = n_{\text{larger}} - n_{\text{smaller}}. \tag{B.8}$$

A large value of Δn leads to an opaque object or a paint with good hiding power, while a small Δn gives a translucent object or a paint with poor hiding power.

Watercolors tend to be more translucent when first applied than when dry. The value n_{H_2O} is greater than n_{air}, so that Δn involving the watercolor pigment becomes larger upon drying.

The relative hiding power of various whites in a common binder, say linseed oil, with $n = 1.48$, can be evaluated using their indices of refraction:

$$\begin{aligned} &\text{titanium dioxide} && \Delta n = 2.72 - 1.48 = 1.23, \\ &\text{lead white} && \Delta n = 2.01 - 1.48 = 0.53, \\ &\text{zinc white} && \Delta n = 2.00 - 1.48 = 0.52. \end{aligned}$$

Titanium dioxide produces the most opaque paint of the three, with the opacity of lead white and that of zinc white being quite similar to each other.

Photon Absorption: Visible, Infrared, and X-rays

C

The observation of the visible colors of a painting and the analysis of a painting by low-energy infrared (IR) and by high-energy x-ray photons all depend on the absorption of photons by the materials in the painting. The absorption mechanism is the same for all three regions of the electromagnetic spectrum, but the effects differ. In the visible region, absorption of selected wavelengths leads to the appearance of color, because the absorbed wavelengths are absent in reflected light. In the infrared at wavelengths of about 2 microns, the absorption of photons is greatly reduced for many pigments, and we can look through the paint layers and "see" the underpainting. For x-rays, the absorption of photons depends strongly on the number of electrons, or the atomic number, of the elements in the pigments. Pigments containing lead (lead white) or mercury (vermilion) are strong absorbers of x-rays. Thus an image of paint containing these pigments can be seen on x-ray sensitive photographic plates.

Photons are absorbed in a solid through a process known as the photoelectric effect, whereby a photon interacts with an electron by giving all its energy to the electron. In effect, the photon disappears, and energy is transferred to an electron. The photoelectric process is responsible for the absorption of visible light with energies of 2 to 3 electron volts (eV) as well as for x-rays with energies a thousand times greater than that of visible light. Electrons and photons are intertwined. A photon is created by an electron losing energy in a transition to an empty level. A photon is absorbed (disappears) by an electron gaining energy from the photon.

The absorption of photons in solids depends on the number of electrons that can accept a transfer of energy from the photon. Not all electrons meet this criterion. Some electrons are so tightly bound to their

orbital path around the atomic nucleus that the photon energy is unable to break the bonds. Other electrons are involved in the bonding between atoms and cannot be freed by the energy of the incident photons. For example, ordinary window glass is transparent to visible photons but is strongly absorbent to ultraviolet radiation, where the photons have energies only a few times greater than that of visible light. A similar situation is true in the infrared region, in which pigments are transparent to infrared energy but opaque to the higher-energy photons in the visible spectrum.

Photon absorption in the visible region of the spectrum depends on the atomic arrangement of the atoms and their bonding. Silicon (Si), a semiconductor with atomic number (Z) of 14, is transparent to infrared radiation, but aluminum, a metal with one fewer electron than Si (Z = 13) is strongly absorbing to infrared and visible radiation. Pure silicon is strongly absorbing to visible light, but silicon combined with oxygen is transparent. For the energetic photons in the x-ray region, photon absorption is much easier to predict and is independent of the details of atomic arrangement. It depends primarily on the electron concentration per unit volume. Since the concentrations of atoms per unit volume differ by a factor of only 2 or 3, the electron concentration in two materials can be estimated from the atomic number Z, which is equal to the number of protons in the nucleus, or, equivalently, to the number of electrons in the atom. Lead (Z = 82) absorbs x-rays much more efficiently than aluminum (Z = 13) and consequently is used in shielding around x-ray apparatus. X-ray absorption does depend on the energy of the x-rays and decreases with increasing x-ray energy E. Absorption is nearly proportional to the inverse cube of the energy (i.e., absorption is proportional to $1/E^3$) and hence decreases as x-ray energy increases.

In spite of the different material dependencies in the description of visible light and x-ray absorption, the mathematical description is the same for the two: the exponential decay law. This decay law is a result of the fact that each successive interval of equal thickness of a sample absorbs an equal fraction of the photons passing through it. Each successive interval, however, receives fewer photons than the preceding interval because photons have been absorbed in the previous intervals. For example, if the first interval absorbs one-half of the photons, then only half of the original number of photons are incident on the second interval, which absorbs one-half of these, i.e., one-fourth of the original number of photons incident on the sample. A third interval would absorb one-eighth the original number, and so on.

C.1 Mechanism for the Absorption of Light

The formula for the absorption of light in the simplest case starts with a beam of light of intensity (or flux of photons) I that has just penetrated

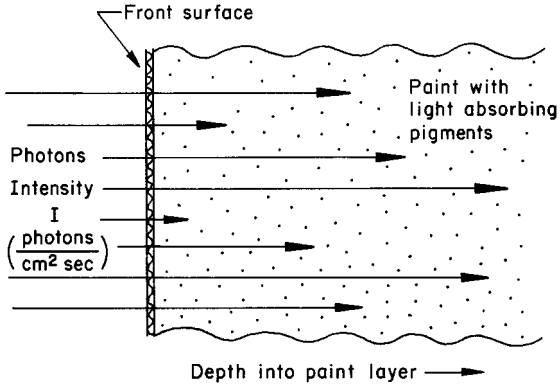

Fig. C.1. Schematic of light rays penetrating to different depths into a paint film with photon-absorbing pigment particles.

into a material with a uniform concentration of absorbing pigments. We ignore reflection and refraction. The photons penetrate into the material and are absorbed at different depths (Figure C.1).

The mechanism for absorption is that a photon transfers all its energy to an electron in the absorbing pigment. The photon is "lost" from the light beam by being absorbed in a single event. The electron is excited by the gain in energy to a higher energy state in the electron configuration around the atom in the pigment. This single event, the transfer of photon energy to an electron and the disappearance of the photon, is closely related to the photoelectric effect described in Appendix A, although here the electron is not ejected from the material. The electron is ejected from the atom in the pigment by the absorption of an x-ray. The atom is left in an excited state. As we will see in Appendix F, the de-excitation of the atom leads to the emission of x-rays.

The decrease in intensity of the light (or photon flux) as the beam penetrates into the material can be visualized if we separate the absorbing material into sets of thin slices, all of a thickness t (Figure C.2). The material is homogeneous, and the thickness t is chosen so that only a small fraction of the light is absorbed in passing through each layer. The symbol A is used to denote the fraction absorbed. The fraction of light absorbed in the first layer is AI, where I is the incident intensity; the amount of light transmitted through this layer is $(1 - A)$ times the incident intensity. For example, if the fraction of light absorbed per layer is 10% of the incident flux, then for 100 incident photons incident on the first layer, $AI = 0.1 \times 100$, or 10 photons will be absorbed and 90 transmitted to the second layer.

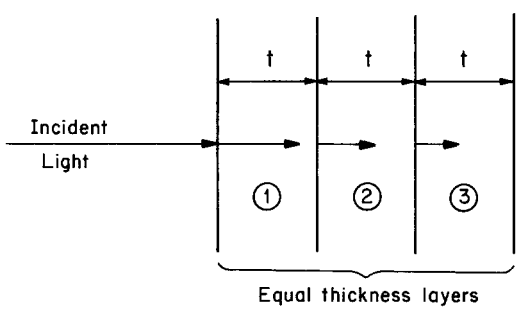

Fig. C.2. Light incident on a light-absorbing material that is represented by a stack of equivalent layers of thickness t. The lengths of the arrows decrease as the light penetrates, showing the decreasing intensity of light.

The light intensity incident on the second layer is $(1 - A)I$, and $A(1 - A)I$ will be absorbed on the second layer. The amount transmitted through the second layer is $(1 - A)^2I$. To continue our example, with 90 photons incident on the second layer, $A \times 90 = 0.1 \times 90 = 9$ photons will be absorbed and 81 transmitted. That is,

Layer 1: I photons incident, $AI = 0.1 \times 100 = 10$ absorbed, and
$(1 - A)I = (1 - 0.1)100 = 90$ transmitted;
Layer 2: $(1 - A)I = 90$ photons incident, $A(1 - A)I$
$= 0.1(0.9)100 = 9$ absorbed,
and $(1 - A)(1 - A)I = (0.9)(0.9)100 = 81$ transmitted.

This process continues, with fewer photons being transmitted into layer 3, layer 4, and so on, and fewer photons being absorbed in each successive layer, although the fraction A absorbed remains constant.

The absorption of photons is given in more general form in Table C.1 for an absorbed fraction A.

For n layers, the total absorption T_A in all layers for absorbed fraction A will be

$$T_A = A + A(1 - A) + A(1 - A)^2 + \cdots + A(1 - A)^{n-1}. \qquad \text{(C.1)}$$

The first term in equation (C.1) represents the absorption by the first layer. The second term represents the absorption by the second layer, and so forth.

The total transmitted light T_T through n layers is

$$T_T = (1 - A)^n. \qquad \text{(C.2)}$$

Equation (C.1) is more conveniently written using an exponential function. Using an absorption coefficient α, the intensity of light at depth t, $I(t)$ for an incident intensity I_0, is given by

$$I(t) = I_0 \exp(-\alpha t), \qquad \text{(C.3)}$$

where α is given as a fraction per distance such as 0.1 per mm. Figure C.3 shows the intensity of light as a function of penetration distance into materials with two different absorption coefficients. The exponential decrease is illustrated on a linear scale by the curves in Figure C.3. An increase in α leads to a decrease in penetration. At the depth where the product αt equals unity, the intensity has dropped by $1/e$, or a factor of about 0.37, times the incident intensity.

These relations rely on the fact that the fraction of light that is absorbed is independent of the intensity of the incident light. For a given

TABLE C.1

Transmission for Absorbed Fraction *A*

	Incident on layer	*Absorbed in layer*	*Transmitted through layer*
layer 1	I	AI	$(1 - A)\ I$
layer 2	$(1 - A)\ I$	$A\ (1 - A)\ I$	$(1 - A)^2\ I$
layer 3	$(1 - A)^2\ I$	$A\ (1 - A)^2\ I$	$(1 - A)^3\ I$
layer n	$(1 - A)^{n-1}\ I$	$A\ (1 - A)^{n-1}\ I$	$(1 - A)^n\ I$

Amount of light incident on, absorbed in, and transmitted through equivalent layers with absorbed fraction A and flux I incident on layer 1.

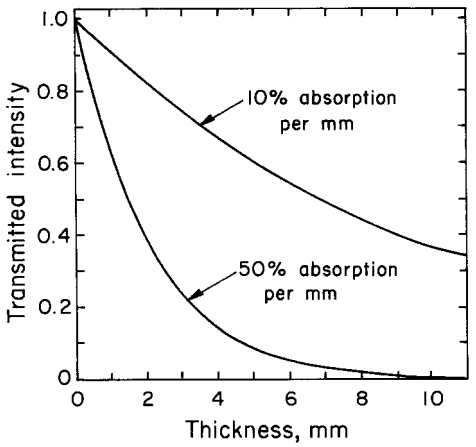

Fig. C.3. The intensity of light transmitted through an absorbing material as a function of thickness d in mm for (1) 10% absorbance and (2) 50% absorbance per mm (from T.B. Brill, *Light* (Plenum Press, New York, 1980)).

wavelength of light, each successive equi-thickness of the medium absorbs an equal fraction of light passing through it, but the amount of light the layers receive is successively decreasing. Hence, the intensity of light passing through a medium will decrease with depth. The exponential attenuation coefficients apply for x-rays as well as photons in the visible portion of the electromagnetic spectrum. The exponential relation is derived in the following:

The number of ΔI of photons that are absorbed in a given thickness Δx is proportional to the incident intensity I, or the number I incident on it, times the thickness Δx, which is proportional to the number of electrons available to absorb photons:

$$-\Delta I \text{ is proportional to } I\ \Delta\ x, \qquad \text{(C.4)}$$

where the minus sign indicates that absorption *decreases* the number of photons.

If we use the symbol α to denote the absorption coefficient, where α is the fraction of photons absorbed per unit thickness, then (C.4) can be written:

$$-\Delta I = \alpha I \Delta x, \qquad \text{(C.5)}$$

or in standard differential notation as

$$-dI = \alpha I\ dx. \qquad \text{(C.6)}$$

This equation can be integrated from the surface at $x = 0$ to a depth x, which leads to the relation that the intensity $I(x)$ at depth x is given by

$$I(x) = I_0 \exp(-\alpha x), \qquad \text{(C.7)}$$

where I_0 is the intensity of photons at $x = 0$.

The absorption coefficient is a number per unit distance, such as 0.1 per cm, which can be written 0.1 cm^{-1}. At a depth x where αx equals unity (in this example, $x = 10$ cm, since $0.1 \times 10 = 1$) the number of photons decreases by a factor of $1/e$, or 0.37 (the value of $e \approx 2.718$).

For small values of αx, for example $\alpha x = 0.01$, equation (C.7) can be approximated by a linear function:

$$I(x) = I_0(1 - \alpha x). \qquad \text{(C.8)}$$

The analytical section of almost every art museum contains an x-ray generating system for examining works of art. Such a system produces high-energy, short-wavelength photons (for example 17.4 keV x-rays have $\lambda = 0.071$ nm = 0.71 angstrom, and 8.04 keV x-rays correspond to $\lambda = 0.154$ nm = 1.54 angstrom). As shown in Figure C.4, a painting is placed over x-ray sensitive film and is irradiated with x-rays. The film after exposure and development reveals regions where the x-rays have been absorbed.

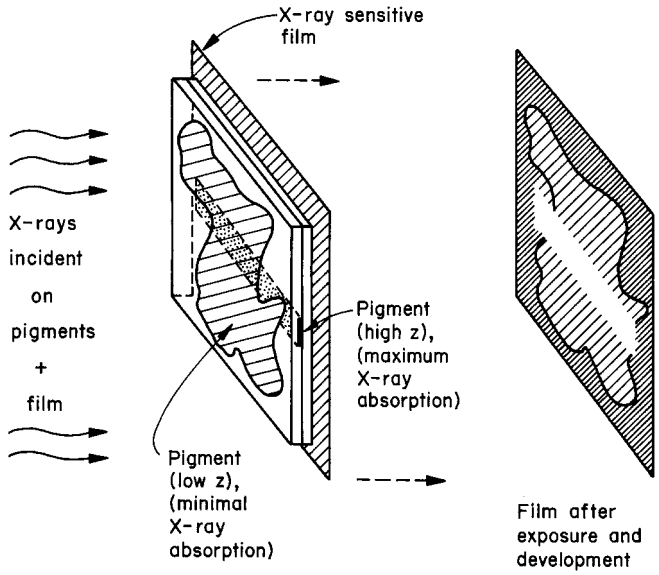

Fig. C.4. Procedure for x-radiography of paintings. An x-ray sensitive film is placed behind a painting. The x-rays incident on the painting are absorbed at different depths depending on the density and atomic number of the pigment particles. The transmitted x-rays expose the film emulsion. The amount of darkening of the developed film is a measure of the intensity of transmitted x-rays and hence the amount of x-ray absorbing pigments.

For x-rays, photoelectric absorption (where the x-ray gives up its energy in a single interaction with an electron) is the major cause of the attenuation of the photons penetrating the material.

The intensity I of x-rays transmitted through a thin foil of material for an incident intensity I_0 follows the exponential attenuation relation of equation (C.3) with a change in the nomenclature from α to μ to follow the convention in standard x-ray usage:

$$I = I_0 \exp(-\mu x) = I_0 \exp[(-\mu/\rho)\rho x], \tag{C.9}$$

where ρ is the density of the element (g/cm^3), μ is the linear attenuation coefficient, and μ/ρ is the mass attenuation coefficient given in cm^2/g. Note that x-ray absorption is not influenced by the crystal structure of the pigment, but only by the number of atoms per unit volume and the thickness of the pigment layer.

Table C.2 gives the density and mass absorption coefficient at two wavelengths of several elements found in artists' pigments. One notes from the table that the mass absorption coefficient tends to increase with increase in atomic number (Z) and that the absorption coefficient is greater (in some cases a factor of ten greater) for the longer-wavelength (lower-energy) photons. There are apparent anomalies with the absorption of Cd at 0.711Å, less than that of arsenic. This, as we will see in Appendix E, is due to the electronic structure and binding energies of

TABLE C.2

Atomic Number (Z), element, density ρ in grams/cm^3 (pigment) and mass attenuation coefficient (μ/ρ) in cm^2/gram at wavelengths of 0.711 and 1.54Å,

			Mass attenuation Coeff. (cm^2/gm)		
Z	*Element*	*Density (gm/cm^3)*	*17.4 keV 0.711Å*	*8.04 keV 1.542Å*	*Pigment*
22	Titanium	4.51	23.25	202.4	titanium white
26	Iron	7.87	37.4	304.4	ochre, sienna
29	Copper	8.93	49.3	51.5	malachite
33	Arsenic	5.78	65.9	75.6	king's yellow
48	Cadmium	8.65	27.3	229.3	cadmium red
80	Mercury	13.55	114.7	216.2	vermilion
82	Lead	11.34	122.8	232.1	Naples yellow

electrons. Figure C.5 gives the mass attenuation coefficient as a function of energy for several elements. This shows both the strong energy dependence of the absorption coefficient (μ/ρ decreases with increasing energy) and the five- to tenfold jumps in absorption at specific energies. These jumps occur when the energy of the photon exceeds the binding energy of a set electron, thus leading to an increase in absorption. For example, at 8 keV incident photon energies the absorption of iron (Fe,

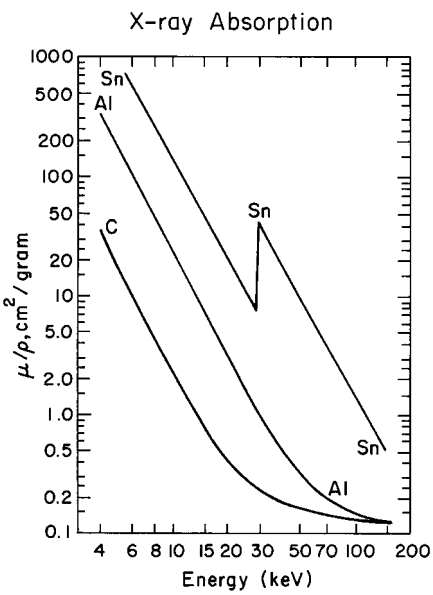

Fig. C.5. The x-ray mass-absorption coefficient (μ/ρ) in cm^2/gram versus x-ray energy in kilo electron volts (keV) for carbon (C), aluminum (Al), and tin (Sn). The sharp increase in absorption for Sn at 29.2 keV corresponds in energy to the K-shell, binding energy (*Taken from* Feldman and Mayer, *Fundamentals of Surface and Thin Film Analysis*, (North Holland, New York, 1986)).

$Z = 26$) can exceed that of tin (Sn, $Z = 50$). A factor-of-two difference in absorption coefficient can make a factor-of-ten difference in x-ray attenuation due to the exponential nature of the absorption process (equation (C.9)) because

$$e^{2.3} = 10.$$

Therefore, details of underlying drawings can be revealed in an x-ray radiograph if the underlying pigments have a higher absorption coefficient than the covering layer; for example, vermilion covered by titanium white.

C.2 Infrared Reflectography and Hiding Thickness

When it comes to the study of undersketching rather than underpainting, scientific emphasis switches to *infrared* reflectography. X-rays are scarcely able to make any distinction between a plain chalk ground (Fig. C.6) and one only slightly altered by addition of a thin sketch line in charcoal and bone black. But infrared radiation of wavelengths around 2.0 microns, having penetrated the upper paint layers, in particular the pigment, will be reflected at the level of the sketch and by virtue of their contrast will sharply distinguish between the whiteness of the ground and the darkness of the sketching medium. Then, although the human eye does not see the infrared image reflected from the undersketching, it is able to see that image once it has been converted to a visible one using a vidicon television system (Figure C.7). *Infrared reflectography* may facilitate the localization of retouchings, damaged areas, etc., and has therefore been used as an aid in the restoration of paintings. Infrared reflectography, however, has been most successful in partially re-

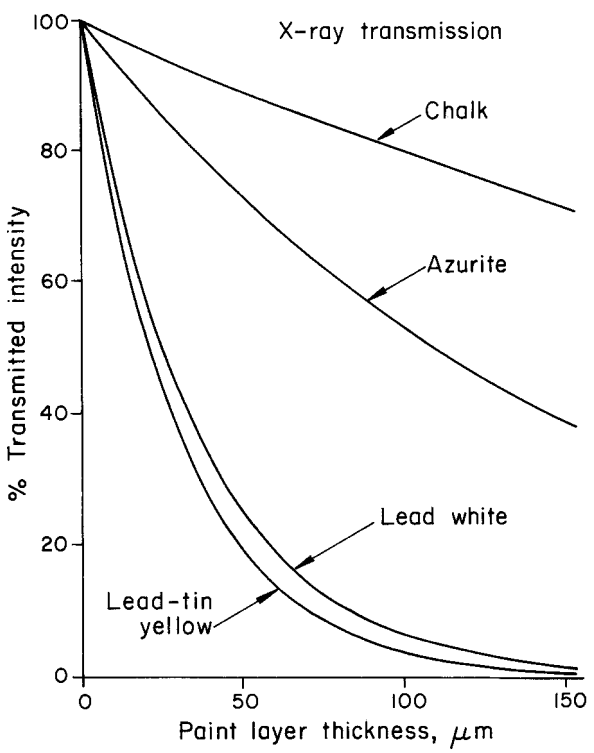

Fig. C.6. X-ray transmission characteristics for various pigments in an oil medium for an oil binder-to-pigment ratio of 0.2 for chalk, azurite, lead white and lead–tin yellow.

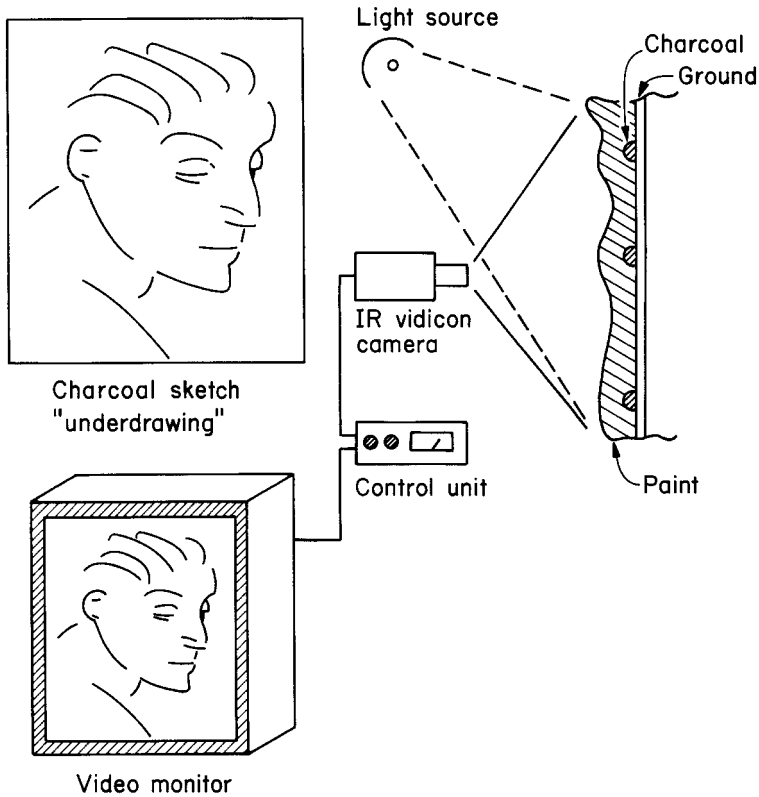

Fig. C.7. Schematic diagram of the application of infrared (IR) reflectography to reveal the presence of a charcoal sketch underneath an IR-transparent paint layer. An IR vidicom camera is used to display the image on the video monitor.

vealing underdrawings such as are frequently encountered in medieval panel paintings. In Flemish fifteenth-century painting a mixture of chalk and animal glue was applied on a carefully prepared oak panel to form a smooth ground. The artist then made a drawing with a brush, using paint with bone black as pigment on this ground. This underdrawing was then the guide for the overlying paint layer.

Different pigments have different reflection and absorption properties at different wavelengths. When viewed in the visible spectrum each pigment has a certain thickness that is required (hiding thickness) to cover up an underlying pigment. In the present case we are interested in finding photon wavelengths at which the underlying pigments can be detected. Our focus is to observe the carbon-containing pigments used in underdrawings.

In the detection of underdrawings the hiding ability of the paint has to be minimized. Long-wavelength infrared (IR) radiation (1.2 to 2.2 mi-

cron, μm) is used to decrease hiding ability or to increase the paint layer thickness (hiding thickness) required to cover up, or "hide," an underlayer of charcoal or other pigment.

The paint-layer thickness cannot be modified, and therefore the only way to penetrate it is to decrease absorption scattering. From fundamental light scattering theory it is known that for nonabsorbing particles, small in themselves compared to the wavelength of incident radiation, scattering decreases with increasing wavelength. Because paints consist of pigment particles embedded in a medium, by increasing the wavelength, the hiding ability of the paint layers will decrease. The absorption of paints used in fifteenth-century Flemish paintings is not strong in the near infrared except for the carbon-containing pigments used in underdrawings.

In Figure C.8 the hiding thickness X_D has been plotted against the wavelength λ for a number of pigments encountered in medieval paintings. For all wavelengths it has been assumed that the reflectance of the underdrawing is constant. It is seen from Figure C.8 that lead white and vermilion show only a moderate increase in X_D with λ. The increase in hiding thickness is most pronounced for verdigris, a pigment that covers well in the 0.7 μm region but shows a rapid increase in hiding thickness at larger wavelengths. Ochre also covers well in the visible region of the spectrum, but its hiding ability, defined as $1/X_D$, decreases rapidly with λ. The green pigment malachite, which is very frequently used in Flemish primitive painting in landscapes and trees, also covers considerably less in the region beyond 1.0 μm. The covering thickness of vermilion is almost constant over the wavelengths displayed in Figure C.8. Although the hiding thickness as a function of the wavelength can only be approximated, Figure C.8 shows that X_D increases by a factor of 2 to 3 from the visible spectrum to $\lambda = 2.0$ μm. This increase is enough to predict a considerable improvement in detectability of underdrawings using imaging devices capable of detecting radiation up to 2.0 μm. The ability of infrared photography to partially reveal underdrawings can be explained by the increase in X_D from the visible to the photographic infrared spectral region, which for thin paint layers is often sufficient. A comparison between calculated X_D values and measured layer thicknesses in actual Flemish primitive paintings shows that in the spectral region around 2.0 μm, the paint thicknesses are less than the hiding thicknesses and an underdrawing may thus be detected.

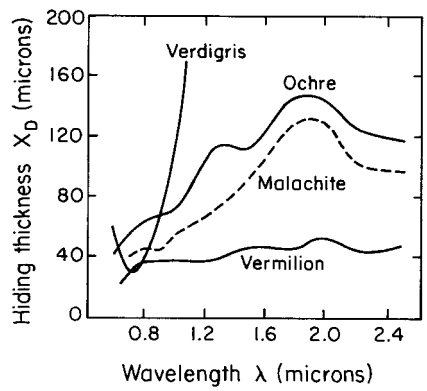

Fig. C.8. The hiding thickness, X_D, plotted against wavelength in microns of light in the infrared region of the spectrum. The hiding thickness is the thickness that is required to hide an underlayer. All the pigments were ground with linseed oil with pigment volume content (PVC) between 11% and 31%: vermilion (PVC = 11%), malachite (PVC = 21%), raw ochre (PVC = 31%), and verdigis. (*From*, J.R.J. Van Asperen de Boer, "Infrared Reflectography," thesis, University of Amsterdam, 1970.)

The Chromaticity Diagram

D

The sensation of color depends primarily on the composition of light, which is a mixture of white light and colored light (which in itself can be a mixture of wavelengths as in the case of purple). The colored light may have a dominant wavelength, or *hue*, and the extent to which the hue dominates is known as saturation (or chroma). The saturation decreases as the hue is diluted with white light.

There are three types of receptors in the eye that respond to different wavelengths (Chapter 4). This leads to attempts to chart colors by a mixture of three primary lights. Figure D.1 shows James Clerk Maxwell's color triangle with the three apexes representing three primary colored lights: blue-violet, orange-red, and green. A great number of colors, *but not all* of them, can be produced by mixing lights of the three primary colors. A specific color, for example an unsaturated greenish blue (cyan), can be represented by a point on the triangular grid.

In order to represent *all* colors, 3 imaginary, or "ideal," primaries are used. The Commission Internationale de l'Eclairage (CIE) defined in 1931 (modified in 1967) the chromaticity curve with standard observer and 3 ideal standard sources. The chromaticity diagram is constructed (Figure D.2) by drawing a color triangle with 3 ideal (but nonexistent) primary colors at each corner: red, blue and green. For example, the x-axis shows the amount of ideal green that would be mixed with blue to form a given color.

Superimposed on the triangle is the CIE chromaticity curve, which places the band of pure spectral colors as a *solid* curved line from violet up to green and down to red. The *dashed* line connecting 400 and 700 nm represents the nonspectral colors of purple obtained by mix-

ing violet and red light beams. All the colors that we can see are contained within the area bounded by the solid and dashed lines. The central point W of the diagram is the white produced by an equal mixture of the three primaries.

We can represent a mixture of two spectral lights as a point on the line joining the light point on the spectral curve. The dotted line in Figure D.2 joins the blue light at 480 nm with the yellow light at 580 nm. Following the dotted line, we would proceed from spectral (or saturated) blue to pale blue to white to pale yellow to saturated yellow. Thus, a mixture of the correct amounts of 480 nm blue light and 580 nm yellow light gives any of the colors located in between. Similarly, the purple colors can be formed by a mixture of red light with violet light as specified by the dashed line. A pair of colors which can produce

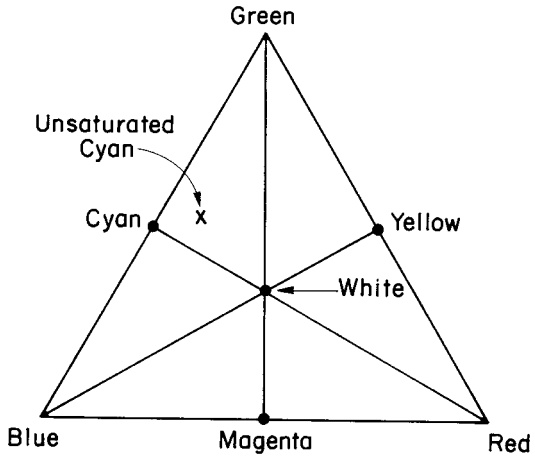

Fig. D.1. The color triangle attributed to James Clerk Maxwell. At the apexes are the additive primary colors, and at the edges, the subtractive colors. Many, but not all, colors can be represented as a mixture of the three color lights. The nearer a point is to an apex, the higher is the proportion of light of the color represented by that apex. (*Adapted from* H. Rossotti, *Colour* (Princeton, 1983)).

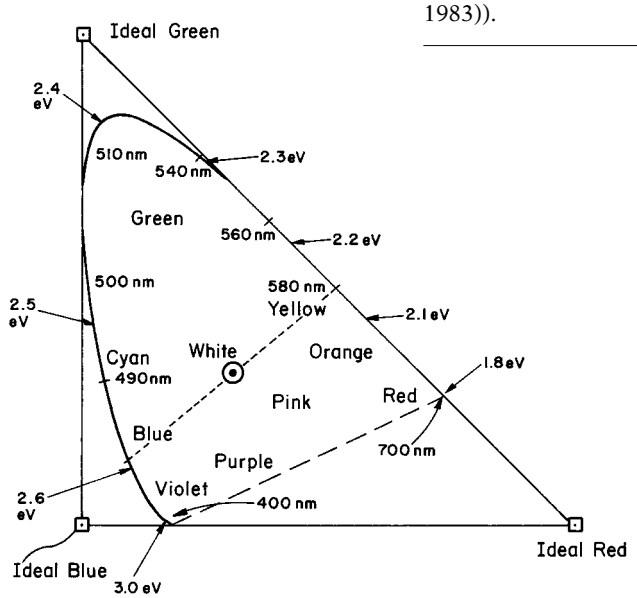

Fig. D.2. The CIE chromaticity diagram showing wavelengths in nanometers (nm) and energies in electron volts (eV). The area enclosed by the curved line and dashed segment includes all visible colors. The pure spectral colors lie along the curved edge. (*Adapted from* Nassau, *The Physics and Chemistry of Color* (Wiley, New York, 1983)).

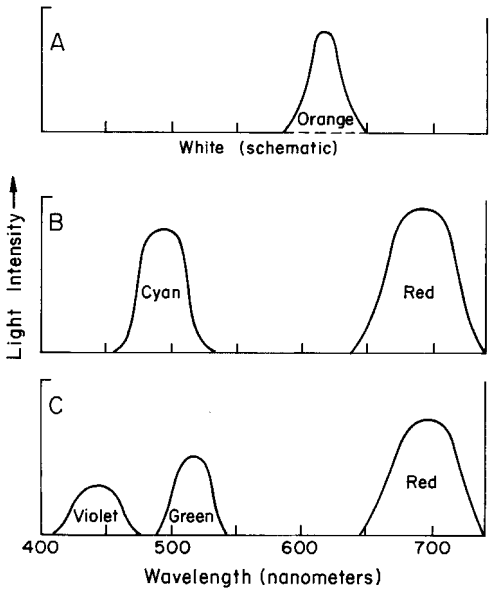

Fig. D.3A,B,C. Different ways of obtaining metameric beams of pink light. Each implies mixture with white light to obtain pink light, (A) by orange light, (B) by mixing red with cyan, or (C) by mixing red, green, and violet. To the eye, these metameric colors would all appear the same. (*Adapted from* Nassau, *The Physics and Chemistry of Color* (Wiley, New York, 1983)).

white (the line joining the two colors passes through the white point, W) are called a *complementary* pair. Thus blue light and yellow light form a complementary pair as do orange (600nm) and blue-green 488 nm, also called "cyan". We can now use the point W as the origin and describe color as a mixture, in a certain proportion, of white light of a given wavelength. This wavelength is referred to as the *dominant* wavelength and the color associated with this dominant wavelength is called the *hue*. We thus describe the sensation of color in terms of hue. The amount of hue that makes up the composition of light is known as *saturation* (also designated as *chroma*). The dominant wavelength points on the spectral curve (solid line in Figure D.2) are fully saturated. As the dominant wavelength or hue is diluted with white light, the saturation decreases. For example, to describe a beam of pink-appearing light as an unsaturated orange hue of 620 nm.

There are many ways to produce the pink light (or any other point): one hue plus white, two spectral colors, or three spectral colors. These light mixtures are illustrated in Figure D.3 where (A) shows orange and white, (B) blue-green (cyan), and red and (C) violet, green, and red. These three mixtures would appear the same to the standard observer.

Periodic Table and Crystal Structure

E

E.1 Electrons, Nuclei, Isotopes, and Atomic Number

An atom is made up of a very small but heavy central nucleus with a positive charge, surrounded by a negatively charged cloud of electrons. Most atoms are on the order of 1.0 to 2.4 angstrom (Å) in diameter, where 1Å = 10^{-8}cm. (1Å = 10^{-10} meter = 0.1 nanometer).

The nucleus of an atom is much smaller yet, typically with a diameter of 10^{-13} cm, or 10^{-5}Å. In spite of this size difference, virtually all of the mass of an atom is concentrated in its nucleus. An electron, which has a negative charge, weighs only 1/1836 as much as the lightest of all atoms, that of the hydrogen atom, which consists of a single proton plus an electron.

An atomic nucleus is built from two major kinds of particles: protons and neutrons. A proton carries one unit of positive charge, which balances the negative charge on an electron. The neutron is uncharged. The standard unit for measuring masses of atoms is the atomic mass unit (amu) defined such that the most common kind of carbon atom weighs exactly 12 amu. On this scale, a proton has a mass of 1.00728 amu. Protons and neutrons usually are thought of as having unit masses (1 amu) unless exact calculations are called for. On this scale, an electron weighs only 0.00055 amu. The charge and mass relationships among these three fundamental particles are summarized in Table E.1.

Electrons surround an atom (Figure E.1), and the nucleus is small and deeply buried, so that the outer part of the electron cloud is all

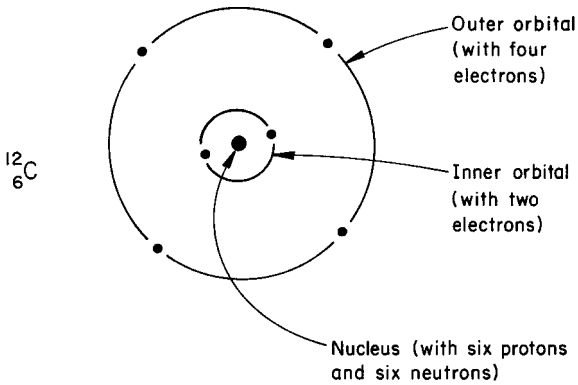

Fig. E.1. Schematic of the planetary model of the carbon (C) atom where the electron orbits are displayed as two circular orbits with two electrons in the inner (K-shell) orbital and four electrons in the outer (L-shell) orbital. Carbon-12 with 6 protons and 6 neutrons is denoted by the symbol $^{12}_{6}C$.

TABLE E.1

Fundamental Particles of Matter

Particle	*Charge*	*Mass (amu)*
Proton	+1	1.00728
Neutron	0	1.00867
Electron	−1	0.000549

Atomic and nuclear particles listing particle, charge, and mass in atomic mass units (amu) where the carbon-12 atom has 12 amu.

that another atom "sees." It is the electron cloud that gives each atom its chemical character. Since the number of electrons in a neutral atom must equal the number of protons in its nucleus, the number of protons indirectly determines the chemical behavior of the atom. All atoms with the same number of protons are defined as the same chemical element, and the number of protons is its atomic number; *Z is the symbol designating atomic number*. A list of the first elements in order of increasing atomic number is given in Table E.2. The atomic number Z is written as a subscript before the symbol.

TABLE E.2

The First Eleven Elements

$_{1}H$	=	hydrogen, a gas
$_{2}He$	=	helium, a noble gas
$_{3}Li$	=	lithium, a soft, reactive metal
$_{4}Be$	=	beryllium, a harder metal
$_{5}B$	=	boron, a borderline nonmetal
$_{6}C$	=	carbon, a nonmetal and the fundamental atom in living organisms
$_{7}N$	=	nitrogen, major component of the atmosphere
$_{8}O$	=	oxygen, the other main component of the atmosphere
$_{9}F$	=	fluorine, a relatively scarce nonmetallic element
$_{10}Ne$	=	neon, an inert gas closely resembling helium
$_{11}Na$	=	sodium, a soft, reactive metal similar to lithium

Table of elements in the first rows of the periodic table listing the chemical symbol with subscript for atomic number (Z).

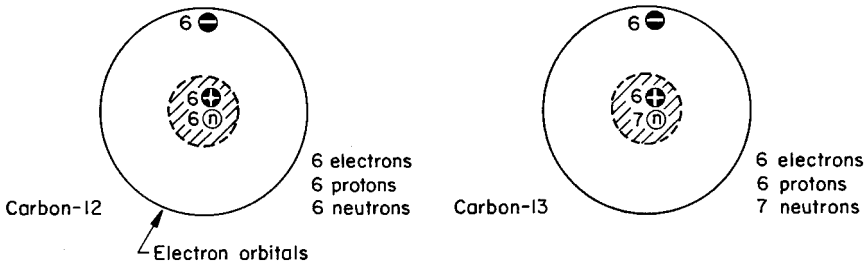

Fig. E.2. Schematic of the stable isotopes of carbon (C) both of which have the same atomic number Z with 6 electrons. Carbon-12 has 6 protons and 6 neutrons and carbon-13 has an extra neutron.

Atoms usually have about the same number of protons and neutrons. The sum of the number of protons and neutrons, i.e., the total number of nucleons, is the mass number. The number of nucleons is indicated by a superscript in front of the chemical symbol: ^{12}C would indicate a carbon atom with 12 nucleons. Atoms with the same atomic number Z but with different numbers of neutrons in the nucleus are called *isotopes* of the same chemical element.

Most of the naturally occurring elements exist as mixtures of several isotopes. For example, of the carbon found on this planet, 98.9% is carbon-12, or ^{12}C, which has six protons and six neutrons. Most of the remaining carbon, 1.1%, is carbon-13, with one additional neutron, Figure E.2. Both of these isotopes are stable, but carbon-14 is radioactive, and is present in minute amounts only because it is being produced constantly by cosmic-ray bombardment of nitrogen in the upper atmosphere. Carbon-14 is the basis of radiocarbon dating.

Because isotopes of the same element have such similar chemical properties, the ratio of isotopes ordinarily is unchanged during chemical reactions. What is important to chemical behavior is not the number of neutrons in an atom, but the number of protons, because this determines the number of electrons, and electrons give rise to all of the important chemical properties of the elements.

E.2 Periodic Table

The first attempt to organize the elements in some systematic fashion occurred over a century ago. In 1869, Dmitri Mendeleev classified the elements by arranging them in order of increasing atomic weight. It was found that similar chemical and physical properties recurred periodically, which led to the concept of a "periodic" table. In 1913, H. Mose-

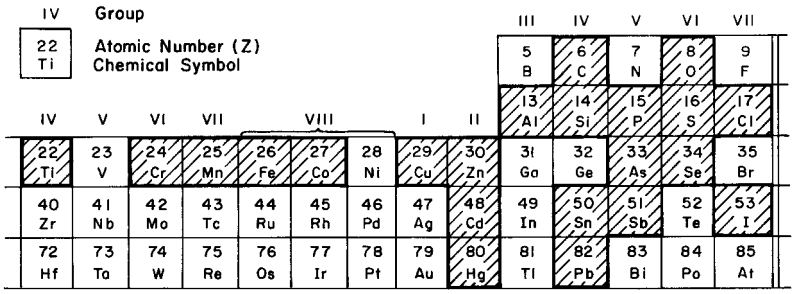

Fig. E.3. The pigment periodic table. This is an abbreviated form of the periodic table showing the elements used in paint pigments (shaded elements) arranged in columns by groups (Roman numerals) that have similar chemical behavior. The atomic number *Z* and chemical symbol are displayed. Table E.3 gives the element name, symbol, and pigments.

TABLE E.3

Elements Used in Pigments

Name	*Symbol*	*Atomic No. (Z)*	*Pigments*
Carbon	C	6	carbon black, calcium carbonate
Oxygen	O	8	lead oxides, chromates
Sodium	Na	11	lapis lazuli, French ultramarine
Aluminum	Al	13	ultramarine, cobalt blue
Silicon	Si	14	smalt, quartz
Phosphorus	P	15	cobalt yellow
Sulfur	S	16	lithopane, vermilion
Chlorine	Cl	17	patent yellow, platina yellow
Titanium	Ti	22	titanium white
Chromium	Cr	24	chrome yellow, veridian
Manganese	Mn	25	manganese blue, raw and burnt umber
Iron	Fe	26	hematite, yellow ochre
Cobalt	Co	27	cobalt blue, cobalt yellow, cerulean blue
Copper	Cu	29	azurite, malachite
Zinc	Zn	30	zinc yellow, zinc white
Arsenic	As	33	orpiment, emerald green
Selenium	Se	34	cadmium red
Cadmium	Cd	48	cadmium red, cadmium yellow
Tin	Sn	50	lead–tin yellow, cerulean blue
Antimony	Sb	51	antimony vermilion
Barium	Ba	56	lithopane, barium yellow
Mercury	Hg	80	vermilion, cinnabar
Lead	Pb	82	lead white, Naples yellow, red lead, litharge

List of elements used in pigments by name, symbol, atomic number (*Z*), and pigment name.

ley found that the atomic number Z could be used with better success, and periodic tables are now constructed based on Z.

The underpinning of the periodic table is in the electron configuration. It is the outermost electrons that determine the chemical behavior, since it is these electrons that participate in the bonds between atoms.

An abbreviated form of the periodic table—based on elements used in pigments—is given in Figure E.3. Elements in the same vertical column such as C (carbon) and Si (silicon) have similar properties. In Table E.3 the elements are arranged in increasing atomic number Z along with the chemical symbol and name. Some of the pigments used with a given element are also listed.

The inorganic pigments are composed of two or more elements in the periodic table. The pigments can be oxides such as Pb_3O_4 (red lead) or sulfides such as CdS (cadium sulfide, cadium yellow) or more complicated structures containing three or more elements such as $BaCrO_4$ (barium chromate, barium yellow, or lemon yellow).

E.3 Structure of Pigment Crystallites

The regularity of the external form of crystals suggests that crystals are formed by the regular repetition of identical building blocks (Figure E.4). When a crystal grows in a constant environment, the shape remains unchanged during growth, as if identical building blocks were being added continuously. The building blocks are atoms or groups of atoms: A crystal is a three-dimensional periodic array of atoms. This was learned in the eighteenth century when mineralogists discovered that the index numbers of the directions of all faces of a crystal are exact integers.

There is an extensive formalism to the description of crystal systems. For our purpose we can regard them as lattices of atoms. Figure E.5 gives a few of the conventional cells, and Figure E.6 shows the notation used in Table E.2 to describe the atoms.

When crystals are well formed, it should be possible to identify them as belonging to one of the seven crystal systems. The chemical substance usually has already been unequivocally assigned to one system on the basis of x-ray diffraction analysis. Six of these systems, diagramed in Figure E.5, are defined as follows:

Cubic: Three mutually perpendicular axes with equal atomic spacing.

Tetragonal: Two mutually perpendicular axes having equal spacing, with different spacing along the axis perpendicular to the other two.

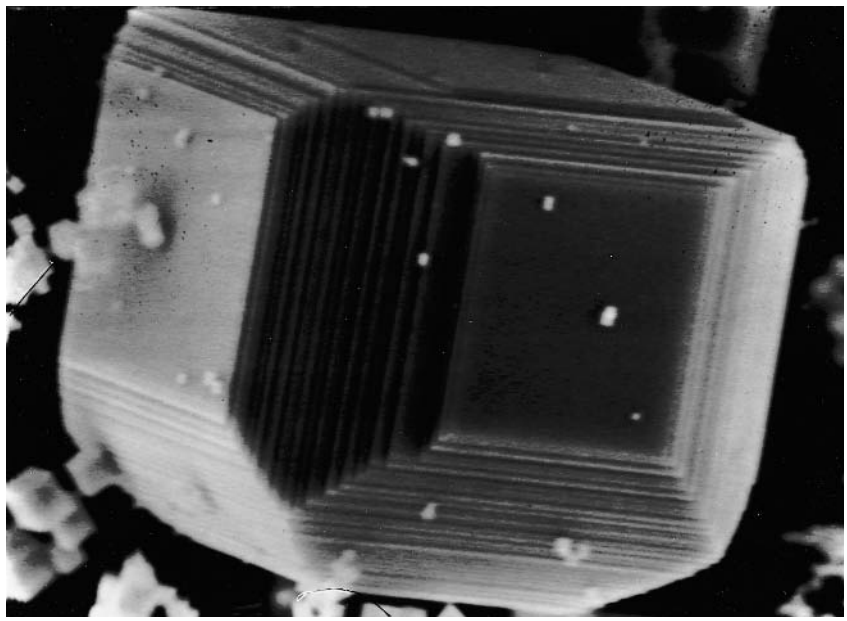

Fig. E.4. A scanning electron microscope (SEM) micrograph of a crystal of magnesium oxide (MgO). The crystal faces and the growth steps are evident on the cubic crystal. The legend at the bottom shows that the microscope was operated at 3.0 kilovolts (kV) with a magnification of 60,000 (60.0K), and the white dot markers indicate a length of 500 nanometers (0.5 microns), which indicates that the crystal is somewhat over 1 micron in size with a top growth face of 0.5 by 0.5 microns. (Micrograph by Bob Roberts, Arizona State University.)

Hexagonal: Two axes 120° apart with equal atomic spacing and different spacing along the axis perpendicular to the plane of the other two.

Orthorhombic: Three mutually perpendicular axes with unequal atomic spacing.

Monoclinic: Two perpendicular axes with unequal spacing, the third nonperpendicular axis with different spacing.

Triclinic: Three oblique axes with unequal spacing.

Inorganic pigments are characterized by the presence of crystalline particles. These particles have a particular crystal structure as given in Figure E.5 and Table E.4. Four structures, rhombohedral, hexagonal,

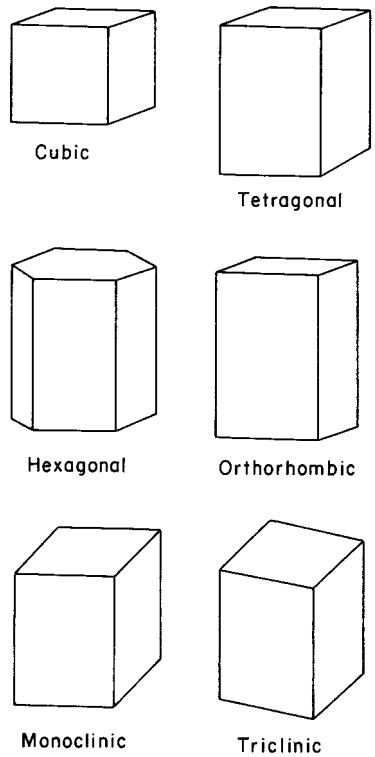

Fig. E.5. Six crystal systems that are found in pigment crystallites.

tetragonal, and monoclinic, are characteristic of the pigments. Even though two red pigments may have the same structure—vermilion and red ochre are both rhombohedral—the spacings between atoms and planes are different. X-ray diffraction allows one to measure the planar spacings and hence to identify the pigments.

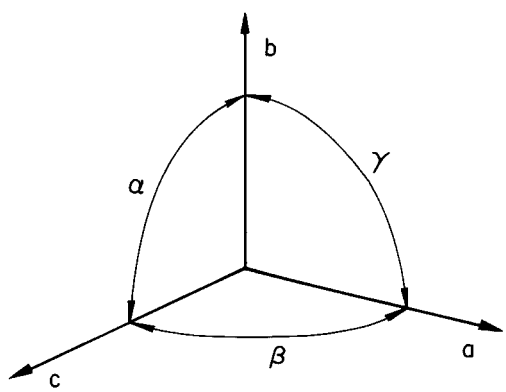

Fig. E.6. The notation for the three axes and angles used to describe the crystal systems in Table E.4.

TABLE E.4

System	*Axial Lengths and Anles*	*Bravais Lattice*
Cubic	Three equal axes at right angles $a = b = c$, $\alpha = \beta = \gamma = 90°$	Simple Body-centered Face-centered
Tetragonal	Three axes at right angles, two equal $a = b \neq c$, $\alpha = \beta = \gamma = 90°$	Simple Body-centered
Orthorhombic	Three unequal axes at right angles $a \neq b \neq c$, $\alpha = \beta = \gamma = 90°$	Simple Body-centered Base-centered Face-centered
Rhombohedral	Three equal axes, equally inclined $a = b = c$, $\alpha = \beta = \gamma \neq 90°$	Simple
Hexagonal	Two equal coplanar axes at 120°, third axis at right angles $a = b \neq c$, $\alpha = \beta = 90°$, $\gamma = 120°$	Simple
Monoclinic	Three unequal axes, one pair not at right angles $a \neq b \neq c$, $\alpha = \gamma = 90° \neq \beta$	Simple Base-centered
Triclinic	Three unequal axes, unequally inclined and none at right angles $a \neq b \neq c$, $\alpha \neq \beta \neq \gamma \neq 90°$	Simple

Seven crystal systems indicating axial lengths, angles, and Bravais lattice.

E.4 X-RAY CRYSTALLOGRAPHY

The atomic structure of a crystal is deduced from the way it diffracts a beam of x-rays in different directions. A crystal is built of countless small structural units, each consisting of the same arrangement of atoms; the units are repeated regularly like a wallpaper pattern, except that in a crystal the pattern extends in three dimensions in space. The *directions* of the diffracted beams depend on the repeat distances of the pattern. The *strengths* of the diffracted beams, on the other hand, depend on the arrangement of atoms in each unit. The wavelets scattered by the atoms interfere to give a strong resultant in some directions and a weak resultant in others.

The easiest way to approach the optical problem of x-ray diffraction is to consider the x-ray waves as being reflected by sheets of atoms in the crystal. When a beam of monochromatic (uniform wavelength) x-rays strikes a crystal, the wavelets scattered by the atoms in each sheet combine to form a reflected wave. If the path difference for waves reflected by successive sheets is a whole number of wavelengths, the wave trains will combine to produce a strong reflected beam. In geometric

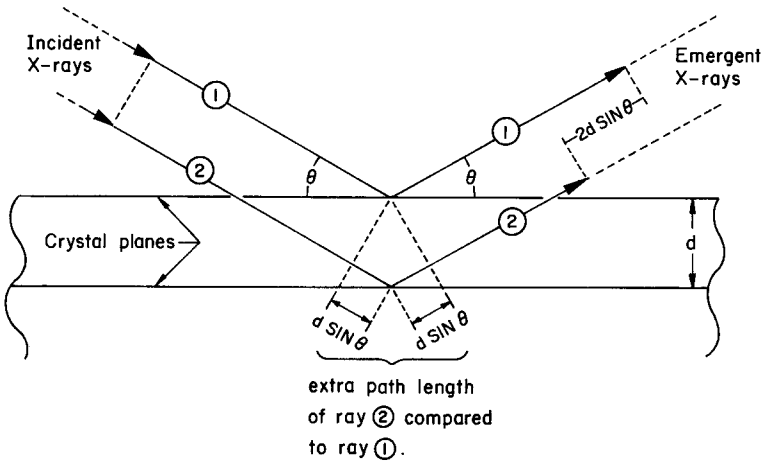

Fig. E.7. Diffraction of an incident beam of monochromatic (equal wavelength) x-rays by two parallel planes of atoms separated by a distance d in the crystal. The difference in the two path lengths is $2d\sin\theta$. If the path length difference is a whole number of wavelengths $n\lambda$, the waves will combine to produce a strong reflected beam (Bragg's law).

terms (Figure E.7), if the spacing between the reflecting planes is d and the glancing angle of the incident x-ray beam is θ, the path difference for waves reflected by successive planes is $2d \sin \theta$. Hence the condition for diffraction is

$$n\lambda = 2d \sin \theta, \tag{E.1}$$

where n is an integer and λ is the wavelength. This relation is called Bragg's law.

The atoms of a given crystal can be arranged in sheets in a number of different ways, as shown in Figure E.8 for a cubic lattice. The equa-

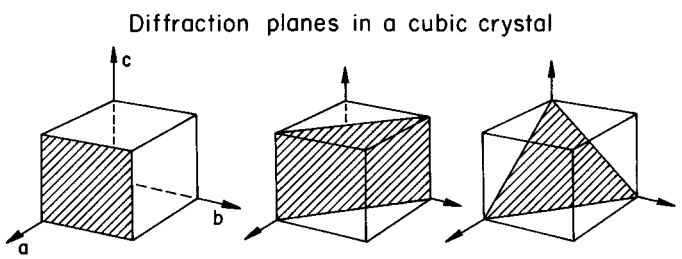

Fig. E.8. Three planes in a cubic crystal that can act as diffraction planes for x-rays. The shaded areas represent one of a family of parallel planes.

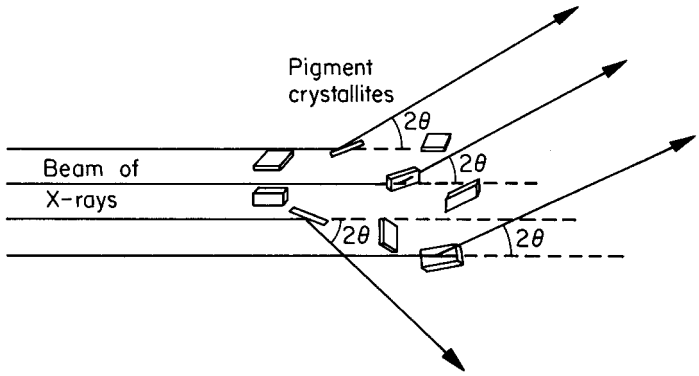

Fig. E.9. X-ray diffraction produced when a beam of x-rays strikes a paint sample containing pigment crystallites. Those crystallites oriented to the beam at a Bragg angle θ will reflect the beam to produce a cone of reflected x-rays about the incident direction of semiangle 2θ.

tion for reflection can be satisfied for any set of planes whose spacing is greater than half the wavelength of the x-rays used.

The general method of x-ray crystallography is the powder method, used when the material is available only in microcrystalline form such as found in the pigments in a paint layer. The x-rays fall on a mass of tiny crystals in all orientations, and the beams of each order form a cone (Figure E.9). When powder photographs are made, arcs of the cones called diffraction patterns are intercepted by a film surrounding the specimen. The powder method is used mainly in pigment analysis when one removes a sample from the painting.

Electron Energy Levels and X-ray Emission

F

In this appendix we focus on the identification of elements in pigments by means of the characteristic energies of emitted x-rays (high-energy photons, typically with energies between 1 and 10 keV). The x-rays are emitted when atoms are bombarded with energetic photons or particles such as electrons or protons. The emitted x-rays are characteristic of the atom itself and are not influenced by the crystal structure of the pigment. For example, the x-rays emitted from lead atoms (Pb) would have the same energies whether they were emitted from lead in chrome yellow (lead chromate, $PbCrO_4$) or lead in massicot (lead oxide, PbO). We start by describing the characteristics of yellow pigments.

F.1 Yellows and Pigment Anachronisms

The elements iron (Fe), arsenic (As), lead (Pb), tin (Sn), chromium (Cr), antimony (Sb), cadmium (Cd), and oxygen (O) are contained in various inorganic yellow pigments. Table F.1 lists six of the pigments and their composition.

Prior to the seventeenth century the choice of yellow pigments was limited to (1) lead–tin yellow (Pb_2SnO_4), and (2) ochres of various hues, prepared from naturally occurring iron oxide ores. Orpiment was an alternative to these but an unpopular one, since its arsenic content made it poisonous and offensive-smelling. The glass colorant, the lead antimonate Naples yellow, was introduced in the seventeenth century into the artist's palette as an alternative to ochre. Vauquelin's

TABLE F.1

Six Inorganic Yellow Pigments and Their Composition

Name	*Composition*
1. Orpiment (king's yellow)	Arsenic sulfide ($As_2 S_3$)
2. Lead–tin yellow	Combined oxides of Pb and Sn ($Pb_2 Sn O_4$)
3. Yellow ochre	Mainly iron oxide ($Fe_2 O_3$) with alumina and silica
4. Naples yellow	Lead antimonate ($Pb_2 Sb_2 O_7$)
5. Chromium yellow	Lead chromate ($Pb Cr O_4$)
6. Cadmium yellow	Cadmium sulfide (CdS)

isolation of chromium as an element, in 1798, led to development of chromium yellow ($PbCrO_4$) about a decade later, and Stromeyer's isolation of cadmium in 1817 inspired production of cadmium yellow (CdS) early in the 1830s. By this time lead–tin yellow seems to have been totally eclipsed.

There are several different techniques that can be used to distinguish among the yellow pigments. Spectral reflectance curves can be used. X-ray diffraction (Appendix E) provides one positive means of identification, although a small sample (a few micrograms is usually sufficient) must be removed from the painting. The third technique, the subject of this appendix, is the excitation of characteristic energy x-rays. The spectra of the characteristic x-ray energies provides a "fingerprint" of the elements in the pigment. The presence of lead and antimony (Naples yellow) can be determined and distinguished from that of lead and tin (lead–tin yellow). All three techniques—infrared spectroscopy, x-ray diffraction, and x-ray emission—are used for positive identification of the elements.

F.2 ELECTRON SHELLS

Electrons in atoms behave as though they were grouped into levels or shells, with all electrons in one shell having approximately the same energies, but with large energy differences between shells. Each shell can hold only a certain maximum number of electrons. If one shell is filled, then an additional electron will be forced to go into a higher-energy, less stable, shell, and this electron will be lost easily during chemical reactions. Conversely, if an atom lacks only one or two electrons to complete a shell, the atom will have a strong attraction for electrons, and can take them away from the type of atom mentioned previously. A completely filled electron shell, with no vacancies and no extra electrons outside, is a particularly stable situation for an atom.

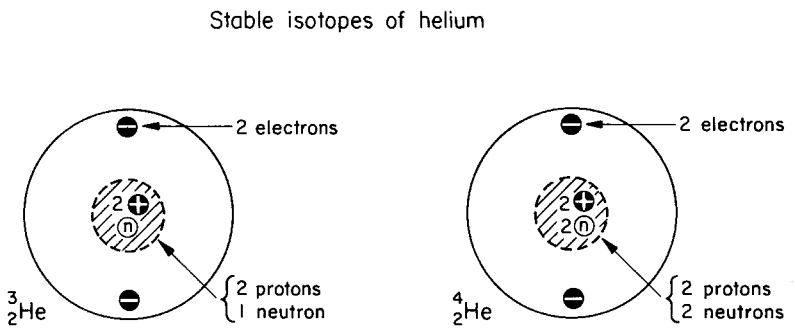

Fig. F.1. The stable isotopes of helium that contain two electrons. Helium-3, ^3_2He contains 2 protons and one neutron, while the much more abundant helium-4, ^4_2He, contains 2 protons and 2 neutrons.

Not only can atoms gain and lose electrons, they can share them in covalent bonds. When they do, all the shared electrons contribute to filling vacancies in the outer electron shell of each atom. The helium atom with filled shell, Figure F.1, is stable and does not form molecules.

The innermost shell (called the 1s or K shell) in any atom can hold a maximum of only two electrons, and the second shell (denoted by L shell) can hold eight. A helium atom has its single shell filled with two electrons.

F-2.1 The Bohr Atom: In 1913 Niels Bohr proposed a model for the hydrogen atom in which the electron moved in a circular orbit around the nucleus. Not all orbits were possible, according to Bohr, but only those that met certain conditions. The orbit with the smallest size would have one complete electron wave around its circumference; the next allowable orbit would have two complete waves, and then three, four, and so on. The only allowed orbits were those for which the total circumference was an integral number n of wavelengths. The orbits are shown in Figure F.2. The radius a_0 of the smallest orbit is known as the Bohr radius, with a value of 0.53×10^{-8} cm, where 10^{-8} cm = 1 angstrom (Å).

The energy corresponding to the orbital state n of the hydrogen atom is given by

$$E_n = -\frac{E_0}{n^2}, \tag{F.1}$$

where E_0 is another collection of physical constants, which for hydrogen has a value of 13.6 eV. The allowed energy levels for hydrogen are diagramed in Figure F.3. By convention, energy is expressed relative to that of an ionized atom, with the electron at rest but infinitely far away. The energy of any atom with its electron still bound to it must be less

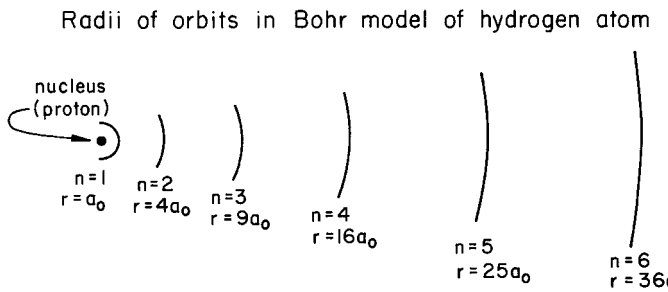

Fig. F.2. Radii of orbits in the Bohr model of the hydrogen atom where a_0 is the Bohr radius and n is an integer.

than zero or negative. Positive energy refers to the kinetic energy of the removed electron if it is not at rest. For atomic hydrogen, the lowest-energy state, with the 0.53 radius orbit, has an energy of $E_1 = 13.6$ eV. Atomic hydrogen in this state is 13.6 eV more stable than an ionized atom. Thus 13.6 eV is the ionization energy of atomic hydrogen. Although the numerical value is calculated from first principles in the Bohr theory, it agrees exactly with the measured value of the ionization energy of hydrogen.

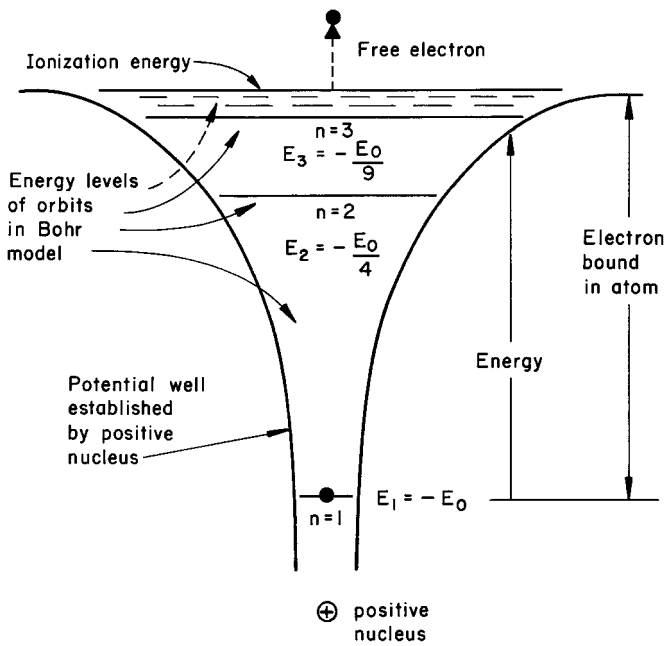

Fig. F.3. Energy levels of allowed orbits in the Bohr model of the hydrogen atom. The energy levels are depicted as constrained in a potential well established by the positive charge of the proton in the nucleus of the hydrogen atom. The energy levels E_n are given by E_0/n^2 with $E_0 = 13.58$ eV, which represents the ionization energy required for complete removal of the $n = 1$ electron.

F-2.2 Wave Mechanics: A quantum or wave theory was developed in the 1920s by Erwin Schrödinger and Werner Heisenberg. As in the simpler Bohr theory, the energy of an electron in an atom is restricted to certain values, or is quantized. Four quantum numbers instead of one are required to describe the state of an electron in an atom, and they are designated n, l, m, and M_s. The average distance of the electron from the nucleus depends primarily on n, which is called the *principal quantum number*. The geometry of bonding around

the atom depends primarily on quantum number *l*, called the *orbital-shape*, or *azimuthal, quantum number*. The energy of an electron in an atom is a function of n and to a lesser degree of l; usually, all m states for given n and l values have the same energy. There is a fourth quantum M_s, which denotes the spin of the electron. Electrons can have two spin states (spin up or down).

F.3 Electron Binding Energies

Every elemental atom has electrons in orbitals whose energy provides a unique signature called characteristic energies that identify the element. The binding energy E_B is the energy required to remove an electron from a specific orbital to a position at rest outside the atom. In Figure F.4 we show schematically the innermost orbitals (n = 1, 2, and 3) and the labels *K, L, M* used in x-ray notation to identify the specific orbitals. At the side we show the actual binding energies in kilo electron volts (keV) for two elements. The symbols at the side (1s, 2s, 2p, 3s . . .) are the electron notation. Table F.2 gives the x-ray notation.

The binding energy is the difference in the total energy between the initial and final states of the atom in which one electron has been removed. That is, it requires an input energy of one binding energy E_B to remove an electron from a state characterized by E_B. In Figure F.4 we use the x-ray symbols where the K-shell refers to n = 1, L shell to n = 2, and L_1 refers to the 2*s* subshell.

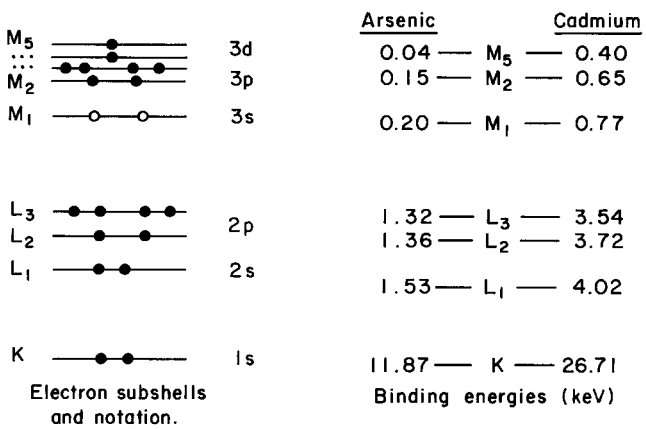

Fig. F.4. Schematic of the energy levels of an atom indicated by the x-ray symbol (K, L_1, L_2, . . .) and the electron shell 1s, 2s, 2p, . . .). On the right side, the binding energies in kilo electron volts (keV) in the various shells of arsenic and cadmium are given.

TABLE F.2

Number of Electrons and X-Ray Symbols

Atomic levels				
n	*l*	*Electron Shell*	*Number of Electrons*	*Singly Ionized Atom X-ray Symbol*
1	0	1s	2	K
2	0	2s	2	L_1
	1	2p	6	L_2
				L_3
3	0	3s	2	M_1
	1	3p	6	M_2
				M_3
	2	3d	10	M_4
				M_5
4	0	4s	2	N_1
	1	4p	6	N_2
				N_3
	2	4d	10	N_4
				N_5
	3	4f	14	N_6
				N_7
5	0	5s	2	O_1

Notation for atomic levels with principal (*n*) and azimuthal (*l*) quantum numbers, electron shell, number of electrons in the shell, and x-ray symbol for singly ionized atom with a vacancy in the shell.

Three aspects to note about binding energies E_B:

(1) E_B increases approximately as Z^2.

(2) E_B (K-shell) is nearly a factor of ten greater than E_B (L-shell), which in turn is nearly a factor of ten greater than the binding energies in the M shell.

(3) Each shell and subshell have a characteristic E_B.

Tabulated values of the binding energy (Table F.3) also show these same trends. These values are important because an incident photon must have an energy $E = hf$ greater than E_B to eject an electron from the shell. For example, a 2.0 keV x-ray would have sufficient energy to eject a silicon (Si) K-shell electron (E_B = 1.839 keV) but not enough for a phosphorous (P) K-shell electron (E_B = 2.149 keV). The same considerations are true for L-shell electrons. A 2.0 keV x-ray would eject an arsenic (As) L-shell electron (E_B = 1.4 keV) but not the L electrons of cadmium (Cd) (E_B = 3.5 keV).

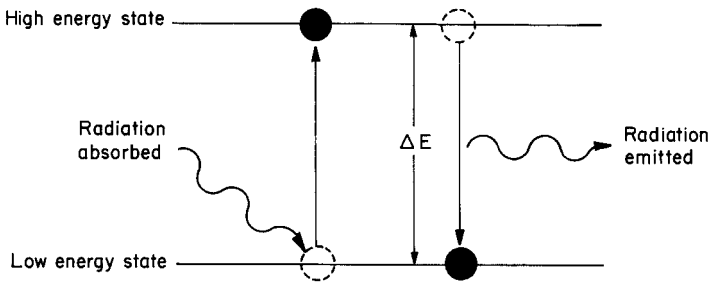

Fig. F.5. Two energy levels separated by an energy ΔE. Radiation is absorbed in an electron transition from the low to the high energy state. Radiation is emitted in the transition from the high to the low energy state.

F.4 X-RAY EMISSION

Bohr proposed that an atom can absorb radiation only at a frequency f that corresponds to the difference in energy ΔE between two allowed quantum states:

$$\Delta E = hf. \tag{F.2}$$

This is illustrated in Figure F.5. An electron cannot jump from a lower to a higher energy state unless this exact amount of energy is supplied to it. Conversely, when an atom in a higher state falls to a lower state, the frequency of radiation given off is dictated by the relationship just given.

For x-ray emission, when an electron is ejected from a K-shell, a vacancy (unoccupied electron state) is left in the K-shell. The atom is in an excited state. The atom can lose some of its excitation energy by emitting a photon (x-ray). The emitted x-ray has lower energy than the incident photon, as illustrated in Figure F.6. The K-shell vacancy is formed by an incident x-ray with energy greater than E_B(K), the binding energy of the K-shell electron. To fill the vacancy an electron makes a transition from the L_3 state. (Binding energies for L-shell electrons are less than those of K-shell electrons.) The energy of the emitted x-ray (notation is Kα x-ray

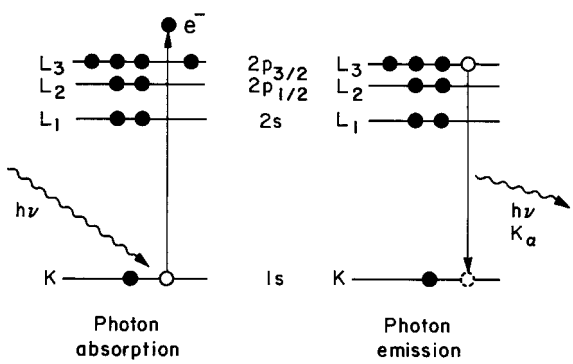

Fig. F.6. Energy levels showing that a photon is absorbed in transferring its energy to a K-shell electron, and an x-ray (K_α x-ray) is emitted when an electron in the L_3 shell makes a transition to the unfilled K-shell.

TABLE F.3

Electron Binding Energies in Kiloelectron Volts (keV) for Elements Commonly Used in Pigments. Electron Energies are Given for Specific Subshells (K, L_3, M_5, N_7).*

			Electron Binding Energies in keV			
Element	*Symbol*	*Z*	*K*	L_3	M_5	N_7
Aluminum	Al	13	1.56	0.07	–	–
Silicon	Si	14	1.84	0.10	–	–
Phosphorus	P	15	2.15	0.14	–	–
Sulfur	S	16	2.47	0.16	–	–
Titanium	Ti	22	4.97	0.46	0.002	–
Chromium	Cr	24	5.99	0.58	0.002	–
Iron	Fe	26	7.11	0.71	0.006	–
Cobalt	Co	27	7.71	0.78	0.003	–
Copper	Cu	29	8.98	0.93	0.002	–
Zinc	Zn	30	9.66	1.02	0.009	–
Arsenic	As	33	11.87	1.32	0.04	–
Selenium	Se	34	12.66	1.44	0.06	–
Cadmium	Cd	48	26.71	3.54	0.40	0.009
Tin	Sn	50	29.2	3.93	0.48	0.024
Antimony	Sb	51	30.49	4.13	0.53	0.032
Mercury	Hg	80	83.10	12.28	2.30	0.10
Lead	Pb	82	88.0	13.04	2.48	0.14

*Compilation from Feldman and Mayer, *"Fundamentals of Surface and Tin Film Analysis"* (North Holland, 1986).

where K_α denotes the most intense line) is given by the difference in binding energies:

$$hf(K_\alpha) = E_B(K) - E_B(L_3). \tag{F.3}$$

Table F.4 gives energies of the K x-rays, E (K_α). The value for Si K x-rays is 1.74 keV. From Table F.3, the binding energy of the Si K-shell is E_B (K) = 1.84 keV, and that of the Si L_3 shell is E_B (L) = 0.10 eV. The difference in energies is

$$\Delta E = E_B(K) - E_B(L) = 1.84 - 0.01 = 1.74 \text{ keV}.$$

This is, of course, the energy of the K_α x-ray lines.

There are other ways to de-excite the atom. An L_2 electron could fill the vacancy, giving rise to a slightly lower energy electron, since $E_B(L_2) > E_B(L_3)$. An electron could make a transition from an M shell (say M_5) to fill the K-shell vacancy (Figure F.7), giving rise to a K_B electron. This is not very probable because electron transitions are most likely from adjacent shells: L to K, a K_α x-ray or M_5 to L_3, an L_α x-ray.

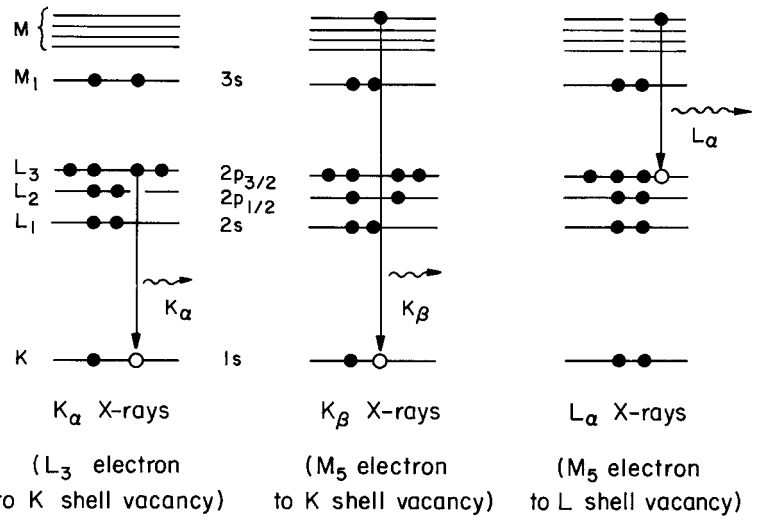

Fig. F.7. Schematic of x-ray emission process where electrons in filled orbitals make transitions to inner shell orbitals with unoccupied (vacant) states. The x-ray energy equals the difference in binding energy between the filled outer shell and vacant inner shell.

The transitions between two $l = 0$ zero shells, 2s to 1s, or 3s to 2s are forbidden by the dipole selection rules.

The energies of the L_α and M_α x-rays are also given by differences in binding energies:

$$\begin{aligned} L_\alpha &: hf(L_\alpha) = E_B(L_3) - E_B(M_5), \\ M_\alpha &: hf(M_\alpha) = E_B(M_5) - E_B(N_7). \end{aligned} \tag{F.4}$$

The energy E of the incident radiation determines from what shell and subshell the electron will be ejected (and a vacancy formed) with the requirement that E be greater than E_B. The highest probability is from shells with energy closest (but lower than) to the incident energy. The difference in electron binding energies determines the energy of the characteristic x-ray lines.

F.5 X-RAY-, ELECTON-, AND PROTON-INDUCED X-RAY EMISSION

In the preceding sections we have discussed the formation of electron vacancies in inner shells ($n = 1, 2, \ldots$) by incident x-rays. Characteris-

TABLE F.4

X-Ray Energies in keV for Characteristic X-rays* Emitted from Elements in Common Pigments

			X-ray Energies keV			
Element	*Symbol*	*Z*	K_α	K_β	L_α	M_α
Aluminum	Al	13	1.49	1.56	–	–
Silicon	Si	14	1.74	1.83	–	–
Phosphorus	P	15	2.01	2.14	–	–
Sulfur	S	16	2.31	2.46	–	–
Titanium	Ti	22	4.51	4.93	0.45	–
Chromium	Cr	24	5.41	5.95	0.57	–
Iron	Fe	26	6.40	7.04	0.70	–
Cobalt	Co	27	6.93	7.65	0.78	–
Copper	Cu	29	8.04	8.92	0.93	–
Zinc	Zn	30	8.63	9.58	1.01	–
Arsenic	As	33	10.53	11.73	1.28	–
Selenium	Se	34	11.21	12.66	1.38	–
Cadmium	Cd	48	23.11	26.10	3.13	0.39
Tin	Sn	50	25.20	28.50	3.44	0.46
Antimony	Sb	51	26.28	29.73	3.60	0.50
Mercury	Hg	80	70.18	80.25	10.0	2.20
Lead	Pb	82	74.25	84.93	10.533	2.34

*In x-ray notation, the capital letter (K, L, M, . . .) indicates the shell containing the vacancy. The subscript $_\alpha$ indicates the most intense line. The electron transitions are: K_α (L_3 to K), K_β (M_5 to K), L_α (M_5 to L_3), M_α (N_7 to M_5).

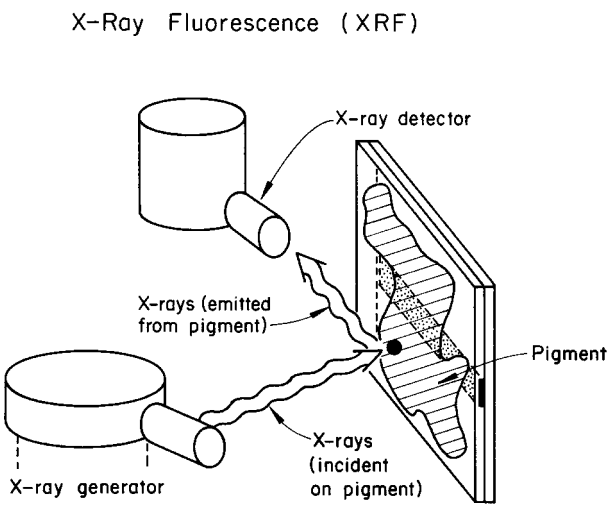

Fig. F.8. X-ray fluorescence (XRF) in which x-rays incident on a painting generate inner shell vacancies in an atom of a pigment particle. Characteristic x-rays are emitted from the atom, and their energies are measured in the x-ray detector, which allows identification of the atom.

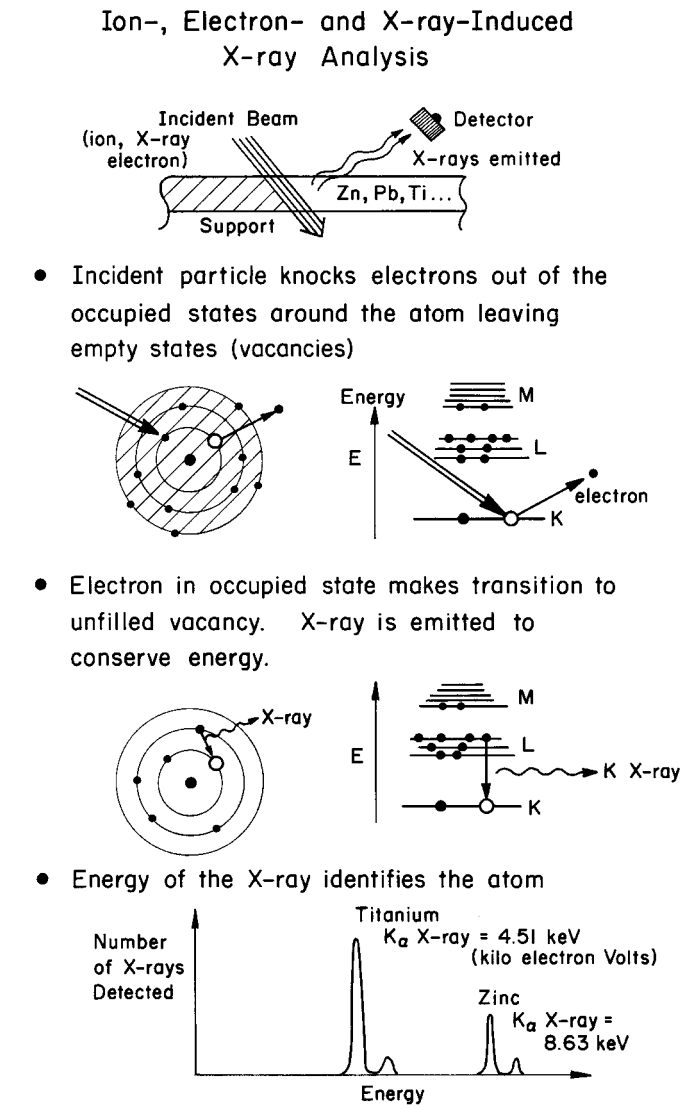

Fig. F.9. Comparison of ion-, electron-, and photon-induced x-ray emission.

tic x-rays are emitted in the subsequent electron transistion to fill the vacancy. This process is called *x-ray fluorescence* (XRF).

The apparatus for generating x-rays is simple, and x-ray fluorescence is used for in situ examination of works of art (Figure F.8). The disadvantage is that the x-ray beam strikes a large area, millimeters to a centimeter in diameter. This large beam area limits the system in analysis of sample areas and paint cross sections. The advantages of XRF are that

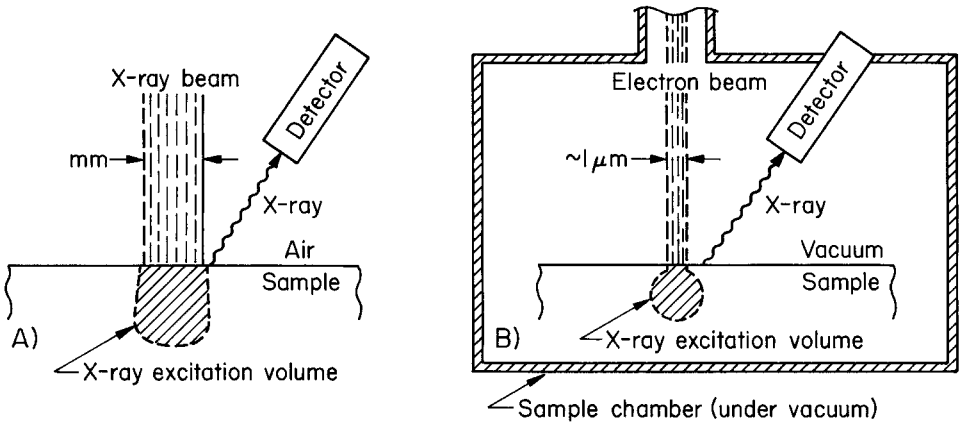

Fig. F.10A,B. Comparison of (A) x-ray and (B) electron beam generated x-ray emission. X-ray fluorescence (XRF) analysis is carried out in air but has a larger beam spot, typically millimeters (mm) in diameter, whereas the electron beam has a smaller size (less than one micron) but the analysis is carried out in a vacuum chamber, which requires removal of the sample from the painting.

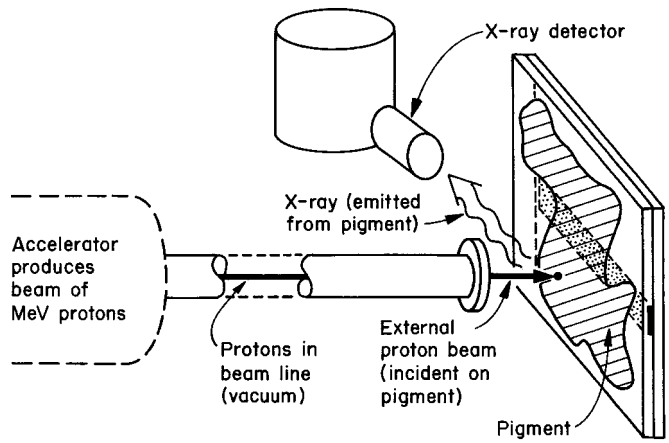

Fig. F.11. Schematic diagram of the setup for proton-induced x-ray emission (PIXE). The million electron volt (MeV) proton beam is produced in an accelerator, and the protons travel in vacuum to the thin window at the end of the beam line. The protons have sufficient energy (usually 3.5 to 5 MeV) to pass through the window and to travel in air to the painting. The emitted x-rays are detected in a system similar to that used in XRF and electron microprobe analysis.

the analysis is carried out in air and that portable units (x-ray generator and detector) are used to analyze pigments without removing samples from the painting.

The x-ray emission process is independent of the manner in which the vacancies are formed. Energetic electrons and ions can also be used

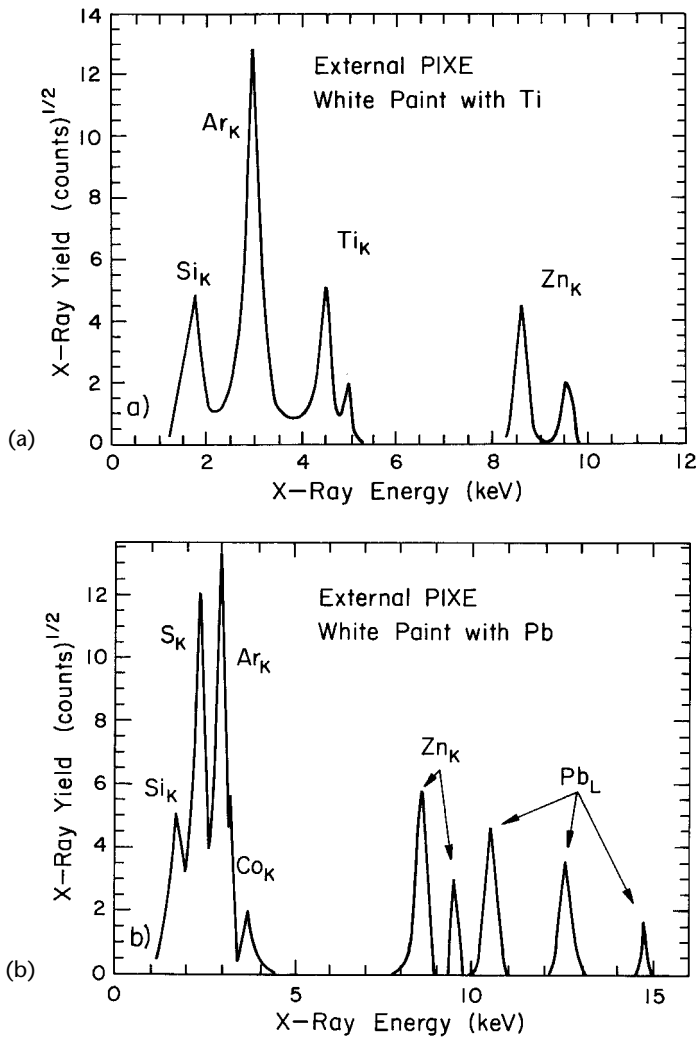

Fig. F.12a,b. External proton beam analysis (PIXE) is shown of two white paints (a) titanium (Ti) white and (b) lead (Pb) white. The spectra are displayed as the yield of x-rays (the number of x-rays incident on the detector for a fixed analysis time) in square root of the number of detected x-rays (counts) versus x-ray energy. The argon (Ar) signals are generated by the proton's passage through air, which contains argon. Titanium K-shell (Ti_K) is shown in (a) and lead K-shell (Pb_L) in (b).

to create vacancies as long as the incident electron energy E_{electron} is greater than the binding energy of electron in the shell. Figure F.9 is a summary of the three methods of pigment analysis by x-ray emission.

Electron-induced x-ray emission is called electron microprobe analysis (EMA) because the incident electron beam can be focused to a one-micron diameter spot size (a microprobe). In comparison with x-ray fluorescence (Figure 10a), the striking drawback to the electron microprobe technique is that the pigment sample must be mounted in vacuum (Figure 10b) because of the small penetration distance of electrons in air. A paint fragment must be removed from the sample, placed in a potting compound, and polished so that a cross section of the pigment layers can be examined in the vacuum chamber of the electron microscope. The penetration of 20-keV electrons is only 40 microns, so that top-surface irradiation by 20-keV electrons would produce x-rays only in the outermost layers.

Protons of MeV energies produced by a particle accelerator can also produce electron vacancies (Figure F.11). The process is called proton-induced x-ray emission (PIXE). Figure F.12 shows PIXE spectra of titanium white (Figure 12a) and lead white (Figure 12b). Comparison of the two spectra show that both have peaks from pigments containing zinc (zinc white) as well as argon (Ar) due to the passage of the proton beam through air before striking the painting (argon is a noble gas present in air at 0.93%). The presence of the titanium peaks in Figure 12a and lead peaks in Figure 12b serve to identify the two white paints.

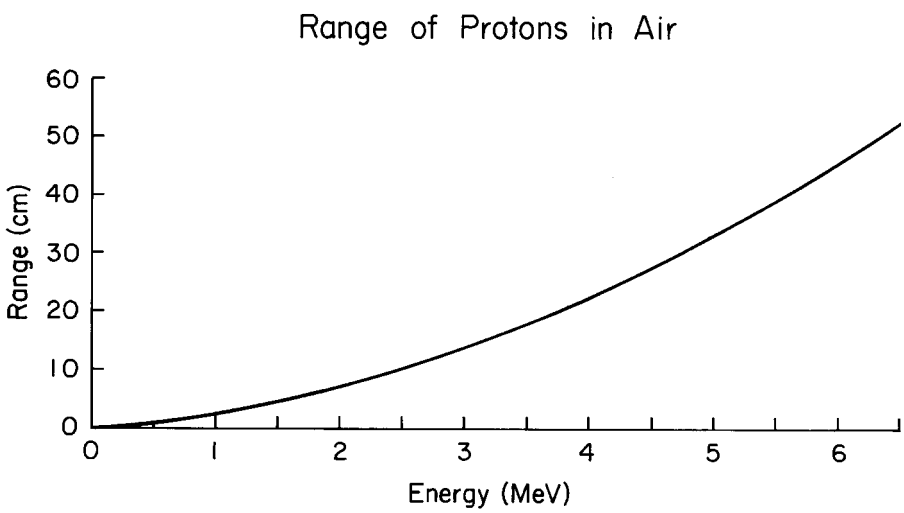

Fig. F.13. The range of protons in air. A 4-million electron volt (MeV) proton can travel nearly 25 cm (10 inches) in air before it loses all its energy in collisions with air molecules along its path.

The range of 5-MeV protons in air is many centimeters. Consequently, the protons can be taken out into the air (external beam analysis), as shown in Figure F.13. The range of 5-MeV protons in paint layers is somewhat greater than 200 microns. Thus, nearly the full thickness of a multilayer painting may be analyzed.

Nuclear Reactions and Autoradiography

G

G.1 Nuclear Reactions

In this section we present the basic terminology and concepts involved in nuclear reactions. We are primarily concerned with two reactions:

(1) The nucleus can be excited to a higher energy state (analogous to promoting an electron to a higher energy state in atomic spectroscopy); the nucleus can then de-excite by γ-ray emission (γ is the Greek letter gamma)

(2) A different nucleus Y may be formed as a result of the nuclear reaction between an incident proton or neutron and the target nucleus X.

In most nuclear reactions we have two particles or nuclei interacting to form two different nuclei. Thus

$$\underset{\text{Reactants}}{a + b} \quad \rightarrow \quad \underset{\text{Products}}{c + d}$$

Although there is no theoretical limitation on what a, b, c, and d can be, as a practical matter each side of the equation usually includes a very light particle. If we designate the particle by a lowercase letter, we can write a nuclear reaction as

$$a + X \rightarrow b + Y.$$

In a common shorthand notation, one would write

$$X(a,b)Y.$$

A nucleus with four neutrons and three protons is designated by

$${}^{7}_{3}X,$$

where the *subscript* is the atomic number Z, the number of protons, and the *superscript* is the total number of nucleons, which we term the mass number A. More generally, therefore, a nucleus is designated by

$${}^{A}_{Z}X.$$

A specific nuclear reaction is

$${}^{1}_{0}\mathrm{n} + {}^{10}_{5}\mathrm{B} \rightarrow {}^{4}_{2}\mathrm{He} + {}^{7}_{3}\mathrm{Li}.$$

where ${}^{4}_{2}He$ is an alpha (α) particle. In shorthand,

$$^{10}\mathrm{B(n,}\alpha\mathrm{)}^{7}\mathrm{Li}.$$

The reactant and product light particles are placed in parentheses and separated by a comma. The terms most frequently used are given below.

Nucleon	Either a proton or a neutron.
Nuclide	A specific nuclear species with a given proton number Z and neutron number N.
Isotopes	Nuclides of the same Z and different N.
Isobars	Nuclides of the same mass number A, where $A = Z + N$.
Alpha (α)	A helium nucleus: two protons and two neutrons.
Beta (β)	An electron or positron emitted in a reaction (beta decay).
Gamma (γ)	A high-energy photon.

In our treatment of atomic reactions and the stable nucleus, the four particles are electron, photon, proton, and neutron. In nuclear reactions and radioactive decay we have particle and antiparticle as well as the subnuclear particle the neutrino. The positron, or antielectron, e^{+}, is identical to the electron, but with positive charge. The positron can be produced along with an energetic electron (electron–positron pair production) by interaction of a gamma ray of energy greater than 1.022 MeV ($2m\,c^2$) with a nucleus or electron. Other particle/antiparticle pairs can be produced, such as proton–antiproton, which requires 1896-MeV pho-

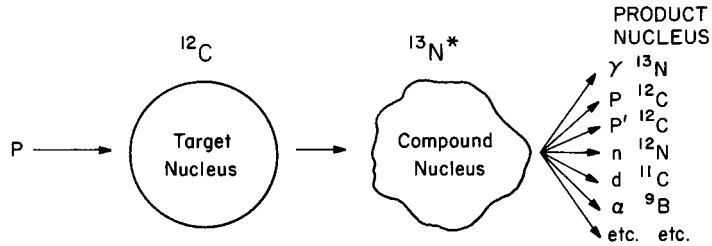

Fig. G.1. Schematic representation of a nuclear reaction in which a proton (p) strikes a carbon-12 (^{12}C) nucleus and forms a radioactive nitrogen-13 ($^{13}N^*$) nucleus, which decays by emission of gamma (γ) rays leaving a product nucleus of ^{13}N, or by emission of protons (p) leaving a product nucleus of ^{12}C, or by emission of neutrons (n), deuterons (d), alpha (α) rays, and others.

tons. Our interest is primarily in beta rays, electrons, and positrons, because of their emission in beta decay. In beta decay, neutrinos and antineutrinos with symbol υ and $\bar{\upsilon}$ are required for conservation of energy. The neutrino has such weak interactions with matter and hence is so difficult to detect that as a practical matter we ignore neutrinos in our description of beta decay.

Let us consider the irradiation of nuclei in a flux of protons, specifically proton irradiation of ^{12}C (Figure G.1). If the protons have sufficient energy to overcome the coulomb barrier, they may actually be captured by the nucleus to form a "compound nucleus." The compound nucleus is now in a highly excited state and can now de-excite in many different ways by emitting γ-rays, protons, neutrons, alpha particles, etc. The incident protons can, however, also transfer sufficient energy to single nucleons or groupings of nucleons (such as deuterons and alphas) that they may be directly ejected from the nucleus. Examples of such direct interactions are (p,n) (p,α), (α,p), and (α,n) reactions. Compound nucleus reactions are more likely at relatively low energies, whereas the probability for a direct interaction increases with energy.

G.2 Radioactive Decay and Decay Law

A nuclear reaction can take place through the formation of a compound nucleus in two distinct stages as follows: (a) the incident particle is absorbed by the target nucleus to form a compound nucleus and (b) the compound nucleus disintegrates by ejecting a particle or emitting a γ-ray. Many nuclei are unstable and decay by emission of electrons or alpha (α) particles. Emission of an electron increases the charge of the

nucleus Z by one unit without changing the mass number A. This is called beta (β) decay. For example, decay of carbon-14 changes the nucleus to nitrogen-14. Alpha decay decreases the charge of the nucleus by two units and the mass number by four units. Nuclei in excited states can lose energy by emitting gamma rays without a change in Z or A.

Radioactive decay is not instantaneous. The time required for half of the radioactive nuclei to decay is called the half-life. Half-lives can be as short as a small fraction of a second or as long as billions of years. This property provides a powerful tool for determining the age of an object containing radioactive nuclei.

If a radioactive nucleus decays by emitting an electron or alpha particle, it is a *one-time event* for the nucleus, which is no longer counted as one of the radioactive species. In this respect, radioactive decay follows the same relation discussed previously for the absorption of photons (x-rays, for example) in a one-event process. A photon is absorbed by interacting with an electron and "disappearing" by giving up all its energy to the electron (photoelectron absorption). The photon is no longer counted as one of the incident photons. In this relation, the number of photons decreases exponentially with depth as the photons penetrate into the material and are absorbed.

Half the number of radioactive nuclei of a given species decay in *one half-life*. If we start with 100 radioactive nuclei at "zero" time with a half-life of one day, then after one day, 50 of the initial radioactive nuclei will remain. We ignore for the moment the statistics of the counting process, in which 50 is only the statistical average in a real experiment. The next day, half of the 50 will decay, and 25 will remain. Every subsequent day the remaining number will decrease by a factor of 2. After 3 days 12.5 will remain, and after 4 days, 6.25 (of course, you cannot actually have fractional nuclei). The number of radioactive nuclei left after a given time is shown as a solid line in Figure G.2 in both a linear and a logarithmic scale. All radioactive decay follows a curve of the same shape. The only thing that changes for different radioactive nuclei is the half-life and hence the scale of the time axis.

In Figure G.2 a linear decay law, in which the number of radioactive nuclei decrease linearly in time, is presented as a dashed line. That is,

$$N = N_0 \left(1 - \frac{t}{2T_{1/2}}\right), \tag{G.1}$$

where N_0 is the original number of radioactive nuclei, N the number remaining after time t, and $T_{1/2}$ the half-life. After one half-life of time has elapsed ($t = T_{1/2}$), one-half of the nuclei remain (the definition of a half-life). However, after two half-lives ($t = 2T_{1/2}$), there are no radioactive nuclei left. *Equation G.1 is obviously wrong.*

What's wrong! We have to start over with our initial assumption, which is that the number of nuclei that decay in a given time interval Δt

is proportional to the number N present at the start of the interval. If we use the notation that the number of nuclei that decay in the time interval is ΔN, then

$$-\Delta N \text{ is proportional to } N\Delta t, \tag{G.2}$$

or

$$-\frac{\Delta N}{\Delta t} \text{ is proportional to } N, \tag{G.3}$$

where the negative sign is used because the number of radioactive nuclei N is decreasing. We can eliminate the "proportional to" by introducing a constant of proportionality λ, the decay constant, so that

$$-\Delta N = \lambda N \Delta t. \tag{G.4}$$

The decay constant is the probability per unit time of the decay of any given nucleus.

Equation G.3 indicates that the rate of decay, the change in N with time, $-\Delta N/\Delta t$, is linearly related to the number N, as we stated at the beginning. We can write the relation in standard differential notation replacing ΔN by dN and Δt by dt in equation (G.4):

$$-dN = \lambda N\, dt. \tag{G.5}$$

We can integrate this equation from time zero to time t and obtain the exponential relation

$$N = N_0 \exp(-\lambda t), \tag{G.6}$$

where N_0 is the number of nuclei at time $t = 0$ (at $t = 0$, $\exp(0) = 1$).

Instead of using the decay constant we can use the inverse of λ, $\tau = 1/\lambda$, which is average time expectancy for the decay of a radioactive nucleus. Equation G.6 then becomes

$$N = N_0 \exp(-t/\tau), \tag{G.7}$$

which we have plotted in Figure G.2 as the solid line.

The symbol τ is also called the "lifetime" and is related to the half-life $T_{1/2}$ as shown below. Recall that the half-life $T_{1/2}$ is the time $t = T_{1/2}$ after which the number N of nuclei has decreased to one-half its original value, $N = 1/2\ N_0$ at $t = T_{1/2}$. Substituting in equation (G.7) we have

$$\tfrac{1}{2}\, N_0 = N_0 \exp(-T_{1/2}/\tau), \tag{G.8}$$

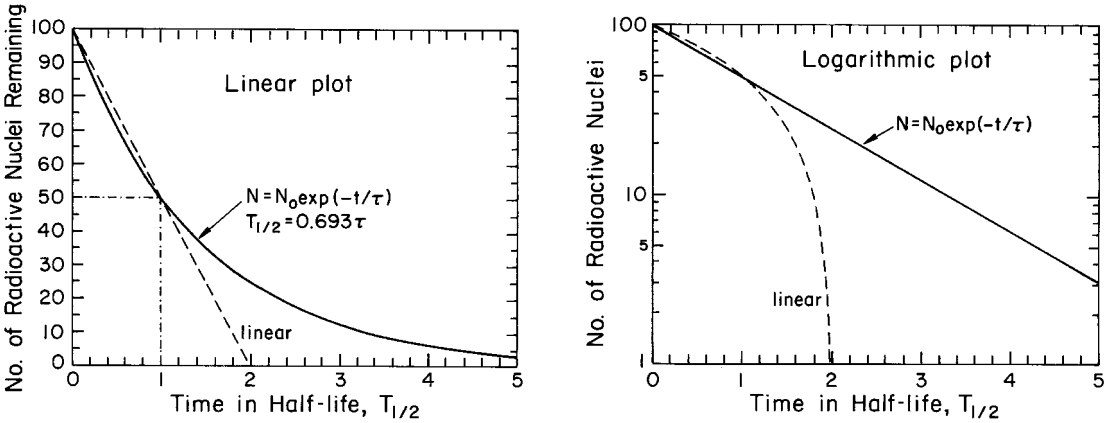

Fig. G.2. Radioactive decay plotted as the number (N) of radioactive nuclei remaining versus the time in half-life, $T_{1/2}$. The upper curve is a linear plot and the lower a logarithmic plot, so the exponential relation appears as a straight line.

or

$$\tfrac{1}{2} = \exp\,(-T_{1/2}/\tau),$$

which on taking reciprocals yields

$$\exp\,(T_{1/2}/\tau) = 2.$$

Then taking the natural logarithm (ln) of both sides, we obtain

$$T_{1/2}/\tau = \ln 2 \approx 0.693.$$

We thus have

$$\boxed{T_{1/2} = 0.693\ \tau.} \qquad \text{(G.9)}$$

In writing on radioactive decay, the expressions lifetime and half-life $T_{1/2}$ are both used.

The exponential function can be approximated for small values of t/τ as a linear relation:

$$N = N_0\ \exp(-t/\tau) \approx N_0\left(1 - \frac{t}{\tau}\right). \qquad \text{(G.10)}$$

For example, if the time t is 1% of the lifetime, then $N = 0.99\ N_0$, or 1% of the radioactive nuclei have decayed. It is because of this linear ap-

proximation that in Figure G.2 the dashed line (linear relation) and solid line essentially coincide for small times. The mathematical function exp is available in most hand calculators, so that it is rather easy to calculate the rate of decay of radioactive nuclei.

G.3 COUNTING STATISTICS

The use of statistical methods is important in counting radioactive decay events. We illustrate this with radioactive dating (see also Appendix K). For the decay of carbon-14, the presently accepted values of the radioactive decay constants are

$$\text{Half-life: } T_{1/2} = 5730 \text{ years},$$
$$\text{Lifetime: } \tau = 8268 \text{ years},$$

where $T_{1/2} = 0.693\ \tau$, as described in equation (G.9). Thus the number of carbon-14 atoms decreases by 1% in every 83 years, indicating that if you can determine the amount of radioactive carbon-14 with sufficient accuracy, then you can determine a time scale.

The time scale is based on the fact that organic matter, while it is alive, is in equilibrium with the cosmic radiation, and the radiocarbon atoms that disintegrate in living things are replaced by the carbon-14 entering the food and growth chain. According to the law of radioactive decay, after 5730 years the carbon that was in the body while it was alive will show half the specific carbon-14 radioactivity that it showed at the time of death. In the disintegration process, the carbon-14 returns to nitrogen-14 by emitting a beta particle.

In radioactive dating one often must detect *small* differences in the amounts of carbon-14 present. The difference between a present sample and one 83 years old (one-hundredth of a lifetime) is only 1% of the amount of carbon-14 present in the two samples. Counting statistics are an important issue. If N is the number of particles counted, then there is a 68% probability that the true value (corresponding to the average rate multiplied by the counting time) lies within the limits where $N \pm \sigma$, where σ, the standard error, is equal to $N^{1/2}$. See Table G.1.

If the error limits are widened to $\pm 2\sigma$, then there is a 95% probability that the true value is contained within them, and for $\pm 3\sigma$ the probability is 99.7%. This statistical uncertainty implies uncertainty about the true value of the radiocarbon age.

TABLE G.1

For $\sigma = N^{1/2}$ the following relations hold:

$N = 100$	$\sigma = 10$, i.e., 10% of N
$N = 1000$	$\sigma = 33$, i.e., 3.3% of N
$N = 10{,}000$	$\sigma = 100$, i.e., 1% of N
$N = 100{,}000$	$\sigma = 330$, i.e., 0.33% of N

Counting statistics for N events with standard deviation σ for $\sigma = N^{1/2}$.

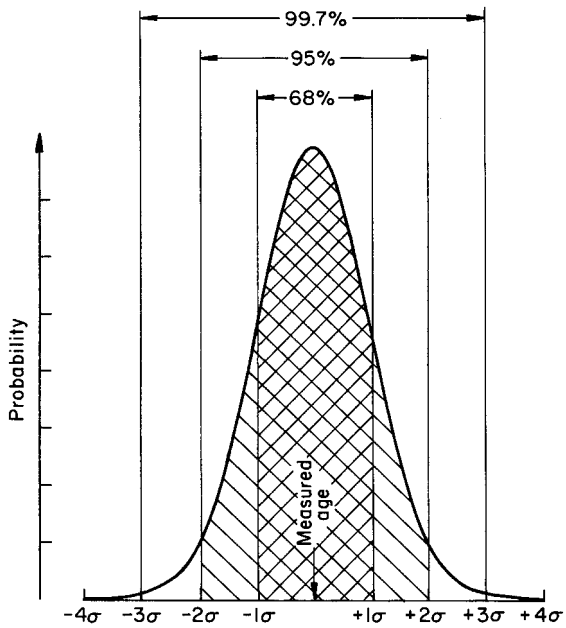

Fig. G.3. Probability curve of a normal or Gaussian distribution plotted versus standard error (or deviation) σ. The probability is 68% that an event occurs within the cross-hatched area between plus and minus one standard deviation ($\pm 1\sigma$). The probability is 95% for $\pm 2\sigma$ and 99.7% for $\pm 3\sigma$ (*Taken from* Aitken, *Science-Based Dating in Archaeology* (Longman, London, 1990)).

The statistical uncertainty is due to the fact that radioactive decay is a random event; that is, the decay of any individual nucleus is a random event in time that we can assign a probability per unit time that the decay occurs. With a million radioactive decays the uncertainty is small—the square root of 10^6 is 10^3—but with one hundred events, the standard is 10, equivalent to 10%, or a dating uncertainty of plus or minus about 830 years for C-14 dating. The probability is plotted as a Gaussian distribution in Figure G.3. This statistical uncertainty due to the randomness of radioactive decay is a fundamental limitation in the precision to which beta activity may be measured. There are also uncertainties besides the statistical one.

G.4 Neutron Activation Analysis and Autoradiography

Almost all of neutron activation analysis depends on the relatively high probability that a slow-moving neutron can be captured by an atomic nucleus. This reaction forms a new isotope with a mass number one unit larger than the target atom:

$$ {}_0^1\mathrm{n} + {}_Z^A X \rightarrow {}^{A+}{}_Z^1 X. $$

In this reaction the atomic number Z of the nucleus is unchanged.

When the atoms of an element are bombarded by neutrons in a reactor, some of them will absorb a neutron and become radioactive. For example, in the case of sodium,

$$ {}_{12}^{23}Na + {}_0^1 n \rightarrow {}_{12}^{24}Na + energy. $$

A sodium nucleus with 12 protons and only 11 neutrons absorbs a neutron to become a sodium nucleus with 12 neutrons. This sodium-24 is radioactive and eventually decays:

$$^{24}_{12}Na \rightarrow ^{24}_{13}Mg + \beta^- + energy.$$

Each sodium-24 atom that decays to a magnesium atom (with 13 protons and 11 neutrons) emits a beta particle (β^-, an energetic electron) and a gamma ray. Energy conservation is provided by the gamma rays. The number and energy of the gamma rays are unique for the decay of sodium-24 and thus constitute a kind of signature. Furthermore, the half-life of the sodium-24 (15 hours) is also a means of identification.

Thus, when a material containing some sodium is irradiated by neutrons in a nuclear reactor, one may (a) show that sodium is present by later observing the energies of gamma rays from sodium-24, and (b) determine how much is present by measuring how many such gamma rays are emitted.

Autoradiography is performed by placing a photographic film in direct contact with a painting after neutron irradiation. In contrast to neutron activation analysis, where gamma rays are detected, in autoradiography, it is the beta-rays (the energetic electrons) that are detected in the film. The gamma rays have such great penetration depths that they hardly interact with the film, whereas the electrons, with their shorter penetration, readily expose the film. In a sense this is a form of beta-radiography as used in watermark analysis, but since the radioactive elements in the painting itself are the source of beta rays, the technique is called "autoradiography."

TABLE G.2

Elements easily detected by neutron activation autoradiographic procedures

Name	*Z*	*Symbol*	*Beta Half-Life*
Sodium	11	Na	15 hours
Aluminum	13	Al	2.3 min
Manganese	25	Mn	2.6 hours
Cobalt	27	Co	5.3 years
Copper	29	Cu*	5.1 min & 12.8 hours
Arsenic	33	As	26.5 hours
Antimony	51	Sb	3 days
Gold	79	Au	3 days
Mercury	80	Hg	

For neutron autoradiography we require that there be a high probability for the formation of a radioactive species that decays by emission of beta particles with a half-life that is not too short or too long. It is clear that quantitative analysis of the amount of an element present depends on *when* the measurement is made after the irradiation.

There are limitations to the method. The most obvious of these are the cases where neutron capture produces a stable isotope, since in such cases no activation occurs. This applies to most of the important light elements such as H, C, N, O, Mg, Si, S, Ti, and Fe. Similarly, if the most abundant isotope yielded a very long-lived radioactive product, the activity produced during an irradiation of some hours or days might still be insufficient for sensitive analysis. Such, for example, is the case for Ca and Ni. Also, when the contrary is true and the product has a very short half-life, decay of the activity may be inconveniently fast and cause problems of measurement as with Li, B, and F. All of these elements except Li, O, and F are readily identified with *prompt* gamma analysis.

In terms of elements found in pigments, for autoradiography where β emission is required for photographic films, the elements most easily

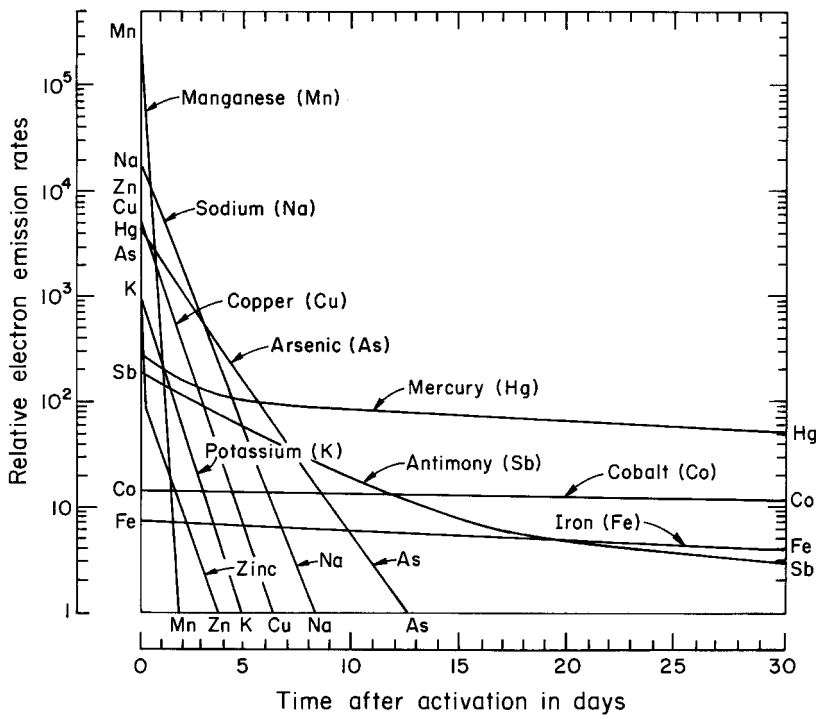

Fig. G.4. Relative rates of energetic electron (beta ray) emission during the radioactive decay of neutron-activated pigments with the painting *Saint Rosalie Interceding for the Plague-Stricken of Palermo* (from Ainsworth et al., *Art and Autoradiography* (The Metropolitan Museum of Art, New York, 1982)).

detected are, in alphabetical order, aluminum, antimony, arsenic, cobalt, copper, gold, manganese, mercury, and sodium. These elements are listed by atomic number Z in Table G.2, which gives β-emission half-life.

Elements that *do not* give good, distinct images are *lead* and *iron* along with *carbon* and calcium, as indicated above. Thus pigments that do *not* cause distinct images are *chalk* (CaCo3), *lead red and white*, *lead–tin yellow,* and the iron in *ochre*. As pointed out by Sayre and Lechtman (Reference E, number 6), "Of these the one which might seem most regrettably absent from the autoradiographic palette is *lead white*, one of the most important pigments in the history of painting."

An indication of the influence of the half-life on electron emission rates is shown in Figure G.4. In autoradiograph film, darkening is caused by electron emission, i.e., beta particles emitted in radioactive decay. All beta particles from elements that were studied were roughly equally effective in producing film darkening. As a result, it appears that for each element its contribution to film darkening at any given time is roughly

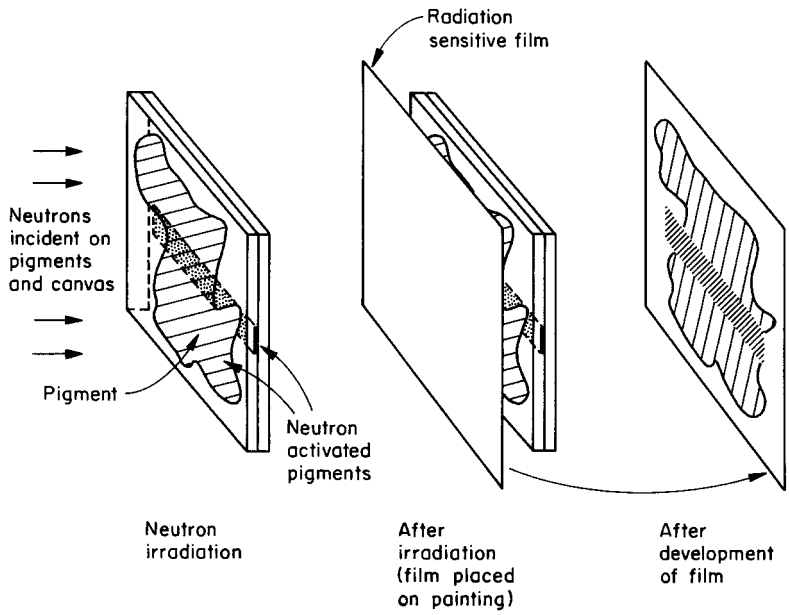

Fig. G.5. The technique of autoradiography. A painting is exposed to a beam of neutrons and is then placed in contact with film at a given time after the neutron activation of the pigments. During the radioactive decay process, beta rays from a radioactive atom in a pigment pass out from the painting and penetrate into the film. Each beta ray exposes the film emulsion along its track. After development of the film, the amount of darkening in a given area indicates the number of beta rays striking the film and hence the amount of radioactive pigment in the painting in the area in contact with the painting.

proportional to the electron emission rate for that element at that time. For every painting a graph such as shown in Figure G.4 is constructed that shows for each element the calculated electron emission rates as a function of the time elapsed after activation. These graphs are valuable in determining which elements contribute to the film darkening in any specific autoradiograph. They facilitate the identification of the pigment or painting material whose image appeared in that autoradiograph.

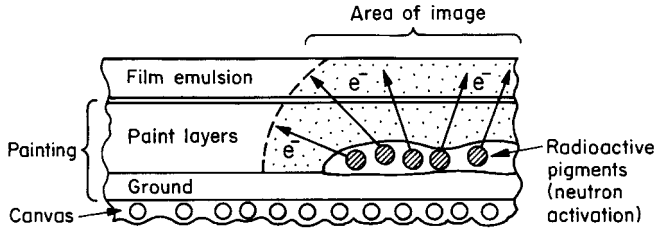

Fig. G.6. A schematic illustration of energetic electrons (beta rays) emitted in radioactive decay of neutron activated pigment particles. The range of the beta rays (shaded area) is about 0.5 mm, depending on electron energy, so that the exposed image in the emulsion corresponds to the location of the radioactive pigment particles.

Autoradiography is a nondestructive technique used here for the examination of underlying paint layers. The painting is placed in a beam of thermal neutrons for a short period of time, and then a series of photographic films is placed in contact with the surface of the painting (Figure G.5). Beta particles (electrons) emitted in the decay of the radioactive elements present in the painting sensitize the film.

Upon development and fixing, the film will show the distribution (location and density) of those pigments and other painting materials that contain radioactive elements at the time of film exposure. The localized nature of the image is due to the short range of the beta rays emitted in radioactive decay. As shown in Figure G.6, the beta rays penetrate the equivalent of only a few paint layers (about 500 microns, or 0.5 mm) and hence blur only the periphery of the image. The deeper-penetrating gamma rays have only a small interaction with the film emulsion. A series of such full-scale photographic images, called autoradiographs, consists of several consecutive exposures: The first ones are short exposures obtained only minutes after neutron activation; later exposures are started hours, days, and even weeks after activation. Film exposure times vary accordingly from several minutes for the first autoradiograph to several weeks for the last one. Because of the differences in the decay times of the radioactive elements, different images are generally observed among the series of autoradiographs.

Organic Binders: Analytical Procedures

H

Contributed by RICHARD NEWMAN, Museum of Fine Arts, Boston

H.1 Introduction

As discussed earlier in this book, many materials, both natural and synthetic, have been used as binders by artists. The binder chosen by a particular artist is influenced in part by both tradition and availability. Animal glues were widely utilized as media by many cultures throughout history, and this is no surprise, considering how readily available the raw materials to make the medium have been and how simple animal glues were to prepare. But in many periods throughout history, artists have been able to work in any of several different media. Different media have quite variable properties that affect how they are used in painting. Among these properties are solubility, the transparency or depth of color that is obtainable with a given pigment, and handling properties—how the paint flows, how quickly it dries, whether it can be applied in very thick and thin layers, and so forth. In many cultures, the choice of medium involved consideration of these other properties. Knowledge of media utilized in paintings can help us to understand the intentions of artists. To some extent, we can use documentary sources to learn about the types of paints used by different artists at various times throughout history. But because such documentary sources are scarce, much of our knowledge comes from analysis of actual samples from painted artifacts. The purpose of this appendix is to introduce some of the modern techniques by which such analysis is carried out.

There are many approaches to analysis of paint binders. Many of the procedures that are useful for the identification of pigments are not very helpful for binding media. For example, determination of the

elements present in a paint sample by an x-ray fluorescence technique can enable much to be said about the pigments in a sample. But most binders consist of the same few elements, and even when there are differences, these elements (carbon, oxygen, hydrogen, nitrogen, and a few others) cannot be nearly as easily detected as the heavier elements (those with higher atomic numbers) that are characteristic of many pigments. Another example is x-ray diffraction, which is quite useful for many pigments (since they are crystalline in nature) but which gives no information on binders (which are not crystalline).

The same basic requirements apply to analytical identification of binders as to pigments. An analysis must be able to be carried out on a quite small sample, since only small samples can usually be taken from paintings. The second requirement is that the analytical technique be capable of providing unambiguous, specific information that can give a positive identification. This second requirement, as we shall see below, is more of an ideal than a reality for most analytical procedures currently applied to the study of paint media. As with pigments, usually the most prudent approach is to apply more than one procedure to a given sample when possible.

The three major approaches currently being utilized are biological stains, Fourier transform infrared spectrometry, and chromatography. We will briefly discuss each in turn below. A bibliography in Reference N gives a few references that can be consulted for more detailed information on these techniques.

H.2 Biological Stains

These are compounds, usually applied in solution, that react in some way with certain types of chemical compounds (or certain types of chemical bonds within compounds) and not with others. The nature of the reaction varies from one stain to another. The majority of stains that have been applied to binder analysis do not provide specific identification of binders, but can give an idea of the general class of binder. The most commonly utilized ones are stains that react in the presence of proteins and stains that react in the presence of lipids (oils). One attractive feature of stains is that they can be applied on cross sections of paint, thus in principal allowing binding media in different layers of a painting's structure to be identified.

The earliest stains utilized for binder analysis were colored compounds that were applied to a sample cross section for a short period of time, after which the sample was rinsed. Under a microscope, layers in the cross section that contain the class of compound for which the stain is specific remain colored by the stain. The stain will have been rinsed away from layers where such compounds are not present. In some cases,

a protein stain and lipid stain could be applied one after the other to a sample, and the results from both could potentially help to identify the binders. Suppose one applies a lipid (oil) stain that stains lipids red, and a protein stain that stains proteins blue. Layers that react with both the lipid and protein stains might contain egg yolk, which contains substantial amounts of both classes of compounds. Layers reacting only to the oil stain probably contain drying oils, while layers that react only with the protein stain could contain any of several protein-containing binders that contain no lipid (such as glue or egg white). Some ambiguity creeps in, however, because a layer that reacts positively to both stains could contain drying oil that has been mixed with a protein-containing binder, and no egg yolk at all.

Akin to normal stains, which are colored compounds viewed under visible light, are fluorescent stains. These are colored compounds that react with general classes of binders to form products that fluoresce in a characteristic fashion when viewed under ultraviolet light. Cross sections can be stained, rinsed, and observed under a microscope fitted with an ultraviolet epifluorescence attachment.

Both the visible-light and fluorescent stains were initially developed for application to fresh biological samples. In old paint samples, the organic compounds have often undergone reactions that can make them more difficult to stain than the fresh compounds would have been. This is one reason why stains can produce somewhat equivocal results when applied to paint samples.

A variation on the normal and fluorescent stains are immunofluorescent stains. These make use of antibodies, which are protein-like compounds capable of reacting only with specific types of proteins. Thus, in theory, egg yolk, egg white, and some other protein-containing binders could be definitively identified. In practice, consistent results have been very difficult to obtain to date, and the technique has been little utilized.

The simplicity of staining, in contrast to the instrumental techniques discussed below, makes it a very attractive method. Even more important, stains ideally can help unravel media in different layers of a cross section in which the media in successive layers may not all have been the same. The techniques described below usually are carried out on isolated samples of individual layers. Separating thin paint layers from one another is difficult, often impossible, so staining is the only current common procedure by which the media in complex paint structures consisting of thin layers can be studied.

H.3 Fourier Transform Infrared Spectrometry

The infrared region of the electromagnetic spectrum is the region on the longer-wavelength side of the visible spectrum. Infrared radiation can-

not be "seen" by our eyes, but we sense it as heat (all hot objects give off considerable infrared radiation). Infrared reflectography, described earlier in this book, uses "near infrared" radiation, that is, infrared radiation just beyond the red part of the visible light spectrum. (The infrared radiation used in IR reflectography goes out to wavelengths of about two micrometers, or two millionths of a meter.) Many pigments are more transparent in near-infrared radiation than they are in visible light, and thus the technique allows underdrawing or underlying paint layers to be seen through overlying thin paint layers. An underdrawing or underpainting that may be totally obscured in visible light can often be readily seen by infrared reflectography.

Radiation in the "mid infrared" region extends from about 2.5 to 25 micrometers (or about 2.5 to 25 millionths of a meter); this is a conventional definition, fairly arbitrary. Just as many materials absorb some of the wavelengths of the visible spectrum and transmit others, many materials also absorb some wavelengths of the mid-infrared region and transmit others. Absorption in the visible range causes electronic transitions, as was discussed in Appendix C. Such electronic transitions also affect the transparency of some pigments in the near infrared region utilized in infrared reflectography. In contrast, mid-infrared radiation is not energetic enough to produce changes in electronic states in atoms or molecules. Instead, mid-infrared radiation can cause chemical bonds to bend or stretch, or cause the atoms in the crystalline lattices of compounds to vibrate relative to one another. Such reactions occur at different wavelengths, depending on the specific compound absorbing the radiation and the types of bonds it contains. Infrared spectrometers are analytical instruments that record the absorption (or transmittance) of infrared radiation by a material as a function of wavelength. The resulting pattern of absorption or transmittance can be used to identify a material, sometimes quite specifically.

In the analysis of painting materials, infrared spectrometry can be used for analysis of many pigments (both organic and inorganic), binders, and varnishes. Many organic compounds with similar chemical compositions and structures have similar patterns of absorption in the IR range. This is true, for example, of the protein-containing binders, such as glue, egg white, casein, and the protein portion of egg yolk (see Figure H.1). Thus, this instrumental technique is useful for the identification of the general class of a binder, but not usually for specific binder identification.

The most modern generation of infrared spectrometers, called "Fourier transform" instruments after the mathematical technique used to compute spectra from the information acquired by the instrument, can be attached to infrared microscopes. With the aid of an infrared microscope, very small specks of paint can be analyzed. Paint chips can also sometimes be sliced very thinly and analyzed, which permits analyses of individual paint layers to be carried out. The technique of infrared microscopy cannot, however, be applied with great success at the mo-

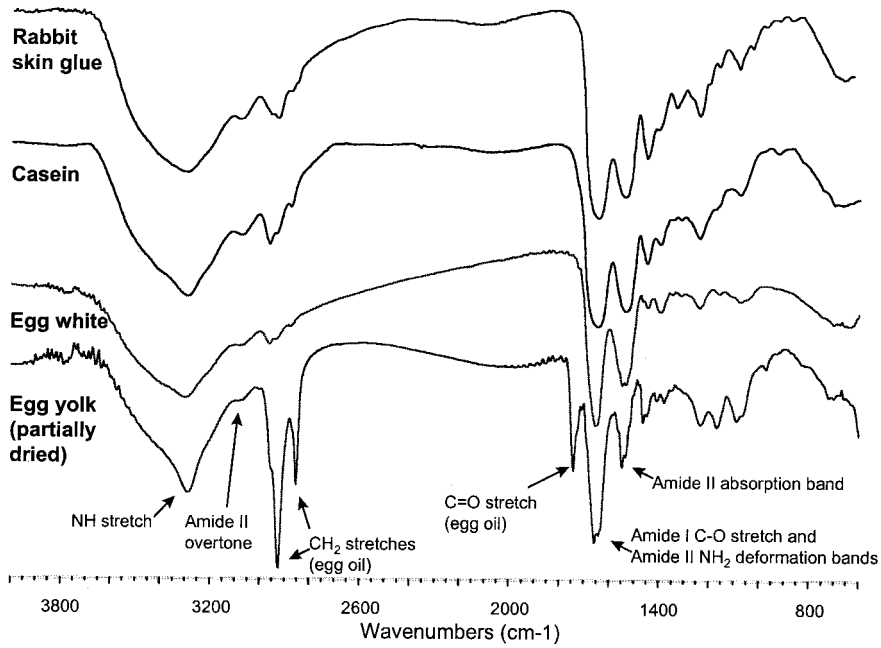

Fig. H.1. FTIR spectra of several protein-containing binders. Rabbit skin glue, the particular casein shown here, and egg white are almost entirely made up of proteins. Although each binder contains different specific proteins, these proteins have virtually identical spectra, and the three binders cannot be distinguished from one another by infrared spectrometry alone. Egg yolk contains a substantial amount of oil in addition to protein. The oil component makes it possible to readily distinguish egg yolk from rabbit skin glue, casein, and egg white. It should be noted, however, that a mixture of one of the nearly pure protein binders and a drying oil would produce a spectrum similar to that of egg yolk, so in certain instances there could be some ambiguity.

ment to cross sections. Infrared microscopy is an attractive technique because of the wealth of information obtainable from a single quite small sample. The sample itself is not damaged or destroyed during the analysis, so it can be used for additional analyses after the IR spectrum is acquired. IR spectrometry is virtually the only common instrumental technique that can simultaneously provide information about both pigments and binding media.

One difficulty in the study of paint samples is the presence of pigments, which often absorb radiation in the mid-infrared range and can partially mask information from the binders in the sample, sometimes to the point where the binder cannot even be generally identified.

One example of general binder identification on a paint sample is shown in Figure H.2. The sample is from the early Netherlandish painting shown in Figure 3.8. The sample contains the pigment lead white

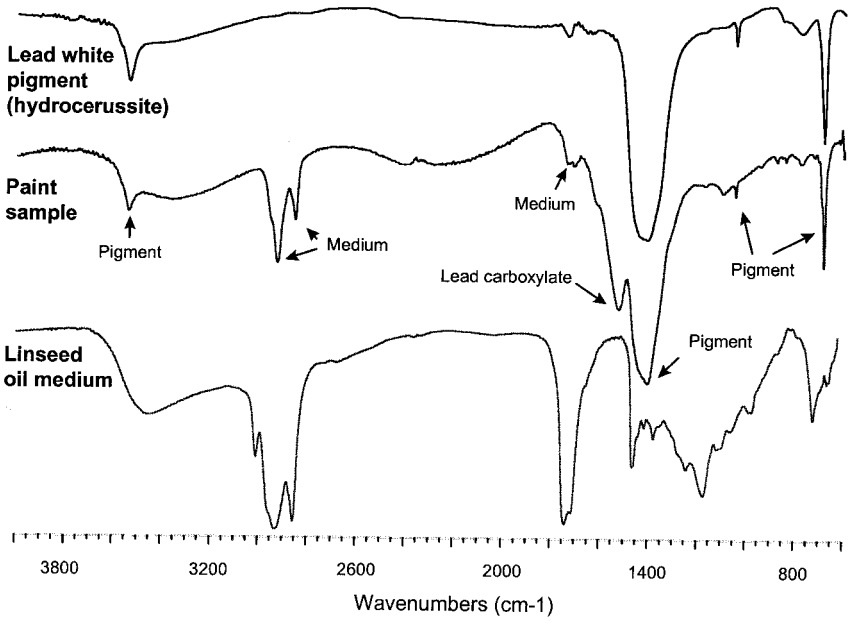

Fig. H.2. FTIR spectrum of a white paint sample from Rogier van der Weyden's *St. Luke Drawing the Virgin*, ca. 1434.
The sample contains lead white pigment (specifically, the compound hydrocerussite) and a drying oil medium (probably linseed oil). The spectrum shows absorption bands for both the pigment and the binder. In addition, interaction between the pigment and medium has produced additional bands, including the large one at about 1550 wavenumbers. This sample spectrum is quite typical for old lead-white-containing oil paint.

and an oil binder. For comparison, reference spectra of lead white and oil are shown. The paint sample probably consists of about 80–90% pigment and 10–20% paint medium, so it is not surprising that the spectrum more closely resembles that of the reference pigment than that of the pure reference binder.

A second example, in Figure H.3, is from a 1938 painting by the American artist Arthur Dove. Analysis of the sample by chromatography techniques (discussed in the next section) showed that the binder contains both wax and drying oil. While the infrared spectrum indicates the presence of oil, the presence of wax cannot be unambiguously established.

IR spectrometry can often produce a general class identification of the binder (for example, oil, protein, or gum). Because of interference from pigments, even this general class identification cannot always be carried out. If a mixture of media is present, identification of the different media may not be, indeed often is not, possible by IR spectrometry alone.

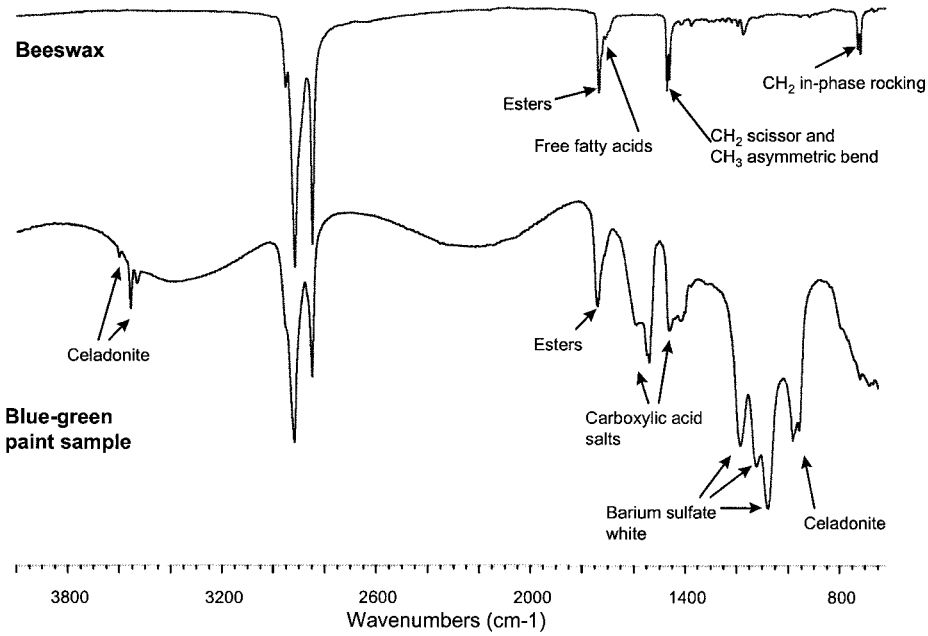

Fig. H.3. FTIR spectrum of a blue-green paint sample from Arthur Dove's *Dancing Willows,* 1941.
Pigments in the sample include two that can be readily identified in the spectrum: the mineral celadonite, the major component of many green earth pigments; and barium sulfate, a white compound. Other features of the spectrum suggest the presence of oil. Also present are fatty acid salts, perhaps a result of interaction between the medium and some pigment in the paint. Analysis of a sample of this paint by gas chromatography/mass spectrometry indicated that the medium also contains some beeswax and a little conifer (probably pine) resin, neither of which can be positively identified in the IR spectrum. The top spectrum is of pure beeswax. The distinctive pairs of bands around 1450 and 720 wavenumbers cannot be seen in the paint sample.

H.4 CHROMATOGRAPHY

Chromatography is the name for a group of analytical procedures widely used in the identification of many organic materials. The name for the general procedure came from its first application in 1906, when an extract from leaves was flushed through a column packed with calcium carbonate. The extract separated into a number of differently colored bands as it passed through the column. Each band essentially represented a different compound contained in the extract.

All chromatographic techniques share a common purpose. They are designed to separate mixtures of several different compounds. At the beginning of a chromatographic examination one has a mixture of compounds. During the course of the analysis, the mixture is separated into

its different parts. Identification of the separated compounds is carried out with reference to standard (known) compounds analyzed under exactly the same conditions. With some modern chromatographic equipment, it is not necessary to actually analyze standards along with an unknown sample—the unknown may be identified with reference to data acquired at a different time, possibly under somewhat different conditions or even on a different instrument.

All chromatographic techniques involve two major components: a carrier or mobile phase, and a stationary material or stationary phase. The mobile phase, usually liquid or gas, carries the sample mixture over or through the stationary phase. There are three principal chromatography techniques that are applied to analysis of binders in paintings. These are thin layer, gas (or gas–liquid, as it is sometimes called), and liquid chromatography, each of which will be briefly discussed below. The mobile phases in these three techniques are liquid, gas, and liquid, respectively.

Chromatography techniques are quite useful for binder identification because, as it turns out, nearly all binders consist of several different compounds, or they consist of material that can be broken down into mixtures of several different compounds. In their natural states, resins and waxes consist of mixtures of different compounds, which can be analyzed by chromatography. For chromatographic analysis, gums, oils, and proteins are usually first chemically broken down into various smaller compounds, which are then analyzed. In the case of gums, oils, and proteins, direct chromatography analysis of the binder, without initial chemical breakdown, is not currently being carried out.

The simplest chromatographic technique is thin layer chromatography. In this procedure, small spots of a solution of the sample are placed near the bottom edge of a glass or plastic plate that has been coated with a thin layer of a very fine-grained inorganic compound (many types of inorganic compounds can be used). Also, along the bottom edge of the same plate are placed spots of solutions of reference materials. The plate is placed in a container that contains a small amount of solvent. The solvent is absorbed by the thin layer of coating and moves up the plate by capillary action, just as water moves up a paper towel that has been dipped in it. As the solvent moves up and past the spots of samples and reference materials, these materials are carried along. The different components of the unknown or reference travel up the plate at different rates, and thus are separated. When the solvent has nearly reached the top of the plate, the plate is removed and dried. If the separation has been successful, a sample will show a series of spots (which correspond to the different compounds found in the sample mixture). If the pattern of spots of the reference materials match the pattern of the unknown, an identification can be made. The spots often are not visible in normal light, but sometimes can be seen in ultraviolet light, or the plate may need to be treated with a chemical that makes the spots visible. Thin layer chro-

matography is a useful technique, but requires somewhat larger samples than do the instrumental techniques discussed below.

Gas chromatography is currently a common technique that may be utilized to identify nearly all types of organic binders. In a gas chromatograph, a small amount of a solution of the sample is injected into the instrument. The solution is immediately heated to a high temperature, which completely volatilizes it (turns it into a gas). The gaseous sample is then swept on a stream of the carrier gas (usually helium or hydrogen) through a long narrow-diameter column that has been coated on its inside with a solid or a liquid that has a very high boiling point. Typical columns are 10 to 30 or more meters in length; diameters are usually from 0.2 to 0.5 millimeters. The column is inside an oven, and analyses are usually made while the temperature of the oven is increased from a fairly low temperature (perhaps 100°C) to a higher temperature (up to about 300°C). The components of the sample mixture generally travel through the instrument at different rates, and come out the other end of the column at different times after injection. Usually, heavier compounds, with higher boiling points, move more slowly than lighter compounds; the exact structure and chemical composition of the compound and the nature of the material in the column also affect the rate of travel. As the components come out the end of the column, they go into a detector, which produces a signal, or peak, in the resulting chromatogram. Just as thin layer chromatography produces only a pattern of separated compounds, analysis of a sample by gas chromatography produces only a chart showing peaks (due to the individual separated compounds) coming out of the instrument at different times. Identification of the peaks is done with reference to standard materials run under the same conditions. The heights of individual peaks is related to the quantity of a compound going through the detector, so with appropriate standards it is possible to determine relative amounts of the various components of a mixture, something that is much more easily done with a gas chromatograph than with thin layer chromatography.

There are two limitations to standard gas chromatography as just described. First, a material must be able to be dissolved in order to be analyzed, and second, the dissolved compound must be able to be vaporized without disintegrating. Although many of the compounds found in natural binders are not volatile, fortunately these nonvolatile compounds can often be turned into a related compound that is volatile by reacting them with certain chemicals, a process called derivatization. Unfortunately, some natural binders are not soluble. It is possible to analyze solid samples, without solution and derivatization, by gas chromatography by utilizing a pyrolysis sampling attachment. A sample placed in a pyrolysis attachment can be heated rapidly to a very high set temperature, which will cause it to fragment into smaller pieces that may be small enough to pass through the gas chromatograph. The fragmentation pattern can be very complex, but with careful control of condi-

tions the pattern is reproducible, and can serve as a sort of fingerprint for a particular binder.

There are many types of detectors that can be attached to a gas chromatograph. A particularly useful one is a mass spectrometer. We will not discuss this type of instrument in this Appendix. However, the mass spectrometer gives more certainty to identification of individual peaks than do most of the other standard types of gas chromatography detectors. A chromatograph coupled with a mass spectrometer is referred to as a gas chromatography/mass spectrometry system (or GC/MS).

High-performance liquid chromatography (HPLC) is currently less widely utilized for binder analysis than gas chromatography, but it too can be used to analyze most of the natural binders. In a liquid chromatograph, a small amount of sample in solution is injected into the instrument. The sample is then carried in a stream of liquid through a column in which separation of the different components of the sample mixture takes place. HPLC columns are typically 15–30 cm long and 1–4 mm in diameter. They are packed with various types of small spherical particles, around which the sample molecules move as they are pushed along in a high-pressure stream of liquid. In the most common variation of liquid chromatography, the liquids used to carry the samples consist of water mixed with certain organic solvents. As in gas chromatography, a detector at the end of the column produces peaks, the heights of which are related to the relative amounts, so this method, too, is easily made quantitative. A limitation of liquid chromatography is that the sample must be soluble. However, it does not need to be volatile, which makes the technique a little more straightforward to apply to some types of compounds than gas chromatography. As with gas chromatography, there are many types of detectors that can be attached to a liquid chromatograph. As with GC, a mass spectrometer can be a very useful detector, but currently LC/MS systems are relatively expensive and have yet to be very widely used in analysis of binders from paintings.

How are different natural binders analyzed by these chromatography procedures? Protein-containing binders are broken down into amino acids, the small molecules from which they are built up, and the amino acids are then analyzed. A given protein will contain over a dozen easily analyzed amino acids, the identities and proportions of which can permit specific proteins to be distinguished from one another. All three chromatography procedures discussed above have been applied to amino acid analysis.

Gum-containing paints are broken down into monosaccharides (simple sugars), which are then analyzed. Some gums contain two, others as many as five, different simple sugars, so analysis can sometimes permit specific gums or mixtures of gums to be identified. Again, all three chromatography techniques have been utilized. In addition to monosaccharides, most gums also contain uronic (sugar) acids. These are more difficult to analyze than the monosaccharides.

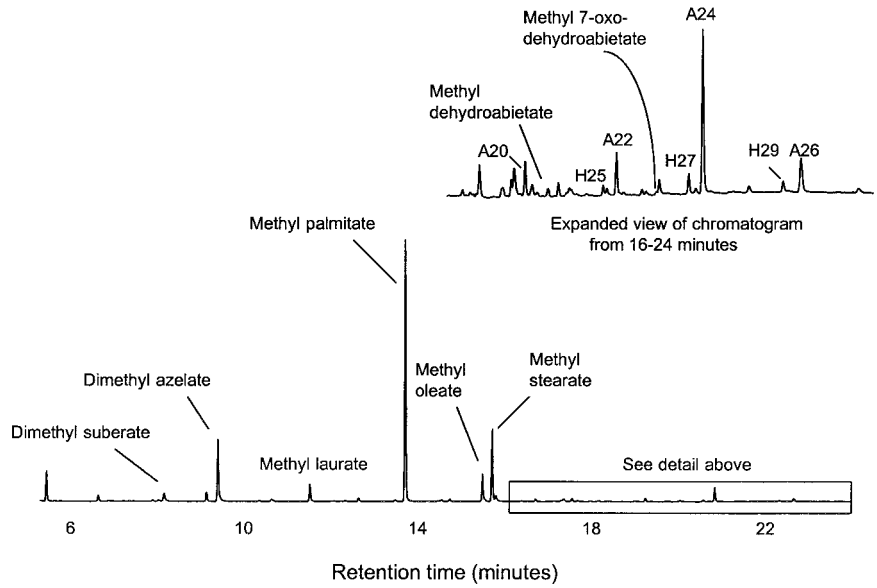

Fig. H.4. Chromatogram of the blue-green paint from Arthur Dove's *Dancing Willows,* 1943.

The sample, whose FTIR spectrum was shown in Figure H.3, was analyzed by gas chromatography/mass spectrometry (GC/MS). Sample preparation involves chemically breaking down the binder and creating derivatives of some of the compounds in the sample (all acidic compounds are converted into methyl esters, which can be much more easily analyzed in a GC than free fatty acids). The major compounds detected, as shown in the chromatogram at the bottom, include saturated fatty acids (mainly palmitic and stearic) and an unsaturated fatty acid (oleic). Also detected are several small dicarboxylic acids (mainly azelaic and suberic). The combination of saturated fatty acids and dicarboxylic acids is typical of paint samples that contain drying oil binders. The upper chromatogram is an expanded part of the overall chromatogram. It shows a number of compounds present at much lower levels than those just noted. These additional compounds indicate that the binder contains two types of material in addition to drying oil. Beeswax is indicated by the pattern of even-numbered saturated fatty acids containing from 20 through 26 carbon atoms, maximizing with the 24-carbon acid (labeled A24). Also indicating beeswax are odd-numbered straight-chain hydrocarbons containing between about 21 and 31 carbon atoms, maximizing with the 27-carbon hydrocarbon (labeled H27). Beeswax also contains a substantial amount of palmitic acid and a small amount of stearic acid, compounds that are also present in drying oils. The chromatogram contains two very small peaks from compounds that are found in conifer resins, such as pine (the specific compounds are dehydroabietic and 7-oxodehydroabietic acids).

Many natural resins contain a large proportion, or at least some, relatively small molecules that are amenable to analysis by GC. At the moment, gas chromatography (and in particular, GC/MS) is by far the most useful technique for the specific identification of resins in small samples from works of art.

That oil paint samples consist to a great extent of large molecules that cannot be directly analyzed by any chromatography procedure. It turns out that such samples can be chemically broken down, to a minor extent, into small molecules that can be analyzed. GC is the technique by which these fragments are usually analyzed at the moment. Although most oils contain essentially the same types of fragments, the relative amounts of these vary to some extent between different types of oils, so that in certain cases the type of drying oil in a paint sample can be identified with some confidence by GC analysis.

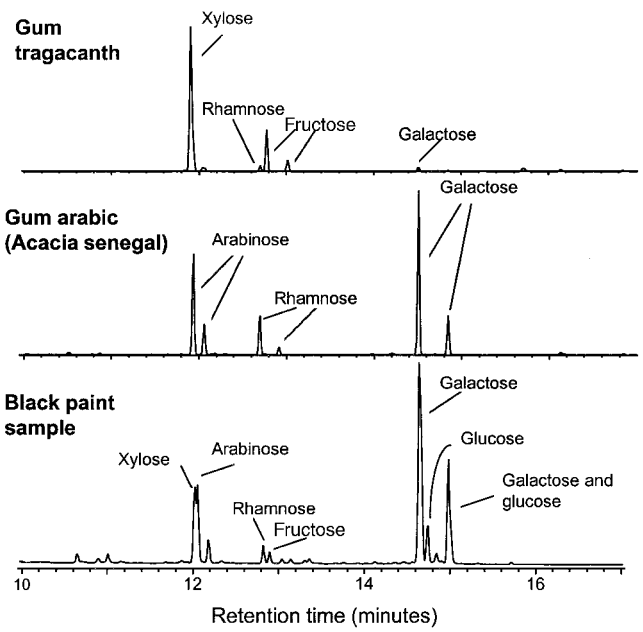

Fig. H.5. Chromatograms of two plant gums and a black paint sample from an ancient Chinese painted wood panel, dated to about A.D. 600. The gums and paint sample were each chemically broken down and derivatized in a manner used to prepare sugar-containing materials for analysis by gas chromatography/mass spectrometry (GC/MS). The analysis detects monosaccharides (simple sugars) that are present in the samples. The result for the paint sample indicates that a plant gum was the binder, although the specific gum cannot be identified. Some contamination from monosaccharides liberated by the breakdown of the wood panel support is also probably present in the sample.

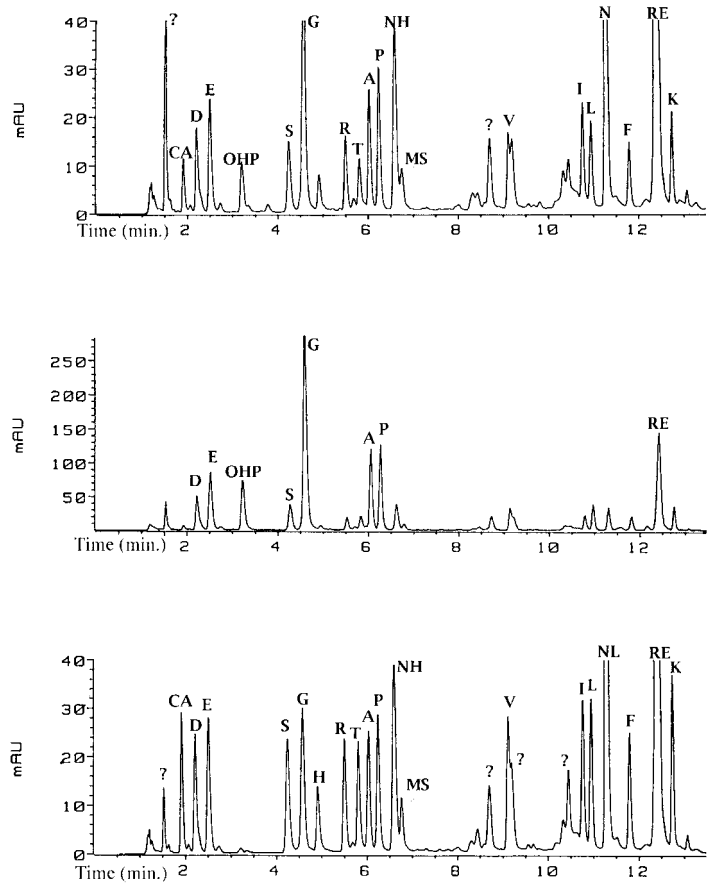

Fig. H.6. Chromatograms of paint samples from *Saint Barbara,* a painting on paper by Edward Burne-Jones, ca. 1866–1870.

These samples were chemically broken down and derivatized in a manner used to prepare protein-containing samples for analysis by high-performance liquid chromatography (HPLC). Each sample was initially allowed to sit in water for a short period of time. The water itself (and whatever part of the sample that may have dissolved) was drawn off and prepared for analysis, as was the remaining solid portion of the sample. This particular procedure often makes interpretation of results from samples that contain more than one protein easier to carry out. The top chromatogram shows the result from the water solution of some paper fibers from the support. The middle chromatogram shows the result from the solid sample of the fibers after the water treatment. Both chromatograms indicate the presence of animal glue; the upper one also suggests the presence of some egg white. The lower chromatogram is from the water-soluble part of a blue paint sample. It indicates the presence of egg white. The chromatograms indicate that the artist used egg white as his paint binder, and glue to seal the paper substrate before paint was applied. Analyses of other paint samples indicated that other (nonproteinaceous) binders were used elsewhere in the painting.

Figure H.4 is a chromatogram from GC/MS analysis of the same paint sample whose FTIR spectrum was shown in Figure H.3. It provides much specific information on the paint binder, indicating the presence of drying oil, beeswax, and a little conifer (probably pine) resin.

Figure H.5 shows how GC/MS can be used to identify carbohydrate-containing media, such as plant gums. The monosaccharides (simple sugars) present in two reference gums are shown, along with the chromatogram of a paint sample from an ancient Chinese painted panel.

Figure H.6 shows chromatograms from analysis of amino acids in samples from a painting on paper. The types and relative amounts of amino acids indicate that the paper substrate was coated (sized) with gelatin (animal glue). The paint layer itself was bound with egg white.

Polarized Light and Optical Microscopy

I

I.1 Polarized Light

Light of a single color can be described as a wave with a specified wavelength or as a stream of photons with a specified energy. Another aspect of light is that it can be polarized with the wave vibrations lying in one plane. Many pigment crystallites respond differently in their ability to transmit light depending on the relation of the plane of polarization to the crystal axes of the pigment. In optical microscopy, the light beams can be polarized by use of filters. Pigments can be distinguished by their unique appearance in polarized light. A description of pigments (see, for example, the book by Feller in References B, Artist's Pigments) includes a description of the appearance of the crystals in an optical microscope when viewed in ordinary light and in polarized light. Thus by use of a light-polarizing optical microscope one can readily identify the majority of crystalline pigments.

Light is emitted from an atom when an electron makes a transition from a higher energy state to a lower energy state (Figure I.1) Conservation of energy applies, so that the energy of light equals the energy difference between the two states. An additional constraint is that angular momentum must be conserved. The emitted photon carries away one unit of angular momentum, shown schematically on the right-hand side of Figure I.1 as a rotating wave of circularly polarized light. Consequently, the energy levels in the electron transition leading to light emission must differ by one unit of angular momentum. The allowed transitions follow selection rules, which are based on the quantum numbers that specify the electron level. For example, an electron in a 2p level (one unit of angular momentum) can make a transition to an

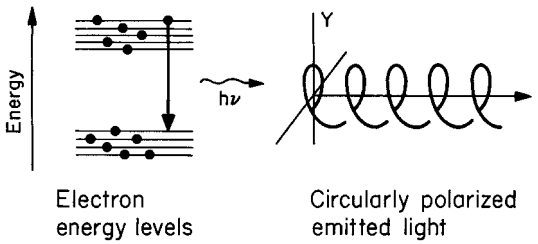

Fig. I.1 Light (photon) emission due to an electron making a transition from a higher to a lower energy state. The emitted light carries one unit of angular momentum. The sketch at the right-hand side shows circularly polarized light.

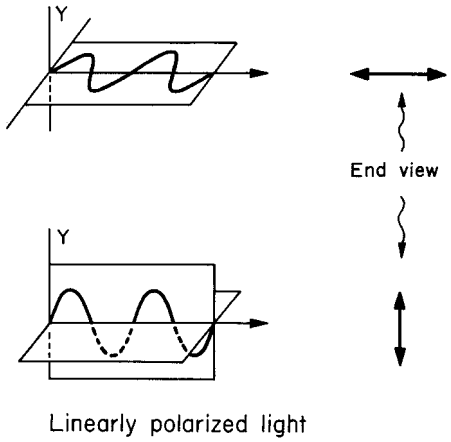

Fig. I.2 Two examples of linearly polarized light where the electric vector of the light wave vibrates in one plane.

empty 1s vacant state and emit a Kα x-ray. The requirement of conservation of angular momentum light emission applies to all photons: infrared, visible light, x-rays, and gamma rays.

Light can be linearly polarized as shown in Figure I.2; the light wave lies on a plane. Figure I.2 shows a horizontal and a vertical plane depiction of two linearly polarized light waves. The arrows on the right side are a conventional notation to indicate the orientation of the plane of polarization and indicate the direction of the electric vector oscillation. An unpolarized beam of light can be represented by two vector components of wave oscillations oriented at right angles to each other.

Human vision does not distinguish between polarized and unpolarized light. However, some materials such as Polaroid can absorb certain orientations of polarized light.

Polaroid represents a class of materials that absorbs light oscillations in one direction but not the component at right angles to the one absorbed. These polarizing materials often contain long particles, rods, or plates, aligned parallel to each other in a regular arrangement. These aligned particles transmit one plane of

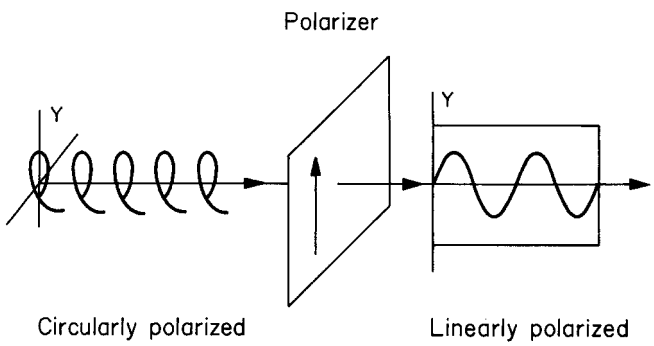

Fig. I.3 Circularly polarized light incident on a polarizer is transmitted as linearly polarized light.

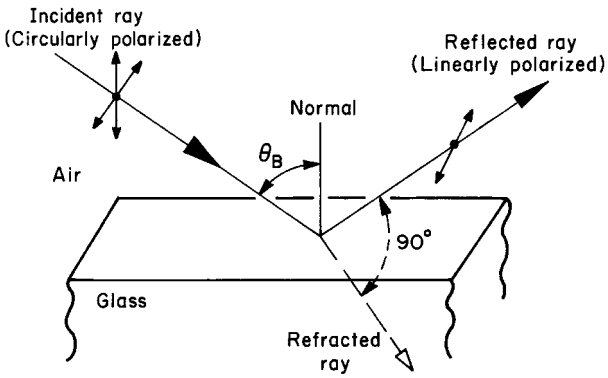

Fig. I.4 Light incident at the Brewster angle θ_B on glass is reflected with complete linear polarization and refracted with a mixture of two perpendicular components.

polarized light and absorb the perpendicular one as illustrated in Figure I.3. The polarizer can transform circularly polarized light into linearly polarized light.

If two polarizers have their orientation axes aligned parallel to each other, the first will absorb half the unpolarized light and transmit linearly polarized light, which is then transmitted without absorption through the second polarizer. The second polarizer is referred to as an "analyzer." If the analyzer is rotated by 90° so that the two polarizers are crossed with their axes perpendicular, the second polarizer will absorb all the light transmitted by the first.

Polarized light can be produced by transmission through polarizers or by reflection from the surface of transparent material such as glass or water. Figure I.4 shows incident light represented by two crossed wave-oscillation vectors. The reflected light is polarized in the plane of the reflecting surface. The refracted beam will contain a mixture of the two orientations. If the incident light is directed at the Brewster angle θ_B, the reflected light is fully polarized, as shown in Figure I.4. At angles other than the Brewster angle, the reflected light is partially polarized.

The Brewster angle is related to the index of refraction n of the material by

$$\tan \theta_B = \frac{n(\text{material})}{n(\text{air})} = n(\text{material}). \tag{I.1}$$

For glass, $n = 1.5$ and $\theta_B = 56.3°$, and for water $n = 1.33$ and $\theta_B = 53°$.

I.2 CRYSTAL OPTICS

The index of refraction n of a transparent medium is defined as the ratio of the velocity c of light in vacuum to the velocity v in the medium:

$$n = \frac{c(\text{vacuum})}{v(\text{medium})}. \tag{I.2}$$

Glasses, liquids, and cubic crystals have a single refractive index and are optically isotropic (the optical properties are independent of direction and orientation of the light to the crystal axes). Other transparent media with lower symmetry (and more complex crystal structure than cubic crystals) are optically anisotropic, and thus have more than one refractive index. The refractive index, and hence the velocity of light in the crystal, depends on the angle between the direction of the beam of light and the axes of crystal symmetry.

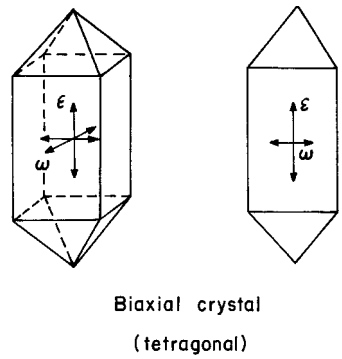

Fig. I.5 A biaxial tetragonal crystal showing the two refractive indices.

Anisotropic crystals in the tetragonal (see Figure I.5) and hexagonal systems have one unique crystallographic direction (the crystals are referred to as uniaxial crystals), and the refractive index is denoted by ϵ for light traveling along this unique direction, the *c*-axis. Perpendicular to the *c*-axis are either two (tetragonal) or three (hexagonal) axes with identical arrangements of the structural unit. The index of refraction is denoted by ω (omega) for light traveling along these axes and perpendicular to the unique *c*-axis. Table I.1 lists some uniaxial pigments and values of the refractive indices ϵ and ω.

The mean refractive index for a uniaxial crystal can be calculated from

$$n_{\mathrm{m}} = \frac{2\omega + \epsilon}{3}. \tag{I.3}$$

Figure I.6 displays the two systems: isotropic (cubic) and anisotropic with uniaxial and biaxial crystals. The biaxial crystals (monoclinic, orthorhombic, biclinic; see Appendix E) have two optic axes, unequal spacings of atoms along three different crystallographic axes, and three

TABLE I.1

Uniaxial Crystals, the Pigment, and Refractive Indices

Compound	*Pigment*	*Omega (ω)*	*Epsilon (ϵ)*
Rutile, TiO_2	Ti white	2.616	2.903
Anatase, TiO_2	Ti white	2.554	2.493
Lead carbonate	White lead	2.09	1.94
Zinc oxide, ZnO	Zinc white	2.00	2.02
Cinnabar, HgS	Vermilion	2.854	3.201
Minium, Pb_3O_4	Red lead	2.40	2.44

Data from R.L. Feller, editor, *Artists' Pigments* (Cambridge University Press, 1986)

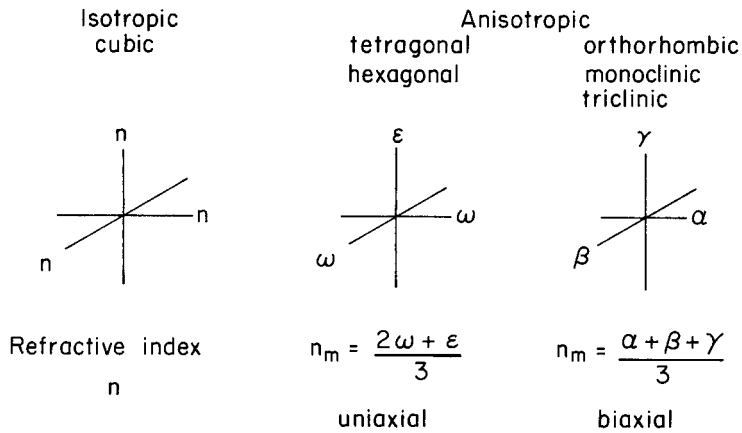

Fig. I.6 Classification of optical behavior of crystals as isotropic or anisotropic.

refractive indices: α (alpha), β (beta), and γ (gamma). The mean refractve index for a biaxial crystal can be calculated from

$$n_{\mathrm{m}} = \frac{\alpha + \beta + \gamma}{3}. \tag{I.4}$$

Table I.2 lists some biaxial pigments.

I.3 Polarized Light Microscopy

The polarizing light microscope is used in the study of materials of paintings because one can identify crystalline pigment materials. The unique characteristic of the polarizing microscope (Figure I.7) is the presence

TABLE I.2

Biaxial Crystals, the Pigment, and Refractive Indices

Compound	*Pigment*	*Alpha (α)*	*Beta (β)*	*Gamma (γ)*
Arsenic disulfide, As_2S_2	Realgar	2.46	2.59	2.61
Arsenic trisulfide, As_2S_3	Orpiment	2.4	2.81	3.02
Copper carbonate	Azurite	1.73	1.758	1.838
Copper carbonate	Malachite	1.65	1.87	1.91

Data from Brill, *Light* (Plenum Press, New York, 1980)

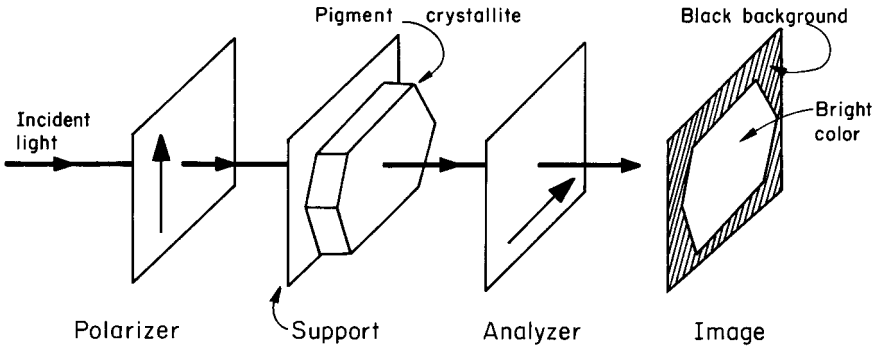

Fig. I.7 Incident light is polarized and passes through the sample and crossed polar analyzer to an image of a brightly colored (interference colored) image of the pigment crystallite.

of two polarizing elements: the polarizer, located in the light path before the sample, and the analyzer, located in the light path after the sample. If the incident light is unpolarized; the polarizer passes only those light waves that vibrate perpendicular to the polarizer transmission direction. If the light passes through an isotropic material, a liquid or glass support, there is no influence on the light. No light will be transmitted through the analyzer whose polarizing axis is perpendicular to the polarizer (crossed polars). If an anisotropic pigment crystal is placed on the support, the crystallite will appear white or brightly colored on the black background.

The colors of the anisotropic pigment materials are bright and characteristically colored against the black background. Color Plate 27 shows red lead pigment particles in plane polarized light with polarizer and analyzer axes aligned and between crossed polars. The green and white colors stand out against the black background.

These colors are not the pigment colors viewed in reflected light, where color is due to light absorption (subtraction) of certain wavelengths and reflection of other wavelengths of the color pigment (see Chapter 3). The colors are interference colors that arise because there are two velocities of light traveling through the crystal. For certain velocity differences and thicknesses the light waves are in phase, and the two components of light constructively reinforce each other. The colors are bright and iridescent, similar to those found in an oil slick on water.

Polarized light entering an optically active anisotropic crystal is resolved into components vibrating in two perpendicular planes. The two vibration directions have different refractive indices, so the light has different velocities in the crystal. The light that was incident on the crystal with wave fronts in phase now emerges with two components. One component is retarded behind the other by a definite amount that depends

on the difference between the two refractive indices and on the thickness of the crystallite (length of the optical path). Interference on recombination of the two components will cause the image to appear colored. Interference will cancel some wavelengths and reinforce others. Anisotropic crystals exhibiting these interference colors are termed *birefringent* or *doubly refractive*.

Cross-Section Analysis of Sample from *Detroit Industry* by Diego Rivera

J

Contributed by LEON P. STODULSKI, Detroit Institute of Arts
JERRY JOURDAN, BASF, Inc.

Buon fresco technique requires applying very finely ground natural and synthetic alkali stable pigments suspended in water onto wet plaster. As the plaster "sets" by chemical reaction with atmospheric carbon dioxide, the pigments become an integral part of the wall surface. This produces a very tough, colored surface. The extent to which this technique produces pigment embedded *in* the wall's surface and not merely *on* its surface was investigated in the laboratories of the Detroit Institute of Arts using a sample taken from the *Detroit Industry* fresco painted by Diego Rivera in 1932–33.

A small fragment of the dark green background from Rivera's south wall's central panel was mounted in polyester resin and sectioned using an ultramicrotome, each slice being between 0.1 to 1 μm thick. The final 0.27-mm thick cross section obtained is shown in reflected visible light at 160× magnification (see Figure J-1a) and in reflected ultraviolet light at approximately 320× magnification (Figure J-1b). In both these photomicrographs, the thin layer of dark green pigment—previously shown by x-ray diffraction analysis[1] to be viridian ($Cr_2O_3 \cdot 2H_2O$)—actually appears to be on top of the white underlying plaster. Even when viewed under 400× magnification, no white or transparent calcium carbonate plaster particles were detected, either on top of or alongside the green pigment particles.

The fresco section was next submitted for analysis by scanning electron microscopic/energy-dispersive spectrometic (SEM/EDS) dot

[1]Table I in Heller, B., "The Conservation of Diego Rivera's Detroit Industry Fresco Cycle," *Preprints* of the American Institute for Conservation meeting, New Orleans, Louisiana (June 1–5, 1988), 94.

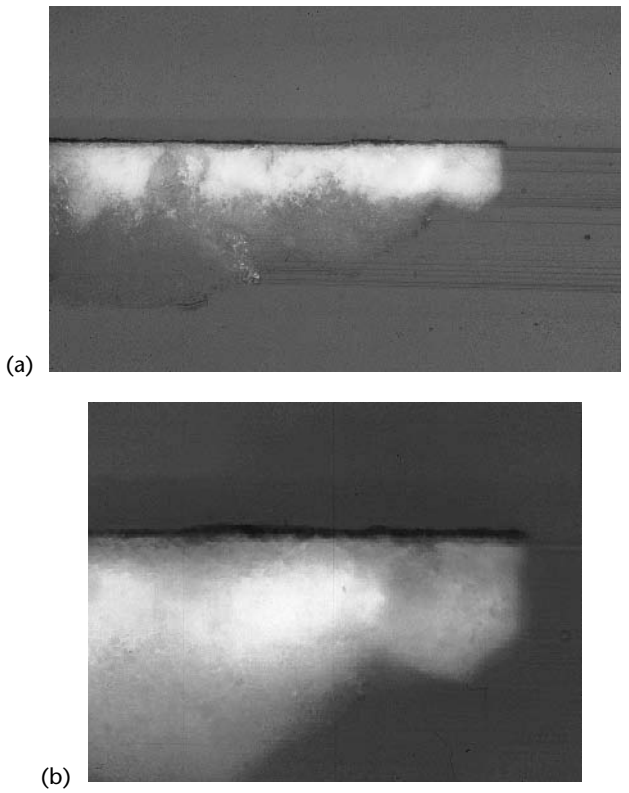

Fig. J.1a,b. Cross section of a small fragment of dark green from Diego Rivera's fresco *Detroit Industry*. Figure J.1a is shown in visible light and Figure J.1b in ultraviolet light. In both photomicrographs, the thin layer of green pigment appears to be on top of the white underlying plaster.

mapping technique.[2] This technique allows the analyst to produce images showing the actual distribution of the elements of interest across the surface of the specimen being analyzed. Ideally, the dot maps of the elements contained in the Rivera cross section would enable us to conclusively show that the plaster particles (containing calcium from calcium carbonate) were located in the same top surface layer as the green pigment particles (containing calcium from viridian) thus proving that the green pigment had indeed become an integral part of the final plaster wall.

The SEM/EDS dot maps obtained are illustrated in Color Plate 28a–g. The portion of the cross section analyzed (a) is the top 270 μm (or 0.27

[2]The instrument used was the AMRAY 1830I scanning electron microscope fitted with an EDAX PV9800 energy-dispersive X-ray spectrometer.

mm) of the fresco. The individual dot maps for chromium (Cr) in red, calcium (Ca) in white, magnesium (Mg) in blue, and sulfur (S) in yellow are shown in b through e, respectively. Color Plate 28f and g are the "composite" dot maps, which exhibit the individual colored dot maps of Cr, Mg, and S, and Ca, Cr, Mg, and S, respectively, overlaid on top of one another. The location in this section of Cr from the green pigment—consisting of a layer having a maximum thickness of about 10 μm (or 0.010 mm)—is illustrated in the individual Cr dot map (b) and in the two composite dot maps (f and g). The important difference between these three dot maps is that g exhibits the location of Ca-containing species across the section, whereas the other two (b and f) do not. It can be clearly seen that the Cr-containing layer appears to be considerably thicker and more extensive in b and f than it is in g. This at first confusing observation is explained by the fact that when two or more different elements are located in the same small area represented by a single dot in a composite dot map, the SEM/EDS computer is programmed to produce an image displaying *only* the color of that element present in the largest amount. Thus, the amount of Cr in g appears to be less than it is in b and f because of the presence of a large concentration of Ca-containing species located in the same small area as many of the Cr-containing pigment particles. Conversely, those areas exhibiting red dots in g are displayed as such because of the preponderance of Cr over Ca species in that area. The difference in thickness and shape of the Cr-containing layer in the two composite dot maps can thus be accounted for by realizing that both Cr and Ca are located close together within the same small area—which is to say that we have concrete visual, if indirect, proof that the Cr-containing green pigment particles are intimately mixed with Ca-containing plaster particles. And this could result only if the green pigment particles are embedded in the present surface of the plaster wall.

Radiocarbon Dating in Art Research

K

Contributed by DUSAN STULIK, Getty Conservation Institute

K.1 Introduction

Since the development of ^{14}C dating by W.F. Libby in the 1940s and 50s, the method has proven to be the best absolute method for chronometric dating of organic and some carbon-containing inorganic materials [K1]. It has become an essential research tool for both archaeologists and geologists [K2]. Even broader application horizons have been opened to radiocarbon dating by use of the accelerator mass spectrometer, which allows routine analysis of submilligram samples. Art curatorship and art conservation are two art research fields that directly benefit from such a development.

There are pronounced similarities between application of radiocarbon dating in archaeology and art research, but there are also major differences that make it difficult simply to take a methodology developed for archaeological research and apply it directly to radiocarbon dating of art objects [K3].

In both fields the application of dating techniques is focused on dating an object of unknown age or on cross-checking the age of an object previously dated by other methods.

Archaeological dating often takes advantage of newly opened archaeological sites and focuses on the identification of disjunctions, disparities, verification of the specimen association, and assessment of the magnitude of temporal hiatuses between the date and the event [K4]. Art research more often deals with an object that long ago was removed from the place of its creation and for which provenance information is not available or that has precipitated questions about its provenance and authenticity. If neither art-historical research nor con-

noisseurship allows placing the object into well-defined temporal relations and there is a suspicion that the object might misrepresent the time of its creation, radiocarbon dating can, together with a range of other scientific tests and methods, provide data that might help to prove or disprove a working hypothesis based on art-historical research methods. For archeological research the extension of the datable range of materials from the currently feasible 40,000 years B.P. (before present) to the theoretically possible 70,000–100,000 years B.P. is a major challenge of accelerator mass spectrometry (AMS) research. Fine-art studies deal with relatively recent time periods (2000 B.C. to the present), but because the focus of the research is more on the work of an individual artist and time-limited artistic movements (comeasurable with a life span of a human being) rather than on the production of periods of civilization, such research would benefit from the results of high- and ultrahigh-precision measurements. Because the majority of art objects are unique, irreplaceable, and relatively small, the ability to date a minimum amount of sample is an extremely critical issue.

K.2 Radiocarbon Dating

The impact of high-energy primary and secondary cosmic rays on atoms and molecules of the upper layers of the earth's atmosphere (lower stratosphere and upper troposphere) results in many nuclear reactions in which a number of neutrons, protons, α-particles and other subatomic particles are produced (Figure K.1). A large portion of neutrons produced by cosmic rays are slowed down by collision with atoms in the atmosphere. The resulting thermal neutrons react with ^{14}N atoms to form a ^{14}C atom and a proton (hydrogen nucleus) through a nuclear reaction (Appendix G):

$$^{14}N + n \rightarrow {}^{14}C + p.$$

Cosmic ray data show that the production rate of ^{14}C atoms averaged over the whole atmosphere is about 2 per g per cm^2 of the earth's surface. In this way approximately 7.5 kg of ^{14}C is produced and added to the world's carbon reservoir every year. The entire carbon reservoir contains close to 4×10^{15} kg of carbon. Most of the carbon is in the form of stable isotopic ^{12}C (98.9%) and ^{13}C (1.1%). After formation, ^{14}C quickly combines with oxygen to form ^{14}CO and later $^{14}CO_2$. This carbon dioxide mixes throughout the atmosphere by air mass movements and turbulences. Once a radiocarbon $^{14}CO_2$ molecule reaches the biosphere, it enters into the carbon exchange cycle. Living organisms are part of the equilibrium. Plants build ^{14}C into their cellular structures by the process of photosynthesis. Other organisms obtain it by ingestion of plant ma-

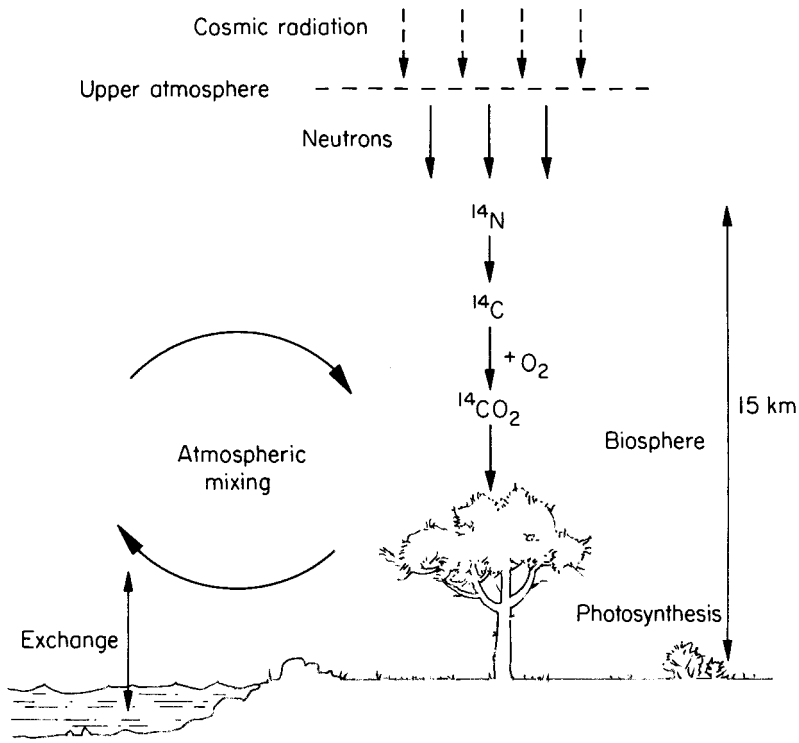

Fig. K.1. Production of ^{14}C and its movement in the earth's biosphere.

terial. The concentration ratio between radioactive isotope ^{14}C and stable carbon isotopes ($^{12}C + {}^{13}C$) is approximately $1{:}10^{-12}$. This concentration ratio stays approximately constant with time and represents the dynamic equilibrium established on a global scale between ^{14}C loss by radioactive decay and cosmic ray production [K1].

Within a living organism the concentration of ^{14}C is also constant and is continuously being replenished from the biosphere carbon exchange reservoir. When an organism dies, the ^{14}C intake process stops, and a finite amount of the ^{14}C fixed in the organism faces the slow process of radioactive decay.

^{14}C is radioactive, and it decays back to ^{14}N by emission of a beta particle (electron) and antineutrino:

$$^{14}C \rightarrow {}^{14}N + \beta + \upsilon.$$

The death of the organism sets a time zero ($t = 0$) on a "radiocarbon clock." The decrease of concentration of ^{14}C in a dead organism follows the exponential radioactive decay law (Figure K.2). This law relates the

number of radioactive atoms A left after time t to the initial number A_0 of radioactive atoms (at $t = 0$):

$$A = A_0 e^{-lt},$$

Where l is a constant equal to the reciprocal value of the mean life t of the radioactive isotope. The mean life is related to the half-life of the radioactive isotope by the equation

$$T_{1/2} = (\ln 2)t, \text{ or } T_{1/2} = 0.693t.$$

Both half-lives and mean lives are specific constants for a given radionuclide. The Libby half-life $T_{1/2} = 5568$ years and Libby meanlife $t = 8033$ years are conventionally used in the calculations of radiocarbon age.

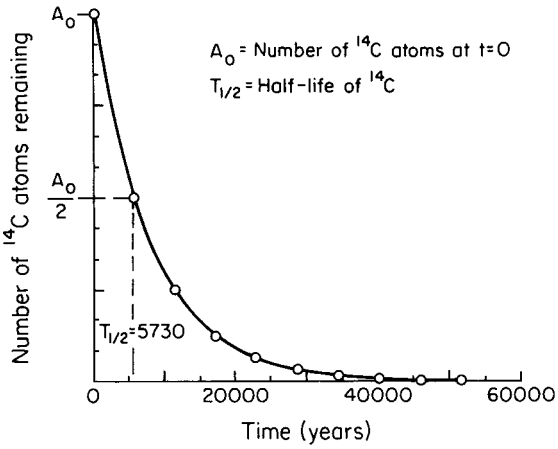

Fig. K.2. Decay curve of ^{14}C.

From 1949 till the late 1970s the only experimental method for measurement of ^{14}C concentration in a given sample was based on the measurement of the radioactive decay rate, the same principle that was originally developed by Libby. The Geiger counter used by Libby was later replaced by gas proportional and liquid scintillation counters. Several other important improvements have been made to increase sensitivity, improve precision and accuracy of the measurements, and decrease sample size requirements. Despite all of these improvements, the conventional counting techniques face the problem of low specific activity of ^{14}C (disintegrations rate per gram of radioisotope).

For example, the activity of recent carbon samples would be 13.6 dpm/gC (disintegration per minute per gram of carbon), for samples 5730 years old the activity would be about 6.8 dpm/gC, and a sample 50,000 years old would have activity of a mere 0.03 dpm/gC. These are very small numbers. In addition to weak signals from ^{14}C, any of radioactivity detector records so-called counter background caused by cosmic radiation or trace radioactivity of surrounding material. This causes a major limitation in age determination of material older than 50,000 years even when modern scintillation counters are used.

Typical sample sizes needed for conventional gas and liquid scintillation counting are equivalent to about 5–10 grams of pure carbon [K5]. The sample needed for dating of material older than 50,000 years is even greater. The dating of older samples is very important for archaeological research but not so critical for fine-art research, which deals mostly with later periods of civilization. In art research a much more critical issue is the problem of minimum sample size. Over the past decades several attempts have been made to date small samples by conventional

counting methods. The mini-gas counters that have been introduced are able to work with sample sizes as small as 100 mg of pure carbon. To achieve the same quality of counting statistics as we can achieve for samples of ordinary sizes, the reduction in sample size has to be compensated by approximately equivalent multiplication of counting time from the usual 24 or 48 hours to several weeks or months. In most of the cases the sample sizes needed for mini-gas counters exceed the amount of material that might be available from the art object or that museum curators or fine-art or antique collectors might agree to provide for such an analysis [K6].

K.3 ACCELERATOR MASS SPECTROMETER

A new era of application of radiocarbon dating came with development of the alternative method of ^{14}C detection based on direct analytical determination of the concentration ratio of ^{14}C and stable carbon isotopes in the analyzed sample [K7].

The conventional ^{14}C counting methods provide information about concentration of ^{14}C in the sample based on radioactive decay and measurement of beta particles emitted from the sample. A more efficient method for ^{14}C measurement would be a direct analytical determination of the isotopic $^{14}C/^{13}C$ and $^{14}C/^{12}C$ ratios of ^{14}C and ^{13}C or ^{12}C. There are about 5×10^{10} ^{14}C atoms in one gram of modern (1950 A.D.) carbon. To detect 1% of ^{14}C in a sample using a beta counting technique would require 80 years of counting time. To detect 1% of ^{14}C atoms in a sample using AMS usually takes less than an hour. Analytical chemists know that one of the most sensitive methods used to measure isotopic ratios is mass spectrometry. In a mass spectrometer the isotopes are separated according to their mass-to-charge ratio. All attempts to use the analytical mass spectrometer for carbon dating have failed. This failure is due to the fact that the $^{14}C/^{12}C$ concentration ratio ranges from about 1.2×10^{-12} for modern carbon to about 3×10^{-16} for samples 70,000 years old. The background of a mass spectrometer does not allow measurement of isotopic ratios smaller than about 10^{-9}. This is due to special interferences of $^{12}CH^{+}_{2}$, $^{13}CH^{+}$, and $^{14}N^{+}$, and molecular ions, which have practically the same mass-to-charge ratio as measured ^{14}C. A special experimental strategy has to be used to achieve a practical elimination of the instrumental background and spectral interferences. Several intricate steps are needed to achieve such a goal.

A schematic diagram of the accelerator mass spectrometer is shown in Figure K.3. A solid sample containing carbon is bombarded by energetic (several keV) cesium ions in the ion source. The impact of the primary ions causes the emission of secondary particles from the surface of the bombarded sample. Emission of secondary particles C_0, C^{+}, C^{-},

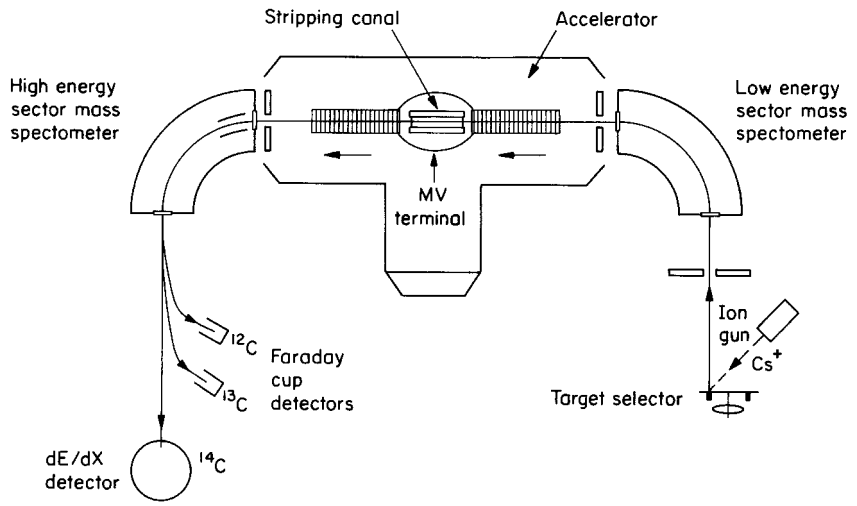

Fig. K.3. Schematic of an accelerator mass spectrometer.

C_n, is called sputtering. Because the cesium bombardment produces relatively high proportions of negatively charged C ions, such an ion source is called a negative ion source. It is used because negative ions are needed for the function of the tandem accelerator and also because it provides the first step in background suppression by discriminating against ^{14}N contamination, which is known not to form stable N^- ions. A strong positive electric field draws the negative ions from the ion source into a low-energy mass analyzer. Using a magnetic field or combination of magnetic and electrostatic fields, a chosen carbon isotope is preselected for the accelerator tube (second step). Selected C^- carbon ions are accelerated in the first half of the accelerator tube to reach the energy of several MeV (2–8 MeV). In the middle of the accelerator tube the energetic carbon ions pass through a gas (Ar, Xe, O_2) or thin film "stripper." During this interaction several electrons of energetic carbon ions are removed (stripped off), and charge reversal of the carbon ion beam (a high proportion of C^{3+} ions is formed for 2–3 MeV accelerators; C^{4+} ions are prevalent for higher accelerating potentials) is achieved. The resulting C^{3+} or C^{4+} carbon ions are accelerated in the second part of the accelerator tube to even higher energies.

No molecular ion can survive electron stripping to the 3+ or 4+ state and during the stripping process all disintegrate (third step) [K8]. After the ion beam passes through the accelerator, molecular fragments are removed from the beam by mass spectra (fourth step). Then an ion beam to be analyzed is directed to a detector, where its intensity is measured (step five). The isotopes ^{12}C, ^{13}C, and ^{14}C can be selected sequentially by

the injection system for transmission through the accelerator and to the detector. Abundant stable isotopes (^{12}C, ^{13}C) are measured using Faraday cup detectors. $^{14}C^{n+}$ ions and a small residue of $^{14}N^{n+}$ are detected using a gas ionization chamber or silicon surface barrier detector capable of measuring both E and dE/dX for each particle, which provides a final (sixth) step in background suppression.

The AMS measuring cycle is divided into a number of detection time periods. The overall relative efficiency of the instrument for ^{12}C, ^{13}C, and ^{14}C is intermittently monitored by measuring targets made from a reference standard material [K7]. The instrument background is also checked using a target made from "dead" carbon. The major advantage of AMS for carbon dating of art objects is its stability to achieve conventional counting precision on submilligram samples. Samples of this size are comparable to samples taken routinely by restorers and conservation scientists for pigment and binding media analysis.

K.4 Reality of Radiocarbon Dating

As described, the principle of radiocarbon dating is simple enough to provide information on the age of dated organic materials. Under real conditions of carbon dating, the situation is much more complicated. There is no analytical method that would not face problems of sample quality, limited validity of basic assumptions, interference, and data interpretation. Issues critical for radiocarbon dating are:

- sampling and contamination
- corrections for isotopic fractionation
- relations between measured and calendar age

K.5 Sampling and Sample Contamination

Analytical chemists know that results of any analysis cannot be better than the quality of the sample used for the analysis. This is also true for ^{14}C dating and particularly for its application in dating museum artifacts. We can get meaningful radiocarbon data only if the dated sample of organic material is indisputably the material that was removed from the live carbon cycle during the time that corresponds to the time of creation of the artifact. This sounds very logical, but without full realization of what this means, there is substantial potential for interpretation error or overinterpretation of radiocarbon data.

Radiocarbon dating is indifferent to the creative force of the artist

or the artist's methods. Radiocarbon dating "sees" only organic materials used during the creative process. Radiocarbon dating cannot provide information about when or by whom a given artifact was created. It can only provide information as to when different organic materials found today as parts of the given artifact were removed from the live carbon cycle. For example, if a baroque wooden sculpture was carved from an old wooden beam taken from a destroyed Gothic church, the radiocarbon dating would not provide information about the date of the carving or the date of the Gothic church, but only about the ages of individual tree rings found in the wood sample. We would not even be able to say when the tree was cut down ($t = 0$ for radiocarbon dating) because the peripheral tree ring under the bark (the last ring grown before cutting) probably would be removed by a carpenter to shape a beam. We would be able to extrapolate our data to provide at least an estimate of when the wood was used as a building material in the church. But in this case, we have to realize that this estimate might be quite misleading if the wooden beam was a later addition or replacement, or if the original tree was "dead" long before it was used to make the beam (natural causes or storage for later use). Sampling of artifacts has to be done with deep understanding of materials (origins of different materials, their participation in the live carbon cycle, and their practical "shelf life"), artist techniques (mixing of materials of different origins), and prevailing customs in handling materials for artistic use (wood aging before use as a support material for panel painting or the tendency to recycle materials for later use). It is also critical to sample a site of the artifact that has a high probability of being part of the original structure of the artifact (part of a panel painting could be a later addition needed to fit a painting to a new frame; a paint sample could be a later overpainting or restoration). A decision on sampling strategy should not be made without consultation with art conservators and art historians involved in the project. If there are any doubts about the originality of the sample site, several samples should be taken from different areas of the artifact. It is better to refuse to work with bad or inadequate samples than to risk sampling error, misinterpretation, or overinterpretation of radiocarbon data. There is also practically no museum artifact untouched by other artists, restorers, or object conservators. Many museum objects have a long history of successive cleaning, repairs, and restorations. There is a high probability that these treatments have changed the original ^{14}C makeup of the object. For example, paraffin wax treatment or acrylic varnish coating represents the introduction of "dead" carbon material and makes the object apparently "older." Treatment with newly produced beeswax or natural resin varnishes would introduce "modern" carbon material, resulting in a positive shift in the apparent radiocarbon dates. A detailed knowledge of past conservation or restoration treatments (very seldom available) or detailed chemical analysis is needed to prepare the

ground for a successful sampling strategy and proper sample pretreatment prior to the radiocarbon dating. The majority of museum historical objects containing organic materials are composed of complex natural materials (cellulose, oils, proteins, waxes, natural resin) and their mixtures (egg tempera–pigment, oil, protein, carbohydrates, natural dyes, and inorganic salts). Detailed knowledge of materials used to create the art object helps to design the pretreatment needed to remove sample contaminations or to identify a component that is the least affected by contaminations and suitable for more reliable age determination.

In the sample preparation step the pretreated sample is transformed into a sample compatible with the radiocarbon dating procedure. Carbon dioxide or volatile hydrocarbons are used for gas counters, scintillating liquid-soluble organic compounds for scintillating counters. For AMS measurements the organic material is transformed to make a small target of graphitic carbon [K9,K10]. Special care has to be taken that sample pretreatment and target preparation steps do not change the carbon isotope composition of the original sample and do not introduce further contaminations [K11].

K.6 Correction for Isotopic Fractionation

Knowing the concentration of ^{14}C in a sample, Libby's mean life for ^{14}C, and the fact that radioactive decay follows the first-order kinetic equation should be enough to calculate the age of the sample. In reality this cannot be done without correction for isotopic fractionation of carbon isotopes [K12]. Each organic material used for radiocarbon dating has a distinct biochemical history. There are small but still measurable differences in physical and chemical properties of compounds of different carbon isotopes. For instance, plant material assimilates $^{12}CO_2$ more easily than $^{13}CO_2$, and $^{13}CO_2$ more easily than $^{14}CO_2$. Resulting isotopic shifts have to be corrected for before the equation describing the radioactive decay is used to calculate the conventional radiocarbon age of the sample

$$T = -t \ln (A/A_0),$$

where T is the conventional ^{14}C age of the sample in years B.P. (before present, 1950), t is the mean life 8033 years, A is the ^{14}C concentration in the analyzed sample, and A_0 is the ^{14}C concentration in the reference 1950 material corrected for isotopic fractionation. The resulting calculation is the so-called conventional radiocarbon age given in uncalibrated years B.P.

K.7 Relations Between Measured and Calendar Age

The basic assumptions of radiocarbon dating are a constant rate of radioactive decay uninfluenced by external factors and constant concentration of ^{14}C in the biosphere. The first assumption has been found correct. The second assumption has been found only approximately correct. The rate of ^{14}C production depends on the stability of cosmic-ray flux. Dendrochronology (tree ring dating method) together with high precision ^{14}C dating allowed for measurement of variation in ^{14}C production back to about 9000 years ago. Long-term variation of ^{14}C production (a sinusoidal variation with a period of about 11,300 years) can be correlated with changes in the earth's magnetic moment. The short-term variations are due to changes in solar activity [K1]. Even activities of man himself have been able to create noticeable changes in ^{14}C concentration within the earth's biosphere. Since the beginning of the Industrial Revolution, coal and oil combustion have injected steadily increasing amounts of "dead carbon" into the atmosphere. This so-called fossil fuel effect in combination with the solar activity effect gives recent organic material a false age of up to about 160 years. In the 1950s and 60s the fossil fuel effect was overshadowed by an increased concentra-

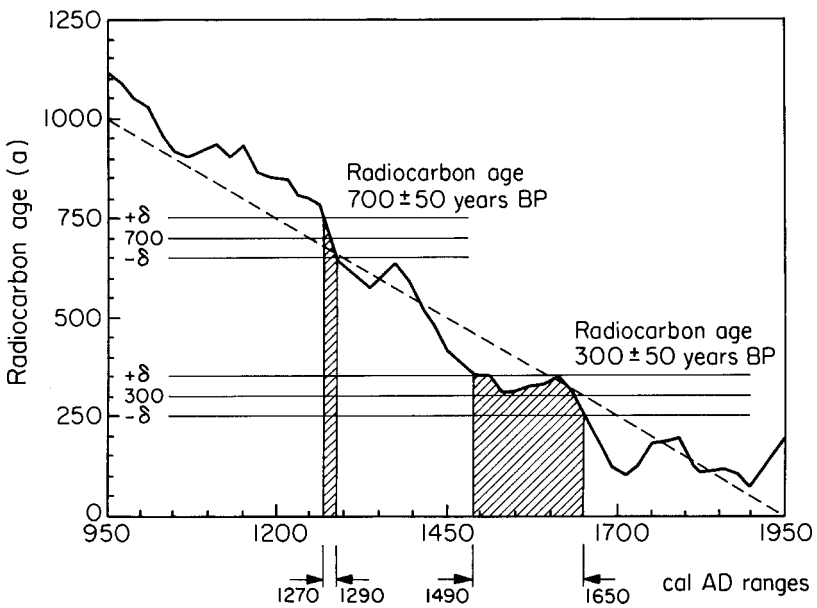

Fig. K.4. Calibration curve (from [K14]) for the last millennium. Two examples show the effect of the calibration curve shape on the range of calibration dates.

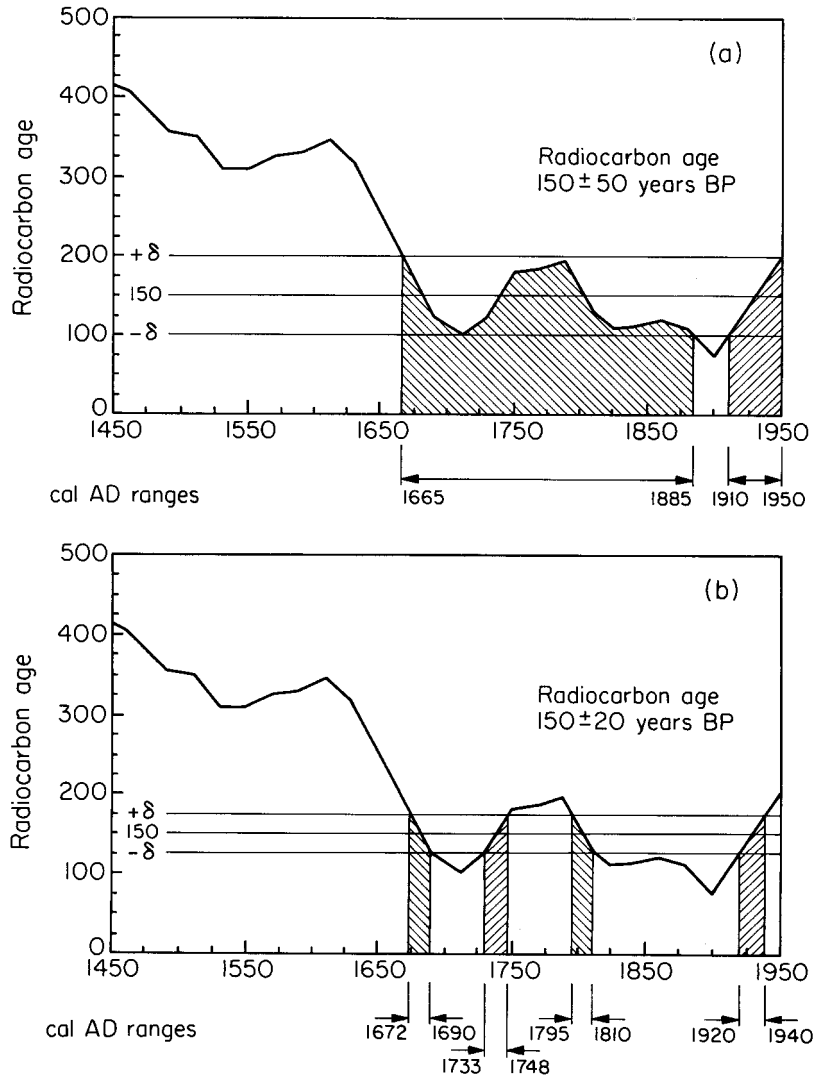

Fig. K.5a,b. The advantage of high-precision measurement in dating relatively recent samples: (a) low-precision measurements; (b) high-precision measurements.

tion of ^{14}C produced by neutrons released during a series of nuclear and thermonuclear bomb tests (bomb effect). Since the moratorium on atmospheric testing in 1963, the concentration of ^{14}C in the atmosphere has been gradually decreasing. Correction for all of the above-mentioned ^{14}C concentration variations can be done using internationally accepted calibration curves derived from radiocarbon and dendrochronological

experiments [K13]. Figure K.4 shows a section of the high-precision calibration curve (without curve error terms) developed by Stuiver and Pearson [K14], which covers several time periods important for art research. The calibration curve is not a monotonic function, and two examples show the effect of the shape of the calibration curve on the width of the calibrated age ranges obtainable from radiocarbon measurements when experimental error terms are included. Calibrated age ranges are not the central dates with error terms but the range of statistically equally valid dates. This age range can be relatively narrow when the calibration curve has a steep slope, or wide when the slope is flat or wiggly.

The shape of the calibration curve for the relatively recent past (≈1650 to 1950 A.D.) is such that for non-high-precision data the calibrated age range covers the whole period from about 1700 A.D. to 1950 A.D. (Figure K.5a). This makes the use radiocarbon results for dating of the last two hundred years before 1950 A.D. very difficult. The situation would improve only marginally with the application of high-precision measurements. In such a case (Figure K.5b) there are several calibrated age ranges corresponding to one conventional radiocarbon age, and other means (complementary scientific methods, art-historical analysis) have to be used to provide a more plausible interpretation.

K.8 Medieval Documents on Parchment

A collection of medieval charters and documents on parchment was obtained by the Getty Conservation Institute as testing material for development of methodology for dating medieval art objects containing proteinaceous materials [K15]. Parchment samples satisfy this application because parchment was often a starting material for the preparation of animal glue, which was widely used as a general adhesive and as a binding medium for a special type of tempera painting called "distemper." Parchment was also used as a substrate for lasting documents, illuminations, and miniature paintings as well as a material for bookbinding. The collection includes a number of legal documents whose age ranges from the late thirteenth century to the middle of the seventeenth century. Several documents are dated, and these can be used as secondary standards for development of the AMS method. Small samples of several square millimeters were cut from the edges of the documents. Prior to chemical treatment the parchment samples were cleaned mechanically using a sharp scalpel. A number of parchment samples were treated with a calcium carbonate wash prior to their use. This was done to make writing on the parchment surface easier. The presence of inorganic carbon from $CaCO_3$ would shift the radiocarbon age (dead carbon effect), and all measures were taken to remove inorganic carbon from the sample prior to the combustion procedure. After mechanical cleaning the

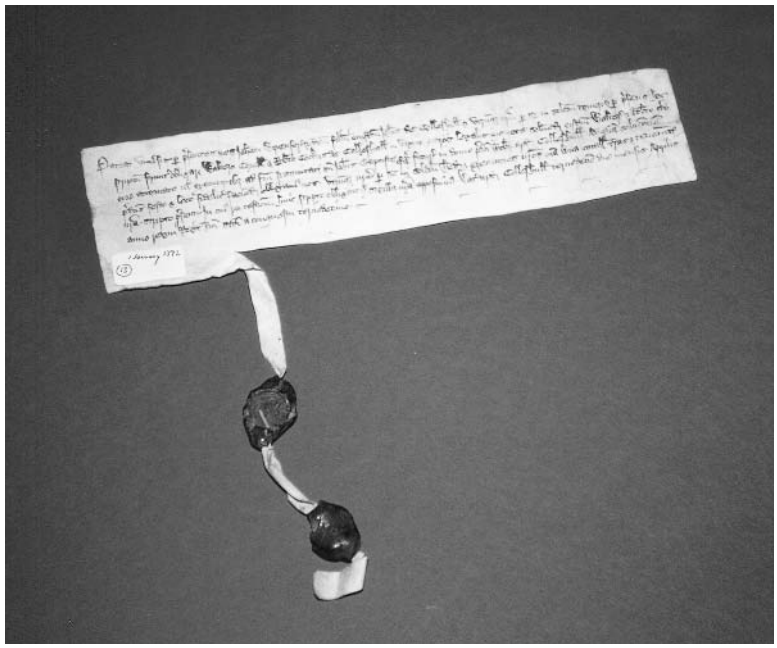

Fig. K.6. Medieval document on parchment; dated November 1420 A.D. (*Photo courtesy* of Getty Conservation Institute.)

samples were cleaned using a standard acid–alkaline deionized water wash. There is a very good correspondence between the calibrated date range and the date of parchment used in 1420 A.D. (Figure K.6).

K.9 CONCLUSIONS

AMS dating shows great potential for art research. The fact that the sample size needed for AMS dating is comparable to the size of samples routinely taken by conservators or conservation scientists for cross-section analysis and for binding media determination opens a number of new and exciting applications. One of the most important applications is direct radiocarbon dating of paint layers on paintings and polychrome sculptures. The limiting factors that make such an analysis difficult are the complex nature of paint materials together with the very severe problem of contamination due to the frequently long history of restoration and conservation treatments that are common to almost all important paintings and polychrome sculptures found in art museums, churches, and private collections. The number of artifacts that have not been re-

stored or repaired is very limited. The radiocarbon dating of a paint layer requires a detailed knowledge of the chemistry of the paint layer. It is important to identify the material used as the original binding medium and develop an experimental strategy that would be able to separate the original material from other materials that were applied later or that permeated the paint layer during restoration and conservation treatments. The current collaborative project between the Getty Conservation Institute and the University of Arizona in Tucson centers on the development of such a strategy. Results of the GCI's Binding Media Analysis Project are used for analysis of the organic portion of both historical and modern paint layers. Advanced methods of analytical separation are used to isolate the critical organic component in the paint layer for AMS target preparation. Scientists of the NSF Radiocarbon Laboratory at the University of Arizona concentrate on the development of a method for preparing and dating submilligram samples and achieving high-precision results from small samples of binding media. The results of our combined effort are very promising, and we believe that the methodology developed for radiocarbon dating of binding media paint layers will bring a new dimension to current and future art-historical and art conservation research.

Dendrochronology (Tree-Ring Dating) of Panel Paintings

L

Contributed by PETER IAN KUNIHOLM
The Malcolm and Carolyn Wiener Laboratory
for Aegean and Near Eastern Dendrochronology
Department of the History of Art and Archaeology
Cornell University

Many European paintings are painted on solid wooden panels or boards, typically oak for Netherlandish paintings. The wood is usually split radially so that, in ideal circumstances, a sequence of annual growth rings from pith to sapwood is present. These sequences are then matched, one against another, by the dendrochronologist and compared with growth sequences whose dates are known from living trees. Absolute dates can thus be assigned to specific annual rings. Sometimes the geographic origin of a board can be determined as well.

L.1 Method

The Material: Oak is not only the most common support for European panel paintings, but is also the most easily dated because of the large number (now in the thousands) of oak panels and oak timbers that have been studied. Paintings also appear, but less commonly, on panels cut from beech, lime, fir, pine, spruce, poplar, and other species. These, too, can sometimes be dated, with the exception of poplar which tends to have enormous rings. For example, the so-called Mellon Madonnas in the National Gallery of Art in Washington, D.C., are painted on poplar panels, each ring of which is about an inch wide. Thus the total ring count for each panel is about two dozen rings, all the same size, and the paintings cannot be dendrochronologically dated. Since many Italian paintings are painted on poplar panels, dendrochronology is therefore an inappropriate analytical technique for

art works south of the Alps. North of the Alps, however, and in the Low Countries in particular, dendrochronology has proven to be an extraordinarily valuable tool.

The Concept: The mechanism that makes tree-ring dating possible is that trees growing in the same climatic region (Europe) or subregions (Eastern Europe vs. Western Europe) respond in a recognizably similar fashion to the same general climatic stimuli. These stimuli may be temperature or rainfall or some combination of the two. In trees from the Eastern Baltic to the English Channel and even across into Great Britain and Ireland, adverse growing conditions will produce narrow annual rings, while favorable growing conditions will produce wide rings (Baillie, 1983). The sequences of such changes over time are unique. Moreover, subtle variations of ring growth, specific to a particular region, sometimes allow the dendrochronologist to determine the precise geographical origin of a panel (Eckstein, Ważny, Bauch, and Klein, 1986). For example, it has been shown that a large number of oak panels now found in a wide variety of Western art collections were cut from trees that grew in the Eastern Baltic (Eckstein, et al., 1986). The boards were shipped west from Gdansk (Danzig), bought on the Amsterdam and Rotterdam docks, and subsequently brought into the studios of Western European artists whose names are household words today. Panels painted on by the same artist or workshop have even been identified sometimes as coming from the same tree (Eckstein and Bauch, 1974; Klein, 1994). One has a mental image of, say, Rembrandt making his way down to the dockyard or to the shop of a middleman, buying a wagonload of oak boards imported from Poland, and bringing them back to his studio. While he paints on panel A, panels B, C, and D from the same shipment lean against the wall of his atelier. Which panel was painted first and which second, however, is beyond the scope of dendrochronology.[1]

The artist's taste or practice must also be considered. If a given artist has all of his known oeuvre on oak, and if a painting attributable to him were to appear on a poplar or lime panel, the investigator might well ask why there has been a new choice of material for the support.

The Technique: A transverse surface must be prepared across the end-grain of the board, which is usually not painted and is normally hidden by the frame. This surfacing is most easily done with a sharp razor blade. The annual rings are counted and measured with a microscope to 1/100 mm. Although early accounts of the dendrochronological analysis of panels show attempts at using a simple loupe or hand-measuring lens with 1/10 mm resolution as in Figure L.1, these have proven to be

[1]Twenty paintings by Lucas Cranach the Elder have now been reported as coming from the same beech tree (Klein, 1994, and personal communication). It is reasonable to assume that they must have been painted at approximately the same time.

Fig. L.1. Attempt with a small hand lens at dating a Byzantine icon painted on juniper boards. A microscope would have been preferable.

relatively unsatisfactory, and the use of a proper microscope is the only acceptable method. For example, the only painted panel I have ever tried to date, a Byzantine icon on juniper boards (Figure L.1), is a classic demonstration of how not to measure panels. An appropriate microscope was not available in the museum, and one of the two boards had as many as 238 rings, some so small that the resolution of the hand lens was not enough to permit me to take sufficiently sensitive measurements. I think one panel had a last ring from 1539, but I cannot tell the date of the second panel until I go back and remeasure the icon with a real microscope.

These microscopic measurements are recorded and plotted on an x, y graph. This graph is then compared and matched with graphs from other panels and from living trees. Figure L.2 from top to bottom shows a cross section of a ninth-century oak board, the graph of its measurements, and a comparable graph from another dated board from the same period. Note how the alternately large and small rings can be matched from one tree to another. These patterns, or "signatures," are unique in time. Statistical methods have been developed to test the probability of any proposed match. A recent detailed exposition of the technique and its applications is by Schweingruber (1988).

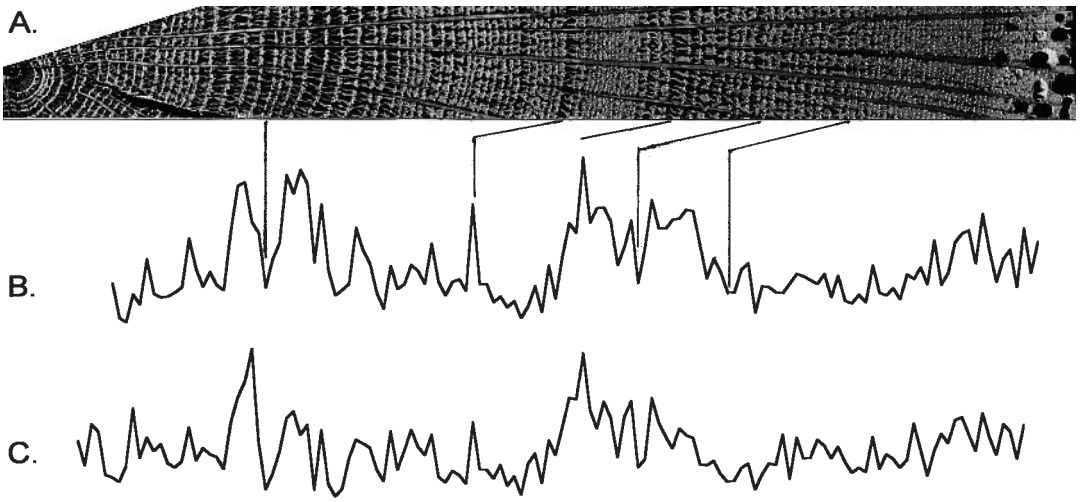

Fig. L.2. Cross section of a ninth-century oak board, graph of its ring measurements, and a comparable graph from another cross-dated board.

In order for the dendrochronological method to be applied successfully, several preconditions are necessary. The sample should preferably have at least one hundred rings to prevent an apparently good but accidental and incorrect fit. The wood must have been cut radially (Figure L.3a). A panel cut in this manner not only provides a more stable surface for the painter but is less likely to warp and shrink than is wood cut tan-

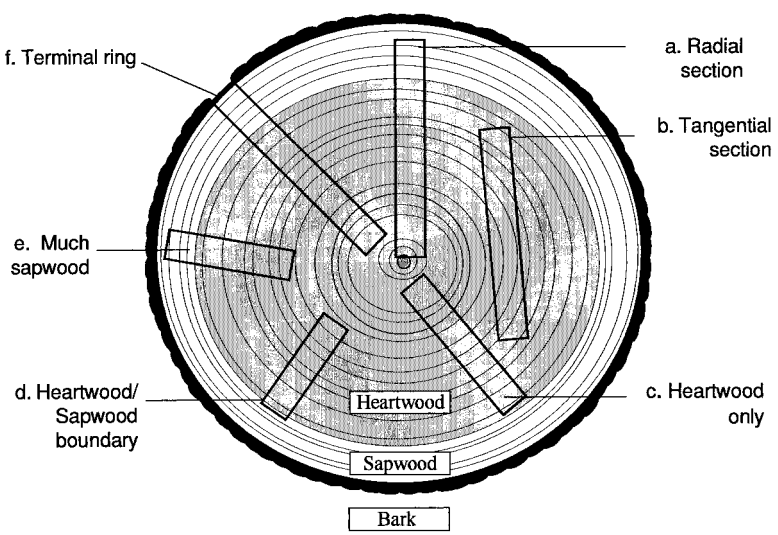

Fig. L.3. Schematic section of a tree from which a variety of panels has been cut.

gentially to the ring growth (Figure L.3b). The latter type of panel will usually not have enough rings to produce a sequence long enough for tree-ring dating. Obviously, the wood should be free of knots and other growth aberrations. Painters, at least those partial to oak panels, almost always are extremely particular in their selection of straight-grained, stable wood, and will avoid such blemishes in their choice of wood for the support.

L.2 LIMITATIONS

Rings Lost to Trimming: If all panels contained a complete ring sequence from pith to bark, dendrochronological analysis would be rather straightforward, but the quality of panels, like the quality of painters, is not equal. Since sapwood (roughly 15 to 30 exterior rings immediately under the bark for oaks) contains sugars that make it subject to insect infestation, the practice in the Middle Ages and Renaissance was to remove some or all of it before painting. This preparation can sometimes cause the loss of some heartwood as well.

Because in oak the number of sapwood rings can be estimated to within a dozen rings (with regional variations; see below), the presence of a considerable number of sapwood rings in the panel permits greater precision in dating. When these exterior rings are missing from the panel, the dendrochronologist is forced to make estimates about the felling year. A panel can be all heartwood with an unknown number of heartwood rings on the recent end missing (Figure L.3c, worst case). It can have at the recent end the heartwood–sapwood boundary (Figure L.3d, better case). It can have a significant number of sapwood rings preserved (Figure L.3e, an even better case). Finally, it can preserve the terminal ring, which grew during the year when the tree was cut down (Figure L.3f, the best case, but extremely rare). Only in this last case is the dendrochronologist able to say exactly in what year the tree was cut.

The Sapwood Problem: For oak, various sapwood estimates exist, ranging from 23 to 41 rings (32 ± 9) for Northern Ireland (Baillie, 1982); 20 ± 6 or 26 ± 7.5 rings for Germany (Huber, 1967; Hollstein, 1980); $15(+9/-6)$ rings for the Baltic (Ważny, 1990); and 26 ± 9 rings for the Aegean (Kuniholm and Striker, 1987). The most recent estimate for oak used by Peter Klein (1993) is 15 years $+4/-2$ for Baltic oak, and 17 years $+6/-4$ for Western European oak.[2] There is evidence that the sapwood ring count varies according to the age of the tree. For other species of trees this convenient sapwood estimation is not applicable. Some species (beech, for example) show little or no difference between heartwood and

[2]Dr. Klein, who has probably analyzed more panels than everybody else combined, now reports (Nov. 1994) that he uses a minimum of nine sapwood rings for Eastern Europe and seven sapwood rings for Western Europe in estimating the earliest possible felling date.

sapwood at all. Other species have wildly varying amounts of sapwood, and anything other than a *terminus post quem* date is impossible. Juniper, on which the icon in Figure L.1 was painted, can have up to 160 sapwood rings.

Time Lost in Seasoning: Another variable is how long the wood was seasoned and/or stored between cutting and painting. Paint will not adhere well to a wet surface, so a certain minimum amount of drying time is necessary before the ground is applied. Estimates based on a number of signed and dated paintings are 5 ± 3 (between two and eight) years for the drying-out period preparatory to the application of the ground and paint by painters of the Dutch and Flemish Schools of the sixteenth and seventeenth centuries (Bauch and Eckstein, 1970). The curing or drying-out period may vary from century to century or from artist to artist. Among the painters in the Cologne School of the fourteenth and fifteenth centuries a longer period of about ten years seems to have been preferred (Klein, 1981).

The Problem of Old or Reused Wood: An artist may have chosen to paint on a panel that was cut and/or used many years—even centuries—earlier. If a dendrochronological date is far too early for the painter in question, other kinds of analysis such as x-radiography should be used to see whether there is any underpainting. One of the greatest discrepancies between a dendrochronological date for a panel and the probable painting date by a well-known artist is over 150 years, on the St. Anne altarpiece by Gérard David (and school) in the National Gallery of Art in Washington (cat. 1942.9.17. a-c), other panels of which were cut only 10–15 years before the painting's execution (P. Klein, personal communication, and Klein's appendix to Hand and Wolff, 1986). This last case is extraordinary rather than the rule.

Other Limitations: Stretchers and frames represent a separate set of problems. Stretchers because of their shape often do not have enough rings to allow for dendrochronological dating. Frames can be older than, contemporary with, or later than the painting, and are probably best left out of any serious dendrochronological study.

Finally, a particular panel might come from a tree with sufficiently erratic growth that it cannot be dated with confidence, no matter how many rings are present, or it could come from a tree growing in a sufficiently complacent environment (e.g., along a river bank with an unchanging amount of available moisture) that it does not match anything else.

L.3 Examples/Case Studies

Example 1 (actual): Peter Klein's comparison of three portraits by Lucas Cranach the Elder (Figure L.4) is an easy example. No sapwood es-

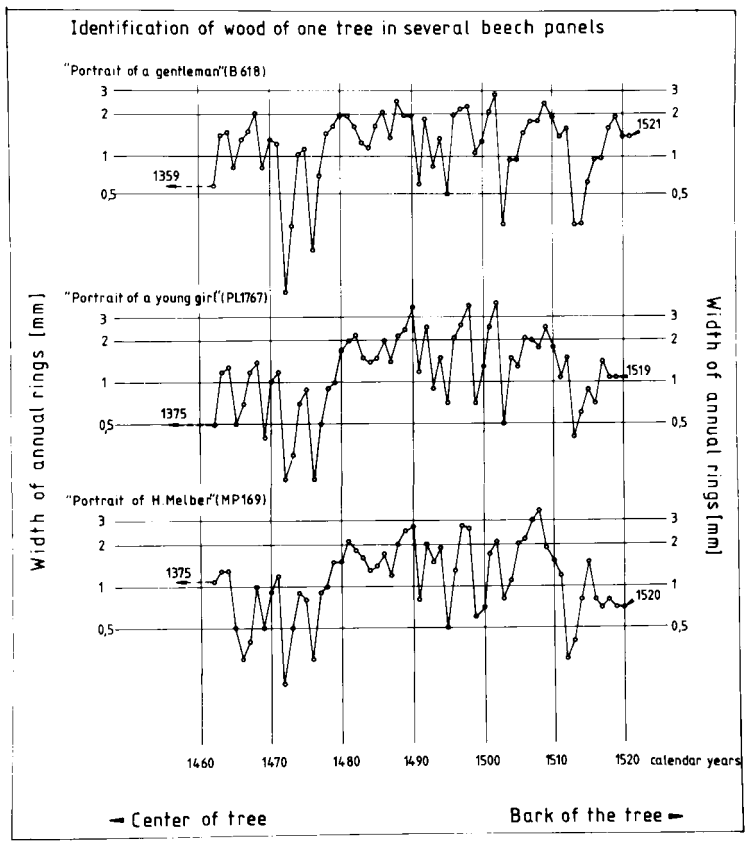

Fig. L.4. Comparison of the growth-ring characteristics of three panels by Lucas Cranach the Elder (after P. Klein, 1986).

timations are involved since the panels are painted on beech, whose heartwood and sapwood rings cannot be distinguished one from another.

Name of Painting	Total Rings	Last Ring	External Date	Difference
(1) *Portrait of a Gentleman*, B618	163	1521	signed 1528	7 years
(2) *Portrait of a Young Girl*, PL1767	145	1519	attrib. l520	1 year
(3) *Portrait of H. Melber*, MP169	146	1520	signed 1526	6 years

Portraits 1 and 3, both signed, seem correctly dated, with a drying-out or storage time of 7 and 6 years, respectively, for their panels. The attribution on stylistic grounds of portrait 2 to 1520, which allows only 1 year between the last preserved ring and the date of painting, should, at first glance, be reconsidered and the date moved—at least on normal dendrochronological grounds—to a slightly later time, especially since other panels from the same tree have now been found on which the 1522 ring is preserved! (P. Klein in C. Grimm, *et al.,* 1994). Painting on this panel cannot possibly have taken place before 1523.

Example 2 (hypothetical): A museum decides to sell a controversial painting, thought to be a Rembrandt self-portrait, in order to pay off its debts. Some Rembrandt specialists claim it is a "mature" portrait from very late in his career. Other specialists say it is only in the manner of Rembrandt but not by his own hand. You, the student dendrochronologist, are called in to help verify the date, and you find, correctly, that the last preserved ring is 1652 when matched against the European oak chronology as a whole. One sapwood ring (1652) is present, so you apply Hollstein's German oak sapwood estimate of 26 ± 7.5 years. You first estimate the cutting date as 1677 (1652 + 26 − 1 because the 1652 ring is a sapwood ring). You modify the ±7.5 years to a round number: ±8 years. You therefore calculate a date for the cutting somewhere between 1667 and 1683. You add 5 years for the curing period, and you tell the museum that its panel was painted on somewhere between 1672 and 1688. Since Rembrandt died in 1669, the museum's painting is not an original but rather that of a copyist or follower of Rembrandt. This seems to clinch the argument about the date, and with great chagrin the museum sells the painting for a fraction of what it would have been worth were it a certifiable painting by Rembrandt himself. You accept a specialist's fee for providing this information, even though unwelcome, to the unhappy museum.

But the museum subsequently claims that you have made a serious mistake. You did not pay attention to the fact that the painting's ring se-

quence matched the Polish oak chronology perfectly rather than the Western European oak chronology, and you should have added the appropriate Polish sapwood amount—somewhere between 12 and 18 rings—to the last preserved ring of 1652. The range for the cutting date would therefore be 1664–1670, which, with a 5-year allowance for seasoning, would yield a revised possible painting date of 1669–1675. The painting is really possibly one of Rembrandt's last masterpieces, and could have sold for ten times more than what the museum got for it. The museum now takes you to court for having sold it bad information. (This example does not take into account connoisseurship and the fact that the museum should have known more about what it was doing. Maybe the museum deserves to be in debt after all.[3])

Example 3 (actual): A triptych by Rogier van der Weyden, the right panel of which is in the Metropolitan Museum of Art in New York (*Christ Appearing to His Mother,* Cat. Metr. 22.60.58) and the remaining two-thirds in the Capilla Real, Granada (*The Nativity* and *The Pietà*), and a second triptych in Berlin-Dahlem (*Miraflores Altar,* Cat. No. 534), provide a final example (Figure L.5). The Metropolitan–Granada altarpiece was thought, on purely art-historical grounds (Wehle and Salinger, 1947), to be the original and the Berlin altarpiece a copy. The Berlin altarpiece has a last preserved (heartwood) ring from 1406. With a median sapwood allowance of 15 years, the felling date should be around 1421, rather early in Rogier's career (Klein, 1981). The wood of the Metropolitan altarpiece, on the other hand, cannot have been cut before 1482 (P. Klein, personal communication), almost two decades after Rogier's death in 1464. Dendrochronology demonstrates that some art-historical opinions must be revised: Berlin has the early painting from Rogier van der Weyden's lifetime. New York and Granada have the posthumous copy.

L.4 SUMMARY

Dendrochronology cannot tell us who painted the panel, or even when the panel was used, but under certain conditions it can tell us where the tree grew, approximately when the tree was cut, and when the prepared

[3]Dr. Klein informs me that this textbook example is flawed since almost all the published sapwood estimates apply to average ring counts for the majority of samples rather than to the extremes for individual trees, and he finds greater variability in Western Europe. A final heartwood ring of 1651 plus a minimum of 7 sapwood rings for Western European oak = 1658, plus a minimum drying time of 2 years = 1660. A final heartwood ring of 1651 plus a minimum of 9 sapwood rings for Baltic oak = 1660, plus a minimum drying time of 2 years = 1662. Both dates are therefore within Rembrandt's lifetime. Moral #1: Beware of averages. Moral #2: Beware of textbook examples. Moral #3: Never accept a fee for providing dendrochronological information.

(a)

Fig. L.5a. "Christ Appearing to His Mother," from Rogier van der Weyden's St. Mary (Miraflores) Altar in Berlin-Dahlem, long thought to be a copy but now demonstrably within Rogier's lifetime.

(b)

Fig. L.5b. The Metropolitan Museum's "Christ Appearing to His Mother," dendrochronologically dated to at least twenty years after Rogier's death.

panel could have been ready for use. It also can tell us about the preferences of certain painters for their supports. If a painter paints only on oak panels, and suddenly a poplar panel appears, allegedly painted by him, one might have immediate grounds for suspicion as to the panel's authenticity.[4]

[4]The Malcolm and Carolyn Wiener Laboratory for Aegean and Near Eastern Dendrochronology is supported by the National Endowment for the Humanities, the National Science Foundation, the Malcolm H. Wiener Foundation, the National Geographic Society, the Samuel B. Kress Foundation, the Wenner-Gren Foundation for Anthropological Research, and individual patrons of the Aegean Dendrochronology Project.

This page intentionally left blank

REFERENCES

REFERENCES

A. COLOR

A-1 J. Albers, *The Interaction of Color* (Yale University Press, 1975).

A-2 T.B. Brill, *Light, Its Interaction with Art and Antiquities* (Plenum Press, New York, 1980).

A-3 M. Hall, *Color and Meaning—Practice and Theory in Renaissance Painting* (Cambridge University Press, Cambridge, 1992).

A-4 K. McLaren, *The Colour Science of Dyes and Pigments* (Adam Hilger Ltd., Boston, 1986).

A-5 K. Nassau, *The Physics and Chemistry of Color* (John Wiley, New York, 1983).

A-6 H. Rossotti, *Colour* (Princeton University Press, 1983).

A-7 S. Saniforth, *Retouching and Color Matching: The Restorer and Metamerism, Studies in Conservation* Vol. 301, pp. 1011–111 (1985).

A-8 M.I. Sobel, *Light* (The University of Chicago Press, Chicago, 1987).

A-9 P. Sloane, *The Visual Nature of Color* (Design Press, New York, 1989).

A-10 D.B. Judd and G. Wyszecki, *Color in Business, Science and Industry* (John Wiley and Sons, New York, 1975) 3rd edition.

A-11 R.G. Kuehni, *Color, Essence and Logic* (Van Nostrand Reinhold Co., New York, 1983).

A-12 F.W. Billmeyer, Jr. and M. Saltzman, *Principles of Color Technology* (John Wiley and Sons, New York, 1981).

A-13 David Falk, Dieter Brill, and David Stork, *Seeing the Light* (John Wiley and Sons, New York, 1986).

A-14 David K. Lynch and William Livingston, *Color and Light in Nature* (Cambridge University Press, New York, 1995).

A-15 David Park, *The Fire within the Eye* (Princeton University Press, Princeton, 1997).

A-16 T. Lamb and J. Bourreau, *Colour, Art and Science* (Cambridge University Press, Cambridge, 1995).
A-17 Richard Dawkins, *Unweaving the Rainbow* (Houghton-Mifflin, Boston, 1998).

B. Artists' Pigments, Materials and Methods

B-1 R.L. Feller, (Ed.), *Artists' Pigments* (National Gallery Art, Washington, 1986) 6th edition.
B-2 A.P. Laurie, *The Painter's Methods and Materials* (Dover Publications, New York, 1967).
B-3 A. Roy, "The Materials of Van Gogh's *Cornfield with Cypresses," National Gallery, Technical Bulletin*, Vol. 11, pp 50–58, 1987.
B-4 D.V. Thompson, *The Materials and Techniques of Medieval Paintings* (Dover Publications, New York, 1959).
B-5 R.H. Harley, *Artists' Pigments, c. 1600–1835* (Butterworth Scientific, London, 1982) 2nd edition.
B-6 H. Kuhn, "Terminal Dates for Paintings Derived from Pigment Analysis" in *Application of Science in Examination of Works of Art* edited by W.J. Young (Museum of Fine Arts, Boston, 1973) pp. 199–205.
B-7 R.J. Gettens and G.L. Stout, *Painting Materials, A Short Encyclopedia* (Dover Publications, New York, 1966).
B-8 R. Mayer, *The Painter's Craft* (Penguin Books, New York, 1979).
B-9 R. Mayer, *The Artist's Handbook* (Viking Penguin Inc., New York, 1981) 4th edition.
B-10 K. Wehlte, *The Materials and Techniques of Painting* (Van Nostrand Reinhold Co., New York, 1975).
B-11 D.V. Thompson, Jr., *The Practice of Tempera Painting* (Dover Publications, New York, 1962).
B-12 J.S. Mills and R. White, *The Organic Chemistry of Museum Objects* (Butterworths, London, 1987).
B-13 R.L. Feller, N. Stolow, and E.H. Jones, *On Picture Varnishes and Their Solvents* (National Gallery of Art, Washington, 1985).
B-14 M.B. Hall, (Ed.), *Color and Technique in Resaissance Painting* (J.J. Augustin, Publisher, Locust Valley, New York, 1987).
B-15 A. Roy, (Ed.), *Artists' Pigments* Vol. 2, (National Gallery of Art, Washington, 1993).
B-16 J. Dunkerton, S. Foster, D. Gordon, and N. Penny, *Giotto to Dürer* (Yale University Press, New Haven, 1991).
B-17 H. von Sonnenburg, *Rembrandt/Not Rembrandt* (The Metropolitan Museum of Art, New York, 1995).
B-18 G. McKim-Smith, G. Andersen-Berdoll, and R. Newman, *Examining Velazquez* (Yale University Press, New Haven, 1988).
B-19 M. Doerner, *The Materials of the Artist and Their Use in Painting* (Harcourt, Brace, Jovanovich, New York, 1984).

B-20 D. Thompson, *The Craftsman's Handbook* [Cennino Cennini] (Dover, New York, 1954).
B-21 G.B. Brown, (Ed.), *Vasari on Technique* (Dover, New York, 1960).

C. SCIENTIFIC ANALYSIS

C-1 L. Bragg, "X-ray Crystallography" *Scientific American*, July 1988.
C-2 B.D. Cullity, *Elements of X-ray Diffraction* (Addison-Wesley, Reading, Mass., 1978) 2nd Edition.
C-3 R.E. Dickerson and I.Geis, *Chemistry, Matter and the Universe*, (W.A. Benjamin, Menlo Park, CA., 1976).
C-4 L.C. Feldman and J.W. Mayer, *Fundamentals of Surface and Thin Film Analysis*, (North-Holland, New York, 1986).
C-5 S.J. Fleming, "An Evaluation of Physics–Chemical Approaches to Authentication" in *Authentication in the Visual Arts* edited by H.L.C. Jaffe, J. Storm van Leeuwen, and L.H. van der Tweel (B.M. Israel BV, Amsterdam, 1979) pp. 103–139.
C-6 V.F. Hanson, "The Curator's Dream Instrument" in *Application of Science in Examination of Works of Art*, edited by W.J. Young (Museum of Fine Arts, Boston, 1973) pp. 18-30.
C-7 M. Hours, *Les Secrets des Chefs-d'oeuvre* (Robert Laffont, S.A., Paris, 1986).
C-8 G. McKim-Smith, G. Andersen-Bergdoll and R. Newman, *Examining Velazquez* (Yale University Press, New Haven, 1988).
C-9 V. Jirat-Wasiutyński, H.T. Newton, E. Farrell, and R. Newman, *Vincent van Gogh's Self-Portrait Dedicated to Paul Gauguin* (Harvard University Art Museums, Cambridge, Massachusetts, 1984).
C-10 D. Bull and J. Plesters, *The Feast of the Gods: Conservation, Examination and Interpretation* (National Gallery of Art, Washington, 1990).
C-11 D. Graham and T. Eddie, *X-Ray Techniques in Art Galleries and Museums* (Adam Hilger Ltd., Bristol, 1985).
C-12 M. Ainsworth "'Paternes for phiosioneamyes': Holbein's Portraiture Reconsidered" *The Burlington Magazine* Vol. 132 (No. 1044), March 1990.
C-13 M.W. Ainsworth and M. Faeries, "Northern Renaissance Paintings—The Discovery of Invention," *Summer Bulletin* (The Saint Louis Art Museum, 1986).
C-14 J.R.J. Van Asperen de Boer, "Infrared Reflectography," Ph.D. thesis, University of Amsterdam, 1970.
C-15 M. Wyld, "Goya's Re–use of a Canvas for Dona Isabel," *National Gallery Technical Bulletin*, Vol. 5, pp. 39–43 (1981).
C-16 C.R. Brundle, C.A. Evans, Jr., and S. Wilson, (Eds.), *Encyclopedia of Materials Characterization* (Butterworth-Heinemann, Stoneham, Ma., 1992).
C-17 Walter McCrone, (Ed.), A. Brown and I.M. Stewart, *The Particle Atlas*, Volume 6, *Electron Optical Atlas and Techniques* (Ann Arbor Science Publishers, Michigan, 1980) 2nd edition.
C-18 B.G. Yacobi, D.B. Holt, and L.L. Kaznerski, (Eds.), *Microanalysis of Solids* (Plenum Press, New York, 1994).
C-19 M.W. Ainsworth, et al., *Art and Autoradiography* (Metropolitan Museum of Art, New York, 1987).
C-20 M.W. Ainsworth, *Gerard David, Purity of Vision in an Age of Transition* (Metropolitan Museum of Art, New York, 1998).

D. Dating and Archaeometry

D-1 M.J. Aitken, *Science-Based Dating in Archaeology*, (Longman, New York, 1990).
D-2 G.F. Knoll, *Radiation Detection and Measurement*, (John Wiley, New York, 1979).
D-3 U. Leute, *Archaeometry*, (VCH, New York, 1987).
D-4 P.A. Tipler, *Modern Physics* (Worth Publishers, New York, 1979).
D-5 R.E. Taylor *Radiocarbon Dating* (Academic Press, Orlando, 1987).
D-6 A. Long, D.J. Donahue, A.J.T. Jull, and T. Zabel, "Tandem Accelerator Mass Spectometry Applied to Archaeology and Art History," in P.A. England and L.V. Zelst, editors, *Application of Science in Examination of Works of Art*, (Museum of Fine Arts, Boston, 1985) pp. 17–21.
D-7 S. Bowman, *Radiocarbon Dating* (University of California Press, Berkeley, 1990).
D-8 H.E. Gove, *Relic, Icon or Hoax? Carbon Dating of the Turin Shroud* (Institute of Physics Publishing, Bristol, 1996).

E. Neutron Activation and Autoradiography

E-1 M. Ainsworth et al., *Art and Autoradiography* (The Metropolitan Museum of Art, New York, 1982).
E-2 W.J. Young, (Ed.), A.A. Gordus, "Neutron Activation Analysis of Streaks from Coins and Metallic Works of Art" in *Application of Science in Examination of Works of Art* (Museum of Fine Arts, Boston, 1973).
E-3 B. Keisch, *Secrets of the Past: Nuclear Energy Applications in Art and Archaeology* US AEC, 1972.
E-4 E.V. Sayre et al., (Eds.) P. Meyers, "The Structure of Works of Art and Historic Artifacts," in *Materials Issues in Art and Archaeology*, Vol 123 in MRS Symposium Proceedings, 1988.
E-5 M. Peisach, "Harnessing the Atomic Nucleus for Elemental Analysis," *S. African J. Chem*, Vol. 40, pp. 209–221 (1987).
E-6 E.V. Sayre and H. Lechtman, "Neutron Activation Autoradiography of Oil Paintings," *Studies in Conservation*, Vol. 13, pp. 161–183 (1968).
E-7 H. von Sonnenburg, *Rembrandt/Not Rembrandt* (The Metropolitan Museum of Art, New York, 1995).
E-8 P. Conisbee, (Ed.), C. Barry, "La Tour and Autoradiography" in, *Georges de La Tour and this World* (National Gallery of Art, Washington, 1996).

F. Art in the Making (National Gallery London)

F-1 D. Bomford, C. Brown, and A. Roy, *Rembrandt* (National Gallery Publications, London, 1988).
F-2 D. Bomford, J. Dunkerton, D. Gordon, and A. Roy, *Italian Painting before 1400* (National Gallery Publications, London, 1989).

F-3 D. Bomford, J. Kirby, J. Leighton, and A. Roy, *Impressionism* (National Gallery Publications, London, 1990).

G. Application of Science in Examination of Works of Art

G-1 Research Laboratory of Museum of Fine Arts, Boston, *Application of Science in Examination of Works of Art* (Arno Press, New York, 1960).
G-2 Research Laboratory of Museum of Fine Arts, Boston, *Application of Science in Examination of Works of Art* (Museum of Fine Arts, Boston, 1966).
G-3 W.J. Young, editor, *Application of Science in Examination of Works of Art* (Museum of Fine Arts, Boston, 1973).
G-4 W.J. Young, (Ed.), *Application of Science to the Dating of Works of Art* (Museum of Fine Arts, Boston, 1978).
G-5 P.A. England and L. van Zelst, *Application of Science in Examination of Works of Art* (Museum of Fine Arts, Boston, 1985).
G-6 A. Gwynne-Jones, *The Life and Works of Sir Joshua Reynolds*, Royal Soc. of Arts. CIV, 1956.
G-7 R.J. Gettens and G.L. Stout, *Painting Materials*, Dover, New York, 1966.
G-8 W.C. McCrone, L.B. McCrone, and J.G. Delly, *Polarized Light Microscopy*, Ann Arbor Science Publ., Ann Arbor, 1978.
G-9 Arie Wallert, private communication.
G-10 J.S. Mills and R. White, *The Organic Chemistry of Museum Objects*, Butterworths, London, 1987.
G-11 L. Masschelein-Kleiner, *Studies in Conservation* 13, 105 (1986).
G-12 S. Barrett and D. Stulik, "Historical Painting Techniques, Materials, and Studio Practice", (The Getty Conservation Institute, 1995), pp. 6–11.
G-13 A.E. Parker and D.C. Stulik, to be published.
G-14 R.P. Haugland, *Molecular Probes*, Molecular Probes Inc. Publ., Eugene (1992).
G-15 M.R. Derrick, D. Stulik, and J.M. Landry, "Infrared Spectroscopy in Conservation Science", (The Getty Conservation Institute, 1999).
G-16 M.R. Derrick, D.C. Stulik, J.M. Landry, and S.P. Bouffard, *Journal of the American Institute of Conservation* 31, 225 (1992).
G-17 C.M. Grzywacz, master's thesis, California State University, Northridge, 1992.
G-18 M.R. Schilling, and H. Khanjian, "Gas chromatographic investigation of organic materials in art objects: New insight from a traditional technique", (Innvoation et Technologie au Service du Patrimoine de l'Humanite, UNESCO/Admitech, Paris), pp. 137–143.
G-19 D.C. Stulik and D.J. Donahue, *MRS Bulletin* 17, 53 (1992).

H. Archaeological Chemistry

H-1 C.W. Beck, (Ed.), *Archaeological Chemistry* (American Chemical Society, Washington, 1974).

H-2 G.F. Carter, (Ed.), *Archaeological Chemistry II* (American Chemical Society, Washington, 1978).
H-3 J.B. Lambert, *Archaeological Chemistry III* (American Chemical Society, Washington, 1984).
H-4 R.O. Allen, *Archaeological Chemistry IV* (American Chemical Society, Washington, 1989).

I. Materials Research Society

I-1 E.V. Sayre, P.B. Vandiver, J. Druzik, and C. Stevenson, (Eds.), *Materials Issues in Art and Archaeology*, Vol. 123, Symposium Proceedings (Materials Research Society, Pittsburgh, 1988).
I-2 C.M. Stevenson and C. Prior, (Eds.), "Microscopic Analysis in Archaeology," *MRS Bulletin* Vol. 14, March 1989.
I-3 P.B. Vandiver, J. Druzik, and G.S. Wheeler, (Eds.), *Materials Issues in Art and Archaeology II*, Vol. 185, Symposium Proceedings (Materials Research Society, Pittsburgh, 1991).
I-4 P.B. Vandiver, J.R. Druzik, G.S. Wheeler, and I.C. Freestone, (Eds.), *Materials Issues in Art and Archaeology III,* Vol. 267, Symposium Proceedings (Materials Research Society, Pittsburgh, 1994).
I-5 P.B. Vandiver, J.R. Druzik, J.L. Galvan Madrid, I.C. Freestone, and G.S. Wheeler, (Eds.), *Materials Issues in Art and Archaeology IV*, Vol. 352, Symposium Proceeding (Materials Research Society, Pittsburgh, 1995).
I-6 M. Ainsworth and J.W. Mayer, (Eds.), "The Science of Art" in *MRS Bulletin* 21, Dec. 1996.
I-7 P.B. Vandiver, J.R. Druzik, J. Merkle, and J. Stewart, (Eds.), *Materials Issues in Art and Archaeology V,* Vol. 462, Symposium Proceedings, Fall 1996 (Materials Research Society, Pittsburgh, 1997).

J. Detection of Fakes in Painting (References to Chapter 8)

J-1 Maryan Ainsworth, *Art and Autoradiography*, The Metropolitan Museum of Art, New York, 1982.
J-2 P. Consibee, (Ed.), C. Barry in "La Tour and Autoradiography" in *Georges de La Tour*, National Gallery of Art, Washington, 1996.
J-3 P. Le Chanu, "The Contributions and Limitations of Scientific Examination and Analysis in the Detection of Forgeries of Old Masters Paintings" presented at the SPIE Conference on "Scientific Detection of Fakery in Art," San Jose, California, Jan. 29, 1998; published in SPIE Conference Series, 1998.
J-4 D. Dutton, (Ed.), *The Forger's Art*, University of California Press, Berkeley, 1983.
J-5 H.E. Gove, *Relic, Icon, or Hoax? Carbon Dating the Turin Shroud*, Institute of Physics Publishing, Bristol, 1996.

J-6 W.J. Young, (Ed.), H. Kühn, "Terminal Dates for Paintings Derived from Pigment Analysis" in *Application of Science in Examination of Works of Art*, pp. 109–205, Museum of Fine Arts, Boston, 1973.
J-7 G. McKim-Smith, Greta Andersen-Berdoll, and Richard Newman, *Examining Velazquez*, Yale University Press, New Haven, 1988.
J-8 W. MacCrone, "1500 Forgeries," *The Microscope*, Vol. 38, pp. 289–98 (1990).
J-9 H. von Sonnenburg, "Paintings: Problems and Issues," Vol. I. *Rembrandt/Not Rembrandt*, Metropolitan Museum of Art, New York, 1996.
J-10 C. Wright, *The Art of the Forger*, Dodd, Mead and Company, New York, 1985.
J-11 C. Wright, *Rembrandt: Self-Portrait*, Gordon Fraser, London, 1982.
J-12 W. McCrone, D.R. Chatier, R.J. Weiss, (Eds.), *Scientific Detection of Fakery in Art*, SPIE-The International Society for Optical Engineering, Bellingham, WA, 1988.
J-13 E. Hebborn, *The Art Forger's Handbook,* The Overlook Press, Woodstock, New York, 1999.

K. Radiocarbon Dating in Art Research

K-1 R.E. Taylor, *Radiocarbon Dating: An Archaeological Perspective*, Academic Press, London, 1987.
K-2 M.A. Geyh and H Schleicher, *Absolute Age Determination*, Springer-Verlag, Berlin, 1990.
K-3 R.E.M. Hedges, *Nucl. instr. and Meth.*, B 52, 1990, p. 428.
K-4 J.J. Hester, *J. Field Archaeol.*, 14, 1987, p. 445.
K-5 R. Gillespie, *Radiocarbon User's Handbook,* Oxford Committee for Archaeology, Oxford, 1984.
K-6 G. Harbottle, E.V. Sayre, and R.W. Stoenner, *Application of Science in Examination of Works of Art*, edited by P.A. van Zelst and I. van Zelst, England, Museum of Fine Arts, Boston, 1985.
K-7 D.J. Donahue, A.J.T. Jull, and L.J. Toolin, *Nucl. Instrum. and Meth.* B, 52, 1990, p. 224.
K-8 M. Suter, *Nucl. Instrum. and Meth.* B, 52, 1990, p. 211.
K-9 J.S. Volgo, J.R. Southen, D.E. Nelson, and T.A. Brown, *Nucl. Instr. and Meth.* B, 5, 1984, p. 289.
K-10 J.S. Slota, A.J.T. Jull, T.W. Lenie, and L.J. Toolin, *Radiocarbon 29*, 1987, p. 363.
K-11 R. Gillespie and R.E.M Hedges, *Nucl. Instr. and Meth.B*, 5, 1984, p. 294.
K-12 D.J.Donahue, T.W. Linick, and A.J.T. Jull, *Radiocarbon 32*, 1990, p. 135.
K-13 M. Stuiver and R. Kra, (Eds.), *Proceedings of the 12th International Radiocarbon Conference June 24–28, 1985, Trodheim, Norway, Radiocarbon 28,* No. 2B, 1986.
K-14 M. Stuiver and G.W. Pearson, *Radiocarbon 28,* No. 2B, 1986, p. 805.
K-15 D.C. Stulik, D.J. Donahue, A.J.T. Jull, and L.J. Toolin, *Radiocarbon 33*, 1991, p. 248.

L. Dendrochronology (Tree-ring Dating) of Panel Paintings

L-1 Baillie, M.G.L., *Tree-Ring Dating and Archaeology*, London: Croom, Helm (1982).

L-2 Baillie, M.G.L., "Is There a Single British Isles Oak Tree-Ring Signal?" *The Proceedings of the 22nd Symposium on Archaeometry: Held at the University of Bradford, Bradford, U.K. 30th March–3rd April 1982* (1983) 73–82.

L-3 Bauch, J., and Eckstein, D., "Dendrochronological Dating of Oak Panels of Dutch Seventeenth-Century Paintings," *Studies in Conservation* 15 (1970) 45–50.

L-4 Bauch, J., and Eckstein, D., "Woodbiological Investigations on Panels of Rembrandt Paintings," *Wood Science and Technology* 15 (1981) 251–263.

L-5 Bauch, J., Eckstein, D., and Brauner, G., "Dendrochronologische Untersuchungen an Eichenholztafeln von Rübens-Gemälden," *Jahrbuch Berliner Museen* 20 (1978) 209–221.

L-6 Bauch, J., Eckstein, D., and Meier-Siem, M., "Dating the Wood Panels by a Dendrochronological Analysis of Tree-Rings," *Nederlands Kunsthistorisch Jaarboek* 23 (1972) 485–496.

L-7 Eckstein, D., and Bauch, J., "Dendrochronologie und Kunstgeschichte, dargestellt an Gemälden Holländischer und Altdeutscher Malerei," *Mitteilungen Deutsche Dendrologische Gesellschaft* 67 (1974) 247–256.

L-8 Eckstein, D., Ważny, T., Bauch, J., and Klein, P., "New Evidence for the Dendrochronological Dating of Netherlandish Paintings," *Nature* 320 (April, 1986) 465–466.

L-9 Fletcher, J., "Tree-Ring Analysis of Panel Paintings," in J. Fletcher, ed., *Dendrochronology in Europe. B.A.R. International Series* 51 (1978) 303–306.

L-10 Hillam, J., and Tyers, I., "Reliability and Repeatability in Dendrochronological Analysis: Tests Using the Fletcher Archive of Panel-Painting Data," *Archaeometry* 37:2 (1995) 395–405.

L-11 Hollstein, E., *Mitteleuropäische Eichenchronologie* Mainz: von Zabern (1980).

L-12 Huber, B., "Seeberg, Burgäschisee-Süd, Part IV, Dendrochronologie," *Acta Bernensia* II (1967) 145–156.

L-13 Klein, P., "Dendrochronologische Untersuchungen an Eichenholztafeln von Rogier Van der Weyden," *Jahrbuch der Berliner Museen* 23 (1981) 113–123.

L-14 Klein, P., "Dating of Art Historical Objects," in D. Eckstein, S. Wrobel, and R.W. Aniol, eds., *Dendrochronology and Archaeology in Europe. Mitteilungen der Bundesforschunganstalt für Forst- und Holzwirtschaft. Hamburg* 141 (1983) 209–222. See long bibliography on pp. 221–222.

L-15 Klein, P., "Age Determinations Based on Dendrochronology," in R. Van Schoute and H. Verougstraete-Marcq, eds., *Scientific Examination of Easel Paintings*. PACT 13 (1986) 225–237.

L-16 Klein, P., "Dendrochronological Analysis of Early Netherlandish Panels in the National Gallery of Art," in J.O. Hand and M. Wolff, *Early Netherlandish Painting*. Washington, D.C. Systematic Catalogue of the Collections of the National Gallery of Art (1986) 259–260.

L-17 Klein, P., Mehringer, H., and Bauch, J., "Dendrochronologische Untersuchungen an Gemäldetafeln und Musikinstrumenten," *Dendrochronologia* 3 (1985) 25–44.
L-18 Klein, P., "The Differentiation of Originals and Copies of Netherlandish Panel Paintings by Dendrochronology," *Le dessin sous-jacent dans la peinture. Colloque VIII* (1989). Louvain-la-Neuve (1991) 29–42.
L-19 Klein, P., "Tree-Ring Chronologies of Conifer Wood and its Application to the Dating of Panels," *ICOM Committee for Conservation* I (1990) 38–40.
L-20 Klein, P., and Ważny, T., "Dendrochronological Analyses of Paintings of Gdansk Painters of the 15th to the 17th Century," *Dendrochronologia* 9 (1991) 181–191. See bibliography for recent references.
L-21 Klein, P., "Dendrochronological Analysis of German Panels in the National Gallery of Art," in J.O. Hand, *German Paintings of the Fifteenth through Seventeenth Centuries*. Washington: National Gallery of Art. (1993) 195–197.
L-22 Klein, P., "Lucas Cranach und seine Werkstatt. Holzarten und dendrochronologische Analyse," in Claus Grimm, Johannes Erichsen, and Evamaria Brockhoff, eds., *Lucas Cranach, Ein Maler-Unternehmer aus Franken*. Augsburg: Haus der Bayerischen Geschichte (1994).
L-23 Kuniholm, P.I., and Striker, C.L., "Dendrochronological Investigations in the Aegean and Neighboring Regions, 1983–1986," *Journal of Field Archaeology* 14:4 (1987) 385–398.
L-24 Schweingruber, F.H., *Tree Rings: Basics and Applications of Dendrochronology*. Dordrecht and Boston: Reidel/Kluwer (1988).
L-25 Ważny, T., *Aufbau und Anwendung der Dendrochronologie für Eichenholz in Polen*. Universität Hamburg: Dissertation, 1990.
L-26 Wehle, H.B., and Salinger, M., *A Catalogue of Early Flemish, Dutch and German Paintings*. New York: The Metropolitan Museum of Art (1947) 30–34.

M. Electrons, the Periodic Table and X-rays

M-1 B.D. Cullity, *Elements of X-ray Diffraction* (Addison-Wesley, Reading, Mass., 1978) 2nd Edition.
M-2 R.E. Dickerson and I. Geis, *Chemistry, Matter and The Universe* (W.A. Benjamin, Menlo Park, CA, 1976).
M-3 L.C. Feldman and J.W. Mayer, *Fundamentals of Surface and Thin Film Analysis,* (North-Holland, New York, 1986).
M-4 R.L. Feller, (Ed.). *Artists' Pigments* (National Gallery of Art, Washington, 1986).
M-5 H.L.C. Jaffe, J. Storm van Leeuwan, and L.H. van der Tweel (Eds.). S.J. Fleming, "An Evaluation of Physics-Chemical Approaches to Authentication" in *Authentication in the Visual Arts,* (B.M. Israel BV, Amsterdam, 1979) pp. 103–139.
M-6 W.J. Young, (Ed.). V.F. Hanson, "The Curator's Dream Instrument" in *Application of Science in Examination of Works of Art,* (Museum of Fine Arts, Boston, 1973) pp. 18–30.

M-7 R.H. Harley *Artists Pigments, c. 1600–1835* (Butterworth Scientific, London, 1982) 2nd edition.
M-8 H. Kuhn "Terminal Dates for Paintings Derived from Pigment Analysis" in *Application of Science in Examination of Works of Art,* edited by W.J. Young (Museum of Fine Arts, Boston, 1973) pp. 199–205.
M-9 J. Orear, *Physics* (Macmillan, New York, 1979).
M-10 P.A. Tipler, *Modern Physics*, (Worth Publishers, New York, 1979).
M-11 T. Tuurnala, A. Hautojarvi, and K. Harva, "Nondestructive Analysis of Paintings by PIXE and PIGME," *Studies in Conservation 30,* 93–99 (1985).
M-12 I.N.M. Wainwright, J.M. Taylor, and R.D. Harley, "Lead Antimonate Yellow," in *Artists' Pigments,* pp. 219–254.

N. Organic Binders: Analytical Procedures

N-1 H. Humecki, (Ed.), M. Derrick. "Infrared Microspectroscopy in the Analysis of Cultural Artifacts," *Practical Guide to Infrared Microspectroscopy.* New York: Marcel Dekker, 1995, 287–322.
N-2 S. Halpine. A New Amino Acid Analysis System for Characterizing Small Paint Samples: Identification of Egg Tempera and Distemper in a Painting by Cosimo Tura. *Studies in Conservation* 37 (1992), 22–38.
N-3 S. Halpine. An Investigation of Artists' Materials Using Amino Acid Analysis: Introduction of the One-Hour Extraction Method. *Conservation Research 1995,* Studies in the History of Art 51, Monograph Series II. Washington, DC: National Gallery of Art, 1995.
N-4 J. Mills and R. White. *The Organic Chemistry of Museum Objects,* 2nd edition. Oxford, England: Butterworth-Heinemann, 1994.
N-5 R. Newman. Binders in Paintings. *MRS Bulletin* 21 (1996), 24–31.
N-6 J. Pilc and R. White. The Application of FTIR-Microscopy to the Analysis of Paint Binders in Easel Paintings. *National Gallery Technical Bulletin* 16 (1995), 73–84.
N-7 T. Bakkenist, R. Hoppenbrouwers, and H. Dubois, (Eds.), S. Schaefer. Fluorescent staining techniques for the characterization of binding media within paint cross-sections and digital image processing for the quantification of staining results," in *Early Italian Paintings Techniques and Analysis* (Maastrict, The Netherlands: Limburg Conservation Institute, 1997), 57–64.
N-8 A. Shedrinsky and N. Baer. The Application of Analytical Pyrolysis to the Study of Cultural Materials. In Thomas Wampler, editor, *Applied Pyrolysis Handbook.* New York: Marcel Dekker, 1995, 125–156.
N-9 M. Striegel and J. Hill. *Thin-Layer Chromatography for Binding Media Analysis.* Los Angeles, California: The Getty Conservation Institute, 1996.
N-10 S. Vallance. Applications of Chromatography in Art Conservation: Techniques Used in the Analysis and Identification of Proteinaceous and Gum Binding Media. *Analyst* 122 (1997), 75R–81R.

This page intentionally left blank

INDEX